MEK Inhibition In Pancreas Cancer

Francesca Vena

A thesis submitted to the University College London for the degree of Doctor of Philosophy

December 2015

CRUK Drug-DNA Interactions Research Group

Department of Oncology

Cancer Institute

University College London

72 Huntley Street, London, WC1E 6BT, UK

DECLARATION

I, Francesca Vena confirm that the work presented in this thesis is my own. Where information has been derived from other sources, I confirm that this has been indicated in this thesis.

ABSTRACT

Pancreatic ductal adenocarcinoma (PDAC) has a poor prognosis and is resistant to chemotherapy. Gemcitabine, a nucleoside analogue, is an important component of treatment for locally advanced and metastatic PDAC, but provides only modest survival benefit. The enzyme Ribonucleotide Reductase (RR) catalyses the conversion of ribonucleotides into deoxyribonucleotides, required for DNA synthesis and repair. Several studies have demonstrated that RR large subunit-1 (RRM1) is associated with gemcitabine resistance in PDAC. The RAS/RAF/MEK/ERK signalling pathways regulates cellular proliferation, differentiation and survival. Targeting downstream effectors of the RAS gene by direct inhibition of MEK (MAPKK) proteins is a rational therapeutic strategy, since aberrant activation of this pathway occurs frequently in PDAC.

In this study, the ability of pimasertib (AS703026), a highly selective and allosteric MEK1/2 inhibitor, to enhance gemcitabine efficacy was tested and the molecular mechanism of their interaction was investigated. Synergistic antiproliferative effects and increased apoptosis were observed when pimasertib was combined sequentially with gemcitabine in human pancreatic cancer cells. Importantly, pimasertib reduced the expression of RRM1 protein and this was associated with sensitivity to gemcitabine. Pre-treatment with the proteasome inhibitor MG132 impaired RRM1 downregulation induced by pimasertib, suggesting RRM1 is degraded through the ubiquitin-proteasome system. Immunoprecipitation experiments indicated enhanced MDM2-mediated polyubiquitination of RRM1 through lys48-mediated linkage following pimasertib treatment, an effect in part mediated by AKT. Finally, the combination treatment of pimasertib with gemcitabine caused significant tumor growth delay in an orthotopic pancreatic cancer model, with RRM1 downregulation in pimasertib-treated mice.

These results indicate MEK as a potential target to sensitize gemcitabine therapy through modulation of RRM1 protein stability and underline the importance of drug scheduling in achieving efficacious antitumor activity. This study has provided mechanistic insights to the synergistic interaction between gemcitabine and pimasertib that could be further investigated in design of future clinical trials.

ACKNOWLEDGEMENTS

First I would like to thank my supervisors Professor Daniel Hochhauser and Professor John Hartley for giving me the opportunity to carry out a PhD under their guidance.

Dear Daniel, thank you very much for your constant support, for keeping up with my mood swings for the entire four years. Thank you for reminding me always to be positive during the hard times, for teaching me how to be a tough and critical scientist and for just being a great PI!

I would also like to thank Dr. Samantha Goodstal for supervising the project from overseas and the MERCK Serono team in Billerica (MA) for funding my PhD.

I would like to thank Dr. Manuel Rodriguez Justo for performing immunohistochemistry quantification and for critical reading of the manuscript.

An important thank you goes to Eleonora Li Causi, my collaborator at the Barts Cancer Institute (London, UK), who helped me with the animal work.

Thank you to all the members of the DRUG/DNA interactions lab: Rouchen, Luke, Helen, Sylwia, Fei, Juanjo, Miguel and Kostas. And to the former members, Raisa and Giammy for mentoring me from the beginning of this tough journey and for our amazing coffee breaks gossiping about the cancer institute life.

A particular thank you to the amazing Trio: Hanna, Michael and Valenti, for keeping up with my pointless dramas about the paper revision, the thesis writing and for all the great Friday nights spent together at the Jeremy Bentham pub after work.

Un grande grazie goes to my ex colleague and friend Valeria. I would not have made it without your support and friendship. I miss you a lot Vale! Thank you to Lucia, Anto and Sebastian for our fun spinning classes at Fitness First together and to Nieves for helping me with my PowerPoint presentations.

To my PhD buddy Jocelyn and our nights out in Mayfair that helped us to distract from our lab life. Thank you to my London partners in crime: Letizia, Pascale, Maddalena and Matilde. Even though they had no idea what a MEK inhibitor is, they have always been interested in hearing about my experiments' progress.

Thank you to all my Italian friends for your long distance support. In particular, to my dear friend Michela and to all my Bolognese friends: Caterina, Agnese, Angela,

Barbara, Simona and Cate. Grazie alla mia Fede, for our millions nights out together, for our trips and for our chats on the phone. You have truly always been there for me and always will.

Thank you to Paul for introducing me to the PhD student's world and taught me how to swim without sinking. You are a great example of how hard work and dedication can lead to great success. Thank you to LIGC! I am so glad to be part of this amazing gospel choir and to have found such great friends.

Now, a very special OBRIGADO goes to Ema for supporting me throughout the final stage of my PhD…the writing! Thank you for being very patient with me, for always understanding me and for standing by my side. You are an amazing person and I am so glad to have you in my life.

The biggest thank you goes to my **big fat Italian family** who has always believed in me. You are the most precious gift life could ever give me.

To my mother, my biggest inspiration: no one could ever do a better job than you! To my great father who always allowed me to follow my dreams. All that I am I owe it to you two.

To my aunt Stefania who followed me everywhere I went: Buffalo, Seattle or London. No matter what part of the world I was moving to she has always come along to make sure I was fine! There is no one quite as special as my older sister Vale who has taught me what the real values in life are.To my grandfather Mario who has watched over me during these four years and to zia Giovanna who transmitted me the passion for medical science.To my cousins Luca, Matteo, Fausto and Martina who represent the most fun part of my life. Marty: you are like sister to me and I am sure you will shine bright like a diamond one day!! To my amazing grandparents: Nonna Luciana (I love you so much) e Nonno Betto, for their unconditional love, tenderness, and words of wisdom.

My curiosity for science began many years ago when as a little child I used to play in my auntie's pharmacy store, wondering why and how these pills would work to cure human diseases. Therefore my last thank you goes to my auntie Dina, who walks beside us every day, to whom this thesis is dedicated

Thank you all for having taken part of this amazing journey.

“It’s the possibility of having a dream come true that makes life interesting” (Paulo Coelho)

To my auntie Dina

COMMUNICATIONS

PRESENTATIONS

- **Poster Presentation** at 10th NCRI cancer conference. 2-5th November 2014, Liverpool (UK). MEK inhibition enhances gemcitabine efficacy by increasing MDM2-mediated ubiquitination and degradation of RRM1. *Vena F, Li Causi E, Hartley J.A, Hagemann T, Goodstal S, Hochhauser D.*

- **Poster Presentation** at EORTC-NCI-AACR 17th-21st November 2014 Barcelona. (Spain). MEK inhibition enhances gemcitabine efficacy by increasing MDM2-mediated ubiquitination and degradation of RRM1. *Vena F, Li Causi E, Hartley J.A, Hagemann T, Goodstal S, Hochhauser D.*

- **Poster Presentation** at UCL Cancer Institute/Colin Woolf Memorial Fund. 18th March 2015, London (UK). MEK inhibition enhances gemcitabine efficacy by increasing MDM2-mediated ubiquitination and degradation of RRM1. *Vena F, Li Causi E, Hartley J.A, Hagemann T, Goodstal S, Hochhauser D.*

- **Poster Presentation** at AACR/Croucher Summer Course in Cancer Biology. 10th-14th August 2015, Hong Kong (CH). The combination of MEK1/2 inhibitor pimasertib with gemcitabine induces schedule-dependent antitumor activity in pancreatic cancer models by reducing RRM1 protein. *Vena F, Li Causi E, Justo-Rodriguez M, Goodstal S, Hartley J.A, Hochhauser D.*

PUBLICATIONS

- *Vena F, Li Causi E, Rodriguez J.M, Goodstal S, Hagemann T, Hartley J.A, Hochhauser D.* (2015). "The MEK1/2 Inhibitor Pimasertib Enhances Gemcitabine Efficacy In Pancreatic Cancer Models By Altering Ribonucleotide Reductase Subunit-1 (RRM1)". Clin Cancer Res.

TABLE OF CONTENTS

LIST OF FIGURES

LIST OF TABLES

LIST OF ABBREVIATIONS

ADAM	Metallopeptidase domain 17
ADM	Acinar-to-Ductal Metaplasia
APC	Adenomatous Polyposis Coli
Ara-C	Cytosine Arabinoside
ATCC	American Tissue Culture Collection
ATP	Adenosine Triphosphate
ATM	Ataxia Telangiectasia Mutated
ATR	Ataxia Telangiectasia Rad3-related
BRAF	V-Raf Murine Sarcoma Viral Oncogene Homolog B
BRCA1	Breast Cancer 1, early onset
BRCA2	Breast Cancer 2, early onset
BSA	Bovine Serum Albumin
CAF	Cancer-associated fibroblasts
CC3	Cleaved Caspase 3
CDA	Cytidine deaminase
CDKN2A	Cyclin-Dependent Kinase Inhibitor 2A
c-Jun	Jun aminoterminal kinase (or JNK)
CRT	Chemoradiotherapy
CT	Cycle Threshold
CI	Combination Index
CRC	Colorectal Cancer
DACH	1,2-Diaminocycloexhane
DBSs	DNA Double Strand Breaks
dC	Deoxycytidine

dCTD	Deoxycytidylate deaminase
dCTP	Deoxycytidine triphosphate
dCK	Deoxycytidine kinase
dFdC	Defluorodeoxycytidine
DMEM	Dulbecco's Modified Eagle's Medium
DMSO	Dimethyslulphoxide
dNTP	Deoxynucleotide triphosphate
dTMP	Deoxythymidine monophosphate
DUBs	DeUbiquitinating enzymes
dUTP	Deoxyuridine monophosphate
ECM	Extracellular Matrix
EDTA	Ethylenediaminetetraacetic Acid
EGF	HER1 or ErbB1, Epidermal Growth Factor
EGFR	Epidermal Growth Factor Receptor
EGTA	Ethylene Glycol Tetra-acetic Acid
EMT	Epithelial-Mesenchynal Transition
ER	Endoplasmic Reticulum
ErbB2	HER2 or ErbB2/neu, Epidermal Growth Factor Receptor 2
ErbB3	HER3, Epidermal Growth Factor Receptor 3
ErbB4	HER4, Epidermal Growth Factor Receptor 4
ERCC1	Excision Repair Cross-Complementation Group 1
ERK1/2	Extracellular Signal-Regulated Kinases
ESC	Embryonic Stem Cells
FA	Fraction Affected
FACS	Fluorescence-Activated Cell Sorting
FAMM	Familial atypical multiple mole melanoma

FDA	Food and Drug administration
FGF	Fibroblast Growth Factor
FGFR	Fibroblast Growth Factor Receptor
FdUTP	Fluorodeoxyuridine triphosphate
FOLFIRI	Folinic acid, Fluorouracil and Irinotecan
FOLFIRINOX	Folinic acid, Fluorouracil, Irinotecan and Oxaliplatin
FOLFOX	Folinic acid, Fluorouracil and Oxaliplatin
5-FU	5-Fluorouracil
FUTP	Fluorouridine triphosphate
Fzd	Frizzled Receptors
GAB2	GRB2 Activating Protein 2
GAPs	GTPase Activating Proteins
GAS	Gamma interferon activation site
GDP	Guanosine DiPhosphate
GemCap	Gemcitabine plus Capecitabine
GEMM	Genetically Engineered Mouse Model
GM-CSF	Granulocyte-macrophage colony-stimulating factor
GTP	Guanosine Triphosphate
GPCRs	G-Protein Coupled Receptors
GPX2	Glutathione peroxidase 2 gastrointestinal
Grb2	Growth Factor Receptor Bound Protein 2
GSH	Glutathione
GSK3β	Glycogen Synthase Kinase 3β
GTP	Guanosine TriPhosphate
GSTZ1	Glutathione Transferase Zeta 1
GO	Glucose Oxidase

HB-EGF	Heparin-Binding EGF
hCNT	Concentrative Nucleoside transporters
HCl	Hydrochloric acid
hENT	Equilibrative Nucleoside transporters
HH	HedgeHog
H_2O_2	Hydrogen Peroxide
HR	Hazard Ratio
HRAS	Harvey RAS
HRP	Horseradish Peroxidase
IGF1R	Insulin-like Growth Factor 1 Receptor
IHC	Immunohistochemistry
IP_3	Inositol 1,3,5 triphosphate
IPM	Intracellular mucinous neoplasms
JAK	Janus Kinase
JNK	c-Jun-N-terminal Kinase
KD	Kinase Domain
KPC	KrasLSL.G12D/+; p53R172H/+; PdxCretg/+
K-RAS	Kirsten Rat Sarcoma Viral Oncogene Homologue
mAbs	Monoclonal Antibodies
MAPK	Mitogen Activated Protein Kinase
MDM2	Mouse Double Minute 2 Homologue
mDNA	Mitochondrial DNA
MEK 1/2	Mitogen-Activating Protein Kinase Kinase 1/2
MEK 4/6	Mitogen-Activating Protein Kinase Kinase 4/6
MET	Met Proto-Oncogene
MMP	Matrix MetalloPeptidase

MPACT	Metastatic Pancreatic Adenocarcinoma Clinical Trial
mTOR	Mammalian target of rapamycin
MTT	Methylthiazolyldiphenyl-tetrazolium bromide
NAC	N-Acetyl-L-Cysteine
NaCl	Sodium Chloride
NADPH	Nicotinamide Adenine Dinucleotide Phosphate
NAOH	Sodium Hydroxide
NER	Nucleotide Excision Repair
NFκβ	Nuclear Factor κβ
NHEJ	Non-Homologous End Joining
Nrf2	Nuclear Factor Erythroid 2-like
NRAS	Neuroblastoma RAS Viral (V-Ras)
NSCLC	Non-Small Cell Lung Cancer
OD	Optical Density
OS	Overall Survival
OH-	Hydroxyl Radical
p16	Cyclin-Dependent Kinase Inhibitor 2A
p21	Cyclin-Dependent Kinase Inhibitor 1A
p27	Cyclin-Dependent Kinase Inhibitor 1B
p38	Mitogen Activated protien kinase p38
p53	Tumor suppressor
p53-R2	p53 inducible Ribonucleotide Reductase subunit-2
PBS	Phosphate buffered saline
PCR	Polymerase Chain Reaction
PDAC	Pancreatic Ductal Adenocarcinoma
PDGF	Platelet-Derived Growth Factor

PDGFR	Platelet Derived Growth Factor Receptor
PDK1	Phosphoinositide-Dependent Kinase 1
PDX	Patient-derived Xenograft
PFA	Paraformaldehyde
PFS	Progression Free Survival
PI3K	Phosphatidylinositol 3-kinase
PIK3CA	Phosphatidylinositol 3-kinase
PIK3CB	PI3-Kinase P110 Subunit Beta
PIP_2	PhosphatidylInositol 4,5-bisPhosphate
PIP_3	PhosphatidylInositol 3,4,5 triPhosphate
PIP4K2A	Phosphatidylinositol-4-Phosphate 5-Kinase Type II Alpha
PKC	Protein Kinase C
PCR	Polymerase Chain Reaction
PTEN	Phosphate and tensin homologue phosphatase
PTB	Phospho-Tyrosine Binding
PTPN12	Protein-Tyrosine Phosphatase G1
Rb	Retinoblastoma
RIPA	Radioimmunoprecipitation Assay Buffer
ROS	Reactive Oxygen Species
RPS6	Ribosomal S6 protein
RR	Ribonucleotide Reductase
RRM1	Ribonucleotide Reductase Subunit-1
RRM2	Ribonucleotide Reductase Subunit-2
RSK	p90 Ribosomal S6 Kinase
RT-PCR	Real Time PCR
RTKs	Receptor Tyrosine Kinases

SDS	Sodium Dodecyl Sulfate
SH2	Src-Homology 2 domain
SH3	Src-Homology 3 domain
shRNA	Short-hairpin RNA
siRNA	Small-interfering RNA
SMAD4	Mothers against decapentaplegic homolog 4
SMO	Smoothened gene
SOS	Son of Sevenless
SPARC	Secreted protein acidic and rich in cysteine
Src	V-Src Avian Sarcoma Viral Oncogene Homolog
TE	Tris-EDTA
TBS	Tris-Buffered Saline
TGF-α	Transforming Growth Factor-α
TGF-β	Transforming Growth Factor-β
TKIs	Tyrosine Kinase Inhibitors
Top1	Topoisomerase I
TP53	Tumour suppressor P53
TK	Tyrosine kinase
TKIs	Tyrosine kinase inhibitors
TKR	Tyrosine kinase receptors
TS	Thymidylate synthase
Ub	Ubiquitin
UV	Ultra-Violet irradiation
VEGF	Vascular Endothelial Growth Factor

CHAPTER 1

INTRODUCTION

1.1 CANCER BIOLOGY

Intense research conducted over the past two decades on cancer cell biology has supported the conclusion that cancer is a complex disease characterised by the sequential acquisition of genomic alterations and importantly, that every human tumor is unique in its genomic mutations (Vogelstein et al. 2013). Tumorigenesis arises from an acquired abnormal and uncontrolled cell proliferation (Croce 2008). Mutations that enable cells to become tumorigenic and ultimately develop cancer affect two classes of genes: oncogenes (with gain of function mutations) and tumor suppressor genes (with recessive loss of function of mutations). Oncogenes are involved in cell proliferation; on the other hand, tumor suppressor genes inhibit cell division (Vogelstein and Kinzler 2004). The acquisition of mutations within these genes drives the transition of normal human cells into malignant cells (Vogelstein and Kinzler 2004). Cells acquire six fundamental physiologic hallmarks capabilities that enable tumor development and growth:

First, they acquire the capability to sustain chronic proliferation. This is achieved for example by not depending solely on mitogenic growth signals but by generating their own growth signals or by becoming insensitive to anti-growth signals (Hunter 1997). Additionally, cancer cells can increase the levels of receptor proteins that stimulate proliferative signalling or activate their downstream components (Hanahan and Weinberg 2011). Excessive amounts of oncogenic signaling (such as K-RAS) can induce cells into a viable but non-proliferative state (senescence) (Collado and Serrano 2010).

Finally, defects in negative feedback mechanisms that control pathways that modulate proliferative signals thus ensuring homeostasis result in sustained cellular proliferation. An example is represented by loss of function mutation of PTEN phosphatase, which leads to amplification of PI3K signaling (Yuan and Cantley 2008).

Programmed cell death (apoptosis) is composed of upstream regulators activated in response to physiological stresses, which in turn activate downstream components responsible for the destruction of the cell (Adams and Cory 2007). Cancer cells acquire the ability to escape programmed cell death pathways, for example through the loss of the *P53* tumor suppressor gene or by increasing antiapoptotic protein expression such as Bcl-2 and Bcl-X_L (Hanahan and Weinberg 2011).

The third biological hallmark acquired by cancer cells is the ability to escape growth suppressor's activity controlling cell proliferation such as the Rb (retinoblastoma-associated) and TP53 proteins. These proteins decide whether a cell should proliferate, undergo senescence (irreversible growth arrest) or trigger apoptosis (Hanahan and Weinberg 2011).

The growth of new blood vasculature, known as angiogenesis, sustains cells proliferation by supplying them with the appropriate nutrients and oxygen (Hayflick 1997). The process of angiogenesis is tightly regulated in normal cells but it is almost always switched on in tumor cells. The ability to induce and sustain angiogenesis can be caused by increased expression of angiogenic inducers (such as VEGF) and downregulation of angiogenic inhibitors. Additionally, oncogenes such as myc or Ras and immune inflammatory cells can turn on angiogenesis from early stages of tumor development (Hanahan and Folkman 1996).

Another important hallmark of cancer cells is the ability of unlimited replicative potential (Hanahan and Weinberg 2011). In normal cells telomeres, regions of repetitive DNA, protect the chromosomes end from degradation or fusion. Without these structures, chromosome ends get damaged, causing a DNA damage response that leads to senescence or apoptosis. During DNA replication, telomeres shorten and ultimately cells stop dividing. Telomere lengths are maintained by telomerase enzymes, whose expression is increased in tumor cells, enabling them to replicate indefinitely (Kim et al. 1994).

Finally, cancer cells are able to invade and metastasise. This process begins with malignant tumor cells escaping the primary tumor site, intravasating into blood vessels and invading adjacent tissues where micrometastases are formed. Ultimately these metastases generate macroscopic tumors and metastasize into distant organs (Fidler 2003). Loss of E-cadherin, a gene responsible for the formation of adherens junctions between adjacent epithelial cells, is frequent in tumors that originate from epithelial tissues and is associated with enhanced invasion and metastasis (Cavallaro and Christofori 2004).

Taken together, this multiplicity of changes is responsible for tumor development and for driving the malignant progression of the disease (Vogelstein and Kinzler 2004).

This thesis will focus on a specific type of gastrointestinal malignancy: pancreatic cancer.

1.2 PANCREATIC CANCER

1.2.1 Overview

Pancreatic cancer, with an overall 5-year survival rate of less than 5% and a median survival of less than 6 months is the 5th leading cause of cancer-related death worldwide (Vogelzang et al. 2012). Early detection is impaired by absence of symptoms, the inaccessible position, which make diagnosis difficult and the lack of specific diagnostic markers (Bardeesy and DePinho 2002) (Costello et al. 2012). In addition, the rapid acquisition of resistance to chemotherapy and the ability to metastasize rapidly contribute to its aggressiveness and mortality rate (Collisson et al. 2012). Only 15-20% of patients are candidates for surgical resection, which represents the only chance for a complete cure (Ottenhof et al. 2011). However, even in this small subset, there is a 5-year survival rate of 20%. The remaining 75-80% of cases are diagnosed with locally advanced or metastatic disease, in which systemic chemotherapy provides only small and temporary benefit and the overall survival is less than 1 year (Von Hoff et al. 2013).

1.2.2 Epidemiology and risk factors

Pancreatic cancer risk increases with advanced age, with less than 10% of patients diagnosed being under the age of 50 years (Deutsch et al. 1999). Tobacco smoking can also increase the risk of pancreatic cancer by 70-100% (Iodice et al. 2008). Furthermore, heavy alcohol consumption and body mass index (BMI) > 35 are environmental risk factors that contribute to the development of this disease. Benign diseases such as type-two diabetes increase the risk of pancreatic cancer by 20 fold (Everhart and Wright 1995) (Raimondi et al. 2009).

Lastly, the inheritance of specific genetic mutations that cause familial syndromes can be related to increased pancreatic cancer risk (Zhen et al. 2015). For example,

individuals with FAMMM (familial atypical multiple mole melanoma) syndrome, characterised by germline mutations in the *CDKN2A* (p16) gene, have a 13-fold increased risk of developing pancreatic cancer (Bartsch et al. 2002) (Lynch et al. 2002). Individuals carrying germline *BRCA2* gene mutations have also a higher risk of pancreatic cancer (Ozcelik et al. 1997) and almost 17% of familial pancreatic cancers carry a mutation within the *BRCA2* gene (Murphy et al. 2002). Finally, germline mutations in the *MLH1* gene, involved in DNA mismatch repair are linked to familial PDAC (Yeo et al. 2002).

Chronic pancreatitis, an inflammatory disease of the pancreas, leads to the transformation of acinar cells into duct-like cells, a process called acinar-to-ductal metaplasia (ADM) (Reichert and Rustgi 2011). ADM can generate pancreatic lesions and develop into malignant PDAC (Reichert and Rustgi 2011). Hereditary pancreatitis, characterised by germline mutations of catyonic trypsinogen gene PRSS1, is associated with increased risk of developing pancreatic cancer (Witt et al. 2000).

Cystic fibrosis is caused by mutation in the cystic fibrosis transmembrane regulatory gene (CFTR), which impairs cyclic AMP mediated chloride function, thus causing duct obstruction due to mucous secretion. This hereditary syndrome can also augment the risk of pancreatic cancer (Maisonneuve et al. 2007).

1.2.3 Biology of pancreatic ductal adenocarcinoma (PDAC)

Pancreatic cancer can be classified into two major categories according to the type of cells it originates from: exocrine and endocrine tumours. Exocrine pancreatic tumours are further divided into adenocarcinomas and a variety of other pancreatic neoplasms. Pancreatic ductal adenocarcinoma (PDAC), a cancer of the exocrine pancreas, is the most frequent type of pancreatic cancer (Warshaw and Fernandez-del Castillo 1992). PDAC is characterised by cuboidal or columnar cells that undergo acinar to ductal metaplasia (ADM). These ductal cells are surrounded by fibroblasts, immune cells, pancreatic stellate cells and excessive production of extracellular matrix (ECM)-rich connective tissue: this phenomenon is referred to as desmoplasia and is a common feature in PDAC tumors (Jaster 2004). The desmoplastic reaction reduces

tumor tissue elasticity and increases tumor interstitial fluid pressure that represents a barrier for many chemotherapeutic agents (Lohr et al. 1994) (Heldin et al. 2004).

PDAC originates from precursor lesions identified as intraductal papillary mucinous neoplasm (IPMN), mucinous cystic neoplasm (MCN) or pancreatic intraepithelial neoplasia (PanIN), the latter being the most frequent pre-lesions to occur and the best characterised (Hruban et al. 2004) (Figure 1.1). PanINs are classified into different grades based on their morphological characteristics and severity of the lesions: PanIN 1A (flat duct lesions), PanIN 1B (papillary duct lesions), PanIN 2 (papillary duct lesions with dysplasia) and PanIN 3 (also known as carcinoma-*in-situ*), which present all the cancer characteristics. PanIN lesions are part of the tumor progression path that ultimately generates invasive carcinoma (Hruban et al. 2001) (Ottenhof et al. 2011) (Fig 1.1). PanIN lesions are characterised by hypovascularity, immune cell infiltration and feature specific genetic alterations that increase in frequency and variety with the progression of PanIN stages. These biological alterations are required for PanIN lesions to progress into invasive carcinoma and are also implicated in the rapid metastatic spread that characterises this malignant disease (Hezel et al. 2006).

1.2.4 Genetic alterations found in PDAC

PDAC is characterised by a series of alterations in multiple genes (Samuel and Hudson 2012). Although less than 10% of PDACs are hereditary and germline mutations of *BRCA2*, *INK4A* have been related with familial PDAC (Schenk et al. 2001, Jaffee et al. 2002), the acquisition of a high diversity of somatic mutations is believed to be the main driver of neoplastic progression (Samuel and Hudson 2012).

A clinical study performing global genomic analyses on PDAC samples identified about 63 genetic alterations affecting almost 12 different signalling pathways, including K-RAS, TGF-β signalling, the HedgeHog and the Wnt pathway (Jones et al. 2008). The four hallmark genetic alterations that characterize PDAC are represented by mutation of *K-RAS*, *TP53*, *SMAD4* and *CDKN2A* genes (Bardeesy and DePinho 2002).

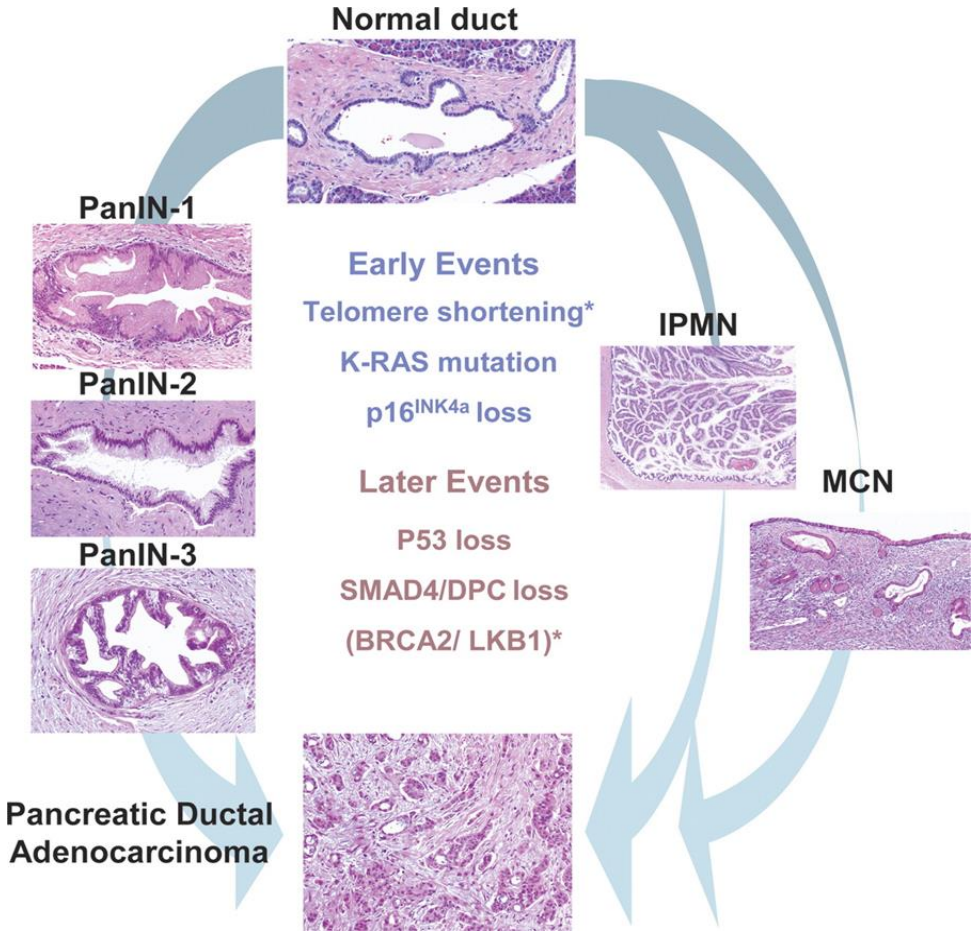

Figure 1.1: Morphologic features and genetic alterations of pancreatic precursor lesions.
Human pancreatic precursor lesions: IPMN, MCN and PanINs. PanINs are graded from I to III and ultimately generate invasive PDAC. Genetic alterations occurring in PanINs are listed (Hezel et al. 2006).

1.2.4.1 Oncogenic K-RAS

RAS proteins are monomeric G proteins and belong to the family of small GTPases (or GTP binding proteins) that control several signalling pathways within the cell (Rajalingam et al. 2007). The MAPK (mitogen activated protein kinase) pathway is one of the many signalling cascades regulated by RAS and promotes cellular proliferation, differentiation and survival (Malumbres and Barbacid 2003). K-RAS mutations are present in almost 90% of PDACs (Morris et al. 2010); however, mutant K-RAS may also be found in chronic pancreatitis or healthy pancreas (Luttges et al. 1999). RAS proteins are bound to GDP or GTP and they function as molecular switches (Pylayeva-Gupta et al. 2011). A point mutation at codon G12 of the *K-RAS* oncogene is the most frequent to occur (Smit et al. 1988). This mutation affects the GTP-ase activity, by reducing GTP

hydrolysis, which leads to constitutive activation of K-RAS and increased stimulation of multiple effector pathways, such as RAF/MEK/ERK and PI3K/mTOR. The persistent activation of these pathways leads to uncontrolled cellular proliferation and transformation (Pylayeva-Gupta et al. 2011). The first studies that investigated the role of the *K-RAS* gene in cancer showed that mutation of *K-RAS* induced the formation of tumors *in vivo*; therefore *K-RAS* has been classified as oncogene (Fernandez-Medarde and Santos 2011).

1.2.4.1.1 KRAS is required for PanIN initiation and development into PDAC

K-RAS mutation is the earliest and most frequent genetic alteration to occur in PanIN lesions (Kanda et al. 2012). Several studies on genetically engineered mouse models (GEMMs) have demonstrated the fundamental role that oncogenic K-RAS plays in the pathogenesis of PDAC (Morris et al. 2010). Mouse models characterised by constitutively activated oncogenic K-RAS developed PanIN lesions similar to the ones observed in the human disease. As the mice aged, these lesions acquired a dense stroma, inflammatory cells and progressed into invasive adenocarcinoma (Aguirre et al. 2003) (Hingorani et al. 2003). A pivotal study on inducible K-RAS^{G12D} mice, in which K-RAS is expressed in pancreatic epithelium in a reversible manner, observed that activation of oncogenic K-RAS followed by induction of acute pancreatitis generated acinar-to-ductal metaplasia (ADM) and infiltration of immune cells that progressed to PanIN formation, as opposed to K-RAS wild type mice in which the damage repaired rapidly and the pancreas resumed its normal histological features (Guerra et al. 2007) (Collins et al. 2012). Furthermore, these inducible K-RAS^{G12D}-driven PDAC models showed complete regression of PanINs and downregulation of PanIN markers in epithelial cells upon K-RAS^{G12D} inactivation indicating that K-RAS activity is required for PanIN progression (Collins et al. 2012).

Although, there is clear evidence showing that K-RAS is essential in the initiation and development of early PanINs, expression of mutant K-RAS alone is not sufficient to cause cellular transformation. For example, an *in vivo* study showed that mice expressing K-RAS mutations in the whole organ developed tumors from only a small percentage of cells (Guerra et al. 2007). Furthermore, induction of oncogenic K-RAS in

mice during early organogenesis led to the development of a tumor-free pancreas with PanIN lesions occurring only after few weeks and progression to PDAC at 1 year (Hingorani et al. 2003). Other genetic alterations have been shown to accelerate or sustain the appropriate levels of oncogenic K-RAS activity required to fully drive the neoplastic process (di Magliano and Logsdon 2013). The introduction of a mutant p53 allele on the *p53* gene in inducible K-RAS mice accelerated PDAC development induced by K-RAS mutations (Collins et al. 2012) and increased metastasis compared to identical mice carrying a null P53 allele (Morton et al. 2010). Furthermore, initiation of PanIN lesions and progression into fully invasive adenocarcinoma in KRAS-driven mice has been shown to be accelerated by introducing mutations within the *SMAD4* and *CDKN2A* genes (Morris et al. 2010). Finally, EGFR activation has been shown to increase the activity of oncogenic K-RAS to initiate pancreatic tumorigenesis (Ardito et al. 2012).

1.2.4.1.2 Oncogenic K-RAS activity affects the tumor microenvironment

The pancreatic tumor microenvironment is characterised by a dense desmoplastic stroma surrounded by inflammatory cells (Hezel et al. 2006). Chronic pancreatitis has been recognised as a risk factor in developing PDAC (Malka et al. 2002). Induction of oncogenic K-RAS in the acinar compartment during embryonic development generated PanIN lesions, which ultimately developed into invasive PDAC, a phenotype not observed if K-RAS was induced during adulthood (Guerra et al. 2007). However, treatment with careulin, which induced pancreatitis, was sufficient to cause transformation of acinar cells into ductal cells and for PDAC development in inducible K-RAS adult mice (Guerra et al. 2007). These observations suggested that inflammatory responses cooperate with K-RAS in promoting PDAC development.

The findings discussed above indicate the crucial role of sustained oncogenic K-RAS activity for pancreatic cancer formation and development and highlight the importance of other genetic alterations or inflammatory stimuli in driving K-RAS induced carcinogenesis.

1.2.4.2 *CDKN2A* gene inactivation

Inactivation of the *CDKN2A* (cyclin dependent kinase inhibitor 2A) tumour suppressor gene is found in almost 90% of sporadic pancreatic adenocarcinomas and usually occurs in high-grade PanIN lesions. The *CDKN2A* gene encodes for the P16/INK4A and $P14^{ARF}$ proteins. Alterations within these genes cause uncontrolled G1/S phase transition, since the inhibition of retinoblastoma (Rb-1) protein phosphorylation by p16 is lost and thus the cell cycle is no longer regulated (Wilentz et al. 1998). Mutation of *CDKN2A* cooperates with activated KRAS to promote tumor progression (Bardeesy et al. 2006).

1.2.4.3 *TP53* mutation

The most common genetic mutation observed in human cancer occurs in the *P53* gene and is associated with poor patient prognosis (Bieging et al. 2014). Upon DNA damage or other oncogenic stresses, P53 is activated and triggers transient cell cycle arrest, senescence or apoptosis depending on the stimulus and cellular context (Bieging et al. 2014).

P53 mutation is usually caused by missense alteration of the DNA binding-domain (Rozenblum et al. 1997) (Freed-Pastor et al. 2012), resulting in loss of wild-type P53 function (Bieging et al. 2014). Between 50% and 75% of PDAC patients carry a mutation of the *P53* tumor suppressor gene, which usually occurs in advanced PanIN3 lesions (Li et al. 2004). The introduction of an inactivating mutation in the *P53* gene accelerated PDAC development in inducible K-RAS mouse models compared to identical mice harbouring a P53null allele, suggesting that this contributes to pancreatic tumor progression (Guerra et al. 2007).

An *in vivo* study has shown that TP53 mutations prevent growth arrest, senescence and promote metastasis in mutant K-RAS mice of pancreatic cancer (Morton et al. 2010). Furthermore, a microarray analysis on human PDAC tissues revealed a direct correlation between mutant P53 accumulation and lymph node metastasis, confirming the prometastatic functions of P53 mutation (Morton et al. 2010).

Finally a recent study generated a pancreatic cancer mouse model by injecting into nude mice KPC cells (generated by the KPC mouse model, characterised by oncogenic K-RAS and mutant $TP53^{R172H}$) whose mutant $TP53^{R172H}$ had been knocked down with short hairpin RNA (shRNA). The incidence of metastasis was significantly lower in mice in which mutant TP53 was depleted compared to mice transfected with control shRNA, indicating that P53 mutation is required to sustain metastatic spread in this murine model (Weissmueller et al. 2014).

1.2.4.4 *SMAD4/DPC4* gene mutation

SMAD4 (mother against decapentaplegic, drosophila, homolog of 4)/DPC4 (deleted in pancreatic carcinoma 4) is a tumour suppressor gene that mediates the TGF-β (transforming growth factor beta) signalling network, which induces growth inhibition (Massague et al. 2000). Loss of SMAD4/DPC4 is frequent in PanINs, thus inducing disruption of TGF-β signalling, which leads to uncontrolled cell proliferation (Massague et al. 2000). A recent study observed that TGF-β1 contributed to the induction of a desmoplastic reaction in PDAC models, a common pathological characteristic in pancreatic tumors, causing impaired drug delivery into the tumor site (Lohr et al. 2001).

1.2.4.5 Other genetic alterations found in PDAC

1.2.4.5.1 The Wnt-β-catenin signalling pathway

The Wnt signalling cascade consists of a family of glycoproteins that bind to receptors of the Frizzled (Fzd) family (Anastas and Moon 2013). The canonical Wnt-β-catenin signalling pathway regulates proliferation and differentiation during embryonic development. Ligands binding to this pathway trigger a signalling cascade that prevents the degradation of β-catenin (Morris et al. 2010). Activation of this pathway and accumulation of β-catenin is frequently found in PanIN lesions of PDAC mice. To establish whether the Wnt pathway is required in pancreatic cancer development, the effects of inhibitors of the Wnt pathway receptor Fzd were examined in mouse models and a delay in PanIN formation and progression was observed (Zhang et al.

2013). Other preclinical results demonstrated that both pharmacological and biological (by using specific siRNA) inhibition of the Wnt pathway significantly blocked proliferation and enhanced apoptosis in PDAC cell lines (Pasca di Magliano et al. 2007). These results indicate that the development of PDAC also depends on the acquisition of genetic alterations within embryonic pathways and provide a strong rationale for developing therapeutic strategies targeting the Wnt signalling cascade for PDAC treatment.

1.2.4.5.2 Upregulation of the Epidermal Growth Factor Receptor (EGFR)

Upregulation of receptor tyrosine kinases, in particular of epidermal growth factor receptor (EGFR) and its ligands, has been found in low-grade PanINs (Tobita et al. 2003) (Morgan et al. 2008). Concomitant activation of oncogenic K-RAS and EGFR signalling accelerates the progression of a different type of pancreatic lesions (IPMN) into invasive neoplasia (Siveke et al. 2007). Preclinical studies have indicated that inhibition of EGFR signalling impairs PDAC development and progression in KRAS-driven pancreatic cancer mouse models (Navas et al. 2012).

As previously mentioned, PDAC is characterised by the formation of metaplastic-duct like cells from the corresponding acinar cells (ADM), a process triggered by chronic pancreatic inflammation (Guerra et al. 2007). A study on oncogenic $Kras^{G12D}$ mice observed upregulation of the EGFR pathway in acinar cells, which strikingly increased upon induction of pancreatic damage caused by cerulein treatment. EGFR activation was detected upon duct cells formation in primary acinar cells explants isolated from the same mice suggesting that EGFR is required in the acinar to ductal transformation both *in vitro* and *in vivo* (Ardito et al. 2012). To confirm this hypothesis, the investigators showed that ADM transformation occurred in acinar cells explants derived from $Kras^{G12D}$ mice after 3 days in culture but was not observed in $Kras^{G12D}$ and $Egfr^{KO}$ mice. K-RAS-driven pancreatic tumorigenesis was suppressed by pharmacological inhibition of EGFR and by depletion of ADAM17, a metalloproteinase involved in EGFR activation (Ardito et al. 2012).

1.2.4.5.3 BRCA mutation

The *BRCA1* and *BRCA2* tumour suppressor genes play a fundamental role in regulating gene transcription, maintaining chromosomal stability and in the repair of DNA double strand breaks (Roy et al. 2012). BRCA mutation induces alterations in the homologous recombination-based DNA repair pathway, thus leading to genomic instability (Venkitaraman 2002). *BRCA2* gene mutations occur at a late stage in pancreatic tumorigenesis (Murphy et al. 2002) (van der Heijden et al. 2004). Tumors harbouring mutant *BRCA* genes have been associated with increased sensitivity to platinum-based chemotherapeutic agents and poly (ADP-ribose) polymerase (PARP) inhibitors. In normal cells, DNA damage is repaired by homologous recombination. However, in BRCA deficient tumors, this process is impaired and double strand breaks cannot be efficiently repaired (Lord and Ashworth 2012). PDAC patients with BRCA mutation who received platinum-based therapies demonstrated a better OS than patients who were treated with non-platinum agents (22 months versus 9 months) (Golan et al. 2014). Therefore, BRCA could be an important prognostic factor for PDAC and there is now increasing interest in exploring whether platinum-based regimens would provide benefit to PDAC patients carrying BRCA2 mutations.

1.2.4.6 Telomere shortening

Telomeres are a region of repetitive nucleotide sequences at the end of a chromosome that protects these ends from sticking to other chromosome ends. Short telomeres induce chromosomal rearrangements through anaphase bridging and breakage-fusion cycles, which generate chromosomal instability (Artandi et al. 2000). Previous evidence classified telomere shortening as a neoplastic event that commonly occurs in pancreatic cancer. Specifically, quantitative fluorescence in situ hybridization (FISH) biopsies on non-cancerous or cancerous pancreatic tissues showed alteration of telomeres function in low-grade to high-grade of pre-cancerous PanIN lesions, a phenomenon that leads to chromosomal abnormalities and as a consequence to the development of invasive PDAC (Matsuda et al. 2015).

1.2.5 Invasive and metastatic properties of PDAC cells

Metastasis is a multistep process in which cancerous cells detach from the primary tumor, invade the surrounding stroma, intravasate into the circulatory systems (blood and lymph) and finally disseminate into distant organs (Valastyan and Weinberg 2011) (Valastyan and Weinberg 2011). Almost 90% of cancer-related deaths are caused by metastasis and not by the primary tumor (Mehlen and Puisieux 2006).

Previous evidence has indicated that metastatic spread occurs at late stage in the clonal evolution of pancreatic cancer and that primary tumors have to proliferate for almost ten years before they acquire the genetic and epigenetic alterations required to produce a metastatic phenotype (Campbell et al. 2010). However, a study that analysed data from a large number of PDAC patients' biopsies adopted a mathematical model to investigate tumor progression and efficacy of chemotherapeutic treatments (Haeno et al. 2012). In this study, the investigators predicted that cancer cells acquire the ability to metastasize during early PanIN stages and observed that chemotherapy was more effective at prolonging survival after tumor resection compared to surgery alone since micrometastases can occur during early tumorigenesis and surgery would only block local tumor progression. These results suggest that systemic chemotherapy should be adopted quickly after tumor diagnosis, even before surgery, to increase the chance of survival (Haeno et al. 2012).

The transition from an epithelial to a mesenchymal phenotype is known as EMT (or epithelial to mesenchymal transition). In this process cells lose their epithelial characteristics and acquire a fusiform morphology, are more motile and express mesenchymal markers (Lee et al. 2006). The EMT process occurs in early premalignant lesions, can be induced by chronic inflammation diseases and has been shown to contribute to pancreatic cancer cell dissemination and metastasis (Polyak and Weinberg 2009).

Different molecular pathways contribute to metastasis formation in PDAC. Cellular migration and tumor metastasis driven by oncogenic K-RAS has shown to be enhanced when K-RAS mutant mice expressed conditional knockout of the *p16 (INK4A)* gene (Qiu et al. 2011). Additionally, loss of SMAD4 (Mazur and Siveke 2012) and increased

production of fibroblastic cells contributes to metastasis dissemination (Xu et al. 2010).

As previously mentioned, a study on pancreatic cancer mouse models revealed that mutant P53 accelerated cell invasion and was required to sustain metastatic spread. Interestingly, in these mouse models, which harboured oncogenic *K-RAS* gene, mutant p53 enhanced metastasis formation by increasing platelet-derived growth factor receptor β (PDGFRβ) expression, an effect that was reversed by genetic knockdown or pharmacological inhibition of PDGFRβ (Weissmueller et al. 2014). The results from this study indicate that anti-PDGFRB therapies represent a potential therapeutic strategy to reduce the metastatic potential of pancreatic cancer in patients harbouring P53 mutation (Weissmueller et al. 2014).

1.3 Current therapies for Pancreatic Ductal Adenocarcinoma

1.3.1 Treatment options for localized disease

Surgical resection is the first treatment choice when pancreatic tumor is still localized and represents the only chance for a complete cure or long-term survival. However, almost 70% of the patients that had a successful surgical resection do not survive due to local recurrence of the disease (Gillen et al. 2010) or due to the development of metastasis (Werner et al. 2013).

The common surgical procedure performed when the tumor is localized to the head of the pancreas is a pancreatic duodenectomy, or Whipple's procedure (after Allen Oldfather Whipple, the initiator of the procedure) and consists of removal of the gallbladder, common bile duct, part of the duodenum, and the head of the pancreas (Michalski et al. 2007).

Among PDAC patients that have had surgical resection, less than 20% live more than 5 years (Hidalgo et al. 2015). For this reason adjuvant treatments have become an important post-operative choice, with the ultimate goal to improve long-term survival (Hidalgo 2010). Several clinical studies have demonstrated that higher median overall survival was achieved in patients treated with adjuvant chemotherapy after surgical resection of the tumor (Neoptolemos et al. 2004) (Oettle and Neuhaus 2007).

Gemcitabine and 5-fluorouracil chemotherapies represent the standard adjuvant regimens used in resected PDAC patients and they will be discussed in detail in the next sections.

1.3.1.1 Adjuvant chemotherapy

5-fluorouracil (5-FU) is a uracil analogue where the hydrogen atom at position 5C is replaced with a fluorine atom (Longley et al. 2003). 5-FU exerts its cytotoxicity by being incorporated into RNA during its synthesis or by inhibiting the Thymidylate Synthase (TS) enzyme. The TS enzyme catalyses the reduction of deoxyuridine monophosphate (dUMP) to deoxithymidine monophosphate (dTMP), thus providing the necessary dTMPs pools for DNA synthesis and repair (Longley et al. 2003).

Intracellular 5-FU is converted into three active metabolites: fluorodeoxyuridine monophosphate (FdUMP), fluorodeoxyuridine triphosphate (FdUTP) and fluorouridine triphosphate (FUTP). The FUTP is incorporated into cellular RNA causing alterations of RNA processing with severe effects on cellular metabolism and survival. FdUMP and FdUTP, in contrast, are the metabolites that mainly cause DNA disruption and TS inhibition.

Gemcitabine, is an analogue of deoxycytidine (Fig. 1.2), in which two hydrogens on the 2 carbons of deoxycytidine (dC) are substituted with two fluorine's (dFdC) (Gesto et al. 2012) and belongs to the class of antimetabolite agents. Gemcitabine represents a standard treatment for PDAC although it provides benefit to only 25% of patients (Burris et al. 1997). The use of gemcitabine as post-operative therapy was supported by the results obtained from a phase III trial in which adjuvant gemcitabine therapy delayed disease recurrence and produced manageable toxicities in patients with resected PDAC tumors. (Oettle et al. 2007).

The first data exploring the effects of adjuvant chemotherapy came from a large multicentre trial known as the ESPAC-1 (The European Study Group for Pancreatic Cancer) (Neoptolemos et al. 2001) (Neoptolemos et al. 2004). In this clinical study, a total of 289 patients with surgically resected PDAC were assigned to receive chemotherapy, chemoradiotherapy, or no treatment. This study showed a 5-year

survival rate of 21% among patients treated with 5-FU compared to an 8% survival rate among patients who did not receive chemotherapy. The median overall survival in patients treated with chemotherapy was 15.9 months compared to the median overall survival of 17.9 months for patients who received chemoradiotherapy (hazard ratio for death of 1.28; 95% CI, 0.99 to 1.66; P=0.5). Overall, this study concluded that adjuvant chemoradiotherapy does not improve survival of resected patients possibly because it delays the administration of chemotherapy, which, in order to be beneficial, should be given immediately after resection (Neoptolemos et al. 2004). The results from the ESPAC trial strongly support the use of adjuvant treatments in resected PDAC patients.

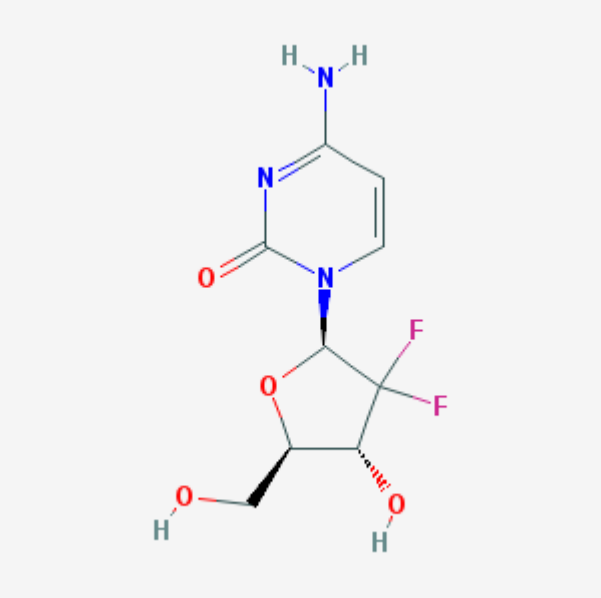

Figure 1.2: Molecular structure of Gemcitabine: 2-deoxy-2,2-difluorocytidine.
Gemcitabine is a cytidine analogue, in which two hydrogen atoms on the 2 carbons of deoxycytidine (dC) are replaced with two fluorine atomos (dFdC).

1.3.1.2 Chemoradiotherapy

Chemoradiotherapy (CRT) is an adjuvant treatment option for some resected PDAC patients and for locally advanced PDAC patients in the USA but is less frequently

adopted in the UK. The results of a study conducted at the John Hopkins hospital demonstrated that adjuvant CRT improved median overall survival in patients with resected pancreatic adenocarcinoma compared to patients that did not receive CRT after surgery (21.2 months vs 14.4 months; P<0.01) (Herman et al. 2008), as opposed to the results observed in the ESPAC trial, supporting the use of CRT after surgical resection in PDAC patients. An important difference with trials consisted on the absence of maintenance chemotherapy in the CRT cohort, which could explain the different outcome of the two results.

Gemcitabine, capecitabine or 5FU are the most common chemotherapies used in combination with radiotherapy (Hidalgo et al. 2015). *In vitro* evidence has demonstrated that gemcitabine sensitizes tumor cells to radiation treatment in a schedule dependent fashion (Ostruszka and Shewach 2000). A recent preclinical study has shown that gemcitabine radiosensitizing effects can be restored in gemcitabine resistant cell lines by upregulation of deoxycytidine kinase (dCK), the enzyme responsible for converting gemcitabine into its active form (Kerr et al. 2014).

A Phase I trial proved that radiation plus twice-weekly administrations of gemcitabine ($40mg/m^2$) was well tolerated and induced antitumor activity in locally advanced PDAC patients, (Blackstock et al. 1999) a result that led to a Phase II trial which further investigated the efficacy of this treatment regimen. However, no significant survival benefit was observed (Blackstock et al. 2003). The same investigators conducted a Phase II study to investigate the effects of radiation plus gemcitabine treatment followed by gemcitabine in patients with resected pancreatic tumor. The combination regimen resulted in a median overall survival of 18.3 months (95% CI=13.7-25.9) (Blackstock et al. 2006).

In agreement with previous findings, randomised trials that compared gemcitabine CRT with 5FU CRT indicated a higher survival benefit in gemcitabine treated patients accompanied by significant haematological toxicity (Zhu et al. 2011). On the other hand, in a recent Phase II trial (SCALOP trial), a survival advantage and less toxic profile were observed with capecitabine-based chemo-radiotherapy compared to gemcitabine-based CRT after a course of induction chemotherapy (Mukherjee et al. 2013).

1.3.2 Treatment options for locally advanced and metastatic disease

PDAC patients with locally advanced or metastatic disease are treated with chemotherapy to prolong survival and improve quality of life. 5-FU represented the only chemotherapeutic option in the advanced settings until 1997 (Kleeff et al. 2007), when a randomized trial conducted by Burris and colleagues showed a better median OS with gemcitabine treatment compared to 5-FU (5.65 months vs. 4.41 months; Long-Rank Test P=0.0025) (Burris et al. 1997). Although the increase in survival was modest, improved quality of life as shown by increased weight gain, reduced pain and a lower toxicity profile was observed in gemcitabine-treated patients; for these reasons, gemcitabine was approved by the Food and Drug Administration (FDA) and became the standard therapy for advanced PDAC treatment (Burris et al. 1997).

Combination therapies in advanced PDAC patients have been an intense subject of investigation (Shi et al. 2012). Several preclinical and clinical studies have investigated whether the addition of targeted therapy to standard chemotherapy would enhance its effectiveness and increase survival. Targeted therapies affect molecular targets involved in cancer cell growth, progression and dissemination and they represent a new treatment choice for many types of human cancers (Huang et al. 2014). Some examples include small molecule inhibitors targeting signal transduction pathways, monoclonal antibodies or angiogenesis inhibitors (Huang et al. 2014). The main limitation of using targeted therapy is the development of drug resistance, which occurs through feedback loop activation of other signalling pathways (Lito et al. 2013). For this reason, targeted therapies are often used in combination with other chemotherapeutic agents.

Up to now, only three clinical studies that involved gemcitabine-based combinations (with chemotherapeutic or targeted agents) or a novel chemotherapy combination have reported significant survival benefit in PDAC (Garrido-Laguna and Hidalgo 2015) The results from these studies are summarized in Table 1.1 and will be discussed in the next paragraphs.

	Gemcitabine vs Gem/nab-paclitaxel	Gemcitabine vs FOLFIRINOX	Gemcitabine vs Gem/erlotinib
Median OS	6.7 months vs 8.5 months	6.8 months vs 11.1 months	5.91 months vs 6.24 months
Median PFS	3.7 months vs 5.5 months	3.3 months vs 6.4 months	3.5 months vs 3.75 months
1-Year survival	22% vs 35%	20.6% vs 48.4%	17% vs 23%

Table 1.1: Clinical trials results in metastatic PDAC patients.
The table illustrates Median Overall Survival (OS), Progression Free Surival (PFS) and 1-year survival rate of patients receiving gemcitabine plus nab-paclitaxel treatment or gemcitabine alone; FOLFIRINOX treatment or gemcitabine alone and gemcitabine plus erlotinib or gemcitabine alone. Table adapted from (Thota et al. 2014).

1.3.2.1 Gemcitabine plus nab-paclitaxel

Paclitaxel is an anticancer agent that acts by stabilizing microtubules and preventing their depolymerisation (Pazdur et al. 1993). Since paclitaxel is a hydrophobic molecule, several formulations have been developed to increase solubility and cremaphore-paclitaxel (Cre-paclitaxel) was the first formulation to be developed. However, this oil solvent induced hypersensitivity reaction and altered paclitaxel pharmacology (Ma and Hidalgo 2013). A later formulation consisting of a solvent-free albumin bound nanoparticle form of paclitaxel (nab-paclitaxel) was developed to limit toxicities of solvent-based formulations (Hoy 2014). Nab-paclitaxel had more favourable pharmacologic properties plus reduced risk of paclitaxel-induced neutropenia, which allowed the use of higher doses compared with the cre-paclitaxel formulation.

A Phase III trial (MPACT) was conducted after the promising results obtained from a Phase-I/II study of gemcitabine in combination with nab-paclitaxel (Von Hoff et al. 2011). The MPACT study involved 861 patients and resulted in a significant improvement in median OS of 8.5 months versus 6.7 months (hazard ratio for death 0.72; 95% CI, 0.62 to 0.83; P<0.001). A better median PFS of 5.5 months versus 3.7 months (hazard ratio for disease progression or death was 0.69; 95% CI, 0.58 to 0.82; P<0.001) and manageable toxicities were also observed in patients treated with gemcitabine plus nab-paclitaxel combination compared to gemcitabine alone (Von

Hoff et al. 2013). These results led to the FDA approval of abraxane® (nab-paclitaxel) for patients with locally advanced and metastatic PDAC.

The molecular mechanisms behind the synergy between gemcitabine and nab-paclitaxel have been investigated. A pre-clinical study demonstrated synergistic antitumor activity between nab-paclitaxel and gemcitabine in the KPC mouse model. This synergistic interaction was associated with paclitaxel-induced downregulation of CDA (cytidine deaminase) protein levels, the enzyme responsible for deactivating gemcitabine, through reactive oxygen species-mediated degradation. Furthermore, an increase in tumor vascularity and a decrease in desmoplastic stroma were induced by nab-paclitaxel treatment, an effect that facilitated gemcitabine accumulation into the tumor (Frese et al. 2012). These results provided novel mechanistic insights into the antitumor activity of nab-paclitaxel.

1.3.2.2 FOLFIRINOX

FOLFIRINOX consists of a combination of three chemotherapeutic agents: 5FU, irinotecan and oxaliplatin plus leucovorin (a folic acid). This chemotherapy regimen has been included as one of the first-line treatment options for metastatic PDAC patients with good performance status since the results of the PRODIGE/ACCORD 11 study: In this Phase III trial, patients treated with FOLFIRINOX showed improved median OS of 11.1 months versus 6.8 months (hazard ratio for death 0.57; 95% CI, 0.45 to 0.73; $P<0.001$), compared to patients receiving gemcitabine alone. Importantly, the 1-year survival was 48.4% with FOLFIRINOX regimen compared to the 20.6% of gemcitabine-treated patients. Patients exposed to this chemotherapy regimen experienced severe toxicities such as neutropenia, neurological and haematological disorders; however, toxicity did not impact the overall quality of life (Conroy et al. 2011). The significance of this study is that chemotherapy prolongs survival in pancreatic cancer.

1.3.2.3 Gemcitabine plus erlotinib

EGFR activation is required for PDAC initiation and progression (Tobita et al. 2003) (Navas et al. 2012). Thus, EGFR represents a rational therapeutic target that could enhance gemcitabine response in PDAC patients. Erlotinib, a tyrosine kinase inhibitor of EGFR induced synergistic antitumor activity in combination with gemcitabine in pancreatic cancer mouse models by antagonizing gemcitabine-induced activation of the MAPK signalling pathway (Miyabayashi et al. 2013).

A Phase III clinical study, which involved a large number of patients with locally advanced or metastatic PDAC, demonstrated that the addition of erlotinib to gemcitabine produced a median OS of 6.24 months versus 5.91 months in patients treated with gemcitabine alone (hazard ratio for death, 0.82; 95% CI, 0.69 to 0.99; P=0.038). A significantly longer progression free survival was also observed with the combination compared to gemcitabine alone, with a hazard ratio of 0.77; 95% CI, 0.64 to 0.92; P=0.04 (Moore et al. 2007). Although the survival benefit was modest, it was clinically significant and led to the FDA approval of this combination regimen for non-resectable PDAC. Other EGFR-targeted therapies have been tested, such as the monoclonal antibody inhibitor of EGFR cetuximab, but so far, the erlotinib plus gemcitabine regimen is the only molecular targeted agent that has demonstrated increased survival benefit compared to gemcitabine alone (Werner et al. 2013) (Philip et al. 2010).

1.3.2.4 Gemcitabine plus capecitabine

Capecitabine is a fluoropyrimidine that is converted into 5FU inside the cell through the sequential action of enzymes present at higher levels in tumor tissues rather than normal tissues (Schuller et al. 2000). Capecitabine has been approved by the FDA as first line single agent for the treatment of metastatic colorectal and breast cancer (Courtin et al. 2013). The gemcitabine plus capecitabine (GemCap) regimen became a treatment option for metastatic PDAC patients with a good performance status, after the results of a meta-analysis, conducted by pooling the results of different trials, showed improved survival benefit and manageable toxicities with the GemCap combination compared to gemcitabine alone (Cunningham et al. 2009).

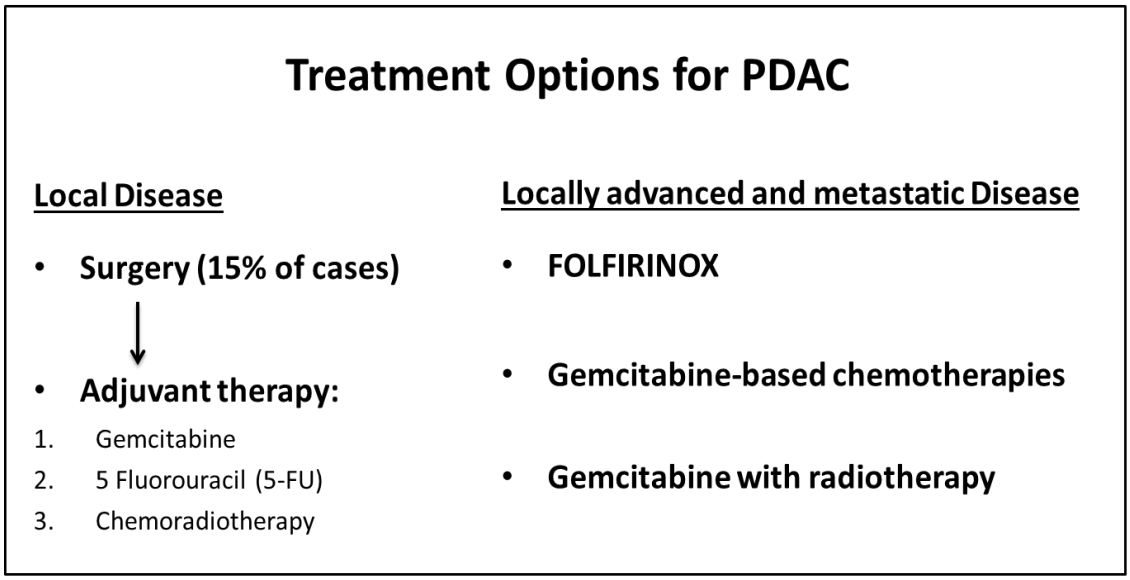

Figure 1.3: Treatment Options in PDAC.

PDAC patients with local disease are candidates for surgical resection, which usually follows adjuvant therapy. Locally advanced and metastatic disease treatment options are: gemcitabine, gemcitabine plus erlotinib, FOLFIRINOX regimen, gemcitabine plus Nab-paclitaxel and gemcitabine plus capecitabine.

1.3.3 Targeting the stromal compartment in PDAC

PDAC is characterised by a dense desmoplastic stroma made of activated cancer-associated fibroblasts (CAFs), inflammatory cells, endothelial cells coated with extracellular matrix (ECM) and poor vascular perfusion (Hidalgo 2010). The stroma contributes to resistance to chemotherapeutic agents because it compromises drug delivery into the tumor site (Neesse et al. 2011).

This stromal reaction occurring in PDAC is in part mediated by constitutive activation of the Hedgehog (HH) signalling pathway, which frequently occurs through mutation of the SMO gene (smoothened gene), an HH activating protein. Although SMO mutations have not been observed in pancreatic cancer, transgenic mouse models of pancreatic adenocarcinoma treated with SMO inhibitors showed decreased accumulation of fibroblasts and increased density of vasculature. This effect was accompanied by enhanced intracellular gemcitabine delivery and increased survival (Olive et al. 2009).

The tumor stroma produces high expression of glycoprotein SPARC (secreted protein acidic and rich in cysteine), which has albumin-binding properties. Since the nab-paclitaxel formulation is based on albumin protein, it was suggested that tumor-SPARC could facilitate drug penetrance into the tumor through its uptake mediated by SPARC proteins (Infante et al. 2007). Results from Phase-I and -II trials obtained from combining nab-paclitaxel plus gemcitabine suggested that SPARC expression was not correlated with patient response to gemcitabine alone or gemcitabine plus nab-paclitaxel treatment (Hidalgo et al. 2015). Mouse models of pancreatic adenocarcinoma were used to further investigate the function of SPARC in the nab-paclitaxel response. In these models, nab-paclitaxel accumulation in the tumor was not dependent on stromal-derived SPARC expression and a similar effect on tumor growth inhibition was observed between SPARC-null mice (in which SPARC was deleted) and SPARC-wild type mice (Neesse et al. 2014) (Hidalgo et al. 2015). These findings indicate that SPARC should not be used in clinical decision making as a predictive biomarker of nab-paclitaxel/gemcitabine response.

The extracellular matrix is enriched with glycosaminoglycans including hyaluronic acid, which has been found to be in excess in almost 87% of human pancreatic cancers

(Jacobetz et al. 2013) (Provenzano et al. 2012) Hyaluran degradation occurs via the action of hyaluronidase enzymes and its accumulation has been shown to be responsible for the poor drug perfusion into the tumor (Jacobetz et al. 2013). The combination of gemcitabine with hyaluronidase enzymatic agents has been evaluated to overcome this stromal barrier and has proved to be effective in KPC mouse models. In particular, mice showed increased survival and enhanced accumulation of gemcitabine into the tumor site due to a reduction of interstitial fluid pressure and a change in the stromal architecture of the tumor (Provenzano et al. 2012).

1.4 Gemcitabine: a deoxycytidine analogue

1.4.1 Clinical pharmacology of gemcitabine

Gemcitabine is administered intravenously, at a dose of 1,000-1,250 mg/m^2 once weekly on a 21-day cycle or day 1,8,15 on a 28-day cycle (Veltkamp et al. 2008). The standard infusion schedule is 1,000mg/m^2 for 30 minutes, which saturates plasma levels of dCK and induces less toxicity compared with higher infusions of gemcitabine (van Moorsel et al. 1997). Gemcitabine is rapidly deactivated through its deamination by cytidine deaminase (CDA) enzyme; in fact, its elimination half-life is between 10 and 30 minutes (Grunewald et al. 1990) (Veltkamp et al. 2008).

1.4.2 Gemcitabine metabolism and uptake

Gemcitabine (2',2'-Difluorodeoxycytidine) is a deoxycytidine analogue, whose structure is analogue of cytosine arabinoside (Ara-C), except for the two fluorine atoms on the 2 position of the sugar ring (Ewald et al. 2008). Being highly hydrophilic, gemcitabine requires intracellular uptake, in order to cross the lipophilic membrane, by specific enzymes called equilibrative (ENTs) and concentrative (CNTs) nucleoside transporters. There are two human equilibrative type (hENT1, hENT2) and three human concentrative type (hCNT1, hCNT2, hCNT3) transporters (Gesto et al. 2012). Previous evidence has demonstrated that gemcitabine uptake across the cell membrane is mainly mediated by hENT1 transporter (Ritzel et al. 2001).

Gemcitabine is a pro-drug, which needs to be transformed into its active drug metabolite by intracellular phosphorylation (Mini et al. 2006). Deoxycytidine kinase (dCK) converts gemcitabine into its corresponding dFd-5'-monophosphate (dFdCMP) form, the rate-limiting step for the production of the active metabolite. Previous studies have shown that dCK has higher affinity for gemcitabine than for Ara-C (Heinemann et al. 1998). dFdCMP is then phosphorylated again into its diphosphate and triphosphate metabolites (dFdCDP and dFDCTP) by pyrimidine monophosphate kinase and other as yet unknown enzymes (Heinemann et al. 1998) (Ohhashi et al. 2008). Gemcitabine triphosphate exerts its cytotoxic effect by inhibiting DNA duplication and ultimately gets inactivated by cytidine deaminase (CDA) into its deaminated metabolite 2', 2'-difluoro-2'-deoxyuridine (dFdU) (Heinemann et al. 1992) (Fig. 1.4).

1.4.3 Mechanisms of action of gemcitabine

Gemcitabine's main mechanism of action is inhibition of DNA synthesis: dFdCTP competes with dCTP (deoxycytidine triphosphate) for incorporation into DNA. After dFdCTP incorporation, the addition of only one more deoxynucleotide by DNA polymerase induces the termination of chain elongation (Huang et al. 1991). Furthermore, the incorporation of an extra single nucleotide prevents dFdCTP from being detected by DNA repair enzymes, thereby replication fork stalling and subsequent double strand breaks occur (Plunkett et al. 1995). dFdCTP can also be incorporated into the RNA strand, inhibiting RNA synthesis in specific cancer cell lines. Another important mechanism of action of the dFdCDP metabolite is inhibition of Ribonucleotide Reductase by covalent binding to RRM1 subunit (Heinemann et al. 1990). Ribonucleotide Reductase (RR) catalyses the production of deoxyribonucleotides (dNTP) required for the synthesis of new DNA, therefore its inhibition results in a decrease of dNTP pools that can be incorporated into the DNA strand (Mini et al. 2006).

Additional mechanisms of action of gemcitabine include induction of apoptosis through activation of caspase signalling or p38 signalling (Pourquier et al. 2002, Chandler et al. 2004) and enhancement of topoisomerase 1 (top1) cleavage

complexes. *In vitro* findings observed an increase in the frequency of collisions between top1 cleavage complexes and replication/transcription forks upon gemcitabine treatment, which caused DNA-strand breaks (Pourquier, Gioffre et al. 2002). Furthermore, topoisomerase 1 deficient cells developed resistance to gemcitabine, confirming top1 poisoning as an important mechanism of gemcitabine cytotoxicity (Pourquier et al. 2002).

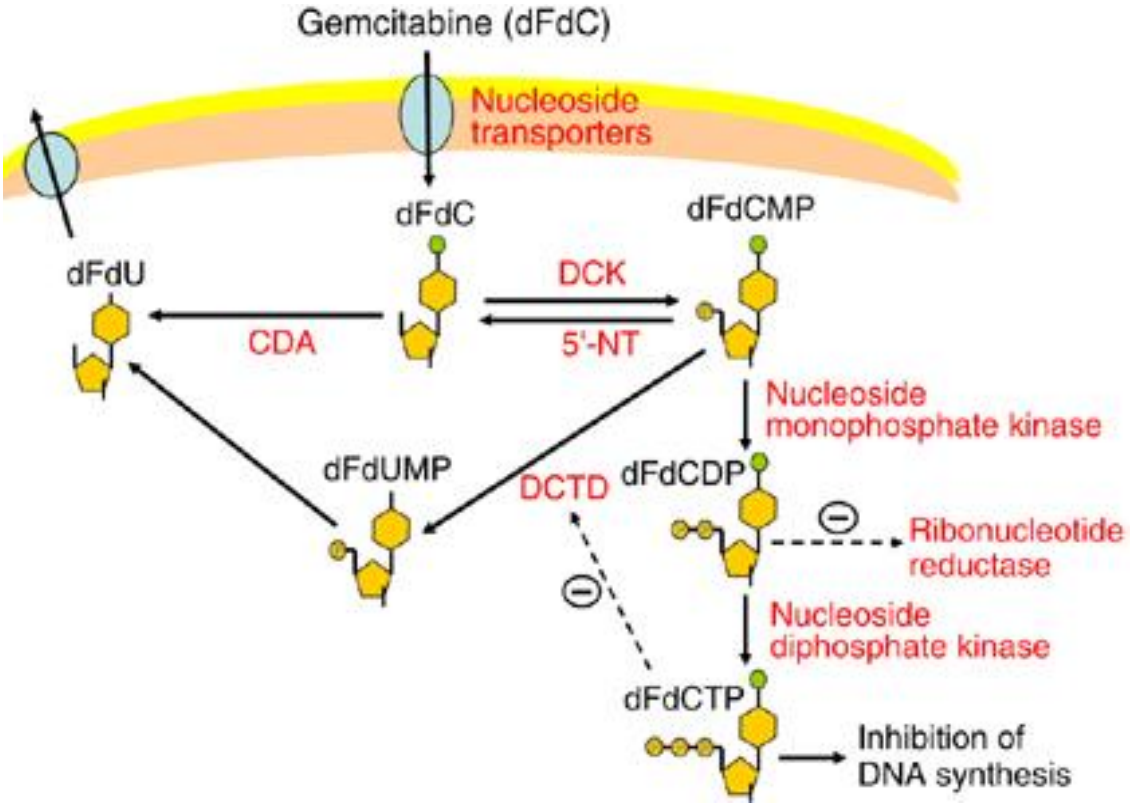

Figure 1.4: Gemcitabine metabolism and mechanisms of action.
Gemcitabine (dFdC) uptake inside the cells occurs through nucleoside transporters. Gemcitabine (dFdC) is phosphorylated into dFdCMP by DCK enzyme. Two additionaly phosphorylation steps occur to convert dFdCMP into dFdCTP molecule. The active form of gemcitabine (dFdCTP) binds and thus inhibits DNA synthesis. In addition, dFdCDP inhibits Ribonucleotide Reductase enzyme activity. Deactivation of gemcitabine (dFdC) into dFdU is mediated by CDA enzyme (Ueno et al. 2007).

1.4.4 Molecular markers associated with gemcitabine response

The main cause of gemcitabine-limited response in PDAC patients is resistance, which can be acquired by pancreatic cancer cells through various mechanisms after drug exposure or can be intrinsic. Acquisition of resistance to gemcitabine is a common event in PDAC patients (Kim et al. 2008). The most extensively studied molecular targets associated with gemcitabine response are shown in Table 1.2.

Molecular Markers associated with Gemcitabine Resistance
Human Equilibrative Nucleoside Transporter (hENT1): main gemcitabine transporter
Deoxycytidine Kinase (dCK) : activates gemcitabine by phosphorylation
Cytidine Deaminase (CDA): gemcitabine inactivating enzyme
Ribonucleotide Reductase (RR): responsible for conversion of ribonucleosides to deoxyribonucleosides triphospahte (dNTPs)

Table 1.2: List of genes associated with gemcitabine resistance.

1.4.4.1 Human Equilibrative Nucleoside Transporter (hENT1)

Human Equilibrative Nucleoside Transporter-1 (hENT1) mediates the active transport of gemcitabine and other pyrimidine nucleosides across the cell membrane, and if expressed at high levels, the amount of gemcitabine uptake inside the cell increases and so does its cytotoxic activity (Yao et al. 2011). A number of studies have suggested that hENT1 expression could be a useful marker in predicting PDAC patient response to gemcitabine therapy after surgical resection. For example, a randomized trial involving resected pancreatic cancer patients receiving adjuvant gemcitabine associated high hENT1 expression with increased survival (Farrell et al. 2009). A similar result was observed after a microarray analysis was performed on tissues from pancreatic cancer patients taking part of the ESPAC (European Study Group for Pancreatic Cancer) 3 trial, who received either 5-FU with folinic acid or gemcitabine. The results from this trial showed no significant difference in overall survival (OS)

between gemcitabine and 5-FU/folinic acid-treated patients. However, among patients treated with gemcitabine, an overall survival (OS) of 26.2 months was observed in patients with high expression of hENT1 compared to 17.1 months in patients with low expression of hENT1 (Greenhalf et al. 2014). Although these results were promising, another Phase-II trial showed no correlation between hENT1 expression and gemcitabine efficacy in metastatic PDAC patients (Poplin et al. 2013). However, the different findings observed among these studies could be associated with the fact that different antibodies were used to quantify hENT-1 expression (Svrcek et al. 2015). Contradictory results have also been found *in vitro*. In fact, overexpression of hENT1 was associated with increased gemcitabine sensitivity of a panel of different pancreatic cancer cells (Mori et al. 2007), whereas another study observed no correlation between the IC_{50} of gemcitabine and hENT1 expression of different pancreatic cancer cell lines (Nakano et al. 2007). These data indicate that there is not yet convincing evidence of the role of hENT1 as a prognostic biomarker of gemcitabine response in PDAC. Additional studies should be conducted before using hENT1 as a predictor of gemcitabine efficacy.

1.4.4.2 Deoxycytidine kinase (dCK)

Gemcitabine phosphorylation by deoxycytidine kinase (dCK), is the necessary step for further phosphorylation to active metabolites and to exert its cytotoxic activity (Heinemann et al. 1988). Overexpression of dCK has been associated with gemcitabine sensitivity in various cancer xenograft models (Kroep et al. 2002).

Immunohistochemical labeling of dCK on 44 tissues from pancreatic cancer patients showed a significant correlation between low/high dCK staining and OS or PFS following gemcitabine treatment. Interestingly, low levels of dCK immunolabeling were detected in older patients, which could in part explain the reason of lower survival rate at advanced age. The findings from this study indicate that immunohistochemical analysis of dCK before start of adjuvant therapy could help predict which patients are ideal candidates for gemcitabine treatment (Sebastiani et al. 2006).

A recent study in bladder cancer models showed that gemcitabine resistant cell lines had significantly low levels of dCK mRNA and protein expression. Additionally, downregulation of dCK expression with specific siRNA resulted in increased gemcitabine resistance in bladder cancer cell lines. In agreement, re-expression of dCK in these cell lines restored gemcitabine radiosensitivity (Kerr et al. 2014). Altogether these results support that dCK is an important predictive marker of gemcitabine efficacy.

1.4.4.3 Cytidine Deaminase (CDA)

Gemcitabine is mainly inactivated to dFdU (difluorodeoxyuridine) by the catabolic enzyme cytidine deaminase (CDA) (Wong et al. 2009). CDA expression has been associated with gemcitabine resistance. Patients with low levels CDA in the plasma, receiving gemcitabine-based combinations exhibited a higher toxicity profile compare to patients with high plasma CDA levels (Ciccolini et al. 2010).

Modulation of CDA expression has also been showed to alter gemcitabine cytotoxicity. This was observed in a pre-clinical study on KPC mouse models, which showed that addition of nab-paclitaxel to gemcitabine produced significant antitumor activity, an effect associated with reduction of CDA protein levels, which was caused by paclitaxel-induced production of reactive oxygen species (ROS) (Frese et al. 2012).

1.4.4.4 Ribonucleotide Reductase (RR)

Ribonucleotide Reductase (RR) controls the rate-limiting step of DNA replication, since uniquely this enzyme catalyses the conversion of ribonucleotide diphosphates into deoxyribonucleotide diphosphates required for new DNA synthesis and repair (Aye et al. 2015). In particular, the hydroxyl at the 2’ carbon of a ribonucleoside diphosphate (NDP) is reduced to a hydrogen to generate the corresponding deoxy (d)NDP. dNDPs are phosphorylated by nucleoside diphosphate kinase to produce dNTPs (Kunz and Kohalmi 1991). Mammalian RRs consist of two homodimers, each of them composed of two subunits: a large subunit RRM1 (90kda) and a small subunit RRM2 (45kda) (Fig. 1.5). When the large subunit associates with the small subunit an active

heterotetrameric enzyme is formed (Nordlund and Reichard 2006). RRM1 can also bind to a subunit analogue of RRM2, which is dependent of p53 activity (p53R2) (Tanaka et al. 2000) (Fig. 1.5). Upon DNA damage, p53R2 expression is induced and forms a complex with RRM1 to provide dNTPs for DNA repair. Additionally, p53R2 is involved in the synthesis of mitochondrial DNA (Tanaka et al. 2000). However, only wild type p53 cells exhibit activated p53R2; mutant P53 cells rely on RRM2 activity (Zhou et al. 2003).

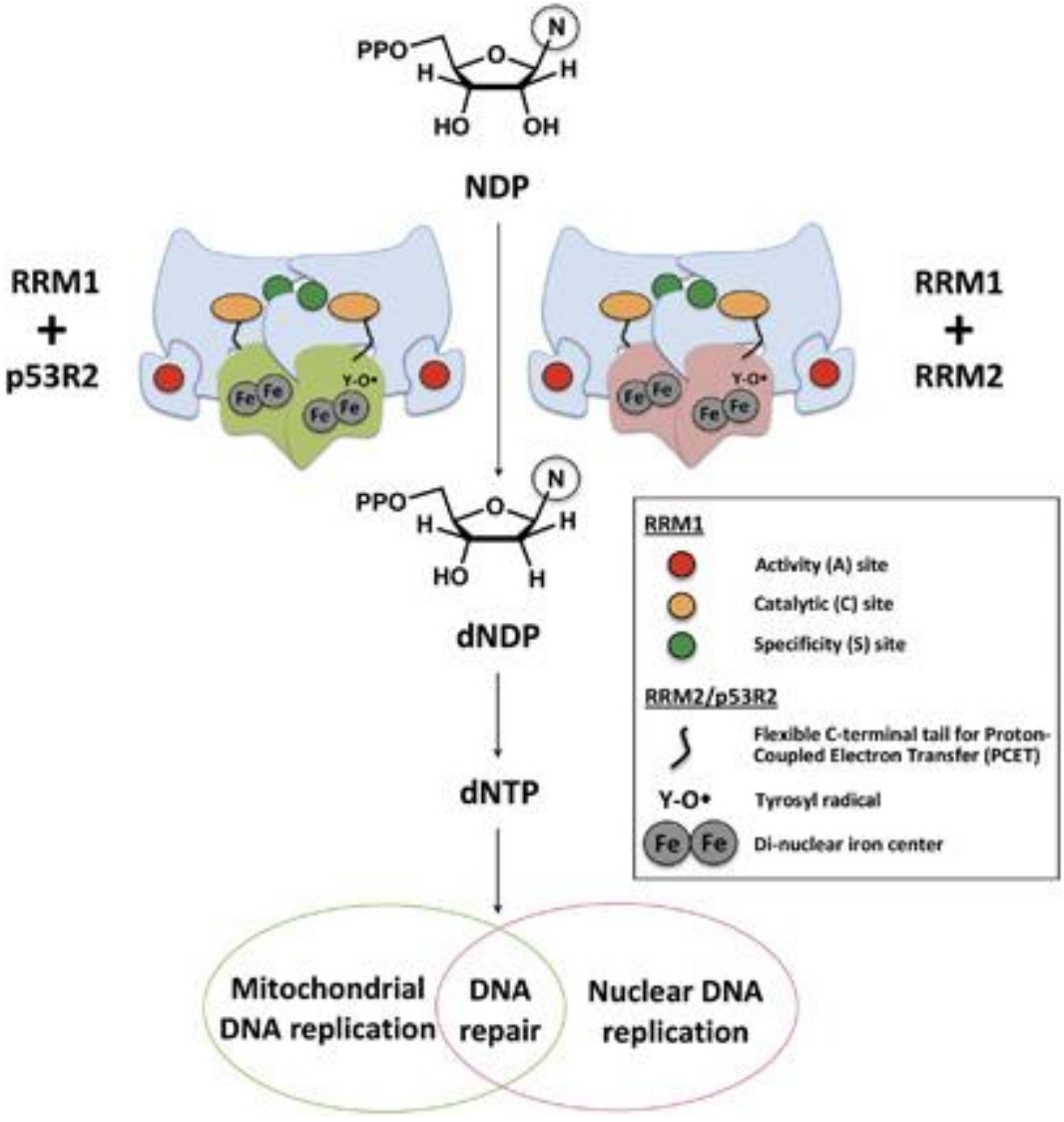

Figure 1.5: Structure of Ribonucleotide Reductase (RR).
The two subunits (RRM1 + RRM2 or RRM1 + p53R2) associate to form the active holoenzyme. RRM1 contains the catalytic site, RRM2 a tyrosil free radical next to a binuclear iron centre. RR catalyses the production of dNTP pools from the corresponding dNDP that are required for new DNA synthesis and repair. (Aye et al. 2015).

The RR enzyme ensures a proper balance of the four DNA nucleotides in order to maintain genomic integrity. Failure of this can lead to DNA strand breaks, enhanced mutagenesis or may induce cell death (Nordlund and Reichard 2006). RR activity is tightly regulated. The RRM1 subunit contains a catalytic site and two allosteric regulatory sites: the first allosteric site controls substrate specificity (S), the other regulates on/off enzyme activity (A). In particular, ATP binding stimulates RR activity, whereas dATP interaction induces feedback inhibition. Substrate specificity is regulated by the nucleotide effectors (ATP, dCTP, dATP, dTTP and dGTP) interaction with the allosteric site S (Nordlund and Reichard 2006). The catalytic domain is active only when RRM2 associates with RRM1. RRM2 subunit contains a tyrosyl free radical next to a binuclear iron centre necessary for the reduction of NDP to dNDP to occur (Reichard 1993) (Fairman et al. 2011) (Figure 1.5). The diferrous ions react with molecular oxygen to generate the protein radical (Aye et al. 2015).

The RR enzyme is also regulated by the cell cycle. Its activity reaches maximum levels during S-phase in order to produce the amount of dNTP pools required in proliferating cells for new DNA synthesis (Chabes and Thelander 2000). The levels of RRM1 protein are in excess and constant throughout the cell cycle because of its long half-life (20h) (D'Angiolella et al. 2012). In contrast, RRM2 protein levels, whose half-life is about 6h, are low in G1 and reach maximum peaks in S phase, as with the mRNA levels (Chabes and Thelander 2000). Cells in G0/G1 phase produce dNTP for DNA repair and for mitochondrial DNA (mtDNA) replication through the activity of the p53R2 subunit, which is constantly expressed at low levels in all phases of the cell cycle and its transcriptional expression is induced upon DNA damage in a P53-dependent way (Tanaka et al. 2000).

CHO cells transfected with cDNA encoding for a mutation in RRM1 activation site, which is resistant to dATP inhibition resulted in a 15-20 fold increase in the spontaneous rate of mutations, indicating the importance of RR activity (Caras and Martin 1988).

1.4.4.4.1 RRM1 overexpression is associated with poor response to gemcitabine in PDAC patients

The large regulatory subunit of Ribonucleotide Reductase (RRM1) is mainly expressed in the cytoplasm and predominantly expressed in cancerous tissues compared to adjacent normal tissues (Wang et al. 2013). From preclinical and clinical studies conflicting results have emerged regarding the biological role of RRM1 in cancer. Several lines of evidence suggest that RRM1 acts as a tumor suppressor gene. For example, RRM1 overexpression suppressed tumorigenicity and reduced metastatic burden in a mouse model of lung cancer (Fan et al. 1997, Gautam et al. 2003). Furthermore, high tumor-associated expression of RRM1 was associated with longer survival and later disease recurrence in NSCLC cancer patients who underwent surgery but did not receive any adjuvant chemotherapy (Bepler et al. 2004). Similar results were obtained from a study conducted on NSCLC patients who had undergone surgery. High RRM1 and ERCC1 (Excision repair cross-complementary gene 1) co-expression was associated with better disease-free survival (DFS) and OS (Zheng et al. 2007).

On the other hand, several findings have demonstrated that RRM1 is associated with gemcitabine resistance (Davidson et al. 2004) (Lee et al. 2010). One of the reasons for RRM1 overexpression being correlated with increased gemcitabine resistance is due to the expansion of dNTP pools that compete with dFDCTP for being incorporated into the DNA strand (Davidson et al. 2004). Additionally, dNTPs inhibit the activity of dCK enzyme, thereby preventing gemcitabine intracellular phosphorylation (Bouffard et al. 1993).

RRM1 overexpression in tumor patients has been associated with poor response to gemcitabine treatment. For example, a result from a clinical study showed that pancreatic cancer resected patients with high RRM1 expression had a better OS and DFS than those having low levels of RRM1 expression. However, among patients who received gemcitabine treatment after tumor recurrence, only those with low RRM1 expression benefited from gemcitabine therapy (Akita et al. 2009).

An oligonucleotide microarray analysis was conducted in gemcitabine resistant cells and parental cells to investigate any significant alterations in gene expression. A

significant upregulation of RRM1 mRNA and protein expression in the resistant cell lines was observed. Importantly, sensitivity to gemcitabine in these cell lines was restored upon RRM1 knock down with specific siRNA (Nakahira et al. 2007). Similar results obtained from RRM1 overexpressing mouse tumor cells, confirmed the ability of RRM1 downregulation (by siRNA) to potentiate chemosensitivity to gemcitabine (Wonganan et al. 2012). Additionally, efficient RRM1 downregulation obtained from systemic administration of RRM1 siRNA complexed with polyethilenimine was achieved in tumors of mice injected with the same RRM1 overexpressing tumor cell line. Importantly, knock down of RRM1 enhanced the antitumor activity of gemcitabine against RRM1 overexpressing tumor-bearing mice further indicating that RRM1 should be evaluated as a target to overcome gemcitabine resistance (Wonganan et al. 2012).

Finally, a clinical study on RRM1 expression was conducted on locally advanced NSCLC patients before they received gemcitabine treatment. A negative correlation between RRM1 gene expression and patient response to gemcitabine was observed, suggesting that RRM1 should be used as a predictive biomarker of gemcitabine therapy in patients with NSCLC (Bepler et al. 2006).

These present findings confirm RRM1 as a prognostic biomarker and modulator of gemcitabine response and suggest RRM1 expression should be evaluated in the design of tailored clinical trials to select patients who might benefit from gemcitabine treatment.

1.4.4.4.2 Ribonucleotide Reductase Inhibitors

RR enzyme has been long evaluated as a therapeutic target in cancer. Inhibitors of RR activity are classified into two main categories: Nucleoside analogues, such as gemcitabine, which bind to RRM1 and form a substrate radical that leads to enzyme inactivation (Chapman and Kinsella 2011). The other class of inhibitors is represented by redox active metal chelators, such as hydroxyurea, which target the di-iron centre of RRM2 subunit (Chapman and Kinsella 2011). Additionally, small interfering RNA (siRNA) strategies that target RR activity have been shown to be effective as a mechanism of chemosensitisation (Wonganan et al. 2012).

1.5 The RAS/RAF/MAPK signalling pathway

1.5.1 System biology of the RAS/RAF/MAPK pathway

Mitogen-activated protein kinases (MAPKs) are a family of protein kinases that phosphorylate specific tyrosine, serine or threonine on target proteins and regulate different and sometimes opposing cellular processes: proliferation, differentiation, invasion, apoptosis and gene expression (Johnson and Lapadat 2002). Mammalian cells have four well-characterised MAPK signalling cascades: 1) extracellular signal-regulated kinases (ERK1 and ERK2), 2) c-Jun amino-terminal kinases (JNKs) 1, 2, and 3, 3) p38 isoforms α, β, γ, and δ, 4) ERK5 groups. The JNK pathway regulates gene transcription, activation of p38 pathway is mediated by inflammatory cytokines or stress stimuli and the ERK pathway regulates cell proliferation among other functions (Johnson and Lapadat 2002).

The RAS-RAF-MEK-extracellular signal-regulated kinase (ERK) (Fig. 1.6) is responsible for the regulation of cell proliferation, differentiation and survival. It is one of the most studied signalling pathways because is often deregulated in human cancers such as PDAC (Xu et al. 2013). This pathway can be activated by different mitogenic stimuli such as growth factors (EGF and TGF-α) (Neuzillet et al. 2012). The binding of a ligand to the receptor leads to its dimerisation followed by autophosphorylation of tyrosine kinase residues. Next, activated receptor tyrosine kinase (RTK) binds adaptor proteins such as the Src homology 2 domain in Grb2 adaptor protein (growth factor-receptor-bound protein 2). The Src domain anchors the GTP exchange factor SOS (Son of sevenless). Grb2-SOS complex physically interacts with RAT sarcoma protein (RAS) molecules, favouring the formation of a RAS-GTP activated state (Downward 2003). Activated GTP-RAS recruits and activates RAF protein, which in turn phosphorylates MEK1/2, ultimately leading to the phosphorylation of the extracellular signal-regulated kinases (ERK1 and ERK2) (Roberts and Der 2007). ERK1/2 proteins can translocate to the nucleus, where they phosphorylate and regulate various transcription factors leading to changes in gene expression involved in the regulation of cell proliferation and survival (Mendoza et al. 2011).The degree of activity of the RAS-ERK signalling pathway depends on the strength and duration of the stimuli and

on other factors such as MAPK phosphatases and scaffold proteins (Neuzillet et al. 2013).

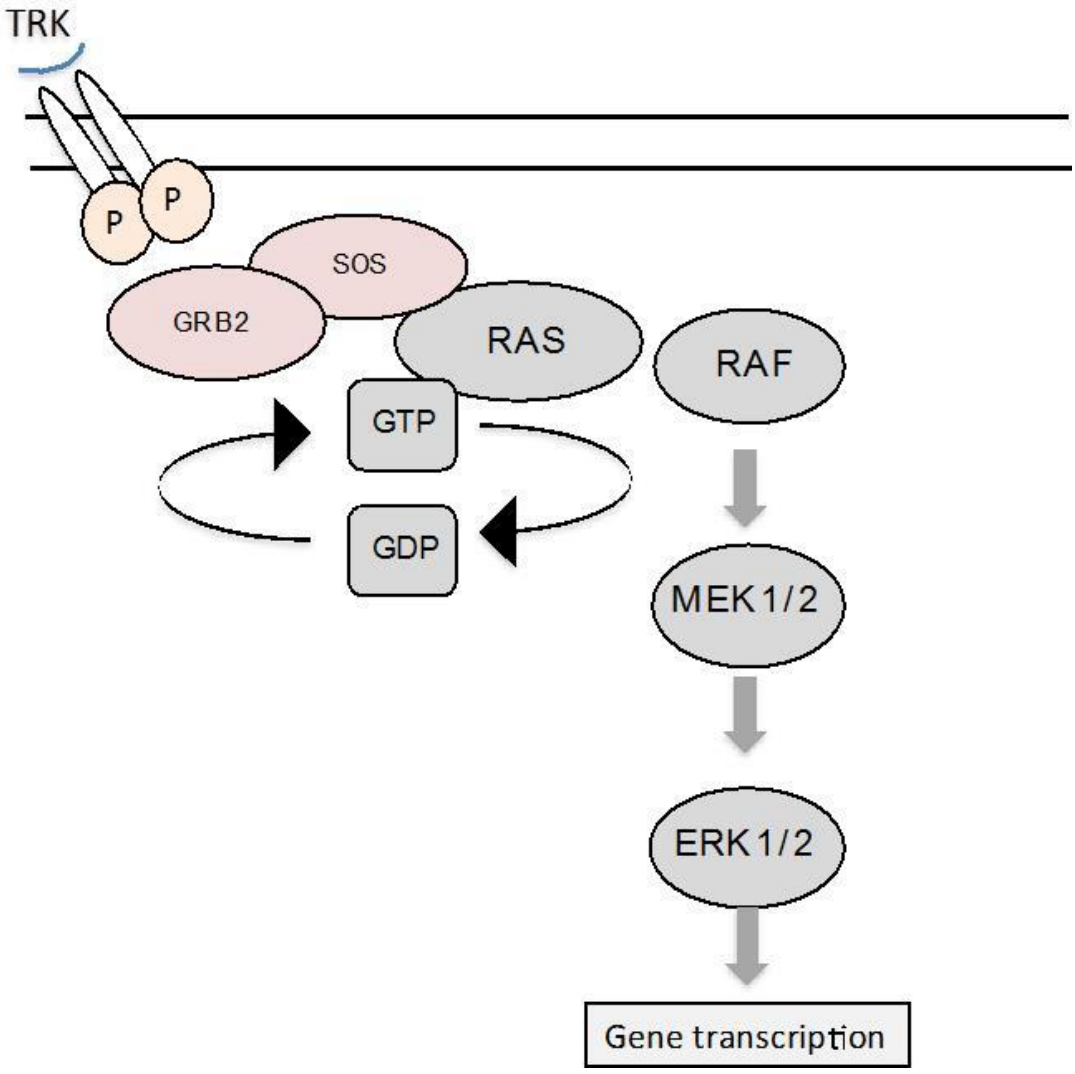

Figure 1.6: The MAPK signalling cascade.
Ligand binding to TRK receptors induces a conformational change that leads to GTP-RAS activation. RAS interacts with and activates RAF, which in turn activates MEK1/2. MEK phosphorylates and activate downstream ERK. Activated ERK enters into the nucleus and induces gene transcription involved in cellular proliferation, migration, and differentiation.

1.5.1.1 Epidermal growth factor receptor

EGFR is a 170kda transmembrane glycoprotein member of the receptor tyrosine kinase (RTK) superfamily, which consists of four members: EGFR or ErbB1 (HER1), ErbB2 (HER2), ErbB3 (HER3) and ErbB4 (HER4) (Yarden 2001). RTKs are characterised by an extracellular ligand-binding region, a single membrane spanning region and a regulatory intracellular region containing the kinase domain (KD). The intracellular region contains the juxtamembrane domain, the N and C lobes that incorporate the Adenosine Triphosphate (ATP) binding site and the carboxyl tail. Furthermore, EGFR, ErbB2 and ErbB4 but not ErbB3 possess an active tyrosine kinase domain in the C-terminal region (Yarden 2001). There are four extracellular domains (I-IV). Domains I and III are responsible for ligand binding, domains II and IV are essential for receptor dimerisation. Monomeric EGFR is in an auto inhibitory tethered conformation in which the dimerization arm is not exposed (domain II). Upon ligand binding to domain I and III, the receptor changes conformation which allows its dimerization and activation. Both the juxtamembrane and the c-terminal domain play a role in the auto-inhibition mechanism as they physically block the ATP binding pocket. (Lemmon 2009).

EGFR can be activated by various ligands including Epidermal Growth Factor (EGF), Transforming Growth Factor-α (TGF-α) and amphiregulin (Normanno et al. 2006). EGFR can form homodimers followed by ligand binding and transmit signal autonomously or form heterodimers. EGFR dimerisation occurs via an asymmetric mechanism of interaction between the C-lobe of one monomer and the N-lobe of another monomer. The activated kinase can then phosphorylate tyrosine residues on the receiver monomer which switch their position and activate each other (Jura et al. 2009). The phosphorylation of the intracellular tyrosine residues leads to recruitment of Src-Homology (SH2) and Phospho-tyrosine Binding (PTB) domains leading to the activation of downstream signalling pathways (Burgess et al. 2003).

EGFR was the first tyrosine kinase receptor to be associated with human cancers (Hynes and Lane 2005). Aberrant activation of EGFR in cancer leads to a range of cellular responses including cell hyper-proliferation, motility and EMT transition and it can occur through both ligand-dependent and independent mechanisms. The first consists of autocrine production of ligands in EGFR overexpressing tumors. The second

includes receptor overexpression via gene amplification, acquisition of somatic mutations and escape from endocytotic degradation (Gschwind et al. 2001).

1.5.1.2 RAS and RAF kinases

RAS, one of the first oncogenes to be discovered, mediates transmission of signals from the cell surface into the nucleus through interaction with many downstream signaling pathways (Goodsell 1999). The family of RAS proteins include Harvey-RAS (HRAS), Kirsten-RAS (KRAS), and N-RAS (Goodsell 1999). RAS proteins do not possess transmembrane domains but are attached to the inner side of the plasma membrane through farnesyl groups. RAS are small GTP binding proteins that function as binary molecular switches. In its inactive state RAS is bound to a guanosine di phosphate (GDP). Guanine nucleotide exchange factors (SoS) regulate the GDP/GTP switch that promotes formation of active RAS-GTP (Roberts and Der 2007). RAS binding to GTPase-activating proteins mediates GTP hydrolysis to guanosine diphosphate (GDP), a mechanism that allows RAS to return into its neutral state (Goodsell 1999).

After RAS activation the effector loop domain of RAS physically interacts with several downstream targets including RAF. RAF proteins are a family of serine/threonine kinases and consist of A-RAF, B-RAF and C-RAF (Lavoie and Therrien 2015). RAF is recruited to the plasma membrane by GTP-RAS through interaction with the RAS binding domain (RBD). RAS binding to RAF leads to RAF dimerization and its catalytic activation (Lavoie and Therrien 2015). RAF phosphorylates downstream MEK1 and MEK2 on two distinct serine residues in their activation loop. MEK activation is usually induced by B-RAF and to less extent by C-RAF or A-RAF (Anderson et al. 1990).

K-RAS mutations represent the most frequent and earliest oncogenic event to occur in PDAC. Activating mutations within the K-RAS gene makes RAS insensitive to GAP protein, which remains constantly in its switched on state. They are generally point-activating mutations, most of which occur at codon 12, by substitution of glycine with aspartic acid, valine or arginine (Thomas et al. 2007).

B-RAF is frequently mutated in melanoma, which results in the hyperactivity of the MAPK pathway; however B-RAF mutation is a rare event in PDAC (Ishimura et al. 2003).

1.5.1.3 Mitogen extracellular signal regulated kinase (MEK or MAPKK) protein

MEK or MAPKKs are a family of proteins that belong to the RAS/RAF/MEK/ERK signalling cascade. MEK proteins are dual-specificity kinases with a molecular weight between 44-46 kDA. Seven MEK proteins have been identified and are involved in four different MAPK signalling pathways but only MEK1 and MEK2 (Fig. 1.6) belong to the RAS-RAF-ERK signalling pathway (Dhanasekaran and Premkumar Reddy 1998). MEK1 and MEK2 share an 80% amino acid identity and are expressed ubiquitously in all mammalians cells. MEK1 is encoded by the gene located on chromosome 15q22.31, MEK2 is encoded by the gene located on chromosome 19p13.3 (Chang and Karin 2001). The structure of MEK protein consists of an amino- terminal domain, a kinase domain, and a carboxyl-terminal domain. The kinase domain represents the catalytic domain, is made of 290 residues and contains the ATP binding site. The carboxyl-terminal sequence contains the domain for versatile docking (DVD), which is made of about 20 aminoacids and represents the binding site of upstream components of the RAS pathway. The N-terminal domain consists of about 70 aminoacids and contains a docking site for interaction with ERK, an inhibitory/allosteric segment and a nuclear export sequence (Roskoski 2012) (Akinleye et al. 2013). The structural difference between MEK1 and MEK2 is represented by the presence of a phosphorylation site (T292) in the proline-rich region in the C-terminus of MEK1 required for the negative regulation of MEK by ERK1/2(Catalanotti et al. 2009) . Activation of MEK1 and MEK2 by upstream serine kinase RAF occurs through phosphorylation of two serine residues at positions 218 and 222 in the catalytic domain. MEK phosphorylates the serine/threonine and tyrosine residues in the activation loop of the downstream ERK substrate (Ohren et al. 2004). The high specificity of MEK is due to the fact ERK represents the only known physiological target and this selectivity renders MEK proteins an attractive target for therapy (Neuzillet et al. 2012).

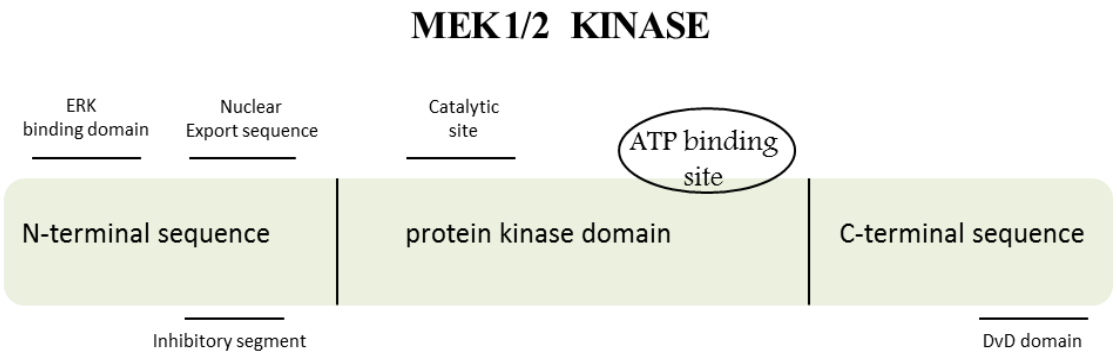

Figure 1.7: The structure of MEK1/2 protein.
MEK proteins possess an N-terminal sequence, a C-terminal sequence and a kinase domain, which contains the catalytic site. Adapted from (Akinleye et al. 2013).

1.5.1.4 ERK kinases

Extracellular signal-regulated kinases ERK1 (44 kDA) and ERK2 (42 kDA) are serine/threonine kinases that show a 70% amino acid similarity. ERK represents the only substrate of MEK and is activated by dual phosphorylation on their tyrosine and threonine residues (Downward 2003). Unlike MEK or RAF protein, ERK has a variety of cytosolic or nuclear substrates. Once activated, ERK dissociates from MEK, and translocate into the cytoplasm or nucleus, where it phosphorylates a large number of proteins such as transcription factors, cytoskeletal proteins and kinases. Elk1, p53 and c-fos are some of the nuclear transcription factors that regulate cell proliferation, survival, as well as angiogenesis and migration, which are activated by ERK (Yoon and Seger 2006). ERK activation promotes cell cycle progression by activating cyclin D1, c-Myc and retinoblastoma protein (Rb). Furthermore, ERK signalling inhibits the activation of pro-apoptotic proteins (Bim and Bad) and stimulates anti-apoptotic members (Bcl-2, Blc-x) (Neuzillet et al. 2014). ERK controls many signalling pathways and gene regulatory circuits. Thus, ERK signalling affects a wide variety of cellular events that include proliferation, differentiation, invasion and survival (Yoon and Seger 2006).

ERKs are inactivated through the removal of phosphatases from the threonine and tyrosine residues generally mediated by MAPK phosphatases (Sun et al. 1993). Additionally, ERK participates in feedback loop mechanisms that inhibit its activity, such as inhibition of upstream RAF or MEK (Slack-Davis et al. 2003).

1.5.2 MEK as a therapeutic target

The RAS/RAF/MEK/ERK signalling pathway is frequently dysregulated in human cancers (Chang and Karin 2001). K-RAS mutation, occurring in 90% of all human PDACs, has a predominant role in the initiation, progression and maintenance of PDAC (di Magliano and Logsdon 2013). Unfortunately the *RAS* oncogene has so far proved to be undruggable (Berndt et al. 2011). For this reason drug development has shifted its focus towards distinct downstream effectors components of oncogenic K-RAS signalling, such as RAF or MEK (McCubrey et al. 2010).

1.5.2.1 The development of MEK inhibitors

MAPKK or MEK belongs to a family of enzymes upstream MAPK or ERK protein. Several MEK inhibitors have been developed as potential therapeutic candidates in human cancer treatments, some of which are under current investigation in preclinical and clinical studies (McCubrey et al. 2010) (Zhao and Adjei 2014), while others have already been proved to give survival benefits in the clinical setting (Flaherty et al. 2012).

The exquisite characteristic of MEK inhibitors is represented by the fact the most of them do not compete with the ATP binding site, but bind to an allosteric pocket adjacent to it; this prevents any undesired side effects caused by inhibition of other protein kinases (Ohren et al. 2004). Additionally, MEK inhibitors are highly selective since the only target of MEK is represented by ERK (Akinleye et al. 2013) (Zhao and Adjei 2014). The binding of a MEK inhibitor to a unique allosteric site induces a conformational change within the activation loop and a deformation of the catalytic site that prevents MEK from interacting with ERK (Sebolt-Leopold and Herrera 2004).

U0126 and PD98059 were the first MEK inhibitors to be developed but because of the poor pharmacological characteristics they did not reach clinical development (McCubrey et al. 2010) (Montagut and Settleman 2009). CI-1040 was the first MEK1/2 inhibitor to be tested in clinical trials after preclinical studies showed its ability to significantly reduce tumor growth in colon cancer and melanoma xenograft models (Sebolt-Leopold et al. 1999) (Collisson et al. 2003). A Phase I study indicated that CI-

1040 was well tolerated by patients and induced antitumoral activity in humans (Lorusso et al. 2005); However, a phase-II study testing CI-1040 on colorectal cancer (CRC), NSCLC, pancreatic and breast cancer patients showed insufficient antitumor activity to advance further development (Rinehart et al. 2004).

A second-generation of inhibitors (such as PD0325901) characterised by better bioavailability and higher potency compared to CI-1040, was later developed (Barrett et al. 2008). Unfortunately, a phase-II study conducted in NSCLC patients who had already received systemic therapy showed no objective responses after treatment with PD0325901 (Haura et al. 2010).

Selumetinib (AZD6244) is a potent MEK1/2 inhibitor that has been tested in several Phase-II trials in different human cancers. For example, selumetinib was given in combination with capecitabine in PDAC patients who did not benefit from gemcitabine therapy. However, no significant improvement in OS was detected (Bodoky et al. 2012). Furthermore, a Phase-II study tested the selumetinib plus dacarbazine combination in BRAF-mutant melanoma patients, but no significant overall survival benefit was observed in these patients compared to patients treated with dacarbazine monotherapy (13.9 months in the selumetinib plus dacarbazine group versus 10.5 months in dacarbazine group; HR 0.93, 80% CI, 0.67-1.28, one-sided $P<0.39$) (Robert et al. 2013). Several other Phase-I, -II and -III trials involving selumetinib are currently underway.

Trametenib is a potent, selective and ATP non-competitive inhibitor of MEK1 and MEK2 activity, which prevents RAF-induced phosphorylation of MEK1, therefore prolonging its effect on ERK1/2 inhibition (Gilmartin et al. 2011). Trametenib has been recently approved for the treatment of unresectable or metastastic B-RAF mutant melanoma after a successful trial showed significant survival benefit for patients treated with single-agent trametenib (Flaherty et al. 2012). Its efficacy has also been evaluated in combination with gemcitabine in metastatic PDAC patients but has shown no improvement in OS and PFS compared to gemcitabine monotherapy (Infante et al. 2014).

1.5.2.2 Pimasertib

Pimasertib, also known as MSC1936369B or AS703026, is a potent, highly selective and orally available small molecule inhibitor of MEK1 and MEK2 protein and belongs to the second-generation class of ATP non-competitive MEK inhibitors. Pimasertib binds to an allosteric site adjacent to the ATP binding site, blocking MEK into an inactive conformation, which prevents it from interacting with and activating downstream ERK (Yoon et al. 2011).

Previous preclinical studies involving pimasertib on PDAC models have not been reported. Nevertheless, the *in vitro* and *in vivo* antitumor activity of pimasertib has been evaluated in other human cancers with aberrantly activated MAPK pathway. The antitumor activity of pimasertib has been evaluated in a preclinical study of multiple myeloma (MM), a disease often characterised by deregulated MAPK signalling pathway (Kim et al. 2010). In this study, pimasertib treatment significantly inhibited growth and induced apoptosis of MM cell lines, patients-derived MM cells and in MM xenograft models; an effect that was not correlated with the B-RAF or K-RAS mutational status of the cells. Immunoblotting analysis showed a significant decrease of P-ERK and increase of P-AKT protein levels up to 72 hours treatment with pimasertib. This was accompanied by a decrease in MAF oncogene expression and a reduction in osteoclastogenesis, suggesting that MEK activity modulates the bone marrow (BM) microenvironment. Moreover, pimasertib enhanced the cytotoxic effect of conventional anti-MM chemotherapies, suggesting that the MEK inhibitors activity should be tested in clinical trials for MM patients alone or in combination with chemotherapy (Kim et al. 2010).

Colorectal cancer (CRC) is frequently characterised by abnormal expression of EGFR. Monoclonal antibodies targeting EGFR (cetuximab, panitumumab) represent treatment options currently in use for metastatic CRC. However, EGFR inhibition benefits only K-RAS wild-type (WT) CRC patients (Di Fiore et al. 2007). The activity of pimasertib on both WT and mutant K-RAS CRC cell lines was examined. As opposed to cetuximab, which induced antiproliferative effects and inhibited EGFR signalling exclusively in WT cells, pimasertib effectively abrogated P-ERK activation and inhibited proliferation in all cell lines tested regardless their K-RAS mutational status (Yoon et al.

2011). Furthermore, pimasertib induced antitumor activity in mutant K-RAS xenograft models of CRC along with a marked decrease of P-ERK expression, in contrast to cetuximab. However, no synergistic effects were observed when pimasertib was combined with cetuximab both *in vitro* and *in vivo* (Yoon et al. 2011).

Another study examined the combination effects between pimasertib and PI3K/mTOR inhibitor in human colon and lung cancer cell lines. Synergistic antiproliferative and apoptotic effects along with sustained blockade of MAPK and PI3K signalling pathways were observed in the combination regimen compared to single agents (Martinelli et al. 2013). Response to pimasertib was not associated with the mutational status of *RAF*, *RAS* or *PI3KCA* genes. Furthermore, the combination of a dual PI3K/mTOR inhibitor (BEZ235) with pimasertib significantly delayed tumor growth in lung carcinoma and CRC xenografts, suggesting that dual inhibition of these pathways could potentiate the efficacy of MEK inhibitors alone (Martinelli et al. 2013).

Finally, pimasertib by inducing a G1 arrest of the cell cycle, enhanced apoptosis caused by BH3 mimetics in AML cell lines and xenograft models suggesting that this combination should be evaluated for future clinical trials of AML patients (Airiau et al. 2015).

Phase-I and II trials testing pimasertib have been conducted and have shown clinical activity both alone and in combination with targeted therapies or chemotherapies. (Delord, J. *et al*. 2010). A clinical trial of pimasertib in combination with FOLFIRI (5-FU, irinotecan, leucovorin) was assessed in mutant KRAS colorectal cancer patients. The maximum tolerated dose (MTD) of pimasertib (45mg per day) was well tolerated by patients. However, the study was unable to progress to Phase-II because of the toxicity induced by dose escalation of pimasertib from 45 to 60mg combined to FOLFIRI (Macarulla et al. 2015).

A Phase-I/II trial involving gemcitabine in combination with pimasertib in metastatic pancreatic adenocarcinoma patients was assessed. Firstly, a Phase-I dose escalation safety run established the maximum tolerated dose of pimasertib (Cutsem EV et al. 2015). The patients participating in this trial were divided in two arms:

- Arm (A): Patients receiving pimasertib 60mg with gemcitabine 1000mg/m^2 simultaneously.
- Arm (B): Patients receiving placebo with weekly gemcitabine 1000mg/m^2.

The primary endpoint of the study was progression free survival (PFS). This trial, which has been recently concluded, showed a median PFS of 3.7 months for arm (A) versus 2.8 months for arm (B) (hazard ratio of 0.883, 95% CI: 0.549–1.42; p=0.608). The OS of arm A and B was 7.3 months versus 8.3 months respectively. Unfortunately the results did not show a clinically significant improvement in PFS and OS, with higher adverse events observed more frequently in patients treated with the combination of pimasertib with gemcitabine (Cutsem EV et al. 2015). This trial was conducted in parallel with our *in vitro* and *in vivo* work on pancreatic cancer models, which demonstrated the importance of administering a sequential combination of pimasertib followed by gemcitabine in order to achieve significant antitumor activity (Chapter 3 and Chapter 5 will explain these findings in detail).

1.5.2.3 Mechanisms of resistance to MEK inhibitors

Despite promising results in preclinical models with MEK inhibitors, several factors cause their limited clinical activity and contribute to the resistance to MEK inhibitors (Zhao and Adjei 2014) .

First, inhibition of ERK blocks negative feedback loops that regulate RAS or RAF signalling, thus enabling stronger reactivation of MEK or other downstream antiapoptotic pathways (Sale and Cook 2014) (Brummer et al. 2003). In agreement with this hypothesis, mutant B-RAF tumors are particularly sensitive to MEK inhibition, since this negative feedback mechanism between ERK and RAF proteins is weak or in some cases non-functional (Friday et al. 2008). Another mechanism of intrinsic

resistance to MEK inhibitors is the EGFR dependent reactivation of parallel signalling pathways such as PI3K/AKT that has been observed in PDAC (Mirzoeva et al. 2013).

Second, oncogenic K-RAS activates multiple effector pathways, thus activation of alternative signalling cascades could rescue cancer cells from the anti-proliferative effects induced by MEK inhibition (Turke et al. 2012) (Steelman et al. 2008).

Third, there are no biomarkers that could predict patients' response to MEK inhibitors and enable patient stratification for personalised treatment (Zhao and Adjei 2014).

Fourth, MEK inhibitors usually exert a cytostatic response, which limits their efficacy and this is one of the reasons why MEK inhibitors are often administered in combination with other cytotoxic agents (McCubrey et al. 2010).

Fifth, the tumor microenvironment has shown to play an important role in the development of resistance to MEK inhibitors. In particular, a recent study reported that MEK inhibitor treatment increased the number of macrophages within the tumor of B-RAF mutant melanoma models, accompanied by a significant increase of TNFα expression (Smith et al. 2014). The increase in macrophages observed was correlated with inhibition of MEK inhibitor-induced apoptosis through TNFα-dependent mechanism. Therefore these results suggest that targeting components of the tumor microenvironment could represent a possible therapeutic strategy to enhance MEK inhibitors sensitivity (Smith et al. 2014).

Novel MEK inhibitor-based combination therapies should be explored to overcome the development of acquired resistance.

1.6 AIMS AND OBJECTIVES

The aim of this thesis is to investigate the biological effects of a novel allosteric MEK1/2 inhibitor (pimasertib) and its ability to enhance gemcitabine cytotoxicity in pancreatic cancer models. Although some gemcitabine-based combinations and novel chemotherapy regimens have shown increased survival benefit compared to gemcitabine monotherapy in PDAC, the survival benefit conferred by these novel treatment options is still limited and there is an urgent need to investigate new therapeutic strategies. The use of MEK inhibitors is a clear rational strategy to sensitise tumours characterised by aberrant activation of RAS effector pathways.

The following objectives will be addressed:

1. **Chapter Three**: aims to investigate the effects of gemcitabine in combination with the MEK1/2 inhibitor pimasertib on human pancreatic cancer cells proliferation, apoptosis and on the regulation of signalling pathways.

2. **Chapter Four**: examines the effects of pimasertib on the modulation of genes involved in gemcitabine metabolism and mechanism of action and the molecular mechanisms by which pimasertib sensitize human pancreatic cancer cells to gemcitabine treatment.

3. **Chapter Five:** investigates the effects of pimasertib plus gemcitabine combination in a syngeneic orthotopic model of pancreatic cancer.

CHAPTER 2

MATERIALS AND METHODS

2.1 MATERIALS

2.1.1 Human and mouse pancreatic cancer cell lines and culture conditions

Human pancreatic cancer cell lines MIAPaCa-2, PANC-1, BxPC-3 and SUIT-2 were purchased from ATCC (American type culture collection), USA.

PANC-1 and MIAPaCa-2 cells were grown in DMEM supplemented with 10% fetal bovine serum, 1% of 200Mm L-Glutamine, 1% of 10,000 units Penicillin-10mg/ml Streptomycin (Sigma-Aldrich, UK). BxPC-3 and SUIT-2 cells were cultured in RPMI-1640 with 10% fetal bovine serum, 1% of 200mM L-Glutamine, 1% of 10,000 units Penicillin-10mg/ml Streptomycin (Sigma-Aldrich, UK). All cell lines were regularly tested for mycoplasma contamination.

TB32048, a pancreatic cancer cell line syngeneic for C57BL/6 mice was derived from the KPC genetic pancreatic cancer mouse model (LSL-KRASG12D/+ LSLTrp53R172H/+Pdx1-Cre) and was kindly provided by Dr. David Tuveson (Cold Spring Harbor, USA). TB32048 cells were grown in DMEM supplemented with 10% fetal bovine serum, 1% of 200Mm L-Glutamine, 1% of 10,000 units Penicillin-10mg/ml Streptomycin (Sigma-Aldrich, UK).

2.1.2 Chemotherapies, MEK inhibitors and other reagents

The MEK1/2 inhibitors AS703026 (pimasertib) and AS703988 were provided by EMD Serono (Billerica, MA, USA). Gemcitabine was provided as a 38mg/ml solution from the pharmacy department of McMillan Cancer Centre (London, UK).

Pimasertib was dissolved in dymethyl sulfoxide (DMSO) to produce a 10mM stock solution and stored at -20°. Gemcitabine was kept at room temperature and used within one month from the opening date.

Gefitinib (Iressa, ZD 1839) was obtained from the London Oncology Clinic (LOC, London), dissolved in DMSO to produce a 10mM stock solution and stored at -20°. The PI3K inhibitor, GDC0942 was purchased from Stratech Scientific Ltd, dissolved in DMSO to make a 10mM stock solution and stored at -20.

MG132, a specific proteasome inhibitor, was purchased from Sigma Aldrich and prepared as a 1mM stock in DMSO, and stored at -20°C until use.

2.2 Methods

2.2.1. Cell Line maintenance

Cells were cultured in 10 or 15cm^2 tissue culture dishes (Thermo scientific) at 37°C in a humidified atmosphere of 5% CO_2 and procedures were carried out in sterile conditions in Class II biological safety cabinets. Cells were routinely passaged by removing the medium and by gently washing once with sterile PBS. Following PBS removal, cells were detached by incubation with 2-5mL of Trypsin-EDTA (volume of trypsin was adjusted to the dimension of the cell culture dish) for 3-5min at 37°C. After detachment, complete medium was added to the cells in order to stop the action of the trypsin (volume of medium was equal to the amount of trypsin used). Cells were then collected and centrifuged at 1000rpm for 5min. The resulting cell pellets were resuspended in fresh medium before reseeding into new culture dishes at a ratio of 1/3 to 1/5 according to the cell line. Cells were passaged for a maximum of two months before being discarded and fresh cultures set-up.

2.2.1.1 Storage and retrieval from liquid nitrogen

Cells were frozen in liquid nitrogen for long-term storage. Cells were plated in 10cm tissue cultured dishes (Corning) and while exponentially growing, were trypsinised and collected by centrifugation as described in the previous section. The cell pellets were then resuspended in 1mL of freezing media [(media supplemented with 20% FBS and 10% dimethylsulphoxide (DMSO) (Sigma-Aldrich)] per culture dish, aliquoted in cryotubes (Thermo scientific) and stored at -80°C for 24-72h prior long-term storage in liquid nitrogen tanks. In order to resuscitate cells from frozen stocks, cryotubes were rapidly warmed-up in a 37°C water bath, after which cells were supplemented with 5mL of fresh medium and centrifuged for 5min at 1000rpm to remove the residual

DMSO. The resulting pellet was then gently suspended in 10mL of fresh media and cells were seeded in a 10cm tissue culture dishes and incubated at 37°C.

2.2.1.2 Cell count

Cells were counted, once resuspended in 10ml of complete growth medium, using a hemocytometer. A hemocytometer has two chambers and each chamber has a microscopic grid etched on the glass surface (4 squares each containing 16 smaller squares all connected by a 25 square grid). The chambers are overlaid with a glass coverslip that rests on pillars exactly 0.1mm above the chamber floor. 15µl of this dilution was loaded into one chamber. The number of cells present in the original solution was determined by counting the number of cells within the 4 large squares. The obtained numbered was then divided by 4 (number of squares) and then multiplied by 2 (dilution 1:2). The total number of cells obtained was multiplied by $1X10^4$, giving the number of cells per ml of suspension.

2.2.2 Assessing growth inhibition

2.2.2.1 Drug scheduling

Cells were diluted 2.5 X 10^4/ml (BxPC-3, MIAPaCa-2 and SUIT-2) or 2.0 X 10^4/ml (PANC-1) and plated in 96 well plates. The following day cells were continuously exposed to increasing concentrations of each drug alone for 96h to determine the cells sensitivity to each drug, their IC50s and to select cell lines with most sensitivity and resistance to gemcitabine. IC50s are defined as the concentrations of drug that result in 50% cell survival compared with untreated cells. Drug combination experiments were carried out by using a fixed dose of pimasertib and increasing doses of gemcitabine. Different drug combination schedules were assessed:

- Gemcitabine and pimasertib were given simultaneously and continuously for 48h.
- Pimasertib was given 4h before gemcitabine for a total of 48h treatment.
- Pimasertib was given 4h before gemcitabine for a total of 24h treatment.

2.2.2.2 MTT assay

A common methodology used to analyse cell viability is the clonogenic assay, which measures the ability of a single cell to proliferate indefinitely, thus to produce a large colony. The clonogenic assay is routinely used to look at the survival effects after exposure to radiation.

Because of the long duration of the experiment, a preferable method used to study chemosensitivity of tumor cells and to perform novel drugs screening is the low-cost MTT (methylthiazolyldiphenyl-tetrazolium bromide) assay, which measures cell viability in an accurate and less time-consuming way. The MTT assay is based on the capacity of viable cells with active mitochondria to reduce the yellow soluble tetrazolium salt (MTT) to form a blue formazan precipitate, a reaction catalysed by dehydrogenase enzymes. It is semi-automated since it can be performed in a 96-well plate and the production of formazan (blue precipitate) can be analysed by a spectrophotometer.

The ability of gemcitabine, pimasertib or their combination to inhibit cell proliferation was measured using this assay. Experiments were conducted in flat-bottom 96-well plates (Corning). 200μL of 2.0-2.5x10^4 cells/mL were plated in each well and left to adhere overnight in full serum medium. Cells were exposed to increasing concentrations of gemcitabine, pimasertib or their combination according to the schedules previously described. Drug dilutions were prepared in complete culture media and 200μL of drug-containing media was added to each well. For every concentration used, four technical repeats were performed and untreated control samples were incubated with complete media supplemented with vehicle DMSO for DMSO-diluted drugs. Following 96h or 48h drug exposure, 20μL of a MTT (5mg/mL)-PBS solution were added to each well and plates were left in the incubator for a further 4h. At the end of the incubation, the cell culture media was removed by gentle aspiration and the formazan crystals were resuspended in 200μL of DMSO. The quantity of formazan, which is directly proportional to the number of viable cells, is measured by recording changes in absorbance at 540nm on a Varioskan Flash Multimode Reader (Thermo Scientific). Percentage proliferation was calculated by averaging the absorbance values obtained from each of the technical repeats and by

normalising the values of drug treated samples to the absorbance values obtained from the untreated control samples (% proliferation= OD of treated/OD of untreated *100).

2.2.2.3 Calcusyn Software analysis

The fraction affected (Fa) obtained from the single drug treatments or from the combination assays were used for the calculation of the combination indices (CI), which describe drug interactions. The Calcusyn Software (Biosoft), based upon the Chou– Talalay method was used for determining CI values, according to a non-fixed ratio design (Bijnsdorp et al. 2011). The Chou- Talalay plot indicates the CI on the y-axis as a function of effect level (Fa) on the X-axis.

CI values were obtained from three independent experiments for each set of combinations, each performed in triplicate, using results obtained from each drug alone and in combination within the same experiment. CI < 1 indicates synergism, 1 < CI > 1 suggests an additive effect, and CI > 1 corresponds to antagonism.

2.2.3 Caspase 3/7 assay

The Caspase-Glo® 3/7 Assay (Promega) is a luminescent assay that measures caspase-3 and -7 activities. The assay provides a luminogenic caspase-3/7 substrate, which, following cleavage generates a 'glow-type' signal produced by a luciferase. 2.0-2.5x10^4 cells were plated in opaque 96 well plates and left to adhere overnight. The following day, drug treatments were performed. 24h or 48h later, the addition of the Caspase-Glo® 3/7 reagent in an 'add-mix-measure' format resulted in cell lysis, followed by caspase cleavage of the substrate and generation of a 'glow-type' luminescent signal detected with the Varioskan Flash Multimode Reader (Thermo Scientific). The luminescent signal detected was directly proportional to the enzymatic activity of caspase 3/7 enzymes indicating apoptosis. Luminescent values in treated samples were normalized to untreated controls and fold increase compared to the controls (assigned a value of 1) was calculated.

2.2.4 Western blotting analysis

2.2.4.1 Protein extraction

Cells were washed twice with ice-cold PBS buffer. Sigma Lysis buffer containing fresh 1.5X protease inhibitor and 1.5X phosphatase inhibitor (Roche, UK), was added to the cells (kept on ice) for few minutes. Next, cells were scraped using cell scrapers (VWR, UK), collected into eppendorf tubes and left on ice for 15 minutes at 4°C. Samples were then pelleted by centrifugation for 15 minutes at 4°C (13,000rpm). The total cell lysate (supernatant) was placed in a fresh eppendorf tube and stored at -80°C.

2.2.4.2 Protein quantification

Proteins were quantified using the colorimetric RC-DC protein assay from Bio-Rad Laboratories. Protein quantification is based on the use of three reagents: A, S, and B. A 1:8 dilution of each protein sample was prepared in order to quantify each sample in triplicate (35μL). A mix of reagent A and S was also prepared (20μl of reagent S with 1ml of reagent A) and 25μL of this mix was added in each well of a flat-bottom 96 well plate. A Bovine Serum Albumin (Sigma-Aldrich) standard curve was used to calculate the protein concentration of the samples under investigation. 10μl of each of the BSA standards (100μg/mL, 200μg/mL, 400μg/mL, 600μg/mL, 800μg/mL, 1000μg/mL) or unknown sample replicates were pipetted per well. 200μL of reagent B was then added to each well and the content of the plate was mixed on a shaking platform for 15min at RT. Absorbance (OD) was measured at 750nm with the Varioskan Flash Multimode Reader (Thermo Scientific). The average absorbance measurement of the blank sample was subtracted from the all the measurements of both standard and unknown samples. A standard curve was then prepared by plotting the average absorbance value of each BSA standard vs. its concentration (μg/mL). The standard curve generated can be used to calculate the protein concentration of each unknown sample.

2.2.4.3 Immunoblotting

25-40μg of protein from samples prepared as in section 2.2.4.1 were centrifuged for 10 seconds, heat-denatured for 5min at 95°C in sample buffer containing 100 mM Tris-Cl (pH 6.8), 4% SDS, 10% 2-mercaptoethanol, 20% glycerol, and 0.02% bromophenol blue (Life Technologies) and loaded on a 7% Tris-acetate, or 4-12% Bis-Tris NuPAGE gel (Novex, Pre-cast gels, Life Technologies). 10x Running NuPAGE [60.5g Tris-Base (Sigma-Aldrich), 89.5g Tricine (Sigma-Aldrich) and 10g of SDS (Sigma-Aldrich)] or 20x MOPS [52.3g MOPS (Sigma-Aldrich), 30.3g Tris-Base (Sigma-Aldrich), 5g SDS (Sigma-Aldrich) and 1.5g EDTA (Sigma-Aldrich)] running buffers were diluted to 1x with distilled water and were used for protein electrophoresis on Tris-acetate or Bis-Tris gels at 175 Volts. The protein marker 'Amersham™ Rainbow™ Marker' (GE Healthcare) was used as a molecular weight protein standard. Proteins were subsequently transferred to polyvinylidene difluoride membranes (Immobilon®-P transfer membrane; Millipore), which had been previously activated by immersion in Methanol (VWR) for 1 min. The transfer buffer was prepared with a 1:10 dilution of a 10x Tris-Glycine buffer [30.3g Tris-Base (Sigma-Aldrich) and 144.1g Glycine (Sigma-Aldrich)] in distilled water and 20% Methanol. Proteins were transferred at 35V for 2.5 hours at RT using the XCell II Blot module (Life Technologies) and membranes were subsequently blocked for 1h at room temperature in blocking buffer containing 5% BSA (Sigma-Aldrich) in 1x TBS, 0.1% Tween-20 (Sigma-Aldrich). All primary antibodies were incubated overnight at 4°C and are listed in Table 2.1. The antibody dilutions were kept at 4°C and supplemented with 0.02% Sodium Azide (Severn Biotech) for at least one month. Anti-rabbit or mouse IgG, HRP-linked Antibodies (Cell Signaling Technologies) were used to detect the primary antibodies binding (dilutions ranging from 1:1000 to 1:5000 depending on the primary antibody used). Membranes were washed three times in 1xTBS-0.1% Tween-20 buffer for 5min following incubation with primary and secondary antibodies. The antibody binding to the protein of interest was detected by enhanced chemiluminescence (ECL system, Amersham) on autoradiography film (Kodak X-Omat). Reprobing of membranes with different antibodies specific for proteins with similar molecular weight (e.g. phosphorylated and total proteins) was performed by stripping the original bound antibody from the membrane with 15 min incubation with the Restore™ PLUS western blot stripping

buffer (Thermo Scientific). Alternatively, protein lysates were re-analysed by western blotting in the exact same conditions.

Antibodies	Dilutions	Dilution buffer	Supplier
Anti-EGFR	1/1000	TTBS 5% BSA	Cell signalling,UK
Anti-P-EGFR Y845	1/1000	TTBS 5% BSA	Cell signalling,UK
Anti-RRM1	1/1000	TTBS 5% BSA	Cell signalling,UK
Anti-ERK	1/1000	TTBS 5% BSA	Cell signalling,UK
Anti-P/ERK	1/1000	TTBS 5% BSA	Cell signalling,UK
Anti-P/MEK1/2	1/1000	TTBS 5% BSA	Cell signalling,UK
Anti-MEK1	1/1000	TTBS 5% BSA	Cell signalling,UK
Anti-MEK2	1/1000	TTBS 5% BSA	Cell signalling,UK
Anti-CDA	1/500	TTBS 5% BSA	Abcam
Anti-RRM2	1/1000	TTBS 5% BSA	Santacruz Biotech
Anti-Calnexin	1/1000	TTBS 5% BSA	Cell signalling,UK
Anti-K48	1/1000	TTBS 5% BSA	Cell signalling,UK
Anti-C-Parp	TTBS 1/1000 BSA	TTBS 5% BSA	Cell signalling,UK
Anti-rabbit-HRP-secondary	TTBS 1/1000 BSA	TTBS 5% BSA	Cell signalling,UK
Anti-mouse-HRP-secondary	TTBS 1/2000 BSA	TTBS 5% BSA	DAKO scientific
Anti-MDM2	TTBS 1/1000 BSA	TTBS 5% BSA	Santa Cruz Biotech.
Anti-p/MDM2	TTBS 1/1000 BSA	TTBS 5% BSA	Cell signalling,UK
Anti-p53	TTBS 1/500 BSA	TTBS 5% BSA	Santa Cruz Biotech.
Anti-β-actin	TTBS 1/3000 BSA	TTBS 5% BSA	Cell signalling,UK

Table 2.1: Primary and secondary antibodies used for western blotting analysis.

2.2.4.4 Densitometry analysis

The ImageJ Software was used to compare the intensity of bands obtained from immunoblotting analysis. Blots were scanned, bands of interest were selected and intensity (pixel density) was measured. The band intensity obtained with the antibody of interest was normalized to the intensity of the respective loading control.

2.2.5 Immunoprecipitation

To investigate protein-protein interaction and RRM1 polyubiquitination, cells were plated at 2-5 × 10^5/mL in 15cm dishes and allowed to proliferate overnight before treatment. Cells were then pre-treated for 1 hour with the proteasome inhibitor MG132 followed by 4h treatment with pimasertib. Approximately 10^7 cells/dish were lysed in 500µL of CelLytic M Cell lysis reagent (Sigma) supplemented with protease and phosphatase inhibitor (Roche) according to manufacturer's protocol. 550-750 µg of protein sample was incubated with 1 µg of anti-RRM1 (Abcam) or anti-MDM2 antibody (Santa Cruz Biotechnology) coupled to protein A beads and left rotating at 4°C overnight. IPs were eluted by boiling in SDS-PAGE loading buffer for 5 min at 95° and analysed by immunoblotting for RRM1, K-48, P-MDM2 and MDM2.

2.2.6 Fluorescence-activated cell sorting (FACS) for cell cycle analysis

Cell cycle alterations were studied by flow cytometry analysis (FACS). BxPC-3 cells were plated at a density of 1 × 10^6 cells in 6 well plates. Twentyfour hour later cells were incubated with the indicated drugs for 48 hours. Cells were washed and harvested by trypsinization and centrifugation (3500 rpm, 5 min). The pelleted cells were washed twice with PBS (0.01 m, pH 7.4) and fixed in cold 70% (*v/v*) ethanol and incubated at -20° overnight. The DNA of the fixed cells was stained with propidium iodide (PI) solution which consists of 50 µg/mL propidium iodide, 0.1 mg/mL RNase A, 0.05% Triton X-100, and PBS (all Sigma-Aldrich) and incubated for 1h at room temperature in the dark before analysis. The cell cycle status of the cells was analysed with FACScan flow cytometer (Becton Dickinson, CA, USA) using Cell Quest™ software (Becton Dickinson, CA, USA).

2.2.7 RNA isolation and real-time PCR

1X10^5 BxPC-3 and PANC-1 cells were plated in a six-well plate. The next day cells were treated with pimasertib or gemcitabine for 24h. Cells were trypsined and collected by centrifugation. Cell pellets were processed with the RNeasy kit (Qiagen) for RNA extraction according to the manufacturer's protocol and concentration was determined using the NanoDrop 2000 Spectrophotometer. 1µg of extracted RNA was transcribed reversely into c-DNA by using Omniscript RT kit (Qiagen) and then used for real Time PCR (RT-PCR). TaqMan dye was used as a detector and the applied biosystem 7500 RT-PCR machine was employed for PCR amplification. PCRs were done in a 20µL reaction volume containing 10µL of 2× buffer/enzyme mix, 1µL of 20× assay mix, 1µL of 20× GAPDH (Hs02758991_g1) endogenous control assay mix and 1µL input cDNA. The following protocol was used: initial incubation at 95°C for 10 minutes followed by 45 cycles at 95°C (15 seconds) and 60°C (1 minute). Cycle Threshold (CT) values, used to calculate the changes in gene expression, and were generated by the Applied Biosystems SDS software. Gene expression analysis ($\Delta\Delta C_T$ method and statistical analysis) was performed with the SABiosciences online tool (http://www.sabiosciences.com/pcr/arrayanalysis.php). Each sample was assayed in triplicates. RRM1 (01040698_m1) and RRM2 (00357247_g1), Assays-on-demand were obtained from Applied Biosystems.

2.2.8 Small interfering RNA (siRNA) transfection

MEK1, MEK2, MDM2, p53 and RRM1 smart-pool siRNA and non-targeting control (scrambled) smart-pool siRNAs were purchased from Thermo Scientific. The siRNA pools (20nmol) were resuspended in 1mL RNAse-free water according to manufacturer's instruction in order to obtain a stock of 20µM. Working stocks of 2µM were obtained by performing a 1:10 dilution of the siRNA aliquots (20µM) in 1x siRNA buffer (Thermo Scientific). Transfection protocols (siRNA concentration, cell density, transfection time, transfection reagent quantity) were optimised for the different cell lines and siRNAs used. Briefly, cells were plated at a concentration of 10^5/ml into 6-well cultured plates and allowed to attach overnight. The following day, both siRNA and DharmaFECT-1 transfection reagent (Thermo Scientific) were diluted in serum-

free Opti-MEM media (Life Technologies) according to the manufacturer's instructions (usually siRNA final concentration range was between 50-100nM) and incubated for 5min at RT. siRNA-Opti-MEM dilution was then mixed with the Dharmafect-Opti-MEM solution by pipetting carefully up and down and the mixture was left at room temperature for 20min. Following incubation, 400μL of the siRNA-Dharmafect solution were added per/well in a total volume of 2mL of antibiotic-free complete medium. The next day transfection medium was replaced with complete medium and cells were then left at 37°C for an additional 24 or 48h. Protein knockdown was confirmed by immunoblotting analysis.

2.2.9 Plasmid transfection

The plasmid pCMV-myc3-HDM2 was a gift from Yue Xiong (Addgene plasmid # 20935) (Zhang et al. 2003) and the plasmid pCMV-myc3-Mdm2 p60 was a gift from Tyler Jacks & Trudy Oliver (Addgene plasmid # 52059) (Oliver et al. 2011).

$1x10^5$ MIAPaCa-2 cells were seeded in six well plates with antibiotics-free media. After 24 hours cells were transiently transfected with pCMV-myc3-HDM2 or pCMV-myc3-Mdm2 p60 (2μG-10μG) using the GeneJuice transfection reagent, according to the manufacturer's protocol (Novagen EMD Bioscience). 48h post transfection, 600μg/mL neomycin (G418) (Sigma-Aldrich) was added to the medium. Transfected cells were incubated for 72 hours keeping selective pressure in the medium before pimasertib treatment.

2.2.10 Treatment studies in murine models

2.2.10.1 Establishment of a syngeneic orthotopic mouse model of pancreatic cancer

The murine pancreatic adenocarcinoma cell line TB32048 was used to establish a syngeneic orthotopic mouse model of pancreatic cancer. TB32048 cells were derived from the genetically engineered mouse model KPC (LSL-$KRAS^{G12D/+}$ $LSLTrp53^{R172H/+}$Pdx1-Cre).

Subconfluent cultures of TB32048 cells were harvested with 0.25% trypsin, re-suspended and washed with PBS. 1 X 10^5 cells were resuspended in ice-cold PBS and ice-cold Matrigel at 1:1 ratio. The mixture was mixed and the suspension was injected.

Six- to eight-week-old C57BL/6 black female mice were used in all *in vivo* experiments according to the Animal Research Ethics and United Kingdom Coordination Committee on Cancer Research Guidelines and Home Office Regulations (Project license PPL70/7411). All animals were housed under specific pathogen-free conditions and all procedures involving animals were conducted according to the requirements of the United Kingdom Home Office Animals (Scientific Procedures) Acts, 1986. After acclimatization for 1 week, mice were anesthetized and laparotomy was performed. Part of the pancreas was well exposed. $1\times10^{\hat{}5}$ TB32048 tumor cells in 30 µL of PBS: Matrigel (1:1) were orthotopically injected into the pancreas using an inoculator with a 30-gauge needle.

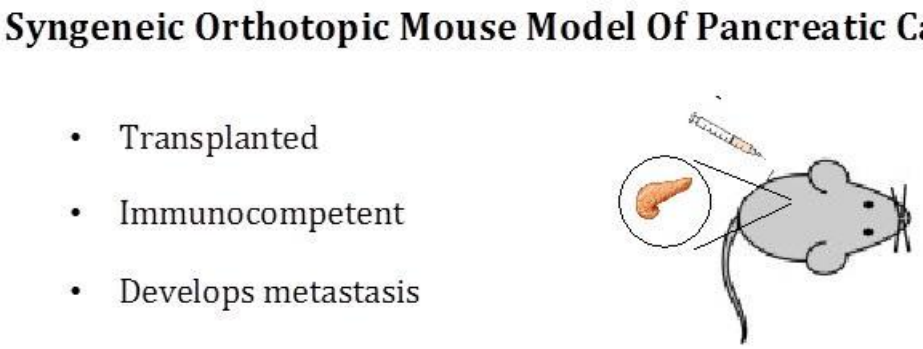

Figure 2.1: Schematic representation of the syngeneic orthotopic mouse model of pancreatic cancer generated.
An orthotopic model of pancreatic tumor was established by implanting TB32048 cells (derived from the KPC mouse model of PDAC) into the pancreas of immunocompetent mice.

2.2.10.2 Drugs treatment schedule in the orthotopic mouse model

After tumors were established, drug treatment was assessed. Gemcitabine was administered intraperitoneally and pimasertib was suspended in 0.5% carboxyl methylcellulose and 0.25% Tween 20 and injected by oral gavage. Mice were treated with gemcitabine 80mg/kg (twice/week), single agent pimasertib at 5mg/kg or

15mg/kg (daily) or sequential combination of pimasertib followed by gemcitabine for a total of 2 5-day treatment cycles. The control mice were treated with 0.5% carboxyl methylcellulose and 0.25% Tween 20 by oral gavage. In the combination cohort, gemcitabine treatment was initiated 4 hours after pimasertib administration. After two treatments cycles of 5 days each all mice were sacrificed. Tumors were excised, weighed and fixed in paraformaldehyde for IHC analysis.

2.2.10.3 Ultrasound analysis

Ultrasound imaging was peformed to measure tumor volumes at the beginning and at the end of each drug treatment using the VEVO2100 high frequency imaging system. Mice were anesthetized using 1.5 liters/min oxygen/isofluorane mixture and then gently taped to the imaging stage. The vital signs were monitored on the VEVO2100 (VisualSonics Inc, Ontario, Canada). Ultrasound images were captured using the abdominal package in B-mode, and three images per pancreas (10 fields/analysis) were captured via 3D-Mode combined with B-Mode for volume analysis following manufacturer's instructions (VisualSonics).

2.2.10.4 Immunohistochemistry (IHC)

Immunohistochemistry was performed to determine specific protein expression in TB32048 tumors. Samples were fixed in paraformaldehyde.4mm paraffin sections underwent automated dewaxing (Leica Bond Dewax AR9222) and endogenous peroxidase was blocked using 3-4% (v/v) hydrogen peroxide (part of Leica Bond Refine Polymer Kit, DS9800). Automated antigen retrieval was then performed on the sections. For Ki67, Cleaved Caspase-3 (CC3) and RRM1, Leica Bond ER2 (EDTA-based, pH9, AR9640) was applied to the slides and they were heated to 100 degrees Celsius (30 minutes for Ki67, p-AKT and CC3 and 10 minutes for RRM1). No antigen retrieval was used for P-ERK. The antibody was used on the slides obtained from mice pancreatic tumors at a dilution of 1/100 (Ki67), 1/1000 (CC3), 1/200 (RRM1 and P-ERK), with 15 minutes incubation or 1/200 (p-AKT), with 30 minutes incubation. Signal visualisation was performed using Bond Polymer (Anti-rabbit Poly-HRP-IgG) for 8 min.

DAB was applied for 10 minutes and then Bond DAB Enhancer (Copper Sulfate-based, AR9432) was applied for 5 min. Cell nuclei were counterstained with haematoxylin. The Leica Bond Polymer Detection Kit (DS9800) was used for peroxidase blocking, visualization and counterstaining. Bond Wash (AR9590) was used for all washing steps between reagent steps.

2.2.10.5 IHC quantification

Immunostaining for RRM1, p-AKT and p-ERK was assessed in at least five fields at 400× magnification. Immunoreactivity was evaluated semi-quantitatively based on staining intensity and proportion. The proportion of staining was scored from 0 to 3 as follows: 3: >50% of positive cells; 2: 10-49%; 1: <10% of positive cells. Intensity of staining was scored from 0 to 3 (0, absent; 1, weak; 2, moderate; 3, intense). The immunoreactive score (IRS) for each sample was determined by multiplying the intensity and the proportion of stained cells.

For ki67 staining the number of positive cells were counted and compared to the total number of nuclei in a field. Values were expressed in percentage. (Nuclear staining in > 40% was considered positive, < 40% was considered negative). For CC3 staining the number of positive cells were counted and compared to the total number of nuclei in a field. Values were expressed in percentage. (Nuclear staining in < 1% was considered negative, between 1-5% was considered positive).

Analysis was undertaken blindly without knowledge of treatment variables. 10 images per slides were analysed.

2.2.11 Statistical analysis

The One-way ANOVA or Two-way ANOVA with Bonferroni post-tests were used to calculate statistical significance for the *in vitro* experiments. *P <0.05, as calculated by GraphPad Prism (version 6.0; GraphPad Software Inc.), was considered statistically significant. Differences in final tumor weights were confirmed using a Student's *t*-test and considered statistically significant when $P < 0.05$.

CHAPTER 3

THE CELLULAR EFFECTS OF PIMASERTIB IN COMBINATION WITH GEMCITABINE IN PDAC

3.1 INTRODUCTION

3.1.1 Interaction of gemcitabine with targeted therapy

Pancreatic ductal adenocarcinoma (PDAC) is a lethal disease for which current therapies are often ineffective (Hidalgo 2010). Gemcitabine, a nucleoside analogue, has represented a standard treatment for PDAC since 1997 (Burris et al. 1997). However, both intrinsic and acquired gemcitabine resistance is a crucial factor, which limits patients' response to treatment (Nakano et al. 2007).

The identification of small molecule inhibitors that could modulate the expression of molecular markers known to impair gemcitabine efficacy represents a key strategy to improve pancreatic cancer patient's response to gemcitabine.

A large number of gemcitabine-based combinations have been evaluated in clinical trials but show limited efficacy. An exception is the combination of gemcitabine plus nab-paclitaxel, which has yielded a small but significant improvement in survival along with manageable toxicities. Thus, this regimen represents one of the standard treatments for locally advanced and metastatic PDAC (Conroy et al. 2011, Von Hoff et al. 2011). Identifying new therapeutic strategies that significantly improve PDAC patients' response to gemcitabine and other chemotherapies are urgently needed.

The RAS/RAF/MEK/ERK signalling pathway regulates fundamental cellular processes such as survival, proliferation, differentiation and invasion (Normanno et al. 2006). The K-RAS oncogene is mutated in almost all PDACs and sustained activation is required for pancreatic tumorigenesis and development (di Magliano and Logsdon 2013). Targeting downstream RAS effectors in cancers characterised by a deregulated MAPK pathway by using inhibitors of MEK protein have proved to be successful in the clinic (Flaherty et al. 2012) and several preclinical studies have demonstrated their efficacy in PDAC model systems (Alagesan et al. 2015). In particular, previous findings have shown improved antitumor activity when gemcitabine was combined with MEK inhibitors in biliary cancer, underling the importance of this drug combination (Xu et al. 2013).

Pimasertib, a potent, highly selective MEK1/2 inhibitor, binds to an adjacent allosteric site, which locks MEK into a catalytically inactive conformation, thereby preventing

any side effects associated with inhibition of other protein kinases (Yoon et al. 2011). Combinations of chemotherapy or targeted therapy with pimasertib caused synergistic antitumor activity in different human cancer where they have been tested (Kim et al. 2010). (Yoon et al. 2011) (Martinelli et al. 2013) (Airiau et al. 2015).

3.1.2 Determining the effects of gemcitabine plus pimasertib combination in human pancreatic cancer cell lines

This chapter aims at investigating the combination effects of pimasertib with gemcitabine. The combination index (CI) theorem derived by Chou-Talay, provides the means for quantifying synergism, additivity or antagonism with a computerised simulation (Chou 2010). CI values describing drug interactions are calculated using the Calcusyn Software. CI values greater than 1 indicate antagonism; values less than 1 indicate synergism. A dose-effect curve of each drug alone has to be determined since each drug has different potency and produces a dose-response curve of different shape (Chou 2010). A non-constant ratio treatment was used to determine the effects of increasing concentrations of gemcitabine with a fixed concentration of pimasertib (≈ IC35) in BxPC-3 and PANC-1 cell lines. CI values from each experiment were derived to accurately quantify the effects of these drugs in combination and characterize their interaction.

3.1.3 Drugs administration schedule affects *in vitro* and *in vivo* response

One of the main challenges in combination therapy is to find the optimal design schedule. Different factors can change the outcome of a patient's response: (a) drugs dosage, (b) the order of drugs administration, (c) the timing between two different administrations and (d) the duration of each drug exposure (Fitzgerald et al. 2006). This concept was well demonstrated by a preclinical study on triple negative breast cancer (TNBC) models, in which the combination effects of an EGFR inhibitor (erlotinib) with doxorubicin was investigated (Lee et al. 2012). Sequential treatment with erlotinib followed by doxorubicin sensitized TNBC cells and xenograft models to DNA damage and enhanced doxorubicin-induced apoptosis, an effect that was

abolished when the sequence was reversed or when the two agents were given simultaneously. Importantly, the synergistic effects obtained by erlotinib plus doxorubicin combination were caused by re-activation of pro-apoptotic pathways induced by sustained EGFR inhibition and whose activity had been abolished by deregulated EGFR signalling (Lee et al. 2012).

Preclinical studies are crucial to investigate the best drug combination schedules, particularly when combined with inhibitors of oncogenic signalling pathways, for the design of new clinical trials. In this present study, the efficacious drug combination design between the MEK inhibitor pimasertib and gemcitabine chemotherapy will be discussed.

3.2 RESEARCH HYPOTHESIS AND AIMS

Hypothesis: MEK inhibitors have been shown to be effective in tumors characterised by genetic alterations within the RAS/MEK/ERK signalling cascade by blocking the transmission of proliferative signals induced by this pathway. Gemcitabine represents a standard treatment for locally advanced and metastatic PDAC patients, however, providing small survival benefit. Gemcitabine-based combinations treatments in PDAC patients have proved promising and some have resulted in FDA approval (nab-paclitaxel plus gemcitabine, erlotinib plus gemcitabine).

This chapter investigates the interaction between pimasertib and gemcitabine in human pancreatic cancer cell lines, aiming to:

- Investigate the effects of pimasertib on the inhibition of human pancreatic cancer cell proliferation and ERK signalling.
- Understand how the combination of pimasertib with gemcitabine affects proliferation and apoptosis.
- Investigate the effects of pimasertib and gemcitabine in modulating the expression of genes associated with gemcitabine resistance.

3.3 RESULTS

3.3.1 Gemcitabine inhibits proliferation of human pancreatic cancer cell lines

The chemosensitivity of a panel of human pancreatic cancer cell lines (PANC-1, BxPC-3, SUIT-2 and MIAPaCa-2) to gemcitabine was evaluated. Cells were treated with increasing concentrations of gemcitabine (0.01µM to 100µM) continuously for 96 hours after which cell proliferation was measured by MTT assay. The concentrations needed to inhibit cell growth by 50% were calculated (IC_{50}). SUIT-2 and BxPC-3 were the most sensitive cell lines, exhibiting an IC_{50} of 14.15nM and 40.97nM respectively, whereas PANC-1 was the most resistant, with an IC_{50} of 10.9µM (Table 3.1). MIAPaCa-2 cell line exhibited an IC_{50} of 69.4nM (Table 3.1). Gemcitabine induced a dose-dependent effect on cell growth inhibition until 100nM dose. As the concentrations of gemcitabine increased (1µM, 10 µM and 100µM) all cell lines reached a plateau of proliferation (Figure 3.1).

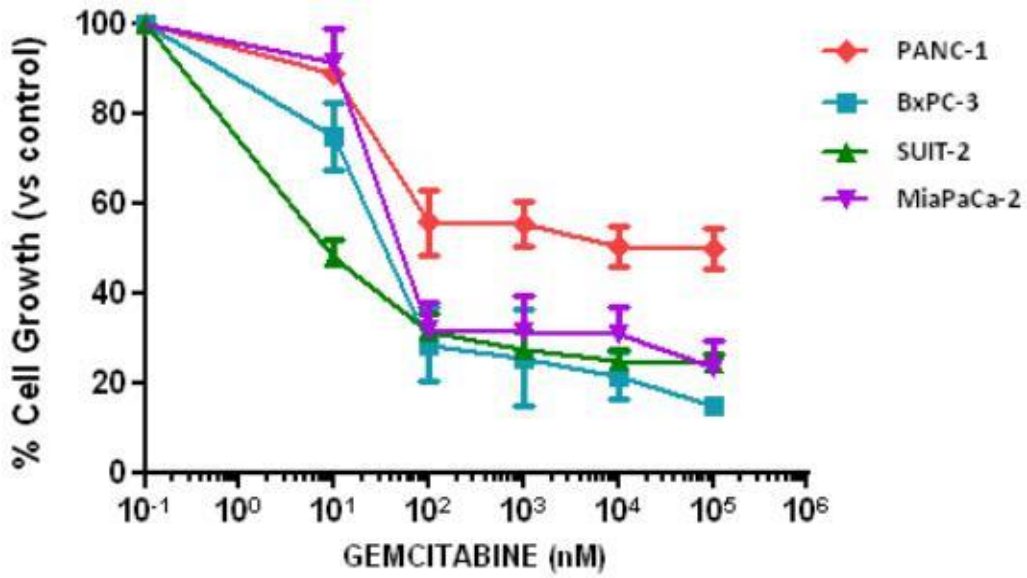

Figure 3.1: Effect of gemcitabine on the proliferation of human pancreatic cancer cell lines.
PANC-1, BxPC-3, MIAPaCa-2 and SUIT-2 cells were treated for 96 hours with increasing concentrations of gemcitabine (0.1µM to 100µM). Inhibition of cell growth was measured using MTT assay. Absorbance values obtained from treated samples were normalized to untreated controls and presented as % proliferation. Each experiment was performed in triplicate and results are presented as mean, error bars ± SD.

BxPC-3 and PANC-1 cell lines were selected to perform drug combination studies and for the mechanistic studies of this project. BxPC-3 cells are wild type for K-RAS and PANC-1 cells harbour an activating point mutation within the K-RAS gene at codon 12 (Loukopoulos et al. 2004). Both BxPC-3 and PANC-1 cells carry an inactivating mutation within the *p53* tumor suppressor gene (Moore et al. 2001). Table 3.1 outlines the main biological characteristics of the cell lines used in this study in terms of their K-RAS and P53 mutations and their gemcitabine IC_{50} values. The concentrations of gemcitabine used for drug combination analyses were selected between the range of 5nM and 100nM, which inhibited cell proliferation in BxPC-3 and PANC-1 cells in a dose-dependent manner (Fig. 3.2).

Cell line	Tissue	K-RAS mutant	P53 mutant	Gem IC_{50}(nmol/L)
PANC-1	pancreas-duct	G12D	R273H	10.9µM
MIAPaCa-2	pancreas	G12C	R248W	69.44nM
BxPC-3	pancreas	Wild Type	Y220C	40.97nM
SUIT-2	pancreas	G12D	R2T3H	14.15nM

Table 3.1: Characteristics of human pancreatic cancer cell lines.
Information for each cell line was obtained from the COSMIC database and the Broad Institute Cancer Cell Line Encyclopedia. IC50 values of gemcitabine were calculated with the GraphPad/Prism6 software.

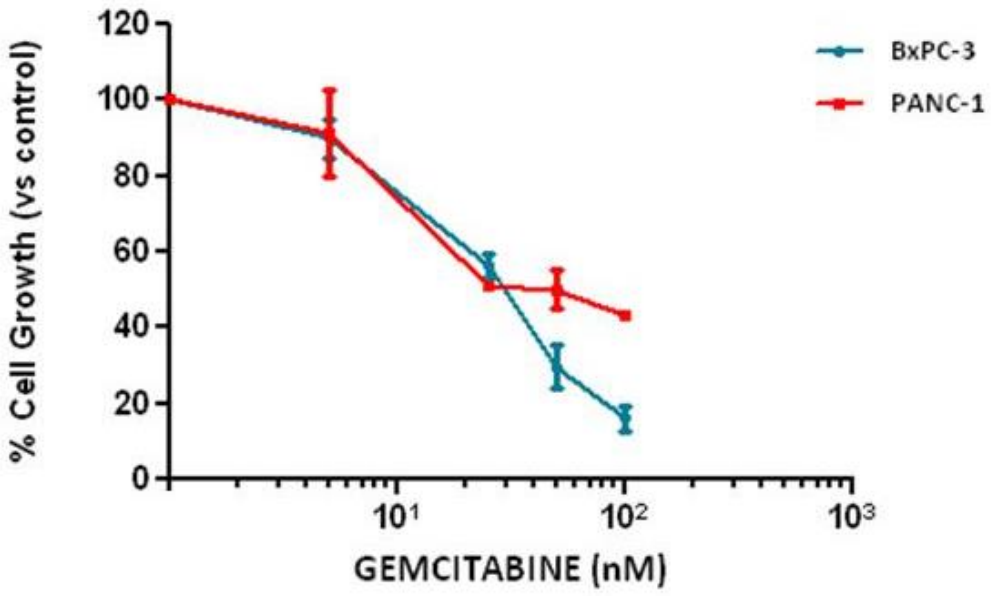

Figure 3.2: Effects of gemcitabine on cell proliferation in BxPC-3 and PANC-1 cell lines.
BxPC-3 and PANC-1 cells were treated for 96 hours with increasing concentrations of gemcitabine (5, 25, 50 and 100nM). Inhibition of cell growth was measured using MTT assay. Absorbance values obtained from treated samples were normalized to untreated controls and presented as % proliferation. Each experiment was performed in triplicates and results are presented as mean, error bars ± SD.

3.3.2 Pimasertib inhibits cell proliferation and activation of ERK signalling in human pancreatic cancer cell lines

Pimasertib acts by inhibiting MEK protein in phosphorylating and thus activating downstream ERK (Yoon et al. 2011). To determine the optimal concentration to use for our combination experiments, the pharmacodynamics effects of pimasertib on ERK pathway inhibition were investigated. Firstly, BxPC-3 and PANC-1 cell lines were treated with increasing concentrations of pimasertib (0.1, 0.5, 1µM) for 24 hours. Pimasertib effectively inhibited P-ERK signalling in both cell lines at all concentrations tested (Fig. 3.3). Next, the effect of pimasertib treatment on ERK signalling over time was analysed. PANC-1 and BxPC-3 cell lines were treated with 1µM pimasertib and total cell lysates were extracted at different times. Both cell lines exhibited total inhibition of P-ERK expression from 30 minutes of exposure with pimasertib, which was sustained over the time course (Fig. 3.4).

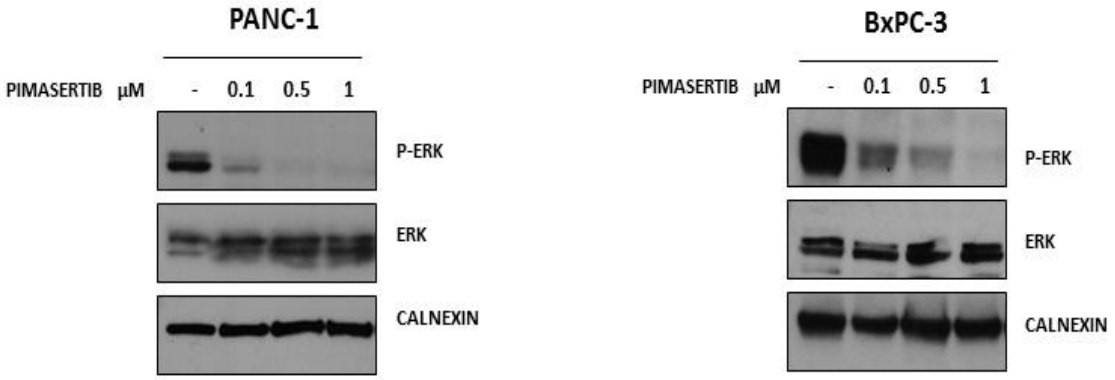

Figure 3.3: Dose-dependent inhibition of P-ERK signaling by pimasertib.
PANC-1 and BxPC-3 cells were treated with increasing concentrations of pimasertib (0.1 µM, 0.5 µM and 1µM) for 24 hours. Total cell lysates were extracted and analysed by immunoblotting with the indicated antibodies. Calnexin was used as loading control. The experiment shown is representative of three independent experiments.

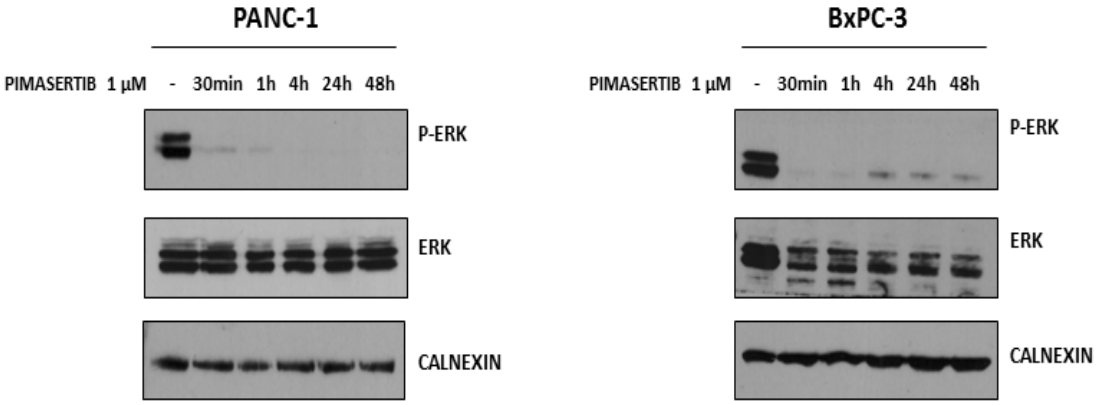

Figure 3.4: Time-dependent inhibition of P-ERK signalling by pimasertib.
PANC-1 and BxPC-3 cells were treated with 1µM pimasertib and harvested at different time points (30min to 48h). Total cell lysates were extracted and analysed by immunoblotting with the indicated antibodies. Calnexin was used as loading control. The experiment shown is representative of three independent experiments.

To determine the responsiveness of pimasertib on cell proliferation, PANC-1 and BxPC-3 cell lines were treated with pimasertib at concentrations ranging from 0.01µM to 10µM, continuously for 48 hours. Inhibition of cell proliferation induced by pimasertib was determined by MTT assay. At 48 hours treatment, BxPC-3 and PANC-1 cells viability was higher than 70% (IC_{70}) at all concentrations of pimasertib tested (Fig. 3.5). A subtoxic concentration of pimasertib (0.5µM) was used for our combination treatments to explore whether pimasertib sensitized cells to gemcitabine-induced cytotoxicity since this concentration, as previously shown, also effectively inhibited ERK phosphorylation (Fig. 3.4).

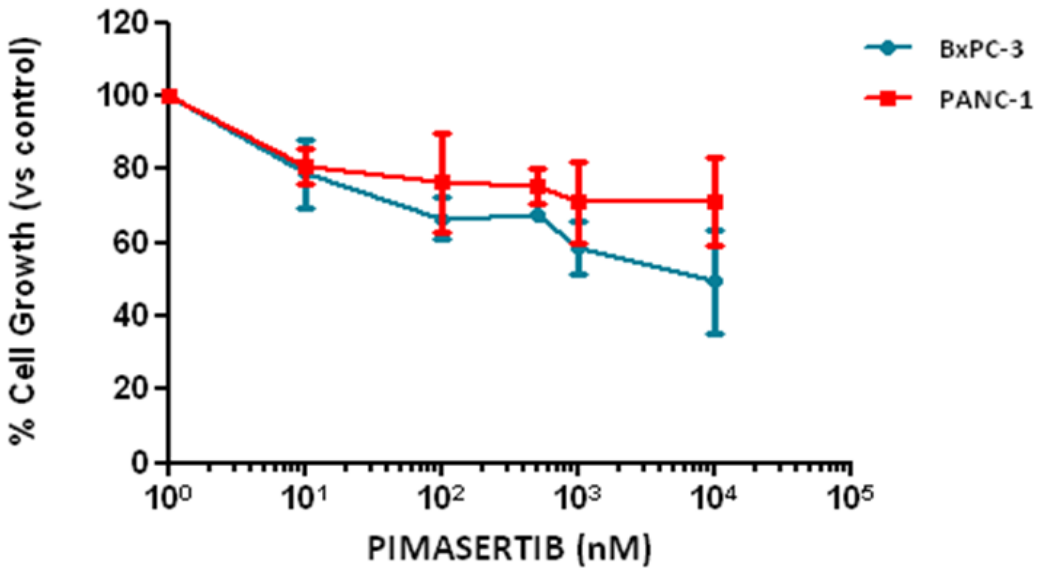

Figure 3.5: Effects of pimasertib on cell proliferation in BxPC-3 and PANC-1 cell lines.
PANC-1 and BxPC3 cells were treated for 48 hours with increasing concentrations of pimasertib (0.01µM, 0.1µM, 0.5µM, 1µM, 10µM). Inhibition of cell growth was measured using MTT assay. Absorbance values obtained from treated samples were normalized to untreated controls and presented as % proliferation. Each experiment was performed in triplicate and results are presented as mean, error bars ± SD.

3.3.3 Cell cycle effects of pimasertib and gemcitabine

Flow cytometry analysis was performed to determine the effects of pimasertib and gemcitabine on the cell cycle. BxPC-3 cell lines were treated for 48 hours with 100nM pimasertib or gemcitabine. Next, cells were harvested, stained with propidium iodide and analysed by flow cytometry. Pimasertib treatment resulted in accumulation in G1 phase as shown by the DNA histograms (Fig. 3.6). On the other hand, gemcitabine increased the percentage of cells in S phase of the cell cycle (Fig. 3.6).

A

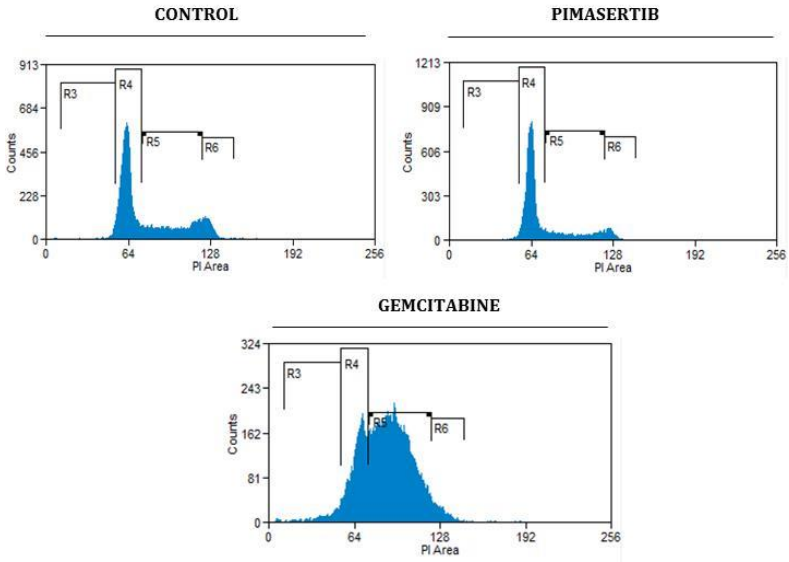

B

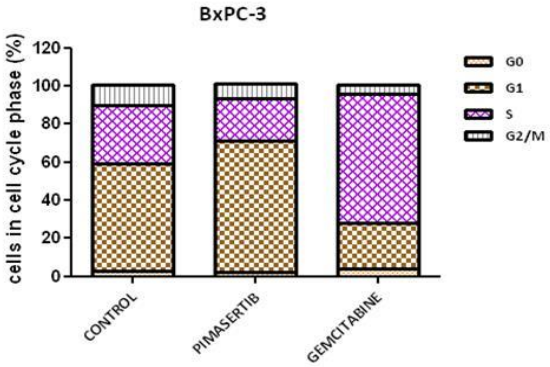

Figure 3.6: Effect of pimasertib and gemcitabine on the cell cycle.
A. BxPC-3 cells were treated for 48 hours with 100nM pimasertib or 100nM gemcitabine. Cells were harvested, stained with propidium iodide and analysed by flow cytometry. Cell cycle distribution is shown. **B.** Bar graphs showing the percentage of cells in each phase of the cell cycle.

3.3.4 Combination of pimasertib with gemcitabine according to a non-constant ratio design

The effect of pimasertib treatment in combination with gemcitabine on the proliferation of BxPC-3 and PANC-1 cell lines was investigated. A non-constant ratio design employing a fixed concentration of pimasertib (500nM), combined with increasing concentrations of gemcitabine (5nM, 25nM, 50nM, 100nM) was applied. A dose-effect curve of each drug alone was also performed.

Three combination schedules were designed:

1. Simultaneous and continuous exposure to pimasertib with gemcitabine for 48 hours.
2. Sequential combination consisting of 4 hour pre-treatment with pimasertib followed by 48-hour treatment with gemcitabine
3. Sequential combination consisting of 4 hour pre-treatment with pimasertib followed by 24-hour treatment with gemcitabine.

The choice of administering pimasertib 4 hours before gemcitabine was associated with the effect observed upon 4 hours treatment with pimasertib on RRM1 protein expression, which will be discussed in detail in this chapter.

Combination indices (CI), which describe the interaction between drugs, were calculated using the methodology of Chou and Talalay, (Chou 2010) with the Calcusyn Software. This software performs a dose-effect analysis based on the mass-action law based theory (Chou 2006). The CI values generated for each drug combination describe the drug interactions. CI values > 1 indicate antagonism, values =1 indicate additivity and values < 1 indicate synergism.

3.3.4.1 Simultaneous administration of pimasertib with gemcitabine induces antagonistic or additive antiproliferative effects

BxPC-3 and PANC-1 cells were exposed to increasing concentrations of gemcitabine (5nM, 25nM, 50nM and 250nM) together with a fixed concentration of pimasertib (500nM) for 48 hours continuously. Inhibition of cell proliferation was determined by MTT assay (Figure 3.7A, 3.8A). The effects of the drugs combination was analysed with the CI method. At all concentrations of gemcitabine tested the combination resulted in CI values > 1 in BxPC-3 cell lines indicating a negative interaction and in CI values ≥ 1 in PANC-1 cell lines indicating an additive or negative interaction. A bar chart of CI values obtained from the simultaneous combination of gemcitabine with pimasertib is illustrated (Fig. 3.7B-3.8B).

A

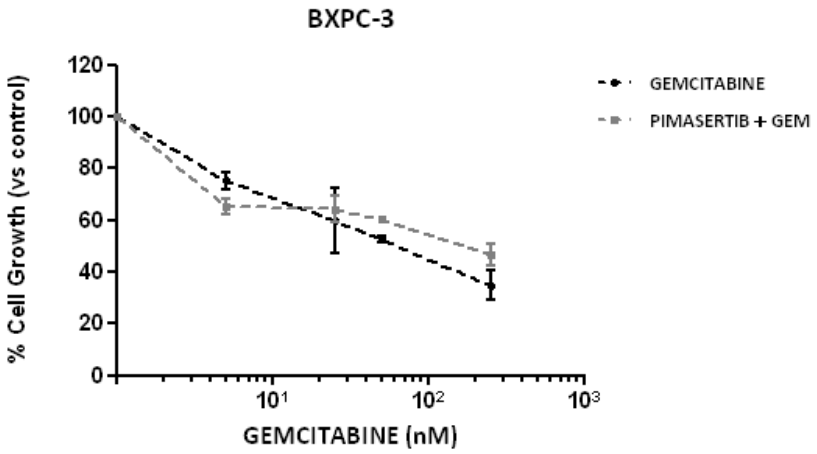

B

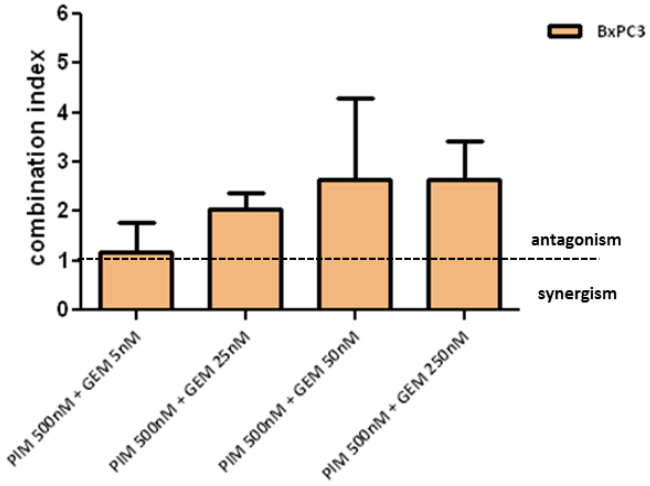

Figure 3.7: Effects of simultaneous treatment of pimasertib plus gemcitabine on BxPC-3 cells proliferation.

A. The MTT assay was used to assess the effect of a 48h simultaneous treatment of 500nM pimasertib with increasing concentrations of gemcitabine (5-25-50-250nM) on the growth of BxPC-3 cells. **B.** Combination Indices (CI) values describing drug combinations were calculated with the Calcusyn program. Experiments were repeated three times and are represented as mean, Error Bars ± SD.

A

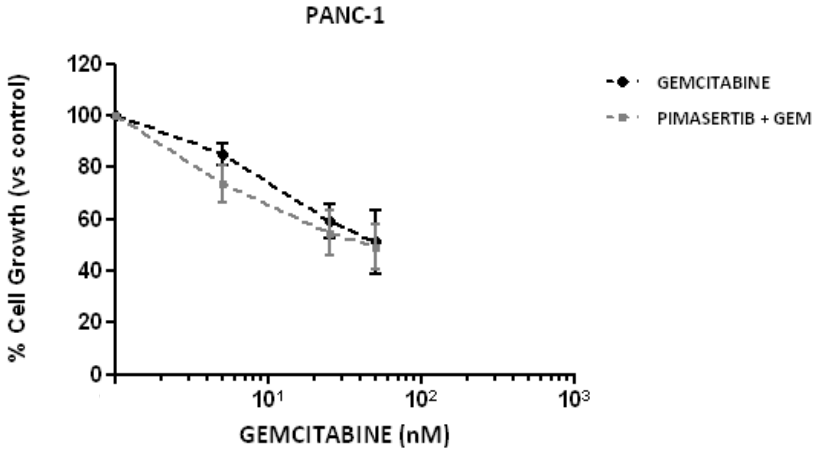

B

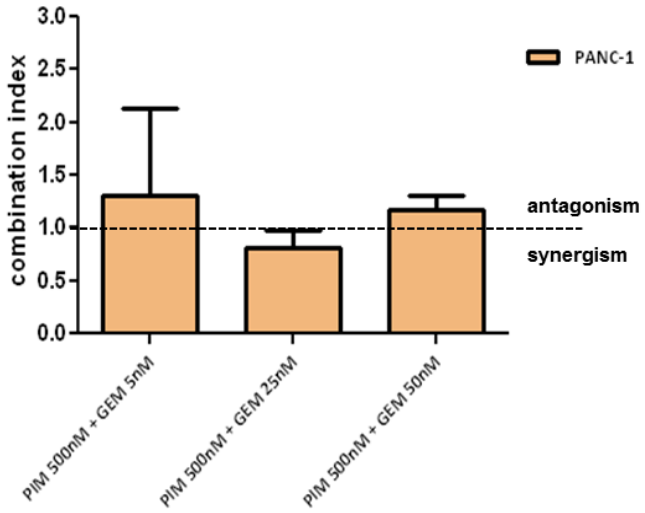

Figure 3.8: Effects of simultaneous treatment of pimasertib plus gemcitabine on PANC-1 cells proliferation.

A. The MTT assay was used to assess the effect of a 48h simultaneous treatment of 500nM pimasertib with increasing concentrations of gemcitabine (5-25-50nM) on the growth of PANC-1 cells. **B.** Combination Indices (CI) values describing drug combinations were calculated with the Calcusyn program. Experiments were repeated three times and are represented as mean, Error Bars ± SD.

3.3.4.2 Sequential administration of pimasertib with gemcitabine induces synergistic antiproliferative effects

Since simultaneous administration of pimasertib with gemcitabine did not produce any synergistic antiproliferative effects (Fig. 3.7-3.8), a different time schedule was evaluated in which the MEK inhibitor was administered prior to chemotherapy. Because we found that pimasertib was able to downregulate an important biomarker of gemcitabine resistance after a 4-hour exposure (These results will be described later in the chapter), we decided to adopt the following sequential schedule of administration: BxPC-3 and PANC-1 cells were pre-treated for 4 hours with 500nM pimasertib after which gemcitabine (5nM, 25nM, 50nM, and 250nM) was administered for 48 hours continuously. Inhibition of cell proliferation was determined by MTT assay (Fig. 3.9A, 3.10A). Interestingly, this time schedule of drug administration induced synergistic antiproliferative effects in BxPC-3 and PANC-1 cell lines as indicated by CI values generated from all concentrations of gemcitabine examined being <1. Bar charts of CI values are illustrated in Fig. 3.9B and 3.10B.

Additionally, a 4-hour pre-exposure to pimasertib followed by a short time exposure with increasing concentrations of gemcitabine (24 hours) showed synergistic growth inhibitory activity (Fig. 3.11A), as shown by the CI values generated from all concentrations of gemcitabine examined being < 1 (Fig. 3.11B).

A

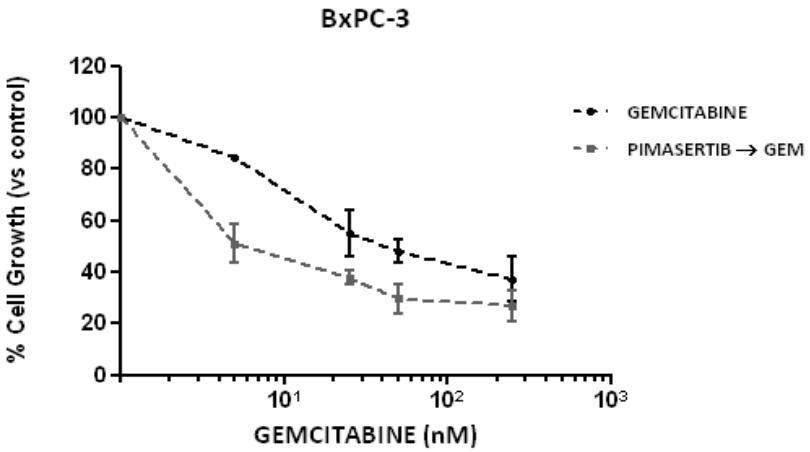

B

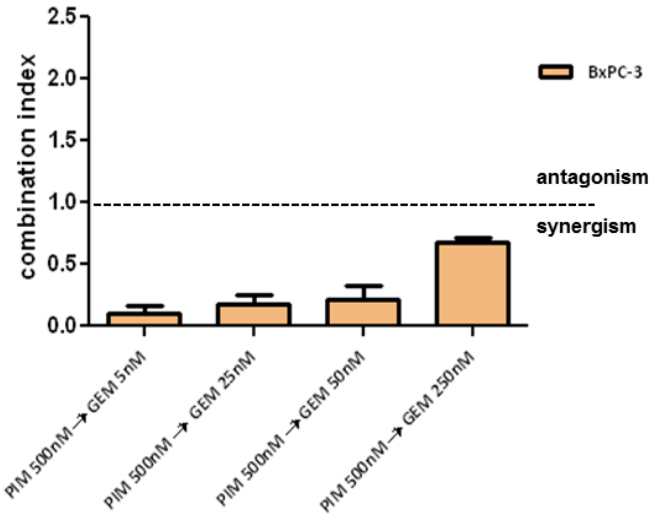

Figure 3.9: Effects of sequential treatment of pimasertib with gemcitabine on BxPC-3 cells proliferation.

A. The MTT assay was used to assess the effect of a 4h pre-treatment of 500nM pimasertib followed by continuous exposure for 48h with increasing concentrations of gemcitabine (5-25-50-250nM) on the growth of BxPC-3 cells. **B.** Combination Indices (CI) values describing drug combinations were calculated with the Calcusyn program. Experiments were repeated three times and are represented as mean, Error Bars ± SD.

A

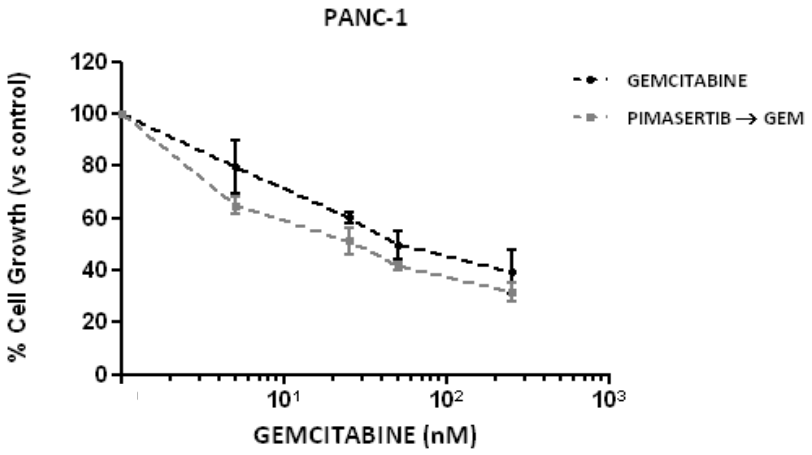

B

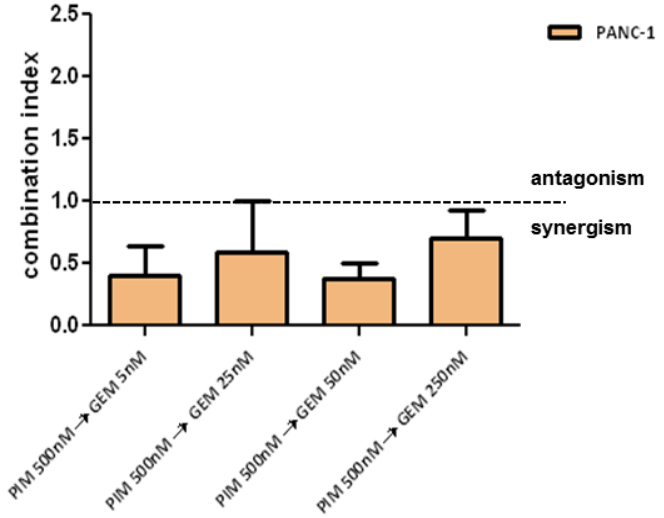

Figure 3.10: Effects of sequential treatment of pimasertib with gemcitabine on PANC-1 cells proliferation.

A. The MTT assay was used to assess the effect of a 4h pre-treatment of 500nM pimasertib followed by continuous exposure for 48h with increasing concentrations of gemcitabine (5-25-50-250nM) on the growth of PANC-1 cells. **B.** Combination Indices (CI) values describing drug combinations were calculated with the Calcusyn program. Experiments were repeated three times and are represented as mean, Error Bars ± SD.

A

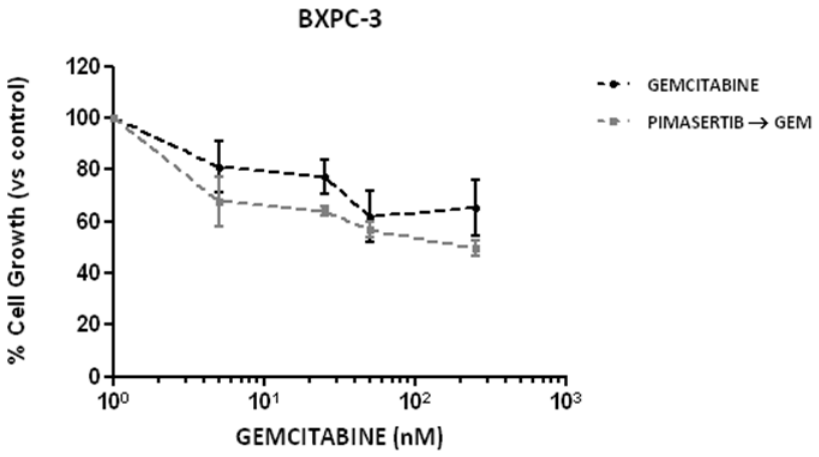

B

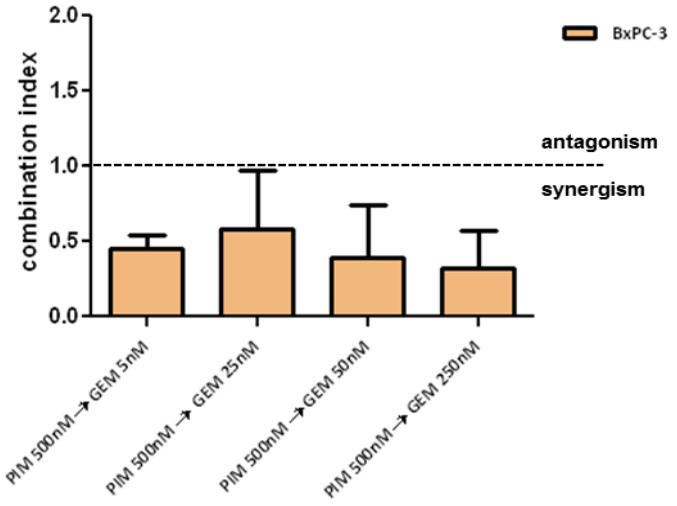

Figure 3.11: Effects of short sequential administration of pimasertib with gemcitabine on BxPC-3 cells proliferation.

A. The MTT assay was used to assess the effect of a 4h pre-treatment of 500nM pimasertib followed by continuous exposure for 24h with increasing concentrations of gemcitabine (5-25-50-250nM) on the growth of BxPC-3 cells. **B.** Combination Indices (CI) values describing drug combinations were calculated with the Calcusyn program. Experiments were repeated three times and are represented as mean, Error Bars ± SD.

3.3.5 Pimasertib enhances gemcitabine-induced apoptosis in a sequence-dependent fashion

One of the mechanisms of gemcitabine cytotoxicity is the induction of cell death which is mainly caused by dFdTCP (gemcitabine triphosphate form) incorporation into DNA (Huang and Plunkett 1995). We sought to investigate whether pimasertib was able to enhance gemcitabine-induced apoptosis. Simultaneous treatment of 500nM pimasertib with 50nM gemcitabine for 48 hours continously did not enhance gemcitabine-induced apoptosis as measured by caspase 3/7 enzyme activity in PANC-1 cells (from 3.38 ± 0.87 fold with gemcitabine alone to 3.43 ± 0.31 with the combination) (Fig. 3.12A) and in BxPC-3 cells (from 2.95 ± 0.78 fold with gem alone to 3.48 ± 0.31 with the combination) (Fig. 3.12B).

A

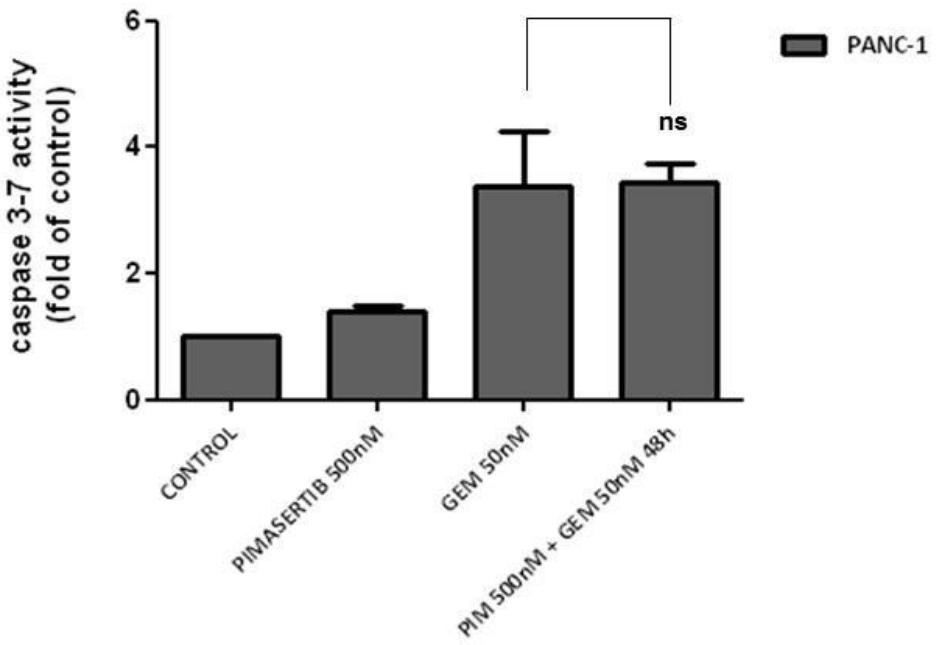

Figure 3.12: Simultaneous treatment of pimasertib with gemcitabine does not enhance apoptosis.
A. PANC-1 cells were treated with 500nM pimasertib and 50nM gemcitabine for 48h continuously. Apoptosis was assessed by measuring the caspase 3-7 enzymatic activity with the Caspase Glo Assay (Promega). Results are presented as fold increase to untreated samples. Each experiment was repeated in triplicate and results are presented as mean, Error Bars ± SD. P values > 0.05 were considered not statistically significant (ns).

B

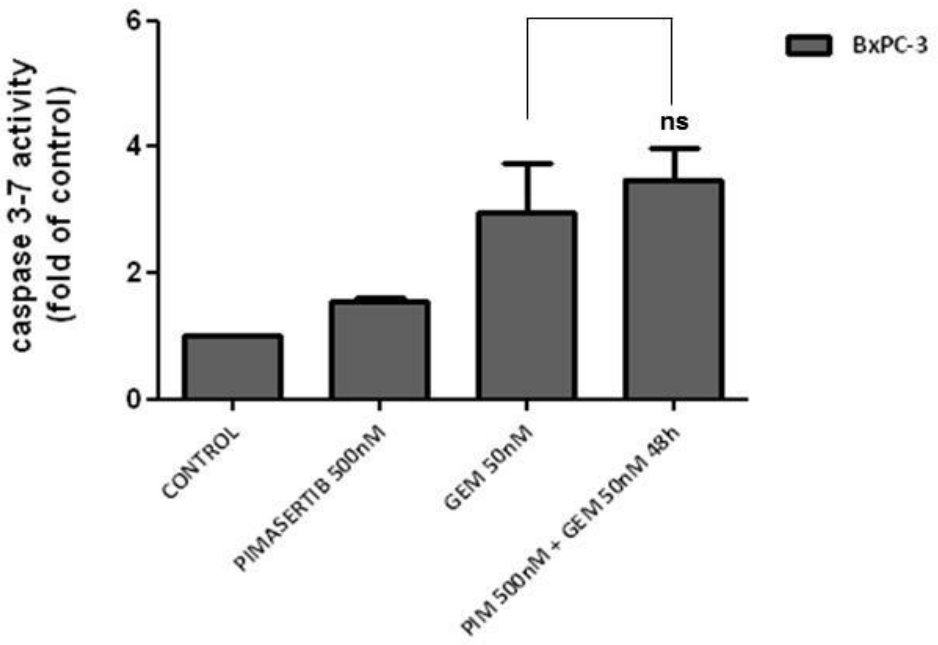

Figure 3.12 continued: Simultaneous treatment of pimasertib with gemcitabine does not enhance apoptosis.

B. BxPC-3 cells were treated with 500nM pimasertib, plus 50nM gemcitabine for 48h. Caspase 3-7 enzymatic activity was measured as an indicator of apoptosis induction. Results are presented as fold increase to untreated samples. Each experiment was repeated in triplicate and results are presented as mean, Error Bars ± SD. P values > 0.05 were considered not statistically significant (ns).

The effect of sequential administration was investigated. A 4-hour pre-treatment with 500nM pimasertib followed by 48 hour treatment with 50nM gemcitabine significantly enhanced gemcitabine-induced apoptosis as measured by the caspase 3/7 enzyme activity in PANC-1 cells (from 1.39 ± 0.12 fold with gemcitabine alone to 2.15 ± 0.42 with the combination) (Fig. 3.13A) and in BxPC-3 cells (from 3.78 ± 0.11 fold with gemcitabine alone to 5.65 ± 0.06 with the combination) (Fig. 3.13B). Treatment with pimasertib alone did not induce any significant increase of apoptosis in both PANC-1 cells (Fig. 3.12A, 3.13A) and BxPC-3 cells (Fig. 3.12B, 3.13B), as has been previously observed in other preclinical studies of pimasertib (Martinelli et al. 2013).

A

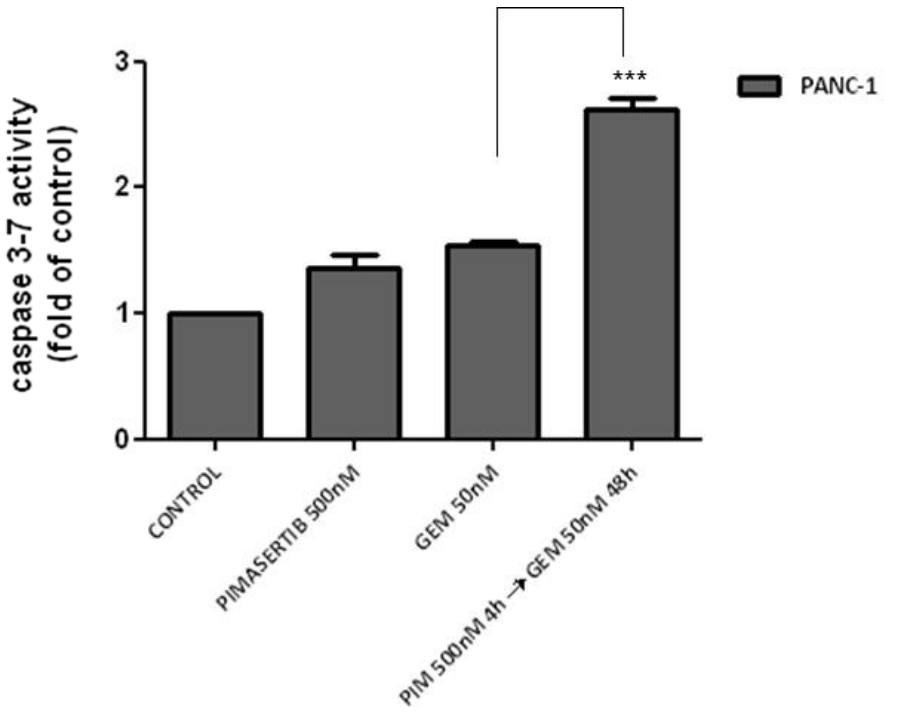

B

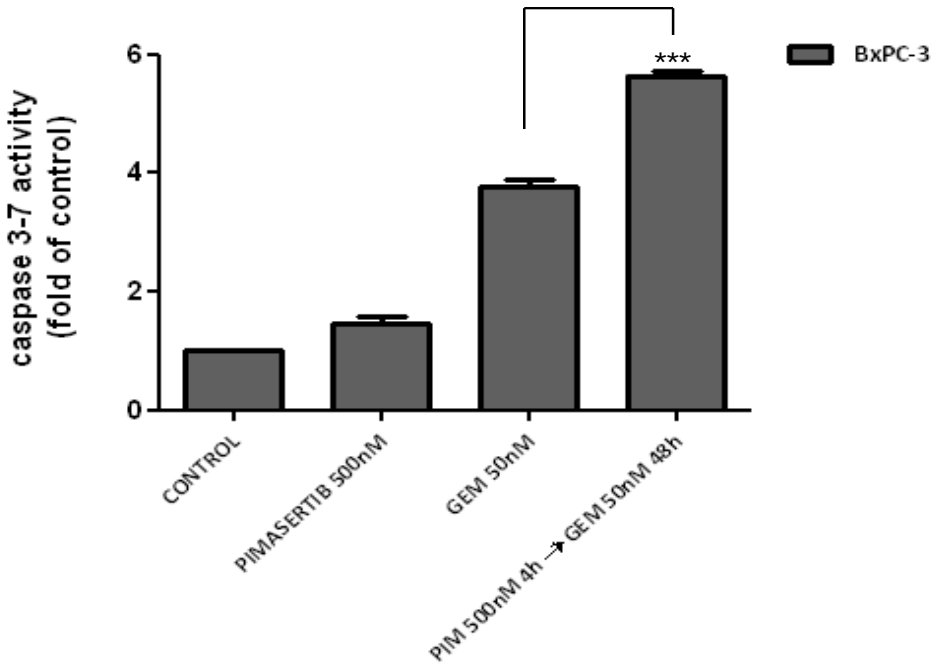

Figure 3.13: Pre-treatment with pimasertib enhances gemcitabine-induced apoptosis.

A. PANC-1 cells were pre-treated with 500nM pimasertib followed by 50nM gemcitabine for 48h. Apoptosis was assessed by measuring caspase 3-7 enzymatic activity. **B.** BxPC-3 cells were pre-treated with 500nM pimasertib followed by 50nM gemcitabine for 48h. Caspase 3-7 enzymatic activity was measured as an indicator of apoptosis induction. Results are presented as fold increase to untreated samples. Each experiment was repeated in triplicate and results are presented as mean, Error Bars ± SD. Stars indicate statistical significance of pimasertib combined with gemcitabine compared to gemcitabine alone (***P<0.001).

We next sought to investigate whether a higher concentration of gemcitabine would produce synergistic apoptotic activity when combined with pimasertib, independent of the time of administration. A 4-hour pre-treatment with 500nM pimasertib followed by 48 hour treatment with 100nM gemcitabine significantly enhanced gemcitabine-induced apoptosis as measured by the caspase 3/7 enzyme activity (from 3.5 ± 0.40 fold with gemcitabine alone to 5.0 ± 0.46 with the combination.) in BxPC-3 cells (Fig. 3.14A), similarly to what observed with 50nM gemcitabine (Fig. 3.13B). However, simultaneous combination of 500nM pimasertib with 100nM gemcitabine for 48 hours significantly reduced gemcitabine-induced apoptosis (from 4.27 ± 0.10 fold with gemcitabine alone to 2.26 ± 0.95 with the combination) in BxPC-3 cells (Fig. 3.14B), confirming the inefficacy of a simultaneous administration of gemcitabine with pimasertib.

A

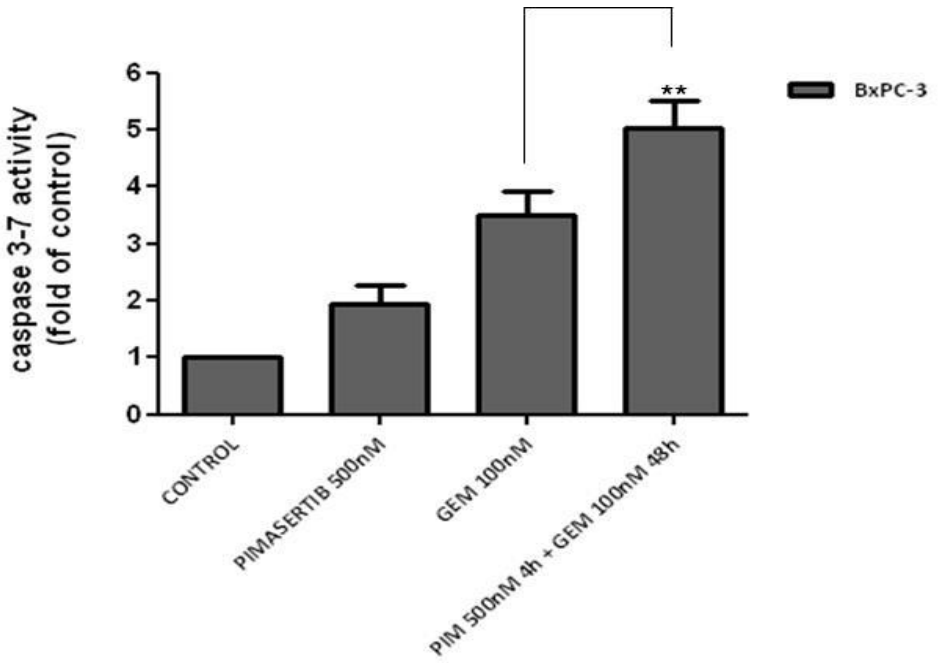

Figure 3.14: Sequential but not simultaneous combination of pimasertib with 100nM gemcitabine enhances gemcitabine-induced apoptosis.

A. BxPC-3 cells were pre-treated with 500nM pimasertib followed by 100nM gemcitabine for 48h. Caspase 3-7 enzymatic activity was measured as an indicator of apoptosis induction. Results are presented as fold increase to untreated samples. Each experiment was repeated in triplicate and results are presented as mean, Error Bars ± SD. Stars indicate statistical significance of pimasertib combined with gemcitabine when compared to gemcitabine alone (**P<0.01).

B

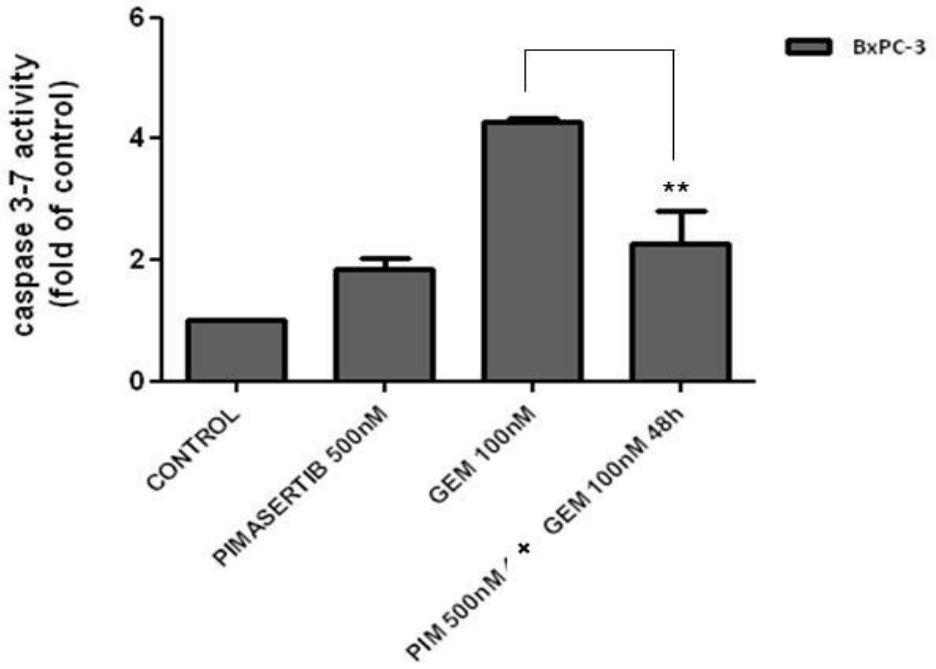

Figure 3.14 continued: Sequential but not simultaneous combination of pimasertib with 100nM gemcitabine enhances gemcitabine-induced apoptosis.

B. BxPC-3 cells were treated with 500nM pimasertib, plus 100nM gemcitabine for 48h. Caspase 3-7 enzymatic activity was measured as an indicator of apoptosis induction. Results are presented as fold increase to untreated samples. Each experiment was repeated in triplicate and results are presented as mean, Error Bars ± SD. Stars indicate statistical significance of pimasertib combined with gemcitabine when compared to gemcitabine alone (**P<0.01).

To further confirm that pimasertib enhances gemcitabine-induced apoptosis immunoblotting analysis was performed on BxPC-3 and PANC-1 cell lysates after sequential treatment with pimasertib plus gemcitabine. The apoptosis marker cleaved-PARP was more strongly induced in cells pre-treated with pimasertib (500nM) followed by gemcitabine (100nM) compared to gemcitabine or pimasertib alone (Fig. 3.15A). Bar graphs showing the quantification of C-PARP immunoblots are illustrated in Figure 3.15B.

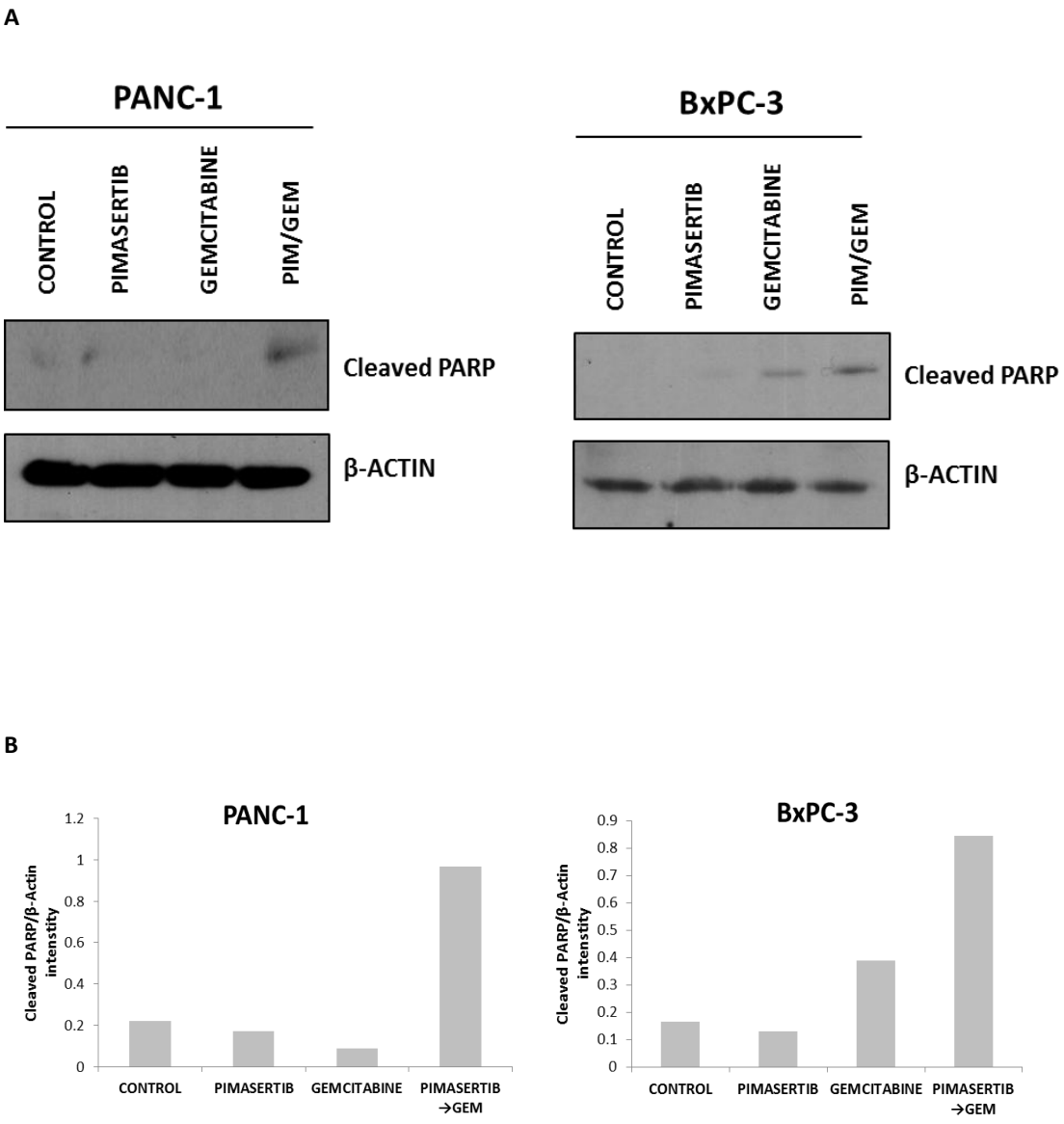

Figure 3.15: Pimasertib plus gemcitabine combination enhances cleaved-Parp expression.

A. PANC-1 and BxPC-3 cells were treated with 500nM pimasertib, 100nM gemcitabine or their combination for 24 hours. Protein levels of cleaved-PARP were analysed by immunoblotting. After drug treatment, proteins samples were extracted and analysed by immunoblotting with the indicated antibodies. β-Actin was used as loading control. **B.** Densitometric analysis of the immunoblots presented in Figure 3.15A. Image J software was used for the quantitation of the western blot bands. Fold increase of C-Parp was calculated by normalization to the loading control and comparison to the untreated sample.

3.3.6 Effects of pimasertib on the modulation of genes involved in gemcitabine resistance

To explore the molecular mechanism behind the synergistic activity observed between pimasertib and gemcitabine we investigated alterations of expression of genes involved in gemcitabine metabolism, transport or activity following pimasertib or gemcitabine treatment.

Cytidine Deaminase (CDA) is responsible for deactivating gemcitabine triphosphate (dFdCTP) by converting it into its inactive form difluorodeoxyuridine (dFdU) (Nakano et al. 2007). Preclinical work on pancreatic cancer mouse models has identified a mechanism by which nab-paclitaxel sensitizes to gemcitabine therapy, as a result of a ROS-mediated reduction in the protein levels of CDA (Frese et al. 2012). The effects of pimasertib and gemcitabine on CDA protein expression were explored. PANC-1 and BxPC-3 cells were treated for 24 hours with 1μM pimasertib, 50nM gemcitabine or their combination. Pimasertib alone caused a reduction of CDA protein expression in PANC-1 cells and to lesser extent in BxPC-3 cells; whereas gemcitabine increased CDA protein expression in BxPC-3 cells (Fig. 3.16). CDA protein levels were not altered upon the combination treatment (Fig. 3.16).

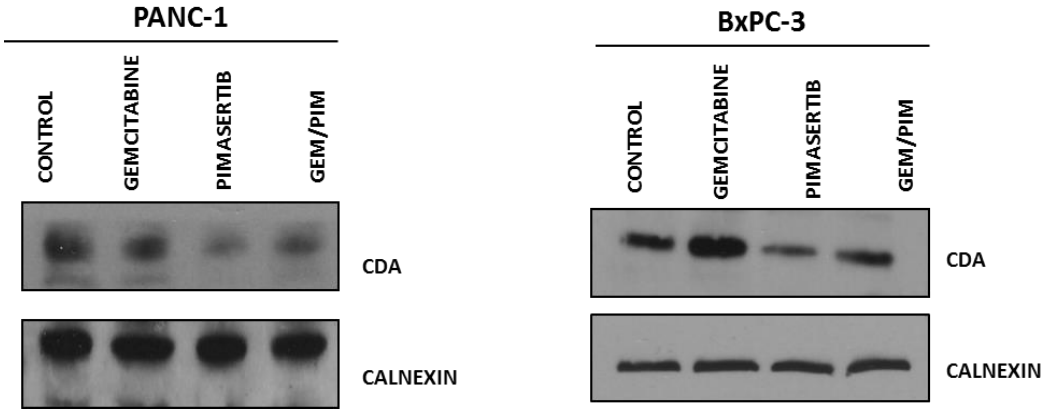

Figure 3.16: Effects of pimasertib on CDA protein levels.
BxPC-3 and PANC-1 cells were treated for 24 hours with 1μM pimasertib, 50nM gemcitabine alone or in combination with 1μM pimasertib. Total cell lysates were analysed by immunoblotting. Calnexin was used as loading control.

We then treated BxPC-3 cells for 24 hours with 1μM pimasertib, 50nM gemcitabine or their combination. The protein levels of RRM1, RRM2 and dCK were analysed by immunoblotting analysis. dCK protein expression was upregulated upon pimasertib and gemcitabine administration in BxPC-3 cells (Fig. 3.17A). RRM2 expression was reduced (Fig.3.17A), and this could be explained by the fact that its protein levels are low in the G1 phase of the cell cycle (Nordlund and Reichard 2006) as pimasertib induces a G1 arrest (Fig. 3.6). A slight decrease in RRM2 protein expression was observed with gemcitabine. Interestingly, treatment with pimasertib alone and in combination with gemcitabine reduced RRM1 protein levels (Fig. 3.17A). Bar graphs showing the quantification of RRM1 immunoblots are illustrated in Figure 3.17B.

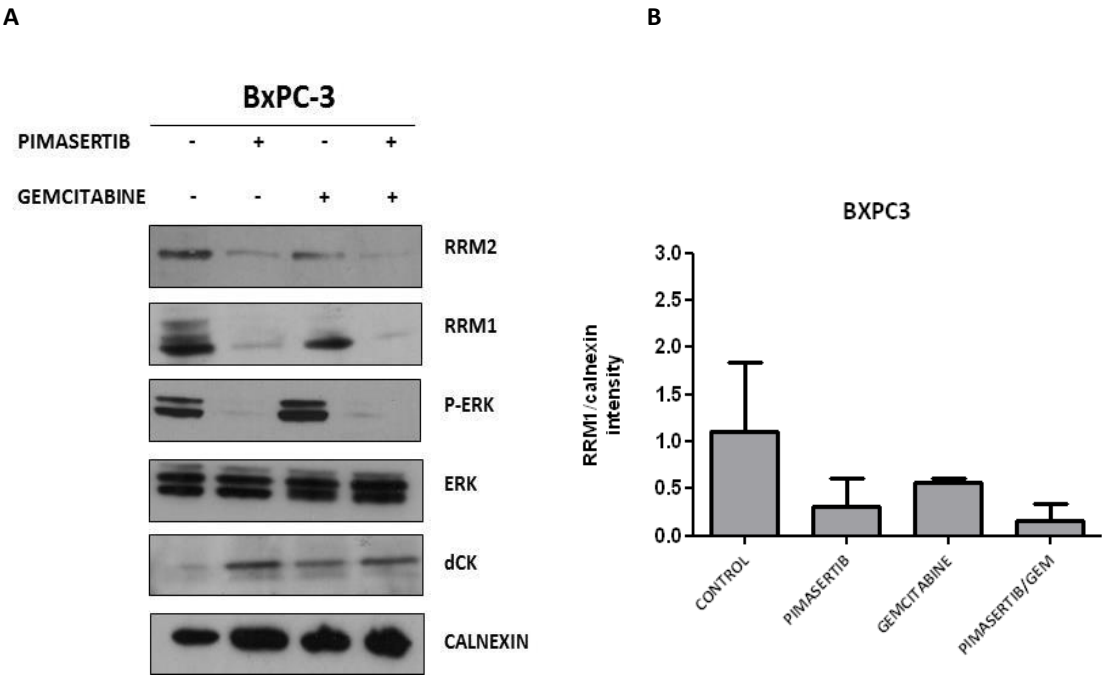

Figure 3.17: Pimasertib reduces RRM1 protein levels.

A. BxPC-3 cells were treated for 24 hours with 1μM pimasertib, 50nM gemcitabine alone or in combination with 1μM pimasertib. Total cell lysates were analysed by immunoblotting. Calnexin was used as loading control. **B.** Densitometric analysis of the immunoblots presented in Figure 3.17A. Results are presented as mean ± SD of three independent experiments. Image J software was used for the quantitation of the western blot bands. Fold decrease of RRM1 was calculated by normalization to the loading control and comparison to the untreated sample.

Downregulation of RRM1 protein was also observed in PANC-1 cell lines after 24h treatment with pimasertib alone or in combination with gemcitabine (Fig. 3.18) but no change in dCK or RRM2 protein expression was found upon gemcitabine or pimasertib (Fig. 3.18A). Bar graphs showing the quantification of RRM1 immunoblots are illustrated in Figure 3.18B.

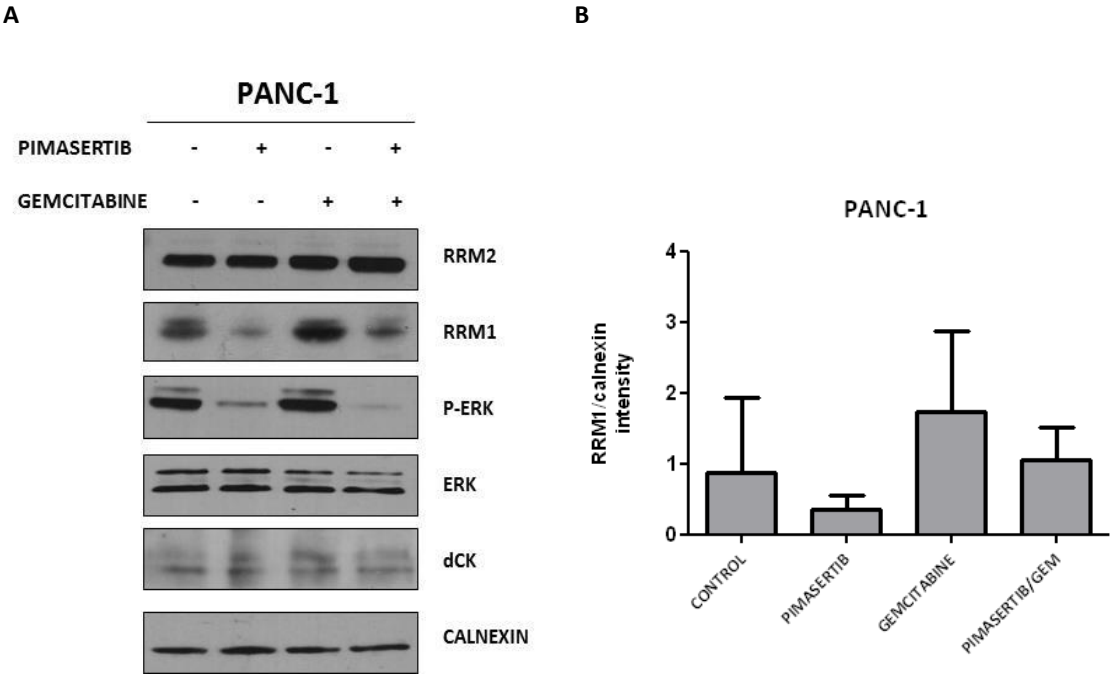

Figure 3.18: Pimasertib reduces RRM1 protein levels.
A. PANC-1 cells were treated for 24 hours with 1μM pimasertib, 50nM gemcitabine alone or in combination with 1μM pimasertib. Total cell lysates were analysed by immunoblotting. Calnexin was used as loading control. **B.** Densitometric analysis of the immunoblots presented in Figure 3.19A. Results are presented as mean ± SD of three independent experiments. Image J software was used for the quantitation of the western blot bands. Fold decrease of RRM1 was calculated by normalization to the loading control and comparison to the untreated sample.

Next, we investigated whether pimasertib induces RRM1 downregulation in other human pancreatic cancer cell lines. SUIT-2 and MIAPaCa-2 cell lines, which had been previously tested for gemcitabine sensitivity, were treated with 1μM pimasertib, 50nM gemcitabine or their combination for 24 hours and protein lysates were analysed by immunoblotting. Pimasertib alone and in combination with gemcitabine reduced RRM1 protein levels in both cell lines tested (Fig. 3.19).

Previous studies have shown that RRM1 protein expression was upregulated in gemcitabine resistant cells (Nakahira et al. 2007). In this present study, gemcitabine increased RRM1 protein levels in PANC-1 (Fig. 3.18), which displayed the highest resistance to gemcitabine, but also in MIAPaCa-2 and SUIT-2 sensitive cell lines (Fig. 3.19). No upregulation of RRM1 was observed in BxPC-3 cells after gemcitabine treatment.

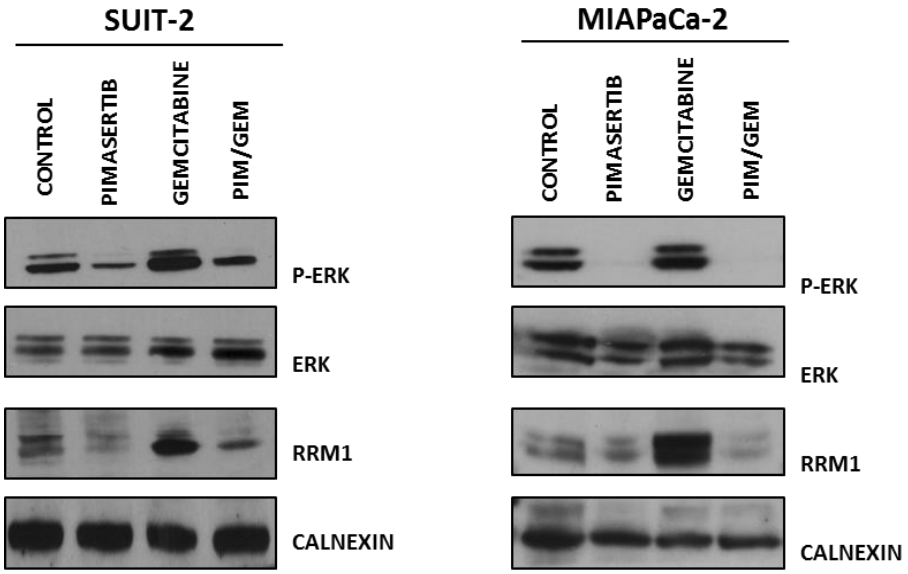

Figure 3.19: Pimasertib reduces RRM1 protein levels in other human pancreatic cancer cell lines.
SUIT-2 and MIAPaCa-2 cells were treated for 24 hours with 1μM pimasertib, 50nM gemcitabine alone or in combination with 1μM pimasertib. Total cell lysates were analysed by immunoblotting. Calnexin was used as loading control.

To explore whether the effect induced by pimasertib on RRM1 expression occurred with other MEK inhibitors, BxPC-3 cells were treated with AS703988 a potent, allosteric MEK1/2 inhibitor. AS703988 inhibited ERK phosphorylation at 1μM and showed the identical effect on RRM1 expression after 24 hours treatment (Fig. 3.20A). Inhibition of ERK phosphorylation and RRM1 protein expression was also observed when AS703988 was combined with gemcitabine (50nM) (Fig. 3.20A). Bar graphs showing the quantification of RRM1 immunoblots are illustrated in Figure 3.20B.

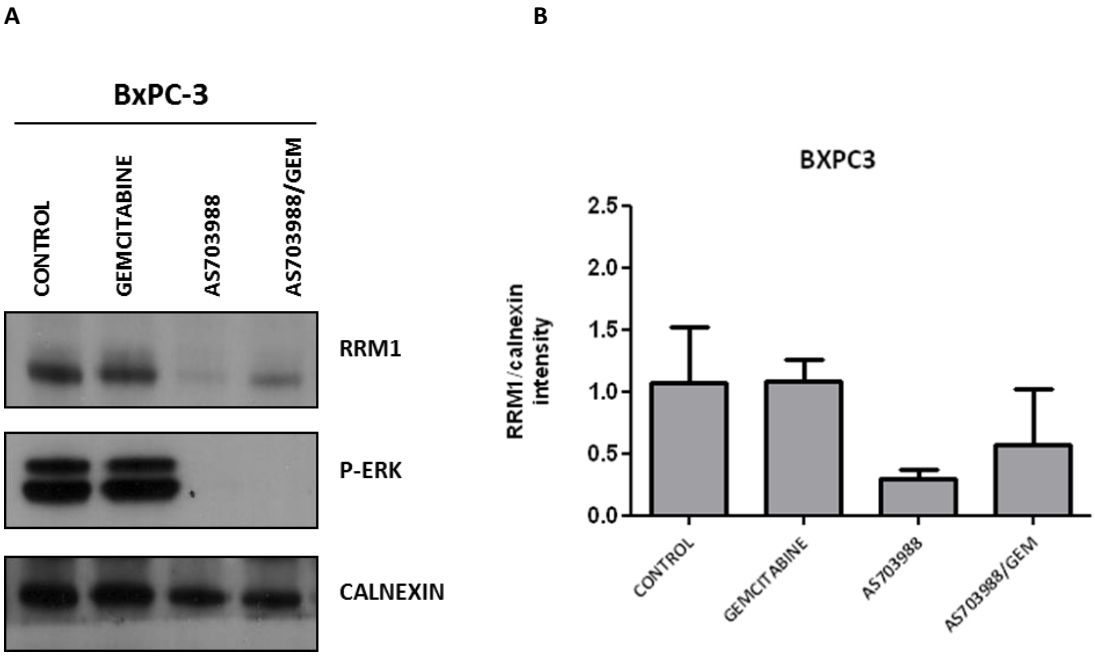

Figure 3.20: The MEK1/2 inhibitor AS703988 alters RRM1 protein expression.

A. BxPC-3 cells were treated for 24 hours with 1μM AS703988, 50nM gemcitabine alone or in combination with 1μM pimasertib. Total cell lysates were analysed by immunoblotting. Calnexin was used as loading control. **B.** Densitometric analysis of the immunoblots presented in figure 3.20A. Results are presented as mean ± SD of three independent experiments. Image J software was used for quantitation of the western blot bands. Fold decrease of RRM1 was calculated by normalization to the loading control and comparison to the untreated sample.

3.3.7 Downregulation of RRM1 protein expression induced by MEK inhibition occurs through a posttranslational modification

To determine whether the effect on modulation of RRM1 expression was specifically associated with inhibition of MEK protein an EGFR inhibitor (gefitinib), which blocks EGFR intracellular phosphorylation, was used to inhibit upstream MEK signalling.

BxPC-3 cells were treated with 1μM gefitinib for 30 minutes, 4 hours and 24 hours. Gefitinib reduced P-EGFR protein expression within 30 minutes after treatment, but did not alter RRM1 protein levels as shown by immunoblotting analysis (Fig. 3.21). Next, we asked whether biological inhibition of MEK protein would have an effect on RRM1 expression. To test this hypothesis we performed siRNA to knockdown the expression of MEK1 and MEK2. Immunoblotting analysis showed reduction of RRM1 protein expression following MEK1 and MEK2 knockdown in PANC-1 (Fig. 3.22A) and BxPC-3 cells (Fig. 3.22B), indicating that the effect on RRM1 protein expression is specifically due to on-target inhibition of MEK protein.

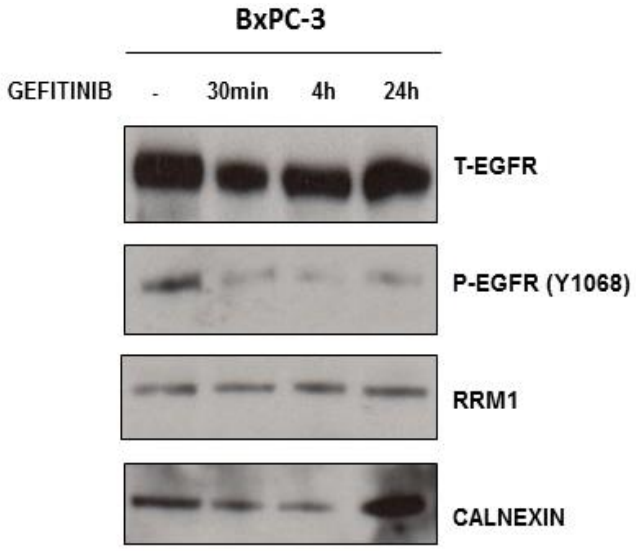

Figure 3.21: EGFR inhibition does not affect RRM1 protein expression.
BxPC-3 cells were treated with 1μM gefitinib and extracted at 30min, 4h and 24h. Total cell lysates were analysed by immunoblotting. Calnexin was used as loading control.

A

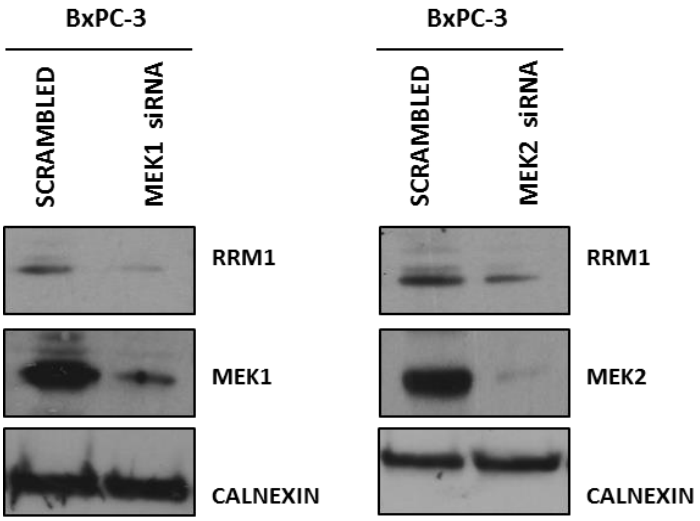

B

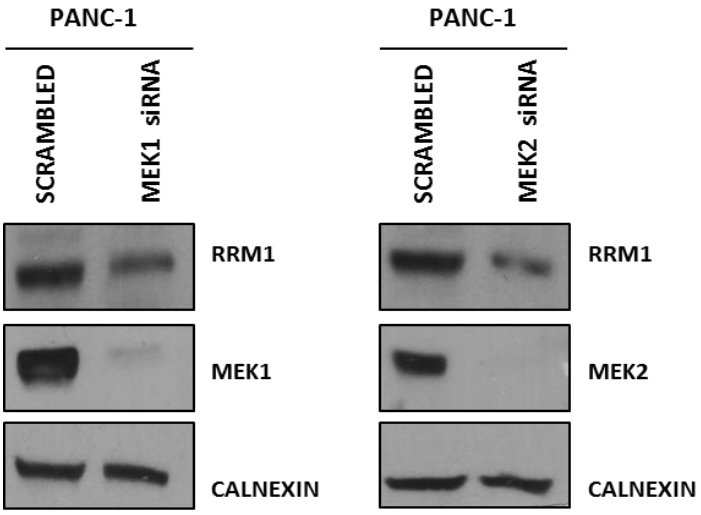

Figure 3.22: Knockdown of MEK1 and MEK2 by siRNA causes inhibition of RRM1 protein.
(A) BxPC-3 and **(B)** PANC-1 cells were transfected with 50nM siRNA targeting MEK1 and MEK2 for 72 hours. Total cell lysates were analysed by immunoblotting. Calnexin was used as loading control.

To assess if RRM1 down-regulation induced by pimasertib occurred at the transcriptional level, BxPC-3 and PANC-1 cells were treated with 1μM pimasertib for 24 hours and mRNA levels of RRM1 and RRM2 were analysed by RT-PCR. While the mRNA levels of RRM2 decreased after 24-hour treatment with pimasertib in BxPC-3 cells and remained constant in PANC-1 cells (Fig. 3.23), the mRNA levels of RRM1 were not significantly altered in BxPC-3 cells and were upregulated upon pimasertib treatment in PANC-1 cells (Fig. 3.24). The basal mRNA levels of RRM1 were higher in PANC-1 cells compared to BxPC3 cells (Fig. 3.24).

In contrast, immunoblotting analysis revealed a substantial reduction of RRM1 protein levels following only 4 hours treatment with pimasertib in BxPC-3 and PANC-1 cells, an effect that was not observed on RRM2 protein expression (Fig. 3.25). These results suggest that pimasertib reduces RRM1 through a post-translational modification.

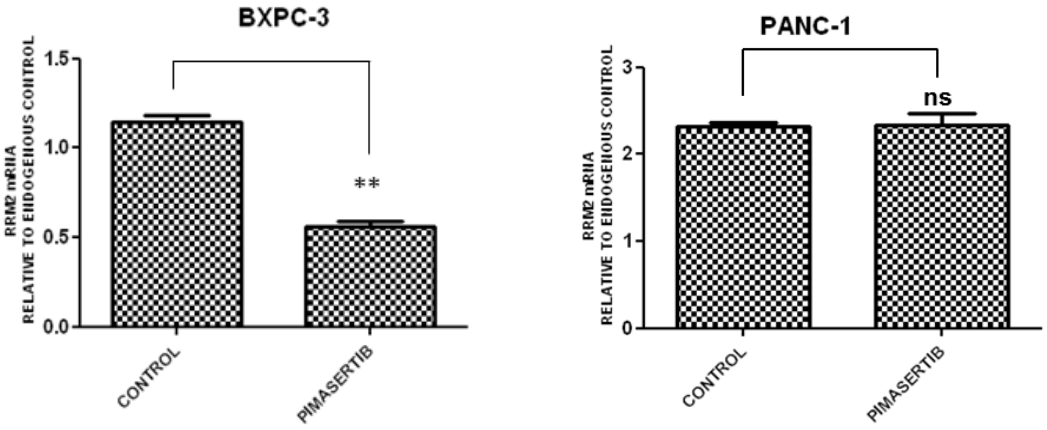

Figure 3.23: Pimasertib effect on RRM2 mRNA levels in BxPC-3 and PANC-1 cells.
Real-time PCR analysis of the mRNA expression of RRM2 in BxPC-3 and PANC-1 cells. Data represent the mean ± SD (n=3) from three independent experiments. Statistical analysis was performed with One Way Anova and Bonferroni post-test (**P<0.01, ns P>0.05).

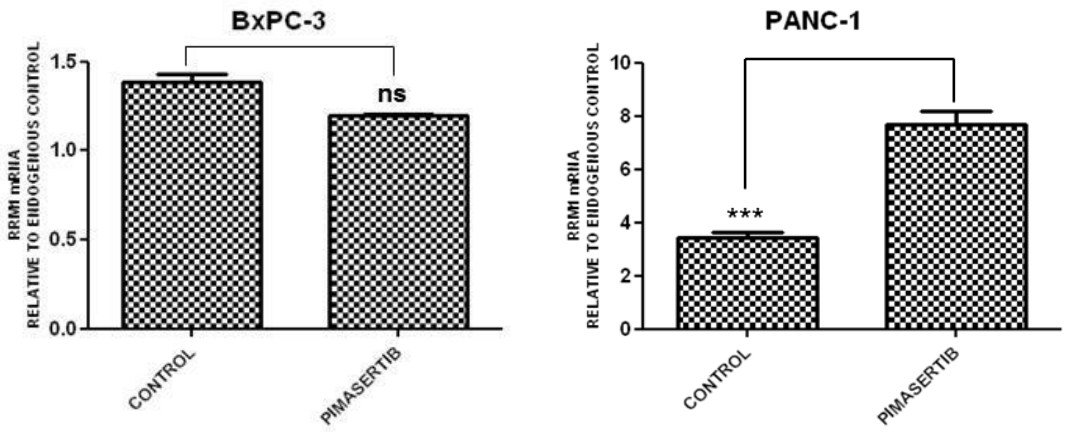

Figure 3.24: RRM1 mRNA levels are not affected by pimasertib in BxPC-3 and PANC-1 cells lines.
Real-time PCR analysis of the mRNA expression of RRM1 in BxPC-3 and PANC-1 cells. Data represent the mean ± SD (n=3) from three independent experiments. Statistical analysis was performed with One Way Anova and Bonferroni post-test (***P<0.001, **ns** P>0.05).

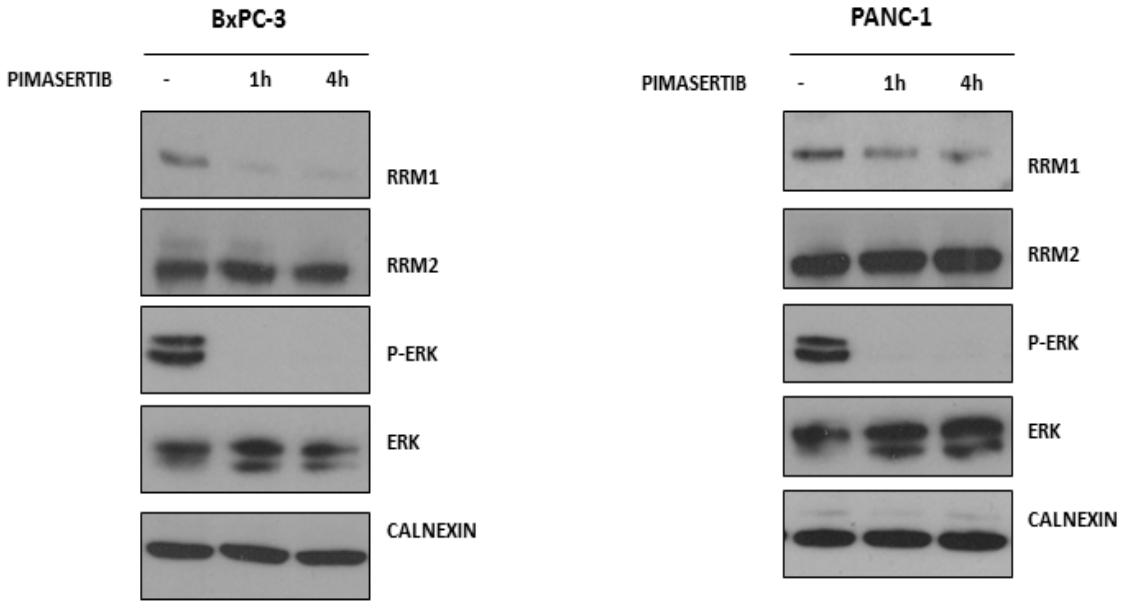

Figure 3.25: Pimasertib reduces RRM1 protein levels after a 4–hour treatment in BxPC-3 and PANC-1 cell lines.
BxPC-3 and PANC-1 cells were treated for 1 hour and 4 hours with 1µM pimasertib. Total cell lysates were analysed by immunoblotting. Calnexin was used as loading control. The experiment shown is representative of two independent experiments.

3.3.8 RRM1 basal protein expression predicts gemcitabine efficacy

To explore whether a correlation existed between gemcitabine cytotoxicity and RRM1 basal expression in human pancreatic cancer cell lines, the IC_{50} values of each cell line were compared with their basal levels of RRM1 protein. Gemcitabine IC_{50} values of each cell line were calculated as previously described (Table 3.2). RRM1 protein expression was analysed by immunoblotting (Fig. 3.26A) and quantified by densitometry (Fig. 3.26B). PANC-1 cells exhibited the highest expression of RRM1 protein and were the most resistant to gemcitabine treatment.

Cell lines	Gemcitabine IC_{50}
PANC-1	10.9μM
MIAPaCa-2	69.44nM
BxPC-3	40.97nM

Table 3.2: IC50 values of BxPC-3, MIAPaCa-2 and PANC-1 cell lines.
BxPC-3, PANC-1 and MIAPaCa-2 cells were treated with increasing concentrations of gemcitabine for 96 hours. MTT assay was assessed to determine cell viability and IC50 values were calculated.

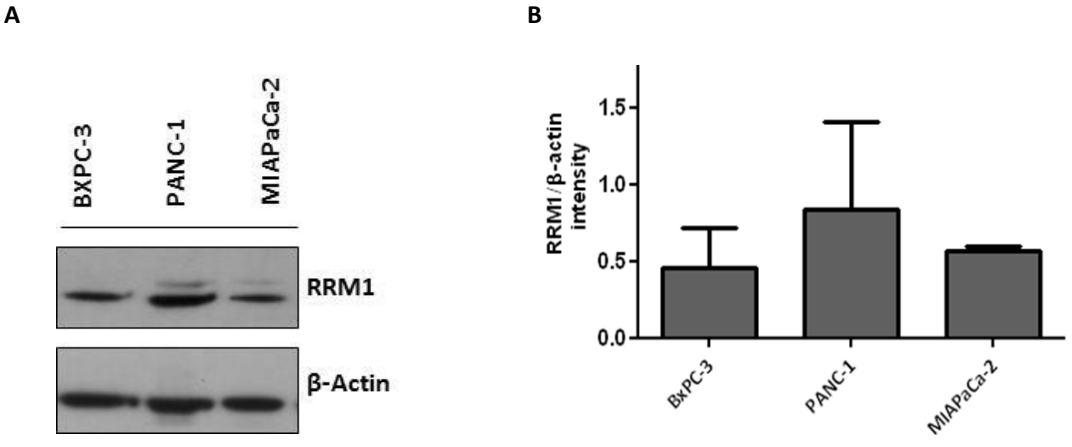

Figure 3.26: RRM1 expression correlates with pancreatic cancer cell sensitivity to gemcitabine.
A. Basal RRM1 protein expression of BxPC-3, PANC-1 and MIAPaCa-2 cell lines was analysed by immunoblotting. β-Actin was used as loading control. **B.** Densitometric analysis of the immunoblots presented in figure 3.28A. Results are presented as mean ± SD of three independent experiments. Image J software was used for the quantitation of the western blot bands.

3.3.9 Inhibition of RRM1 expression by siRNA sensitizes BxPC-3 and PANC-1 cells to gemcitabine

Previous studies have shown that inhibition of RRM1 by siRNA increases gemcitabine efficacy in NSCLC cell lines and sensitizes RRM1-overexpressing mice to gemcitabine cytotoxicity, suggesting that RRM1 is a potential target of chemosensitization (Wonganan et al. 2012).

To confirm RRM1 expression effects on gemcitabine response, BxPC-3 and PANC-1 cells were transfected with specific siRNA against RRM1 for 72h prior to gemcitabine treatment. Immunoblotting analysis was performed and demonstrated that RRM1 specific-siRNA efficiently inhibited RRM1 protein expression in PANC-1 cells (Fig. 3.27A) and BxPC-3 cells (Fig. 3.28A). RRM1 siRNA transfected cells were then treated for 48 hours with 100nM gemcitabine, after which apoptosis was assessed as previously described in section 3.3.5. PANC-1 cells transfected with RRM1 siRNA exhibited enhanced apoptosis upon gemcitabine treatment compared to cells treated with scrambled, as levels of caspase 3/7 activity increased from 2.1 ± 0.42 fold to 4.1 ± 0.93 (Fig. 3.27B). Furthermore, knockdown of RRM1 with siRNA enhanced apoptosis also without drug treatment in PANC-1 cells, suggesting that depletion of RRM1 is cytotoxic in these cell lines (Fig. 3.27B).

Gemcitabine treatment induced a significantly higher apoptotic effect in BxPC-3 cells transfected with RRM1 siRNA compared to cells transfected with scrambled as shown by levels of caspase 3/7 activity (from 6.30 ± 0.91 to 9.71 ± 4.1) (Fig. 3.28B). Additionally, RRM1 knock-down cells treated with gemcitabine exhibited higher levels of cleaved caspase-3 activation compared to RRM1 knock-down cells that did not receive any drug treatment (from 0.96 ± 0.14 to 9.60 ± 1.32) (Fig. 3.28B).

These results confirm the role of RRM1 expression in modulating human pancreatic cancer cells sensitivity to gemcitabine treatment.

A

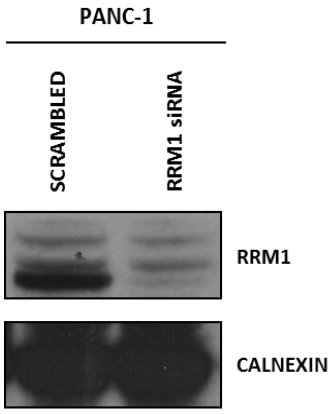

B

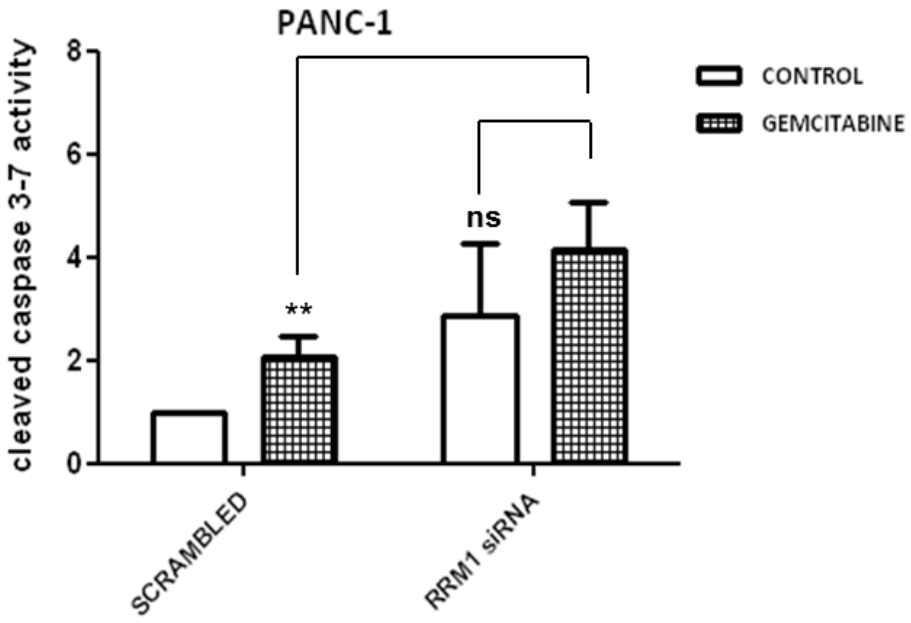

Figure 3.27: RRM1 downregulation sensitizes PANC-1 response to gemcitabine.

A. PANC-1 cells were transfected with 50nM siRNA targeting RRM1 or scrambled for 72 hours and immunoblotted with the indicated antibodies. Calnexin was using as loading control. **B.** Scrambled and RRM1 transfected cells were treated with 100nM gemcitabine for 48 hours after which Caspase 3/7 activity was measured to detect apoptosis. Results are presented as fold increase relative to untreated sample and are shown as mean ± SD (n=3). Stars indicate a significant increase in apoptosis (**, P<0.01) after gemcitabine treatment in PANC-1 cells transfected with RRM1 siRNA compared to cells transfected with scrambled.

A

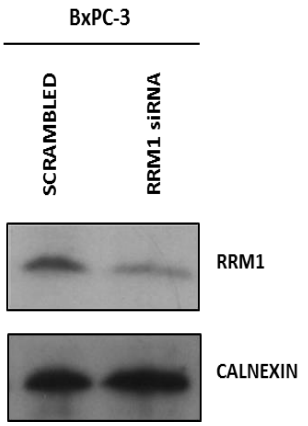

B

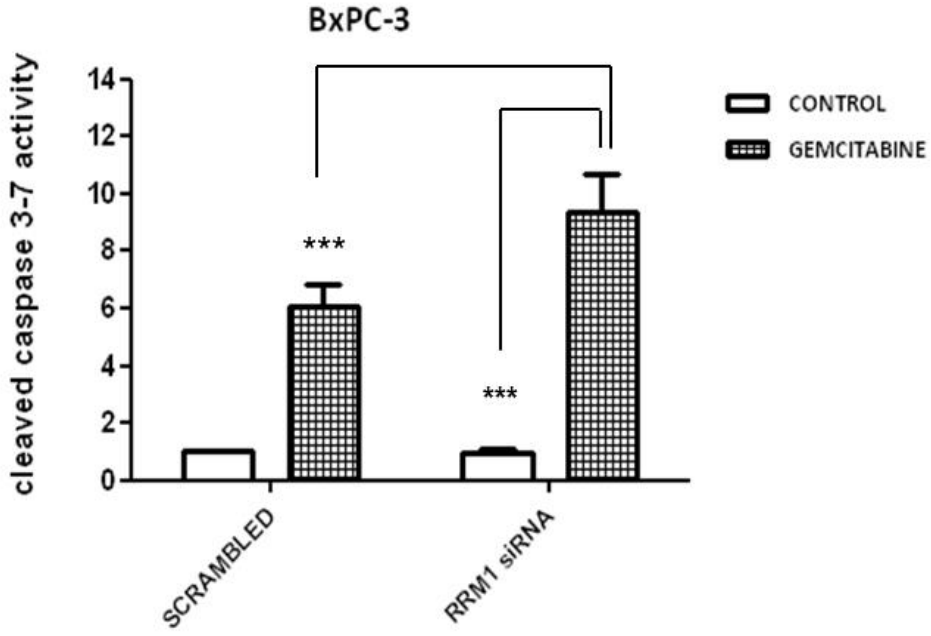

Figure 3.28: RRM1 downregulation sensitizes BxPC-3 response to gemcitabine.

A. BxPC-3 cells were transfected with 50nM siRNA targeting RRM1 or scrambled for 72 hours and immunoblotted with the indicated antibodies. Calnexin was using as loading control. **B.** Scrambled and RRM1 transfected cells were treated with 100nM gemcitabine for 48 hours after which Caspase 3/7 activity was measured to detect apoptosis. Results are presented as fold increase relative to untreated sample and are shown as mean ± SD (n=3). Stars indicate a significant increase in apoptosis (***, $P<0.001$) after gemcitabine treatment in BxPC-3 cells transfected with RRM1 siRNA compared to cells transfected with scrambled and between RRM1-transfected cells non-treated and treated with gemcitabine.

3.4 DISCUSSION

3.4.1 Improving gemcitabine efficacy with MEK inhibitors

The combination of cytotoxic agents with molecular-targeted agents has been the focus of intense study for cancer therapy and has the aim to reduce the acquired resistance to conventional chemotherapy, to lower the doses of highly cytotoxic drugs or to sensitize the action of one drug with the use of another drug (Fitzgerald et al. 2006). Importantly, the combination of two or more drugs aims to achieve a synergistic effect on cell growth inhibition or cell killing compared to single drugs alone. Combinations can include drugs that inhibit a single target, the same signalling pathway but at different levels or two distinguished pathways (Fitzgerald et al. 2006).

In the locally advanced and metastatic setting, the chemotherapeutic agent gemcitabine represents an important standard of care for PDAC patients but the overall surival still remains very low (Seufferlein et al. 2012).

Inhibition of downstream effectors of RAS, such as MEK protein has provided clinical benefit against human tumors (Flaherty et al. 2012). Mutant BRAF melanoma cells rely on ERK for survival (Balmanno and Cook 2009), thus BRAF inhibitors are commonly used for the treatment of metastatic melanoma patients carrying a BRAF mutation since they inhibit ERK signalling in cells with activating mutations of BRAF; however, in most patients, BRAF inhibitors have short efficacy as the tumour reccurs. This is the case of melanoma cells because they are able to overcome BRAF inhibition (Cheng et al. 2013). A Phase III trial involving the MEK inhibitor trametenib was performed on patients with metastatic melanoma harbouring BRAF V600E or V600K mutation that had not previously received BRAF or MEK inhibitors. Trametenib-treated patients showed longer PFS of 4.8 months vs 1.5 months (HR of 0.45, 95% confidence interval (CI), 0.33-0.63 $P<0.01$) and OS rate at 6 months was 81% vs 67% compared to patients receiving only chemotherapy (dacarbazine or paclitaxel) (HR for death = 0.54, 95% confidence interval (CI), 0.32-0.92 $P<0.01$) (Flaherty et al. 2012).

A large Phase II trial was later conducted to investigate the efficacy of trametenib in combination with BRAF inhibitors. Although the adverse effects associated with MEK inhibition were more frequent upon combination treatment, a significant

improvement in PFS was achieved when trametinib was added to BRAF inhibitors. The results allowed the FDA approval of trametenib for clinical use for patients with metastatic melanoma harbouring BRAF V600E/K mutation both as monotherapy and in combination with the BRAF inhibitor dabrafenib (Flaherty et al. 2012). No other MEK inhibitors have so far gained approval by the FDA to be used in the clinic.

In this present study the effects of combining an allosteric MEK1/2 inhibitor (pimasertib) with gemcitabine was evaluated in human pancreatic cancer cell lines. Gemcitabine showed antiproliferative activity with different sensitivities among the human pancreatic cancer cell lines tested (Fig. 3.1). Pimasertib inhibited cellular proliferation (Fig. 3.5) and induced specific target modulation by inhibiting P-ERK signalling in a dose and time dependent fashion (Fig. 3.3-3.4).

Different schedules of drugs administration were evaluated to determine the effects of gemcitabine plus pimasertib in combination. Interestingly, the order in which pimasertib and gemcitabine were administered influenced the cellular response to these agents. In fact, only a short pre-treatment with pimasertib followed by gemcitabine induced synergistic antiproliferative (Fig. 3.9, 3.10, 3.11) and increased apoptosis (Fig. 3.13-3.14A). On the other hand, additive or antagonistic antiproliferative activity and no enhancement of apotosis was observed upon simultaneous administration of the two agents (Fig. 3.7, 3.8, 3.12, 314B) in all cell lines tested. To support these results, an increase in the expression of the apoptotic marker cleaved caspase-3 was also observed upon sequential combination of pimasertib with gemcitabine (Fig. 3.15).

Previous reports have demonstrated how scheduling affects drug treatments. A preclinical study on biliary cancer models aimed to investigate the cytotoxic effects induced by the combination of the MEK inhibitor selumetinib (AZD6244) with gemcitabine. Pre-treatment with selumetinib followed by gemcitabine enhanced the cytotoxicity of the latter, as opposed to simultaneous treatment that did not show any synergistic cytotoxic effect (Xu et al. 2013). The MEK inhibitor led to an accumulation of cells in G1, thus blocking the progression into DNA synthesis where gemcitabine acts. (Xu et al. 2013). The results obtained in this study could draw interest in the antagonism observed in our study after simultaneous treatment of pimasertib with

gemcitabine, since pimasertib caused an accumulation of cells in G1-phase of the cell cycle (Fig. 3.6).

3.4.2 RRM1 protein expression is modulated by MEK inhibition

A limitation of gemcitabine-based therapy is the rapid development of resistance (Nakano et al. 2007). The identification of biomarkers associated with tumor sensitivity to gemcitabine is of high importance to predict patients' response and allow patients' stratification. Furthermore, biomarkers are important in the development of new therapeutic targets (Colburn 2003).

Several studies have demonstrated that modulation of expression of genes that regulate gemcitabine metabolism, transport or mechanism of action can significantly enhance its efficacy (Ogawa et al. 2005, Giovannetti et al. 2006). The ribonucleotide reductase (RR) enzyme catalyses the production of dNTP pools required for new DNA synthesis and repair (Nordlund and Reichard 2006). Several studies have now established that overexpression of RR large subunit 1 (RRM1) is associated with poor response to gemcitabine treatment (Nakahira et al. 2007). Excessive production of dNTP pools produced by RR competes with gemcitabine for incorporation into DNA (Duxbury et al. 2004). Furthermore, RRM1 inhibits the activity of dCK, thus impairing gemcitabine activation (Heinemann et al. 1990).

Previous investigators have demonstrated how modulation of RRM1 or RRM2 expression affects cellular sensitivity to gemcitabine. For example, RRM1 knock down using specific siRNA enhanced sensitivity to gemcitabine both *in vitro* and in cancer mouse models (Nakahira et al. 2007) (Wonganan et al. 2012). Silencing RRM2 with specific siRNA has been reported to enhance gemcitabine-induced cytotoxicity in PDAC cell lines through decrease of NF-kB activity. Furthermore, systemic treatment of RRM2 siRNA in combination with gemcitabine induced a marked suppression of tumor growth accompanied by inhibition of liver metastasis in a mouse xenograft model of pancreatic cancer (Duxbury et al. 2004).

Analysis of pimasertib effects on multiple genes associated with gemcitabine resistance was performed. Interestingly, pimasertib induced a striking reduction of

RRM1 protein levels in all cell lines tested (Fig. 3.17-19). The same effect on RRM1 downregulation was observed with another allosteric MEK1/2 inhibitor (AS703988) (Fig. 3.20) but did not occur in response to an EGFR inhibitor (Fig. 3.21), Furthermore MEK1/2 knock down by siRNA caused a reduction of RRM1 protein expression (Fig. 3.22) indicating that this effect is specifically dependent on MEK inhibition.

Previous reports have observed modulation of RR activity by MEK signalling. Activation of MEK2 protein by serum stimulation increased RR activity by interacting with and regulating the P53R2 subunit, an effect that was impaired by specific inhibition of MEK2. Rapid activation of P53R2 upon MEK2 stimulation allowed efficient production of dNTP pools for prompt DNA repair, which would normally occur over a much longer period of time (Piao et al. 2012).

Another study found a correlation between poor survival and high expression of RRM1 in gastric cancer patients. Interestingly, downregulation of RRM1 using specific siRNA reduced P-MEK and P-ERK levels accompanied by inhibition of gastric cancer cells growth and invasion, indicating RRM1-induced proliferation through activation of MEK signalling (Wang et al. 2013).

Our results showed that RRM1 mRNA expression levels were not reduced by addition of pimasertib (Fig. 3.23-3.24). On the other hand, a reduction of RRM1 protein was observed after a short exposure (4 hours) to pimasertib (Fig. 3.25). These results could also in part explain why the 4-hour pre-treatment with pimasertib is required to sensitize pancreatic cancer cells to gemcitabine cytotoxicity.

Finally, we explored whether inhibition of RRM1 expression would alter human pancreatic cancer cells' response to gemcitabine. As expected, we observed enhanced gemcitabine cytotoxicity in RRM1 depleted cells (Fig. 3.27-3.28), confirming that RRM1 expression affects gemcitabine response. These results are in agreement with previous studies showing that RRM1 inhibition potentiated chemosensitivity to gemcitabine both *in vitro* and *in vivo* (Wonganan et al. 2012) (Nakahira et al. 2007).

3.5 CONCLUSIONS

The results presented in this chapter indicate different sensitivity of human pancreatic cancer cell lines to both gemcitabine and pimasertib and efficient inhibition of ERK activation upon MEK inhibition. The interaction between pimasertib and gemcitabine was investigated and the results indicate MEK as a potential target to enhance gemcitabine efficacy in human PDAC cell lines. Importantly, sequential but not simultaneous administration of pimasertib followed by gemcitabine produced synergistic anti-proliferative and pro-apoptotic effects, underlining the importance of dose and duration of drug treatments in achieving efficacious antitumor activity. The results shown suggest that the enhanced sensitivity to gemcitabine cytotoxicity obtained by a pre-exposure to pimasertib could be explained by its ability to modulate RRM1 protein expression.

These preclinical investigations, which demonstrated that the schedule of administration significantly impacted the mechanism of the combination and, consequently, the efficacy of the combination *in vitro* were performed after the Phase I/II trial examining pimasertib in combination with gemcitabine (which were administered simultaneously) in PDAC patients was initiated (Van Cutsem E, et al. 2015). While clinical data for combinations of MEK inhibitors, like pimasertib, with gemcitabine have been disappointing up to now, we suggest that a modified approach may be considered in future studies, such as using preclinical studies to optimize the right combination therapy schedule before proceeding to clinical trials. Moreover, the establishment of molecular therapies targeting RRM1 should be further explored in the future both in preclinical and clinical settings to enhance the activity of gemcitabine in PDAC patients.

The ability of pimasertib to inhibit RRM1 expression, which has been described in this chapter, is of crucial importance since its expression is associated with gemcitabine resistance and the mechanism by which this occurs will be further investigated in the next chapter.

CHAPTER 4

PIMASERTIB INDUCES POLYUBIQUITINATION AND PROTEASOMAL DEGRADATION OF RRM1

4.1 INTRODUCTION

4.1.1 The Ubiquitin-Proteasome System (UBS): biology and mechanisms

Proteins are subject to a great variety of post-translational modifications. One of them is the formation of a transient bond between a small protein called ubiquitin and a target protein, which is carried out by an enzymatic system: the ubiquitin proteasome system (UPS) (Hochstrasser 2009) (Fig. 4.1).

The UPS machinery depends on metabolic energy for its function and is often used by eukaryotic cells for protein degradation. Other ways in which cells degrade proteins and organelles is through the lysosome, where they are engulfed and degraded by lysosome proteases, or through non-lysosomal proteolysis systems (Almond and Cohen 2002).

The UPS is composed of two main elements: a protein complex referred as the proteasome and a 76 amino acid protein (ubiquitin). Before being degraded by the proteasome, the target protein has to be tagged by ubiquitin (Dahlmann 2007) (Fig. 4.1). This process occurs through three consecutive biochemical steps: in the first step, the cysteine residue of an E1 enzyme (also called ubiquitin-activating enzyme) forms a thioester bond with the C-terminus of ubiquitin through an ATP-dependent reaction. The thioester-linked ubiquitin is then transferred to a cysteine residue of an E2 conjugating enzyme. In the last step, an E3 ligase enzyme catalyses the formation of a covalent bond between the cysteine residue of ubiquitin and the lysine residue of a target protein (Almond and Cohen 2002)(Fig. 4.1).

E3 enzymes can interact with more than one protein substrates at the same time and they determine substrate specificity in the ubiquitination process since they recognize the target protein that will be ubiquitinated (Almond and Cohen 2002). There are two types of E3 ligases. The first type forms a thioester intermediate with ubiquitin and they are called HECT (homology to E6-AP C-terminus) domain ligases. The second type has a RING finger domain and associates directly with the target protein (Lilienbaum 2013). Ubiquitin elongation occurs through the addition of one or more ubiquitin proteins to the first one. Ubiquitin chains are formed through several lysine residues (k11, k27, k29, k6, k33, k48, k63). The different ubiquitin linkages attached to the target protein determines the fate of that protein (Hochstrasser 2009). For example,

substrates that are polyubiquitinated via lys48 ubiquitin chains are recognized by the proteasome for degradation. In the final step, the target protein is then transferred into the proteasome. This complex is composed of a core (20S) and a regulatory subunit (19S). The 20S subunit is made of 4 heptameric rings: two α rings on the outside and two β inner rings, which contain the catalytic sites for peptide bonds cleavage (Orlowski and Wilk 2000). The 19S subunit contains ubiquitin receptors, regulates substrates entry into the proteasome and removes ubiquitin from the target protein. Proteins are unfolded and degraded into short peptides. In addition, ubiquitin proteins are released by deubiquitinating enzymes (DUBs) and can be reused (Hershko and Ciechanover 1998).UPS regulates several processes such as cell division, apoptosis, signal transduction and gene expression, thus its activity is essential for maintaining cell integrity (Hershko and Ciechanover 1998).

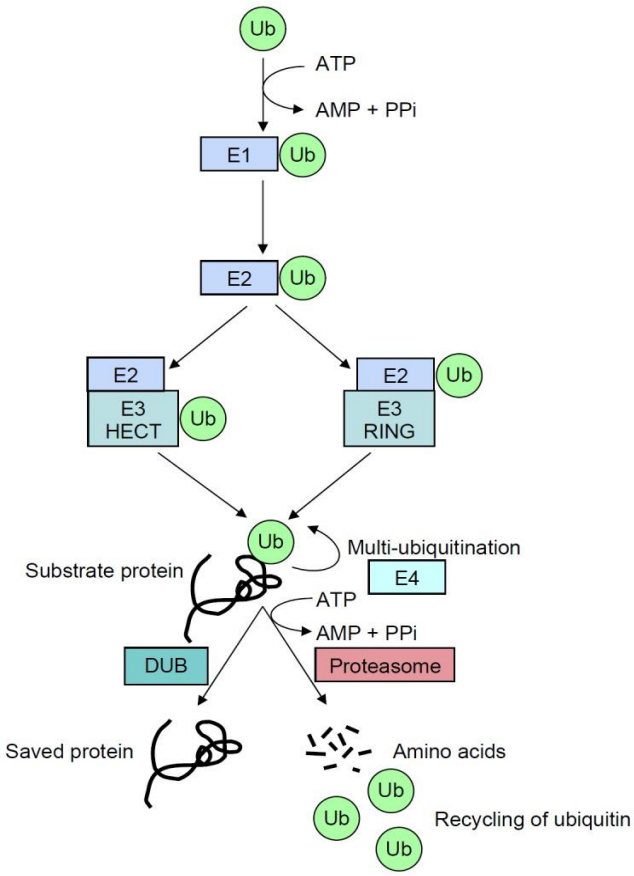

Figure 4.1: The ubiquitin-proteasome pathway.
Ubiquitin (Ub) is attached to an E1 activating enzyme through an ATP dependent process. This reaction leads to a subsequent binding of ubiquitin to an E2 conjugating enzyme. E3 ligase catalyses the formation of an isopeptide bond between Ub and the substrate protein, which is recognized by the proteasome, unfolded and degraded (Lilienbaum 2013).

4.1.2 AKT/PI3K signalling pathway

Phosphoinositide 3-kinases (PI3Ks) are a family of lipid kinases whose main mediator is represented by the serine/threonine kinase AKT that exists in three different variations: AKT1, AKT2 and AKT3 (Hers et al. 2011). PI3 kinases are divided into three different classes. PI3K class IA, the most implicated in human cancers, is a heterodimer composed of a catalytic subunit (p110) and an adaptor/regulatory subunit (p85). The PI3/AKT signalling pathway (Fig. 4.2) is activated by receptor tyrosine kinases (RTKs) or G-protein coupled receptors (GPCR) and sends signal to downstream molecules that ultimately regulate several cellular processes such as proliferation, differentiation and survival (Hers et al. 2011) (Engelman 2009) (Montagut and Settleman 2009). Following RTK activation, PI3K is recruited directly or through docking proteins to the cell membrane where it catalyses the conversion of phosphatidylinositol-4,5-biphosphate (PIP_2) into phosphatidylinositol-3,4,5-triphosphate (PIP_3). PIP_3 mediates the recruitment of AKT and 3-phosphoinositide-dependent kinase-1 (PDK1), which partially activates AKT through phosphorylation on threonine 308. Complete activation of AKT occurs upon phosphorylation of serine 473 from the second mTOR complex (mTORC2). Once AKT is activated, it phosphorylates many proteins involved in different cellular processes such as mTORC1. The phosphatase and tensin homologue (PTEN) is responsible for the negative regulation of this pathway by dephosphorylating PIP_3 thus impairing AKT activation (Mendoza et al. 2011).

4.1.3 PI3K/AKT signalling pathway is deregulated in human cancers

Deregulation of the PI3K/AKT signalling pathway frequently occurs in human cancers and can be caused by several factors:

1) Hyperactivation of the upstream receptor tyrosine kinase (RTK) (such as EGFR)
2) Activating mutations in the catalytic subunit of PI3K (PIK3CA or P110α)
3) Loss of PTEN expression (Vivanco and Sawyers 2002)

Although not a common event, PIK3CA mutation has been reported in pancreatic tumors and even in absence of detectable alterations within the PIK3CA gene, this

pathway is often constitutively activated in PDAC due to loss of PTEN gene (Asano et al. 2004). Furthermore, AKT2 kinase has been found to be overexpressed in 60% of pancreatic cancers (Altomare et al. 2002).

Previous evidence has demonstrated the importance of this pathway in pancreatic cancer (Reichert et al. 2007, Ying et al. 2011). For example, a preclinical study on pancreatic cancer GEM models has indicated that the introduction of an activating mutation of PI3K is critical for tumor maintenance upon loss of oncogenic K-RAS function (Lim and Counter 2005).

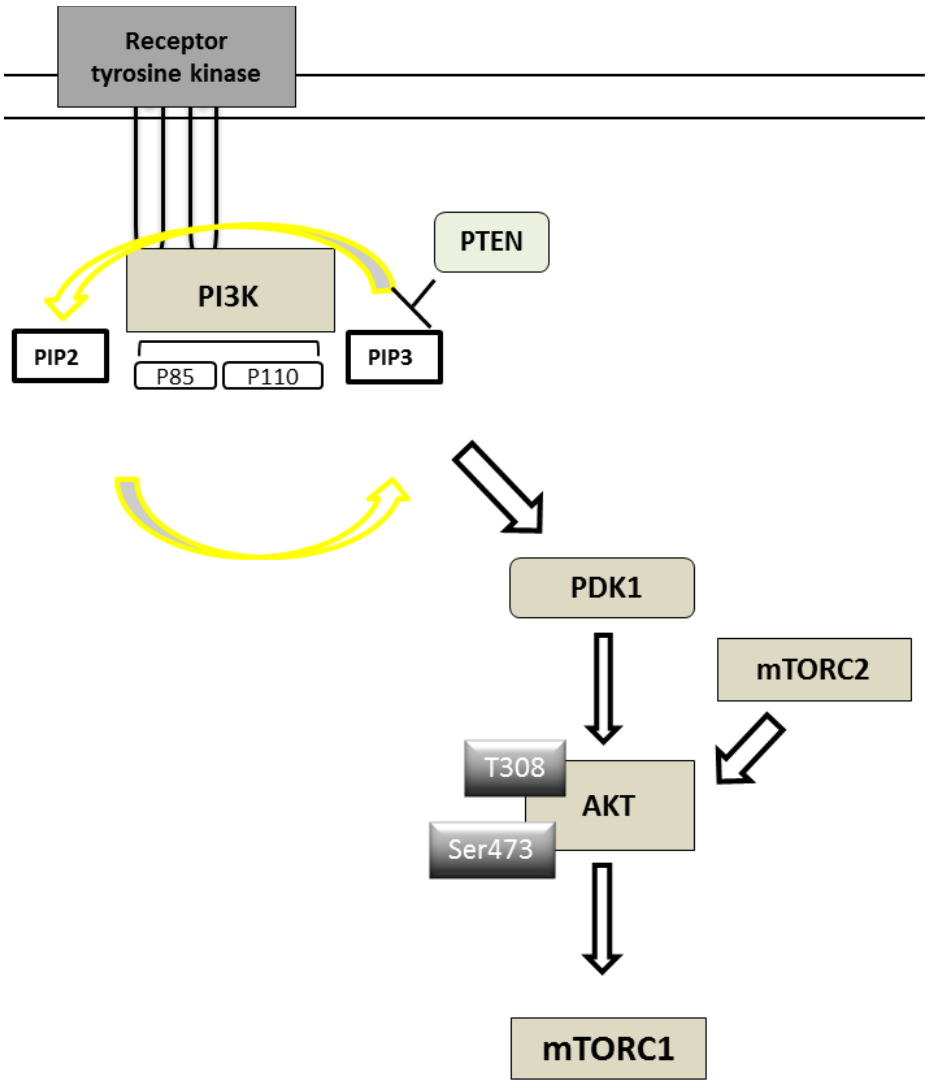

Figure 4.2: PI3K/PDK1/AKT signalling pathway.
Receptor tyrosine kinases (RTKs) activate downstream molecules such as K-RAS. PI3K is recruited and converts phosphatidylinositol-4,5-biphosphate (PIP_2) into its triphosphate form (PIP_3). PIP_3 activates AKT, which in turns activates mTOR.

Compensatory cross talk occurs between different effector pathways activated by oncogenic K-RAS. The RAS/RAF/MAPK and PI3K/AKT signalling pathways interact with each other through various negative feedback loop mechanisms (Liu et al. 2009). For example, an *in vitro* study identified a mechanism of feedback activation of AKT signalling by MEK inhibition, which occurs through blockade of the ERK-inhibitory effect on PI3K recruitment to the EGF receptor (Zhang et al. 2002).

Another report has observed that MEK depletion induced inhibition of a negative feedback loop on ERBB3 receptors, which led to the activation of AKT signalling (Turke et al. 2012). In particular, treatment with a MEK inhibitor was able to suppress the phosphorylation of the EGFR and HER2 juxtamembrane domain, thereby increasing phosphorylation of ERBB3.

Finally, MEK1 protein has been shown to be required for regulating PTEN localization at the cell membrane; therefore inhibition of MEK protein enhances PIP3 concentrations and AKT signalling (Zmajkovicova et al. 2013).

4.2 RESEARCH HYPOTHESIS AND AIMS

Hypothesis: The results presented in Chapter 3 have demonstrated the ability of pimasertib to sensitize human pancreatic cancer cells to gemcitabine in a schedule-dependent fashion. Additionally, we have shown that genetic and pharmacologic inhibition of MEK protein reduces RRM1 protein expression, a key determinant of gemcitabine response. We believe that the downregulation of RRM1 is one of the mechanisms by which pimasertib enhances gemcitabine cytotoxicity, since RRM1 depletion increases gemcitabine-induced apoptosis.

This chapter investigates the molecular mechanisms by which pimasertib reduces RRM1 with the following aims:

- To understand whether RRM1 downregulation induced by pimasertib is caused by its proteasomal degradation.
- To elucidate the mechanism by which inhibition of downstream molecules within the RAS signalling pathway can modulate the expression of an important biomarker of gemcitabine response.

4.3 RESULTS

4.3.1 Pimasertib-induced downregulation of RRM1 protein expression occurs through a post-translational modification

The data presented previously indicate that pimasertib reduces RRM1 protein levels, a mechanism that could in part explain the synergistic interaction observed in the combination of pimasertib with gemcitabine in human pancreatic cancer cell lines. In the previous chapter we showed that RRM1 mRNA levels were not significantly reduced by pimasertib treatment (Fig. 3.24); on the other hand the protein levels of RRM1 were decreased after only 1-hour treatment with pimasertib (Fig 3.25).

To better elucidate the mechanisms responsible for the observed pimasertib-induced rapid downregulation of RRM1 protein, we investigated whether RRM1 protein stability was regulated by the ubiquitin-proteasome system. To do that, we first used the proteasome inhibitor MG132, a peptide-aldehyde, whose structure is similar to the substrates of the chymotrypsin-like active site (Goldberg 2012). MG132 inhibits the activity of the 26S proteasome, the core complex where ubiquitin proteins are degraded, by binding the catalytic active site located in the β-subunits (Goldberg 2012).

A 4-hour exposure with 1μM pimasertib reduced RRM1 protein expression in BxPC-3 and PANC-1 cell lines (Fig. 4.3A). Nonetheless, pre-treatment with 1μM MG132 followed by a 4-hour exposure to 1μM pimasertib impaired the effects of pimasertib on downregulating RRM1 protein expression in both cell lines (Fig. 4.3A), indicating that pimasertib induces RRM1 degradation through the ubiquitin-proteasome pathway. Bar graphs showing the quantification of RRM1 immunoblots are illustrated in Figure 4.3B.

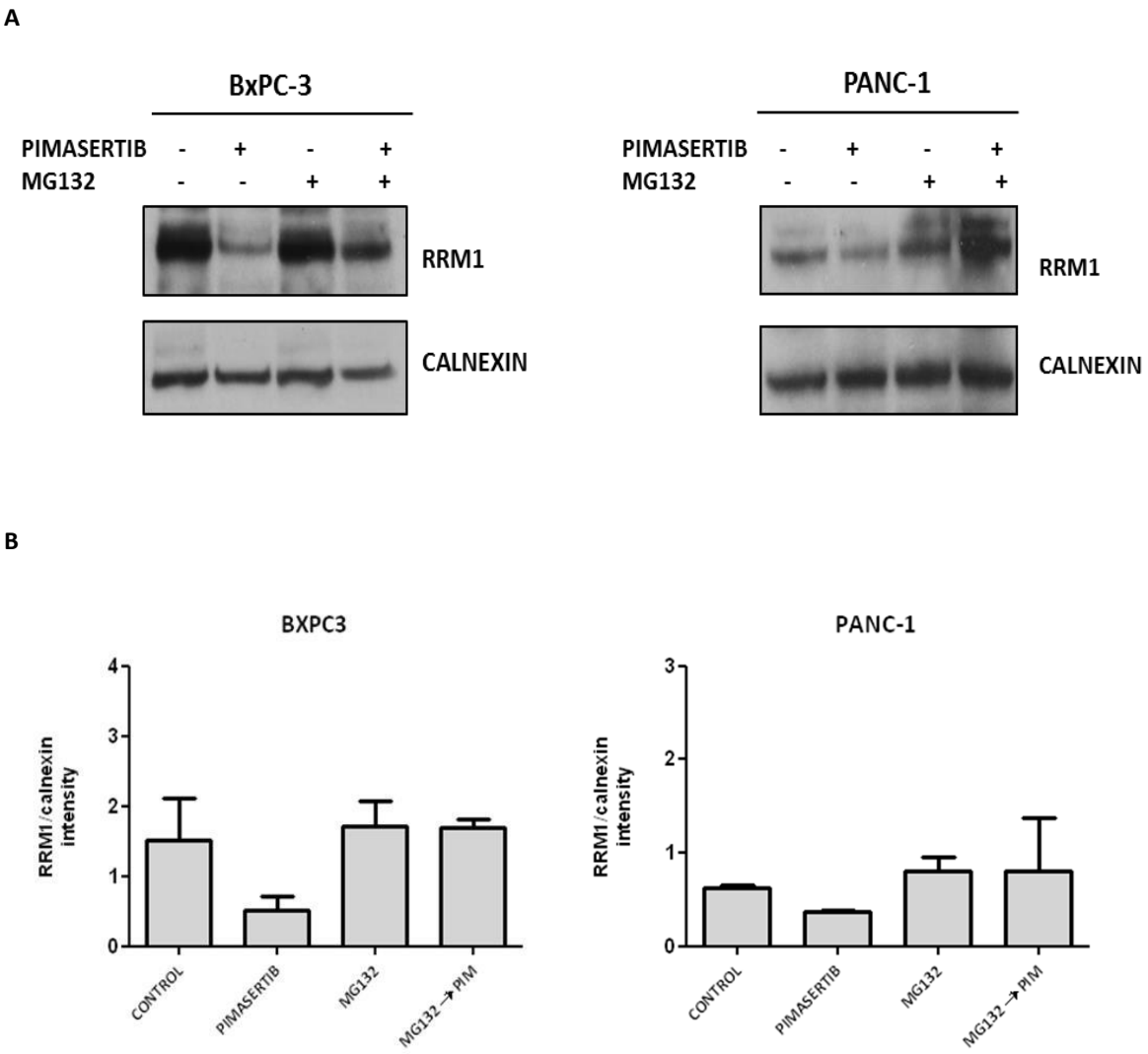

Figure 4.3: RRM1 protein levels are reduced by pimasertib through a post-translational modification.
A. BxPC-3 and PANC-1 cells were pre-treated for 1 hour with 1μM MG132 followed by 1μM pimasertib for 4 hours. Total cell lysates were analysed by immunoblotting. Calnexin was used as loading control. **B.** Densitometric analysis of the immunoblots presented in figure 4.3A. Results are presented as mean ± SD of three independent experiments. Image J software was used for quantitation of the western blot bands. Fold average of RRM1 was calculated by normalization to the loading control and comparison to the untreated sample.

4.3.2 RRM1 is polyubiquitinated through lys48-mediated linkage

Ubiquitin chains are formed through different lysine residues and this phenomenon is referred as polyubiquitination (Hochstrasser 2009). In particular, ubiquitin proteins attached to each other through lysine residues at position 48 target proteins for proteasomal degradation (Xu et al. 2009).

To confirm that the decrease in RRM1 expression induced by MEK inhibition was due to its proteasomal degradation, we explored whether RRM1 undergoes lys48 polyubiquitination. RRM1 was immunoprecipitated from PANC-1 and BxPC-3 cells pre-treated for 1 hour with 1μM MG132 followed by 4 hours exposure to 1μM pimasertib, and immunoblotted with an antibody against Lys48. Proteasomal inhibition (by MG132) produced a ladder of bands at high molecular weights whose intensity increased after pimasertib treatment, indicating that pimasertib enhances RRM1 polyubiquitination through lys48-mediated linkage (Fig. 4.4).

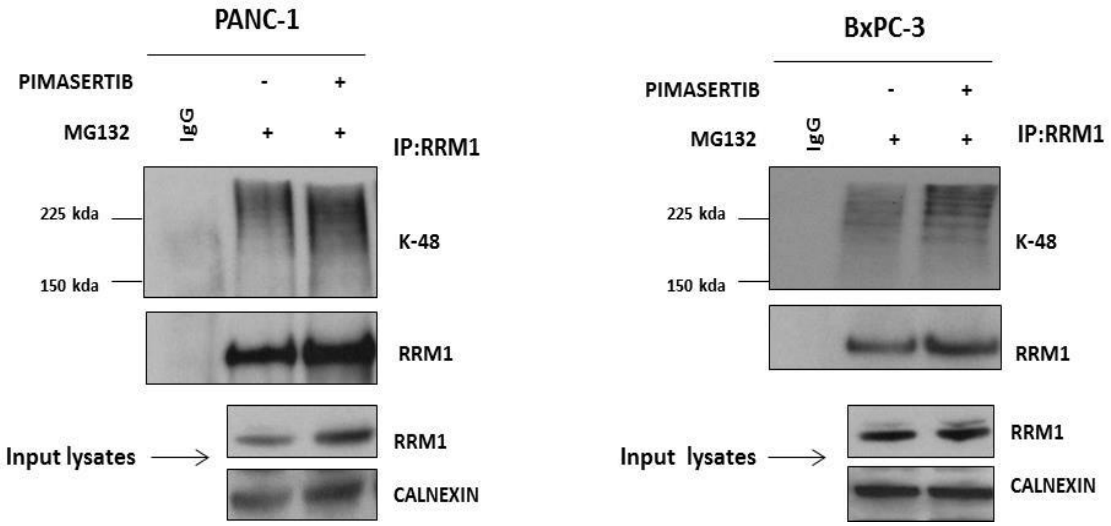

Figure 4.4: Pimasertib enhances polyubiquitination of RRM1.
PANC-1 and BxPC-3 cells were pre-treated for 1 hour with 1μM MG132 followed by 1μM pimasertib for 4 hours. Immunoprecipitation was performed using anti-RRM1 antibody or anti-IgG antibody, and immunoblotted with anti-RRM1 and anti-K48 antibodies. Inputs lysates (25μg/μl) were blotted with RRM1 antibody. Calnexin was used as loading control.

4.3.3 MDM2 inhibition impairs RRM1 degradation induced by pimasertib

To gain insights into how pimasertib promotes RRM1 degradation by the ubiquitin-proteasome pathway, we explored what effects inhibition of RING1-B and MDM2 E3 ubiquitin ligases would have on RRM1 protein stability. The RING1-B protein was selected based on previous findings that showed it to be involved in the ubiquitination and degradation of RRM1 (Zhang et al. 2014). MDM2 was selected because of the results from a recent preclinical study indicating that MDM2 induces proteasomal degradation of the P53R2 subunit of Ribonucleotide Reductase (Chang et al. 2008).

BxPC-3 cells were transfected with RING1-B specific siRNA for 72 hours and total cell lysates were analysed by immunoblotting. Depletion of RING1-B slightly increased RRM1 protein levels compared to scrambled (lane 1 and 4 of Fig. 4.5A), confirming previous results that showed RING1-B mediating ubiquitination and degradation of RRM1. However, treatment with 1μM pimasertib for 4 hours caused downregulation of RRM1 protein expression in cells transfected with scrambled (lane 3) and cell transfected with RING1-B siRNA (lane 2) (Fig. 4.5A), indicating that RING1-B is not implicated in RRM1 degradation triggered by pimasertib, since its depletion does not affect the pimasertib effect on RRM1 protein expression. Bar graphs showing the quantification of RRM1 are illustrated in Figure 4.5B.

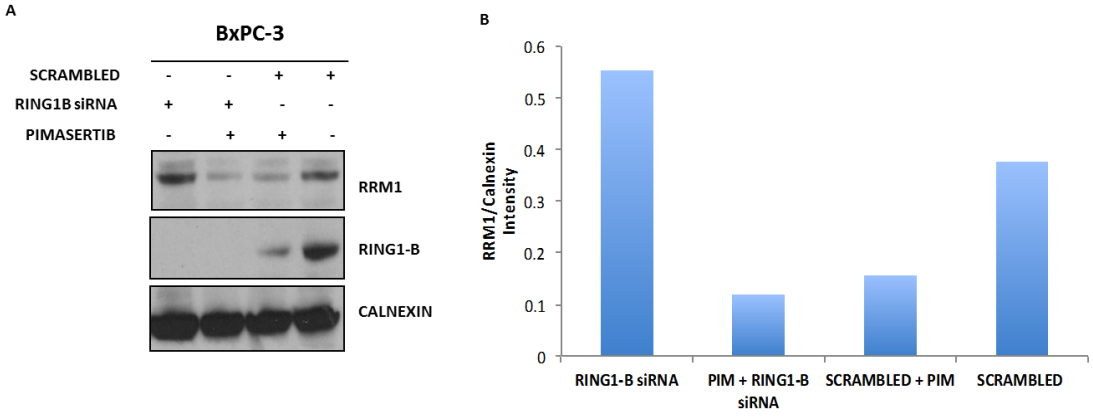

Figure 4.5: RNF2 E3 ligase activity on RRM1 protein stability.
A. BxPC-3 cells were transfected with 50nM siRNA targeting RING1B or scrambled siRNA for 72 hours and treated with pimasertib for the last 4 hours of transfection. Total cell lysates were immunoblotted with the indicated antibodies. Calnexin was using as loading control. **B.** Densitometric analysis of the immunoblots presented in Figure 4.5A. Image J software was used for quantitation of the western blot bands. Fold decrease of RRM1 was calculated by normalization to the loading control and comparison to the untreated sample.

MDM2 mediates proteasomal degradation of other protein targets apart from P53 (Ambrosini et al. 2007). To investigate whether MDM2 was involved in RRM1 degradation, BxPC-3 cells were transfected with MDM2-specific siRNA for 72 hours and RRM1 protein levels were analysed by immunoblotting. RRM1 protein levels accumulated in MDM2 knocked-down cells suggesting that MDM2 is involved in the proteasome-dependent degradation of RRM1 (Fig. 4.6A). When BxPC-3 cells, transfected with siRNA against MDM2, were treated with pimasertib for the last 4h of transfection, RRM1 downregulation was impaired (Fig. 4.6B), suggesting that pimasertib-induced RRM1 degradation occur through MDM2 activity. Bar graphs showing the quantification of RRM1 immunoblots are illustrated in Figure 4.6C.

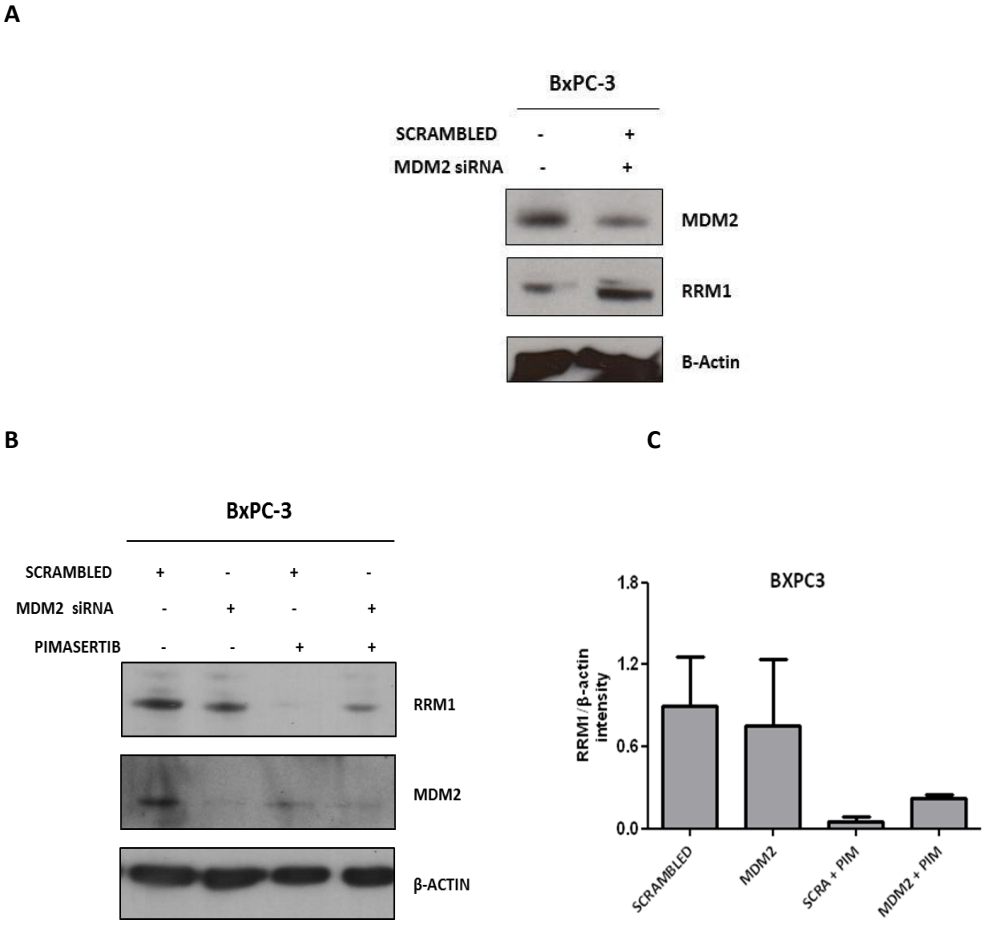

Figure 4.6: MDM2 modulates RRM1 degradation induced by pimasertib.

A. BxPC-3 cells were transfected with 50nM siRNA targeting MDM2 or scrambled for 72 hours and immunoblotted with the indicated antibodies. **B.** BxPC-3 cells were transfected with 50nM siRNA targeting MDM2 or scrambled for 72 hours followed by a 4-hour treatment with pimasertib and immunoblotted with the indicated antibodies. β-Actin was using as loading control. **C.** Densitometric analysis of the immunoblots presented in Figure 4.6B. Fold decrease of RRM1 was calculated by normalization to the loading control and comparison to the untreated sample. Results are presented as mean ± SD of three independent experiments.

To further confirm that MDM2 mediates RRM1 degradation through its polyubiquitination and degradation by the proteasome system, myc-labeled wild-type or truncated MDM2 (p60), the latter lacking the E3 ligase domain, were transiently transfected into the MIAPaCa-2 cell line and treated with pimasertib for 4 hours. Protein lysates were analysed by immunoblotting. When MDM2p60 was expressed, accumulation of RRM1 protein expression was observed compared to MDM2wt (lane 1,2 Fig. 4.7). Importantly, RRM1 downregulation caused by pimasertib administration was impaired in MDM2p60 transfected cells (Lane 3,4 Fig. 4.7). These findings further confirm the involvement of MDM2 in targeting RRM1 for proteasomal degradation.

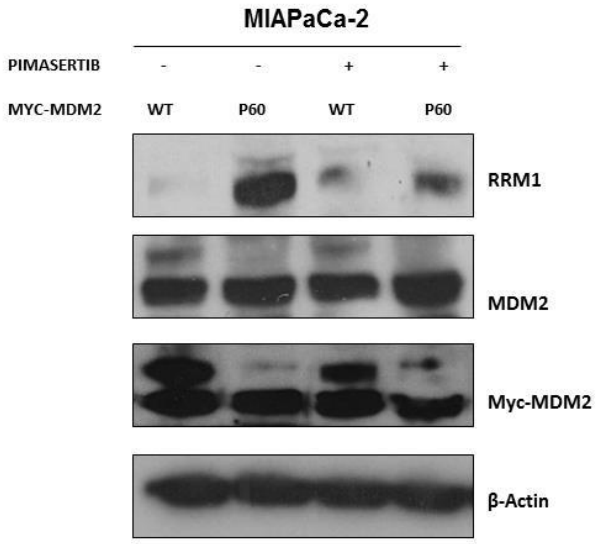

Figure 4.7: RRM1 protein levels are increased in truncated mutant MDM2 cells.
MIAPaCa-2 cells were transiently transfected with MYC-labelled MDM2wt or MDM2p60. After 48 hours, transfected cells were selected with neomycin and treated with pimasertib for an additional 4 hours. Total cell lysates were analysed by immunoblotting with the indicated antibodies. β-Actin was using as loading control.

Nutlin-3 belongs to the class of small molecule antagonists of MDM2 that binds the P53 binding pocket of MDM2, thus disrupting the interaction between p53 and MDM2, which results in the inhibition of P53 degradation (Vassilev 2007). Several studies have demonstrated a P53 independent role of nutlin-3 (Ambrosini et al. 2007). For example, small molecule antagonists of MDM2 can disrupt the binding between MDM2 and E2F1 in P53 mutant cells (Ambrosini et al. 2007). We sought to investigate

if nutlin-3 could alter the effect of pimasertib on RRM1 stability by inhibiting MDM2 E3 ligase activity. BxPC-3 cells were treated with 1μM pimasertib and 1μM nutlin-3 for 24 hours. Immunoblotting analysis showed that treatment with nutlin-3 impaired RRM1 downregulation induced by pimasertib (Fig. 4.8A). Bar graphs showing the quantification of RRM1 immunoblots are illustrated in Figure 4.8B.

A

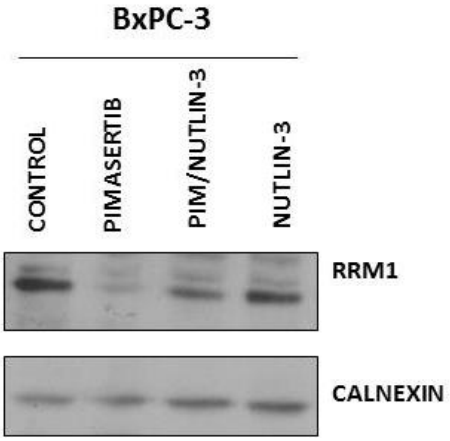

B

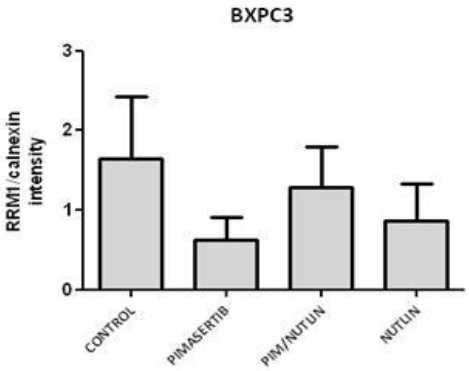

Figure 4.8: The MDM2 antagonist Nutlin-3 impairs RRM1 degradation.
A. BxPC-3 cells were co-treated with 1μM nutlin-3 and 1μM pimasertib for 24 hours and total cell lysates were analysed by immunoblotting with the indicated antibodies. Calnexin was used as loading control. Results are representative of three independent experiments. **B.** Densitometric analysis of the immunoblots presented in Figure 4.8A. Image J software was used for quantitation of the western blot bands. Fold average of RRM1 was calculated by normalization to the loading control and comparison to the untreated sample. Results are presented as mean ± SD of three independent experiments.

4.3.4 RRM1 interacts with MDM2

MDM2 acts as an E3 ubiquitin ligase by interacting with target proteins and regulating their proteasomal degradation(Iwakuma and Lozano 2003). To investigate whether RRM1 was an MDM2-binding protein, immunoprecipitation experiments were performed in BxPC-3 and PANC-1 cells. Endogenous RRM1 bound to total and phosphorylated forms of MDM2 (Serine 166). In particular, the binding between P-MDM2 and RRM1 increased after treatment with pimasertib in BxPC-3 cells and to a greater extent in PANC-1 cells (Fig 4.9).

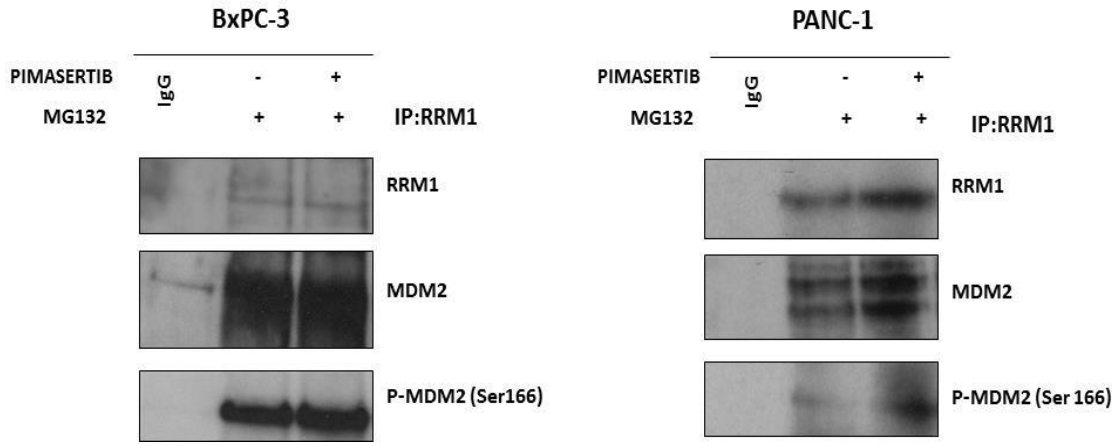

Figure 4.9: Pimasertib enhances MDM2 interaction with RRM1.
BxPC-3 and PANC-1 cells were treated with the same conditions described in Fig. 4.4. Total cell lysates were immunoprecipitated (IP) with control IgG or anti-RRM1 antibody. IP complexes were immunoblotted with the indicated antibodies.

Previous studies have shown that MDM2 is active in a P53 mutant setting (Bouska and Eischen 2009). Our results have shown that MDM2 mediates ubiquitination and degradation of RRM1 in mutant BxPC-3 cell lines. To confirm that the effect observed in our study on RRM1 stability is independent of the functional activity of P53, BxPC-3 cells were transfected with specific siRNA targeting P53 for 72 hours and treated with pimasertib for the last 4 hours of transfection. Total cell lysates were immunoblotted against P53 and RRM1. Inhibition of P53 by siRNA did not affect the reduction of RRM1 protein induced by pimasertib treatment (Fig. 4.10).

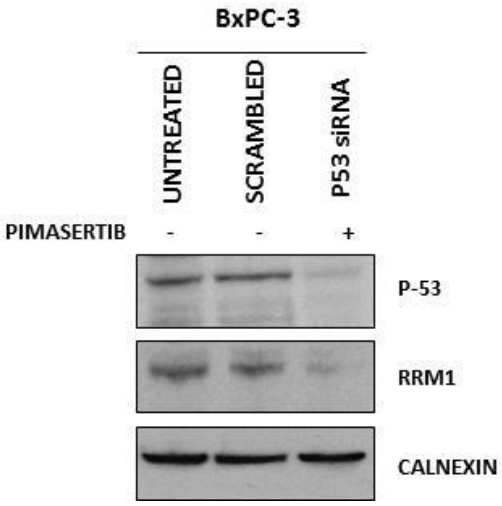

Figure 4.10: Pimasertib-induced downregulation of RRM1 is independent of P53 activity.
BxPC-3 cells were transfected with 50nM siRNA targeting P53 or scrambled for 72 hours and immunoblotted with the indicated antibodies. Calnexin was using as loading control.

4.3.5 Pimasertib induces activation of P-AKT

MEK inhibition has been shown to induce activation of the PI3K/AKT signalling pathway through various feedback loop mechanisms (Zmajkovicova et al. 2013) (Turke et al. 2012). A previous preclinical study has shown activation of AKT signalling by pimasertib in multiple myeloma cell lines (Kim et al. 2010). To investigate whether pimasertib had an effect on AKT, BxPC-3 cells were treated with 1µM pimasertib and extracted at different time point (1h, 4h and 24h). Immunoblotting analysis showed an increase of P-AKT protein levels along with sustained P-ERK inhibition after 1-hour treatment with pimasertib (Fig. 4.11).

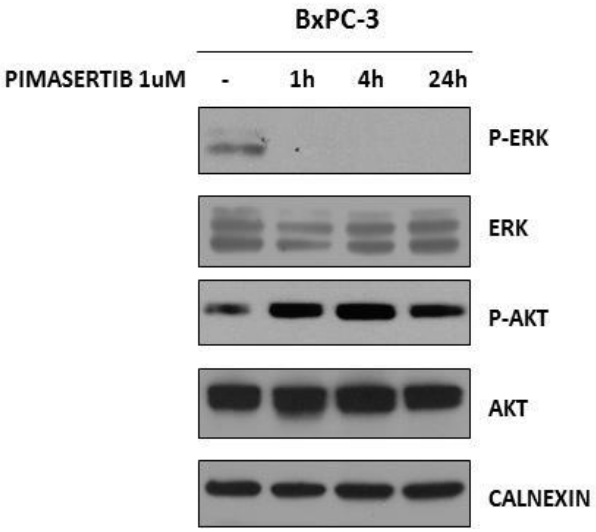

Figure 4.11: Pimasertib induces rapid activation of P-AKT.
BxPC-3 cells were treated for 1, 4 and 24 hours with 1µM pimasertib. Total cell lysates were immunoblotted using the indicated antibodies. Calnexin was used as loading control. Data is representative of two independent experiments.

4.3.6 AKT activation is required for pimasertib-mediated degradation of RRM1

The results presented in Figures 4.7-4.9 show that pimasertib triggers MDM2-mediated polyubiquitination and degradation of RRM1. Previous studies have reported that phosphorylation of MDM2 on serine 166 and 186 can be triggered by P-

AKT, an effect that stimulates MDM2 entry into the nucleus and increases its ability to target P53 (Mayo and Donner 2001) (Zhou et al. 2001). One potential route by which pimasertib enhances MDM2 E3 ligase activity may be the PI3K/AKT pathway, since we have previously shown it is activated by the MEK inhibitor (Fig. 4.11). To explore this hypothesis, BxPC-3 cells were treated with 1µM pimasertib for 4 hours. Total lysates were immunoprecipitated with MDM2 antibody and probed for AKT and P-AKT. Results showed an interaction between MDM2 and AKT (Fig. 4.12). In particular, a strong interaction between MDM2 and P-AKT was observed upon pimasertib treatment (Fig. 4.12), suggesting that P-AKT directly activates MDM2 E3 ligase activity in BxPC-3 cells.

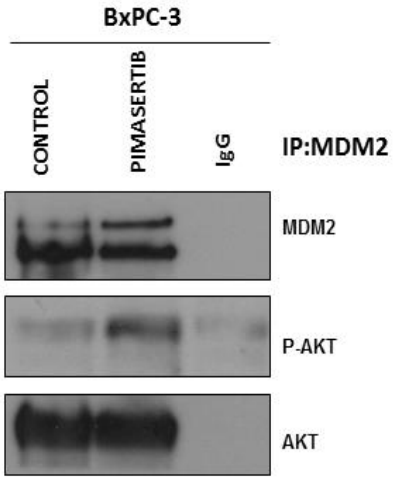

Figure 4.12: MDM2 interacts with P-AKT.
BxPC-3 cells were pre-treated for 4 hours with with 1µM pimasertib. Total cell lysates were immunoprecipitated with anti-MDM2 antibody. Immunoprecipitates were analysed by immunoblotting by using the indicated antibodies.

We then used a selective inhibitor of class-I PI3K (GDC-0941) to determine whether MEK inhibition-feedback activation of P-AKT was implicated in RRM1 degradation. Immunoblotting analysis showed that the combination of both drugs effectively inhibited AKT and ERK phosphorylation, but total levels of ERK and AKT remained unchanged (Fig. 4.13A). Quantitatively, the ratio of P-AKT/T-AKT increased upon 4 hours treatment with 1µM pimasertib (Fig 4.13B). Importantly, 1µM pimasertib plus 1µM GDC-0941 treatment for 4 hours antagonised the effect of pimasertib on downregulating RRM1 protein expression (Fig 4.13A). Based on these findings, we

suggest that AKT phosphorylation induced by MEK inhibition might trigger MDM2-mediated degradation of RRM1.

A

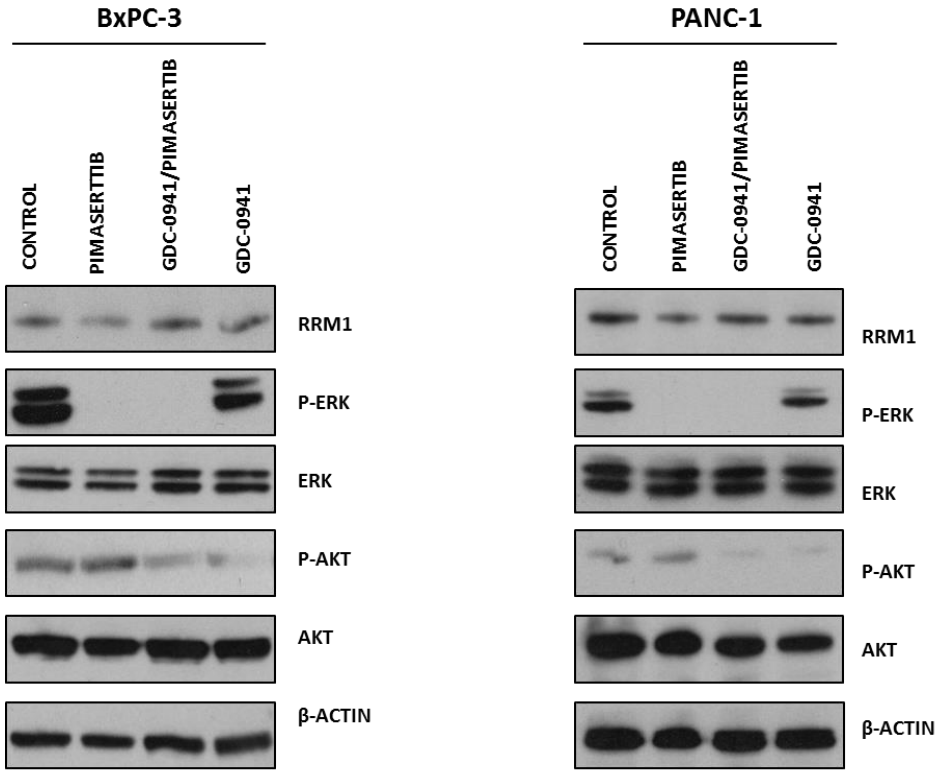

B

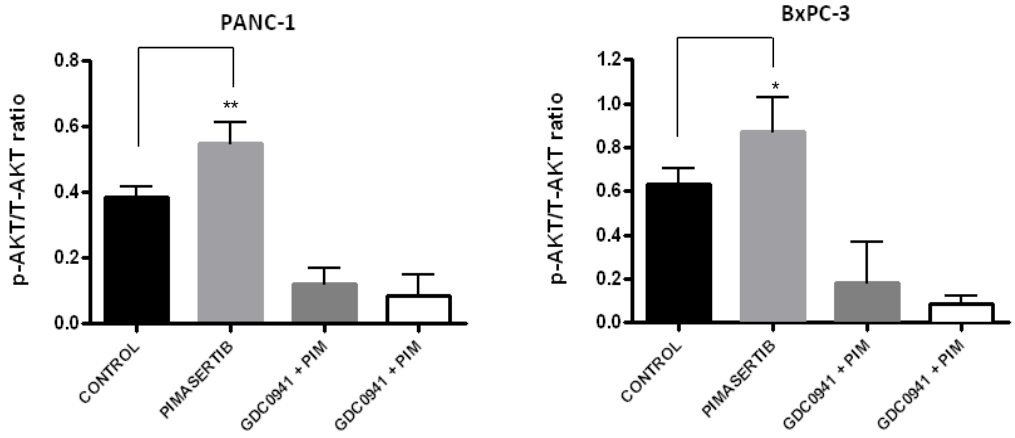

Figure 4.13: PI3K/AKT signalling inhibition impairs the downregulation of RRM1.

A. BxPC-3 and PANC-1 cells were treated for 4 hours with 1μM of PI3K inhibitor GDC-0941 together with 1μM pimasertib and total cell lysates were immunoblotted using the indicated antibodies. β-actin was used as loading control. **B.** Densitometric analysis of the immunoblots presented in figure 4.13A. Results are presented as mean ± SD of three independent experiments. Image J software was used for the quantitation of the western blot bands. Increase of P-AKT/T-AKT was calculated by normalization to the loading control and comparison to the untreated sample.

4.4 DISCUSSION

This chapter presented a series of experiments conducted to investigate the molecular mechanisms by which the MEK inhibitor pimasertib modulates RRM1 protein stability.

4.4.1 Ribonucleotide Reductase stability is modulated by the ubiquitin-proteasome system

Ribonucleotide Reductase (RR) activity is tightly regulated through several mechanisms (Aye et al. 2015). For example, RR regulation occurs through the cell cycle, in which RRM2 protein and mRNA levels reach maximum peaks in S-phase. RR activity is also modulated by the binding of ATP or dATP molecules to the catalytic site of RR (Nordlund and Reichard 2006). Recent findings have shown that RR enzyme stability is regulated by the action of the proteasome pathway. An in vitro study has demonstrated that RRM2 protein stability is regulated by the ubiquitin-proteasome system through Cyclin F, an SCF E3 ubiquitin ligase F-box protein. Upon DNA damage Cyclin F is downregulated in an ATR (ataxia telangiectasia and Rad-3 dependent protein) dependent manner, thus increasing RRM2 stability (D'Angiolella et al. 2012). In the study just described, defective elimination of Cyclin F enhanced RRM2 proteasomal degradation thus producing an imbalance in the levels of dNTPs. Inappropriate production of dNTP pools sensitized cells to DNA damage, which led to genomic instability. (D'Angiolella et al. 2012).

Another example of RR activity being regulated post-translationally came from a pre-clinical study investigating P53R2 activity. RR subunit p53R2 is induced upon DNA damage and associates with RRM1 to supply dNTP pools for DNA repair. However, its mRNA transcription is not induced rapidly enough to provide dNTP for immediate DNA repair (Nordlund and Reichard 2006). Recent findings revealed that ataxia telangiectasia mutated (ATM) phosphorylation on Ser^{72} maintains P53R2 stability, by blocking MDM2-mediated degradation of P53R2 in response to genotoxic stress (Chang et al. 2008). In agreement, mutation of Ser^{72} impaired P53R2 phosphorylation and resulted in hyperubiquitinated P53R2 upon DNA damage. Interestingly, co-immunoprecipitation analysis demonstrated not only a physical interaction between

ATM and P53R2 but between ATM/P53R2 and RRM1 subunit after 30 minutes of UV irradiation, suggesting that RRM1 and P53R2 form a complex, which interacts with ATM *in vivo* (Chang et al. 2008).

Finally, another study identified RNF2 and Bmi1 E3 ubiquitin ligases to interact with and induce RRM1 polyubiquitination. Silencing of both genes induced accumulation of RRM1 protein (Zhang et al. 2014). These results indicate that the ubiquitin proteasome system is involved in the regulation of RR stability. Enhancing the activity of specific E3 ligases within the proteasome pathway could be an effective way to downregulate RR activity and thus overcome gemcitabine resistance.

4.4.2 Pimasertib induces MDM2-mediated proteasomal degradation of RRM1

The P53 tumor suppressor gene is activated in response to stress signals or DNA damage to induce cell proliferation arrest, senescence or apoptosis. P53 is one of the most frequently mutated gene in human cancer (Vogelstein et al. 2000). One of the functions of the murine double minute 2 (MDM2) gene is to bind the N-terminal transactivation domain of P53 and thus inactivates P53 transcriptional activity (Michael and Oren 2003). Additionally, MDM2 acts as an E3 ubiquitin ligase by binding P53 through its RING finger domain and inducing its proteasomal degradation (Freedman et al. 1999). Loss of MDM2 causes embryonic lethality in mice during early development, a phenotype that is rescued by concomitant deletion of P53 (Jones et al. 1995). MDM2 expression is also regulated by P53 and MDM2 inhibits P53 activity; both auto regulatory feedback loop mechanisms are important to maintain P53 levels under normal physiological conditions (Wu et al. 1993). MDM2 is classified as an oncogene because of its property on inhibiting P53 tumor suppressive functions. However, different alternative splicing of MDM2 transcripts exist which do not include sequences encoding for the P53 binding domain, suggesting that MDM2 has also p53-independent functions (Steinman et al. 2004).

Several studies have shown that MDM2 possesses E3 ubiquitin ligase activity against other target proteins, such as the activating transcription factor 3 (ATF3) (Mo et al.

2010), the tumor suppressor protein Rb (Loughran and La Thangue 2000), the androgen receptor (AR) (Zhau et al. 1995) and P53R2 subunit (Chang et al. 2008).

In human pancreatic cancer cells, MDM2 was shown to regulate the expression of target genes involved in cellular proliferation such as *C-jun*, *C-Myc* and *cyclin D1* (Sui et al. 2009).

In this study, human pancreatic cancer cells were treated with the proteasome inhibitor MG132 to explore whether the decrease of RRM1 protein expression induced by pimasertib was due to its degradation through the proteasome system. MG132 prevented RRM1 downregulation caused by pimasertib suggesting that the degradation of RRM1 is proteasome dependent (Fig. 4.3). Additionally, pimasertib caused accumulation of polyubiquitinated RRM1 through Lys48-mediated linkage, which is associated with proteasomal degradation of the target protein (Fig. 4.4) (Tenno et al. 2004).

The results from this chapter have also shown the depletion of MDM2 by siRNA impaired RRM1 degradation induced by pimasertib (Fig. 4.6). Furthermore, in transient transfection experiments we have shown that RRM1 accumulated more in cells overexpressing a truncated form of MDM2, which does not have functional E3 ligase activity (Fig. 4.7).

Small molecule antagonists of MDM2 (Nutlins) have been developed to disrupt the binding between MDM2 and P53 and thus increase p53 signalling only in cells with wild-type p53 (Vassilev 2004). However, nutlins have proved to be active in a mutant P53 setting (Ambrosini et al. 2007). For instance, a study has demonstrated that treatment with nutlin-3 disrupted the binding of E2F1 with MDM2, thus increasing the stability of E2F1. Enhanced activation of E2F1 led to an increase of pro-apoptotic proteins, which enhanced cytotoxicity of cisplatin therapy (Ambrosini et al. 2007). We used the MDM2 antagonist nutlin-3, which block MDM2 E3 ubiquitin ligase activity and observed that administration of nutlin-3 prevented pimasertib-induced downregulation of RRM1, further confirming MDM2 involvement in RRM1 degradation (Fig. 4.8). Finally, to determine whether RRM1 and MDM2 interact we performed co-immunoprecipitation analysis and demonstrated a direct association between RRM1 and MDM2 or P-MDM2 (Fig. 4.9). These results all together confirm

the role of MDM2 in mediating RRM1 proteasomal degradation induced by pimasertib.

4.4.3 The PI3K/AKT pathway is involved in RRM1 degradation induced by pimasertib

MEK inhibitors can induce activation of the PI3K/AKT signalling pathway due to presence of compensatory feedback systems (Zmajkovicova et al. 2013). For instance, recent findings have shown that MEK inhibitors increased AKT phosphorylation through activation of ERBB3 tyrosine receptor, which led to the upregulation of ERBB3/PI3K association. This effect, induced by MEK inhibition, is caused by the loss of ERK-inhibitory feedback action on phosphorylating EGFR T669 and HER2 T667, which inhibits ERRB3 activity. (Turke et al. 2012).

Other reports have demonstrated the role of the PI3K/AKT signalling pathway in promoting MDM2 E3 ligase activity. AKT has been reported to phosphorylate MDM2 at Ser^{166} and Ser^{186}, necessary for its translocation into the nucleus. In fact, depletion of AKT signalling significantly enhanced P53 transcriptional activity and thereby P53-dependent apoptosis (Mayo and Donner 2001).

Additionally, the AKT pathway is involved in MDM2-mediated degradation of the androgen receptor (AR), a transcription factor that mediates the regulation of prostate cell growth and apoptosis (Grossmann et al. 2001). AKT phosphorylates both AR and MDM2 and this leads to ubiquitination and thus degradation of the receptor by the 26S proteasome (Lin et al. 2002). The overall results indicate important mechanisms of regulation of MDM2 activity through PI3K signalling pathway.

In this present study we have shown an increase in P-AKT levels following pimasertib administration (Fig. 4.11) and we asked if this effect could be associated with RRM1 downregulation observed upon pimasertib treatment. Our results first confirmed the existence of a physical interaction between P-AKT and MDM2, which increased after treatment with the MEK inhibitor (Fig. 4.12). Next, we observed that co-treatment of pimasertib with the PI3K inhibitor GDC0941 resulted in impaired downregulation of

RRM1 (Fig. 4.13). These results suggest that MEK inhibition mediates P-AKT activation of MDM2 to target RRM1.

4.5 CONCLUSIONS

The experiments conducted in this chapter reveal new mechanistic insights in the modulation of RRM1 protein stability induced by MEK inhibition in human pancreatic cancer cell lines. In this context we demonstrated that pimasertib triggers RRM1 proteasomal degradation through MDM2 E3 ligase activity. We believe RRM1 degradation contributes to pimasertib effects in enhancing gemcitabine efficacy *in vitro*. Additionally, we propose that pimasertib-induced phosphorylation of AKT might be responsible for the activation of MDM2 to promote polyubiquitination and degradation of RRM1 protein. Further experiments will have to be performed to validate this hypothesis and understand how P-AKT interacts and activates MDM2 protein. RRM1 is a key determinant of gemcitabine response in PDAC. Therefore, understanding the mechanism by which MEK inhibition modulates RRM1 expression is of crucial importance to develop new combination treatments with the aim of improving the small survival benefit provided by gemcitabine therapy. In the next Chapter experiments conducted on a mouse model of pancreatic cancer will be presented to further evaluate and confirm our *in vitro* findings.

CHAPTER 5

EFFECTS OF PIMASERTIB IN COMBINATION WITH GEMCITABINE IN AN ORTHOTOPIC MODEL OF PANCREATIC TUMOR

5.1 INTRODUCTION

5.1.1 *In vivo* model systems to study human cancers

In vivo model systems have been extensively used in cancer research and have proved to be an important tool to investigate the role that specific genetic alterations have in tumor initiation, progression and maintenance (Qiu and Su 2013) (Guerra and Barbacid 2013). Mouse models have accelerated the identification of novel therapeutic drugs for PDAC, whose mechanisms of action can be studied in these models before clinical testing (Hidalgo et al. 2014) (Hidalgo et al. 2015).

5.1.1.1 Human tumour xenograft models

Human tumour xenograft models are widely used in cancer research for the preclinical evaluation of therapeutic drugs and are generated by implantation of human tumour cells in immunodeficient mouse hosts (Rubio-Viqueira et al. 2006) (Qiu and Su 2013). Human tumour xenograft models are used to examine the potential effects of anticancer therapies on tumour regression and long-term survival (Kelland 2004).

Xenograft models can be divided into two categories:

1. Heterotopic mice: when the tumour cells are injected subcutaneously
2. Orthotopic mice: when the tumour cell is injected or implanted directly into the corresponding host organ.

Orthotopic models are more appropriate to investigate the metastatic process since their tumour microenvironment resembles that of the original tumour and they develop distant metastasis in a similar way to what is observed in human cancers (Killion et al. 1998). However, orthotopic models are time consuming and more challenging to generate compared to the corresponding heterotopic models.

Human tumour xenograft models have some limitations: tumours develop very rapidly therefore they do not acquire the full characteristics of a human tumour. Additionally, as these models are immunocompromised, they do not simulate an immune response, which is integral to tumour initiation and progression. For these reasons,

the response to therapy obtained from these preclinical models is not always fully reproducible in the clinical setting (Gopinathan and Tuveson 2008).

5.1.1.2 Genetically engineered mouse models of PDAC

Genetically engineered mouse models (GEMMs) are models in which one or several genes expression has been manipulated to recapitulate the main features of a particular human cancer (Dow and Lowe 2012). The KC mouse model (KrasLSL.G12D/+; PdxCretg/+) is one of the most commonly used GEM models of PDAC (Fig. 5.1). This model was generated by crossing mice carrying $KRAS^{G12D}$ knocked-in allele containing a cassette with transcriptional termination stop codon flanked by LoxP sites (LSL cassette) that prevents expression of the allele, with transgenic mice expressing a bacterial CRE recombinase under the control of a pancreas specific promoter (PDX1). Expression of CRE recombinase removes the stop cassette and activates the $KRAS^{G12D}$ allele specifically in the pancreatic tissue (Hingorani et al. 2003) (Fig. 5.1). After induction of oncogenic $KRAS^{G12D}$, KC mice start developing all three stages of PanIN lesions, acquire ductal morphology and slowly progress to PDAC (Hingorani and Tuveson 2003).

Simultaneous induction of oncogenic $KRAS^{G12D}$ and a loss of function allele of the tumor suppressor p53 led to the development of KPC mice (KrasLSL.G12D/+; p53R172H/+; PdxCretg/+) that develop pancreatic cancers more rapidly and generate liver metastasis that closely resemble that of the corresponding human tumour (Hingorani et al. 2005).

Although these models allow the manipulation of expression of genes frequently mutated in PDAC, the concurrent introduction of these genetic alterations does not reflect the real scenario in which mutations occur in specific stages of tumour development and not at the same time (di Magliano and Logsdon 2013). For this reason, a second model of pancreatic cancer has been developed characterised by spatial and temporal control of $K\text{-}RAS^{G12D}$ expression (Guerra et al. 2007). This model is ideal to investigate how the temporal order of genetic alterations occurring in PDAC determines cancer progression.

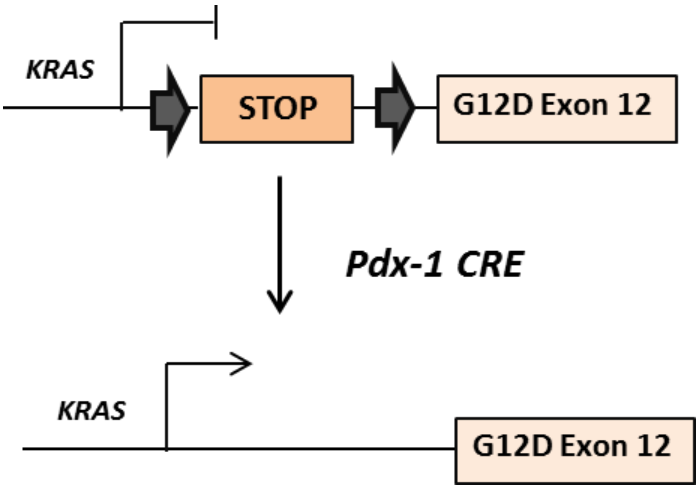

Figure 5.1: Schematic representation of the KC mouse model.
The KC mouse model is generated by crossing a mouse strain containing oncogenic K-RAS^{G12D} preceded by a STOP cassette flanked by two LoxP sites, with a strain containing the Pdx1 promoter-regulated CRE. Endogenous allele of KrasG12D is conditionally activated in the mouse pancreatic tissue by Pdx-1 CRE recombinase, which recognizes the LoxP sites and deletes the DNA sequence (containing the STOP cassette) between the two LoxP sites. Adapted from (Hingorani et al. 2005).

The establishment of GEMMs have helped to study the biology of pancreatic cancer and to validate genes mutation, such as K-RAS as main drivers of pancreatic tumor initiation and development (Frese and Tuveson 2007) (Westphalen and Olive 2012). Additionally, GEM models have proved to be critical tool for the identification of new therapeutic strategies at various stages during tumor development (Olive et al. 2009) (Dow and Lowe 2012). However there are some disadvantages which make their use limited: they are time consuming, requiring almost a year to develop and they are highly expensive to generate (Dow and Lowe 2012). Additionally, it is not possible to define the function that specific genes have in tumor maintenance (Saborowski et al. 2014). Faster and more scalable approaches than knock-out mice have been recently developed; for example, shRNA technology enables the silencing of a gene in a reversible manner, allowing the investigation of gene function in a determined period of time (Dow and Lowe 2012).

Another faster approach compared to GEMMs is the mulltiallelic transgenic mouse model known as GEMM-ESC. This model is generated by injecting mouse embryonic stem cells (ESC) (derived from a GEM model) in a mouse host, whose genome had been modified *in vitro* to carry the essential genetic modifications needed to develop

a particular type of cancer. This system does not require breeding and the mice generated develop tumour within 3 months, therefore they represent an efficient platform for preclinical treatment studies (Dow and Lowe 2012).

5.1.1.3 Syngeneic orthotopic mouse models

Syngeneic orthotopic pancreatic cancer mouse models represent a lower cost and less time consuming alternative to GEMMs (Tseng et al. 2010). To generate these models, tumor cells derived from GEMMs are implanted into the pancreas of immunocompetent mice. Syngeneic orthotopic mouse models develop genetic mutations and an immune response typical of human pancreatic cancer and thus they are a powerful system for exploring novel therapeutic strategies (Tseng et al. 2010).

5.2 RESEARCH HYPOTHESIS AND AIMS

Hypothesis: The MEK1/2 inhibitor pimasertib has demonstrated potent antitumor activity in mouse models of different malignancies (Kim et al. 2010) (Park et al. 2013) (Yoon et al. 2011). However, no *in vivo* studies on pancreatic cancer models involving pimasertib have been published to date. Our results on human pancreatic cancer cell lines demonstrated synergistic activity when pimasertib was combined with gemcitabine and we suggest that this effect is in part due to a significant downregulation of RRM1 protein levels.

We believed that investigating the effects of pimasertib in orthotopic mouse models of pancreatic would be of significance to confirm our *in vitro* findings.

This chapter validates the research hypothesis with the following aims:

- To investigate the *in vivo* antitumor activity of pimasertib in combination with gemcitabine in an orthotopic model of pancreatic cancer.
- To confirm the effects of pimasertib on the MAPK pathway and RRM1 expression in the same mouse model.

5.3 RESULTS

5.3.1 Effects of pimasertib on TB32048 tumor cells

To explore the antitumor activity of pimasertib in combination with gemcitabine *in vivo,* a syngeneic orthotopic mouse model of pancreatic cancer was generated by our collaborators at the Barts Cancer Institute (London, UK). TB32048 murine cells, derived from the KPC mouse model (previously described) were implanted in the pancreas of immunocompetent mice.

Initially, the cellular effects of pimasertib in combination with gemcitabine were evaluated in the TB32048 cell line. As observed in the human pancreatic cancer cell lines (Fig. 3.9-3.10), a 4-hour pre-treatment with 500nM pimasertib followed by a 48-hour treatment with increasing concentrations of gemcitabine (5nM, 25nM, 50nM and 250nM) induced synergistic antiproliferative effects (Fig. 5.2A) as indicated by CI values generated from all concentrations of gemcitabine examined being <1 (Fig. 5.2B). A bar chart of CI values obtained from the sequential combination of gemcitabine with pimasertib is illustrated in Fig. 5.2B).

A

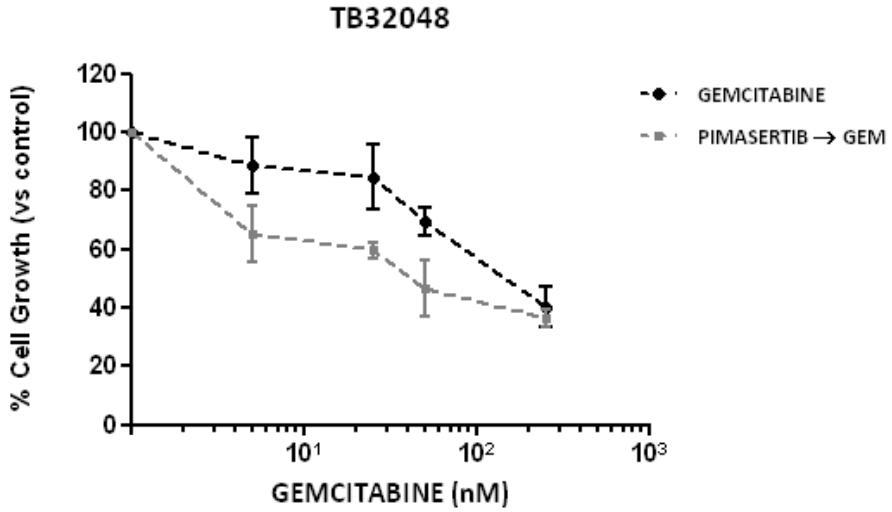

Figure 5.2: Sequential combination of pimasertib followed by gemcitabine induces synergistic antiproliferative activity in KPC cells.

A. MTT assay was used to evaluate the effect of a 4-hour pre-treatment of 500nM pimasertib followed by increasing concentrations of gemcitabine (5-25-50-250nM) for 48 hours on the growth of TB32048 cells.

B

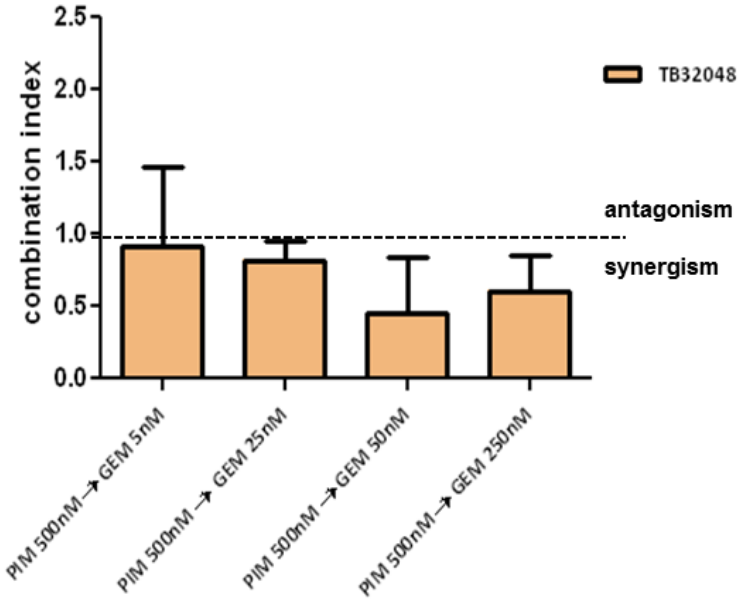

Figure 5.2 continued: Sequential combination of pimasertib followed by gemcitabine induces synergistic antiproliferative activity in KPC cells.

B. Combination Indices (CI) values describing drug combinations were calculated with the Calcusyn program. Experiments were repeated three times and are represented as mean, Error Bars ± SD.

Next, we investigated the effects of pimasertib on MAPK signaling and RRM1 expression on cultured TB32048 cells *in vitro*. Immunoblotting analysis showed inhibition of ERK phosphorylation and reduced RRM1 protein expression after 4 hours treatment with pimasertib and this effect was sustained for 24 hours (Fig. 5.3). Additionally, pimasertib led to an increase in P-AKT protein levels at 4 and 24 hours (Fig. 5.3). We have previously shown that treatment with the PI3K inhibitor GDC-0941 impaired the effects of pimasertib on RRM1 protein expression (Fig. 4.13), suggesting that the PI3K/AKT pathway is involved in RRM1 degradation induced by MEK inhibition. To confirm these results, TB32048 cells were treated with 1μM GDC-0941 and 1μM pimasertib for 4 hours. GDC-0941 treatment inhibited the pimasertib-mediated decrease of RRM1 (Fig. 5.4A). P-AKT/T-AKT quantification was performed by densitometric analysis (Fig. 5.4B).

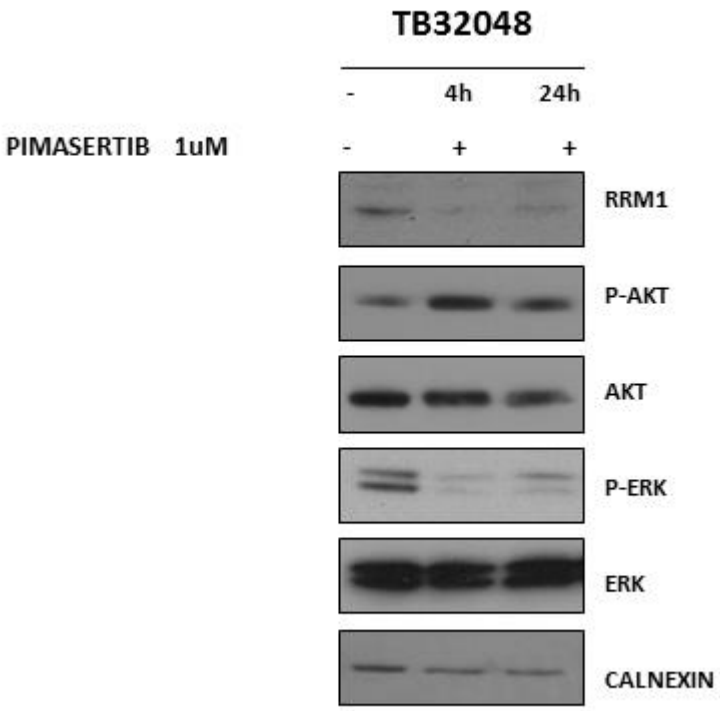

Figure 5.3: Pimasertib reduces RRM1 protein levels in TB32048 cells.
TB32048 cells were treated for 4 and 24 hours with 1 μM pimasertib. Total cell lysates were immunoblotted using the indicated antibodies. Calnexin was used as loading control.

A

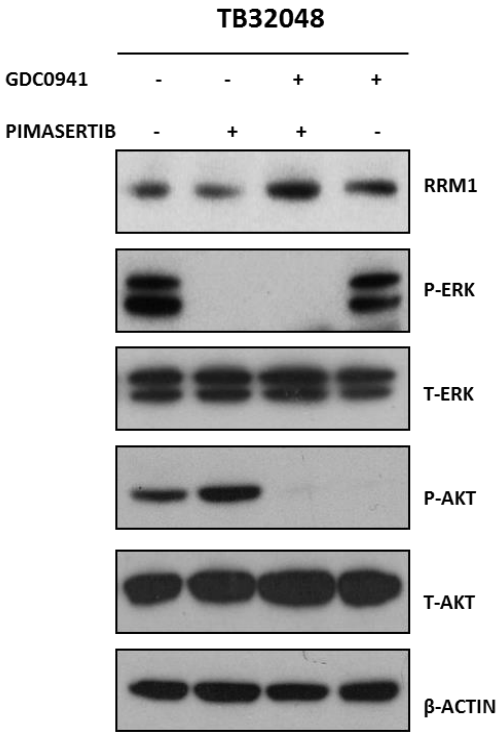

B

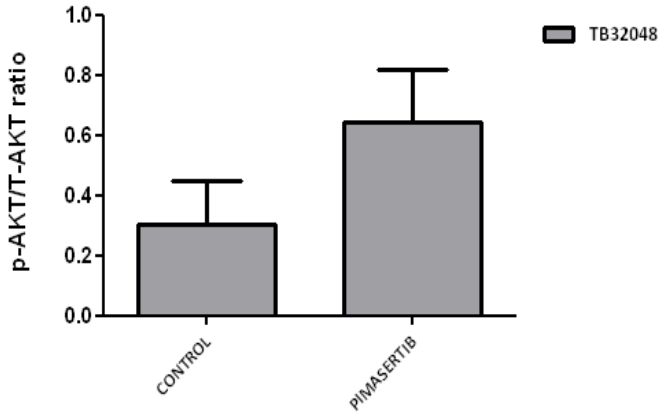

Figure 5.4: AKT inhibition impairs RRM1 downregulation induced by pimasertib in TB32048 cells.
A. TB32048 cells were treated for 4 hours with 1μM of PI3K inhibitor GDC-0941 together with 1μM pimasertib. Total cell lysates were immunoblotted using the indicated antibodies and β-actin was used as loading control. **B.** Densitometric analysis of the immunoblots presented in figure 5.4A. Results are presented as mean ± SD of three independent experiments. Image J software was used for quantitation of the western blot bands. Fold increase of P-AKT/T-AKT was calculated by normalization to the loading control and comparison to the untreated sample.

5.3.2 Combination of pimasertib with gemcitabine induces tumor growth delay in TB32048 mice

To investigate the antitumor activity of pimasertib with gemcitabine *in vivo,* an orthotopic mouse model was generated by injecting a total of 10^5 TB32048 cells in 30 µl of matrigel into the pancreata of 6-week old immunocompetent C57/BL6 black female mice. Two weeks after orthotopic implantation, tumors were established and mice were randomly divided into 4 groups (*n*=6 for each group) to receive the following treatments: 1) 0.5% carboxyl methylcellulose and 0.25% Tween 20 by oral gavage (vehicle), 2) gemcitabine intraperitoneally 80mg/kg (twice/week), 3) pimasertib via oral gavage at 5mg/kg (daily), 4) with pimasertib 5mg/kg (daily) followed 4 hours later by gemcitabine 80mg/kg (twice/week) (Table 5.1).

The choice of pimasertib dose was based on previous *in vivo* experiments conducted on xenograft models at EMD Serono, which showed that pimasertib was well tolerated at doses of 5 and 10mg/kg. The dose of gemcitabine chosen for this study was the same adopted by our collaborators at Barts for other studies in pancreatic mouse models, which gave no evidence of acute toxicity. Additionally, 80mg/kg corresponds to ≈ 450mg/m^2, which is below the standard clinically human dose of gemcitabine given once weekly (1000mg/m^2).

The schedule used in our *in vivo* experiments was designed according to the time of drug administration that produced the best synergistic effect *in vitro*. After two treatment cycles of 5 days each, all mice were sacrificed 4 hours after the last administration of pimasertib, tumor excised, weighed and sectioned for histopathologic analysis.

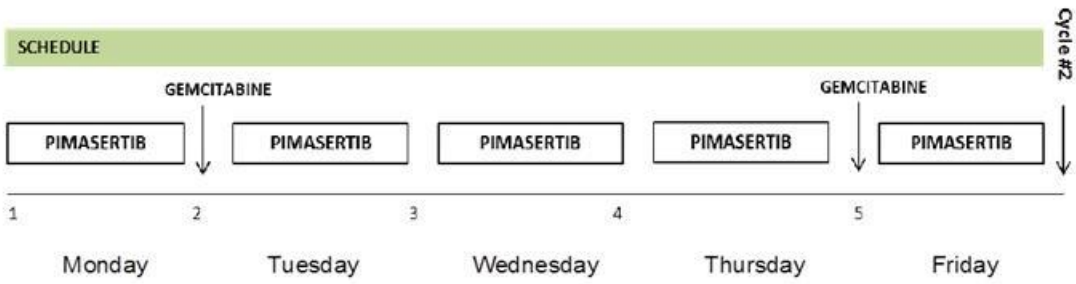

Table 5.1: Schematic schedule of treatments.
The diagram shows an outline of the treatment schedule used in this study. After tumors were established, TB32048 mice were treated with gemcitabine intraperitoneally 80mg/kg (twice/week), pimasertib via oral gavage at 5mg/kg (daily) or with pimasertib 5mg/kg (daily) followed 4 hours later by gemcitabine 80mg/kg (twice/week). Mice were treated for 2 cycles of 5 days each.

Mice treated with pimasertib or gemcitabine alone had no statistically significant difference in tumor weight compared to mice treated with vehicle (Fig. 5.5A). In contrast, the combination cohort resulted in significantly smaller tumors as compared to vehicle (**P< 0.01), gemcitabine (*P< 0.05) or pimasertib (**P< 0.01) (Fig. 5.5A).

A decrease of tumor vasculature density was observed in pimasertib alone and pimasertib plus gemcitabine treated mice compared to the other cohorts (Fig. 5.5B), suggesting an anti-angiogenic effect induced by the MEK inhibitor. Representative gross images of dissected tumors from each group are shown in Figure 5.5B.

A

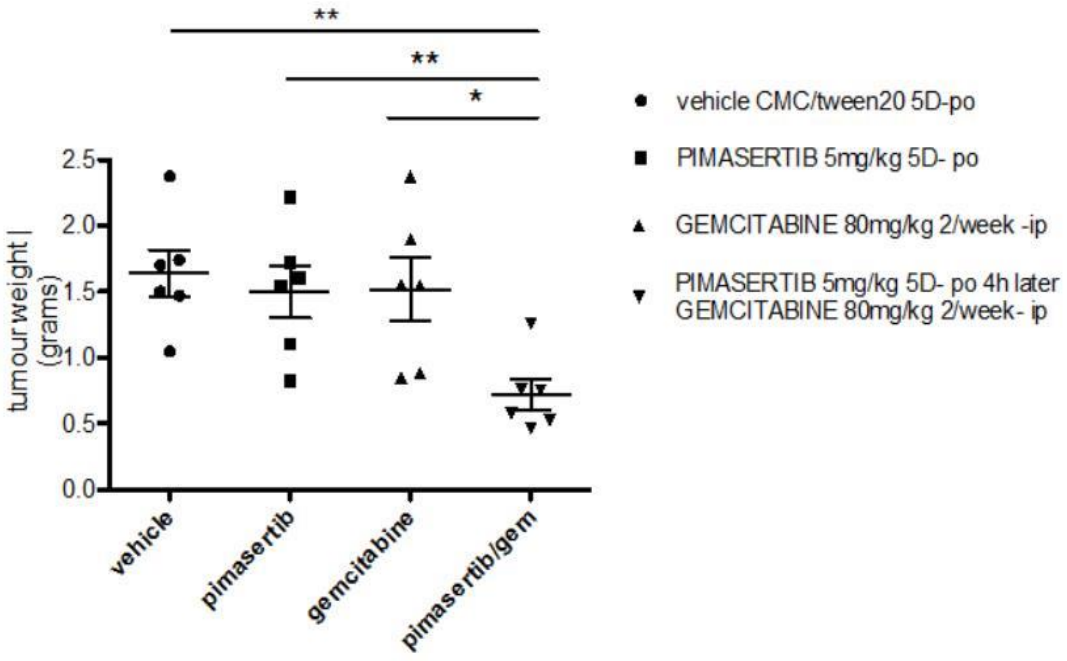

B

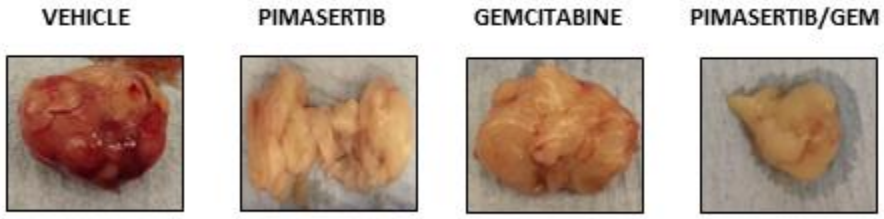

Figure 5.5: The sequential combination of pimasertib with gemcitabine delays tumor growth *in vivo*.
A. TB32048 tumor-bearing mice were treated with vehicle, 5mg/kg pimasertib (daily) by oral gavage, gemcitabine 80mg/kg (twice/week) intraperitoneally or a sequential combination of pimasertib 5mg/kg followed 4 hours later by gemcitabine 80mg/kg. After 12 days, mice were sacrificed and tumor weight was measured. Student's t test was used to determine the statistical significance of differences in tumor weight (**P<0.01 and *P<0.05). **B.** Gross images from representative excised tumors are shown.

Primary tumor volumes were measured using ultrasound imaging before drug treatment and before sacrifice. From these data changes in tumor volume were calculated. Tumor volumes from mice treated with gemcitabine (149mm^3 vs 1112mm^3 $P < 0.001$) or pimasertib alone (90mm^3 vs 673mm^3 $P < 0.001$) significantly increased at the end of the treatment (Fig. 5.6). On the other hand, the average tumor volumes of the combination group were not significantly different before and after treatment (108mm^3 vs 404mm^3 $P > 0.05$) (Fig. 5.6). These results showed that only the combination of pimasertib with gemcitabine was effective at slowing down tumor growth in TB32048 mice. All drug treatments regimens were well tolerated in mice. No signs of acute toxicity were observed with any of the drug treatments.

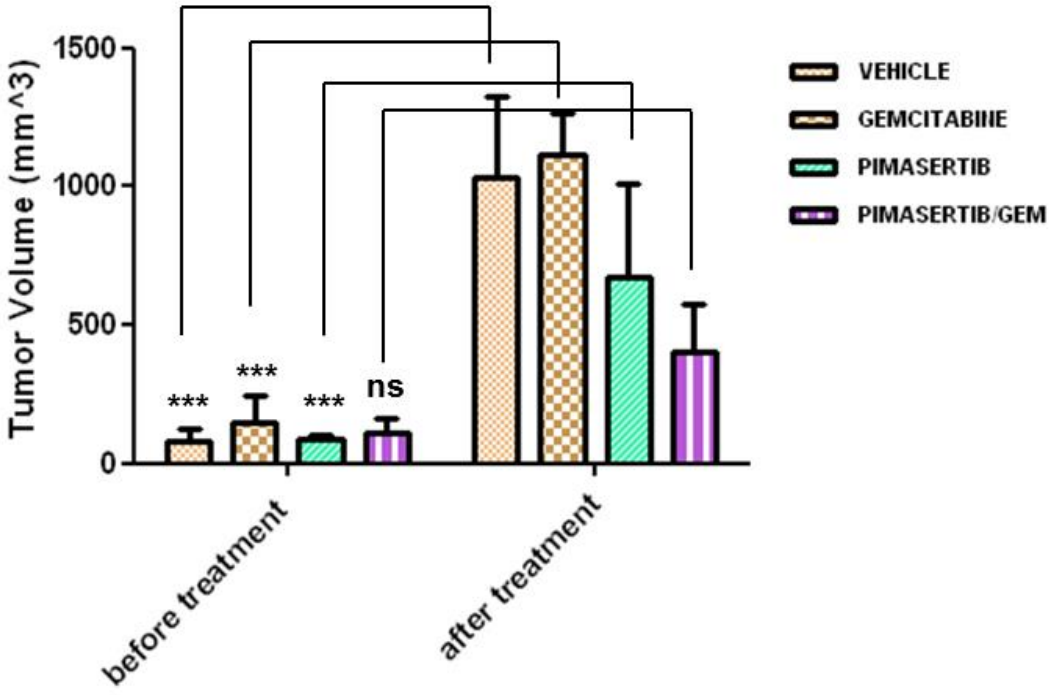

Figure 5.6: Tumor volumes of TB32048 mice before and after drug treatment.
Pancreatic tumor volumes were measured before the start and at the end of each drug treatment by ultrasound analysis. Results are expressed in tumor volume (mm^3). Each data point represents the mean ± SD of 6 mice per treatment group. Statistical analysis was performed using One-way Anova with Bonferroni Post-test (***P<0.001, ns P>0.05).

5.3.3 Pimasertib/gemcitabine combination inhibits proliferation and induces apoptosis in TB32048 mice

Hematoxylin and Eosin (H&E) staining of tumor sections was performed. H&E staining revealed spindle or oval-shaped tumor cells arranged in a weave pattern, indicative of poorly differentiated adenocarcinoma, with mild desmoplastic reaction and variable degree of lymphocytic infiltrate. No difference in tumor morphology was observed among the four groups (Fig. 5.7).

Next, we investigated the effects of pimasertib, gemcitabine or their combination on proliferation and apoptosis in TB32048 mice. Immunohistochemical staining was performed by using antibodies against Ki67, a marker of cell proliferation, and cleaved caspase-3 (CC3), a marker of apoptosis. Reduced nuclear expression of ki67 was observed in mice treated with pimasertib compared to the other treatments (Fig. 5.8A). An increase in the number of CC3 positive cells was observed in mice treated with the pimasertib/gemcitabine regimen compared to the other treatment groups (Fig. 5.8B) suggesting that the antitumor effect of the combination is mediated by induction of apoptosis. On the other hand, treatment with gemcitabine alone did not seem to affect apoptosis of TB32048 mice as it did in human pancreatic cancer cell lines BxPC-3 and PANC-1 (Fig. 3.12-3.14).

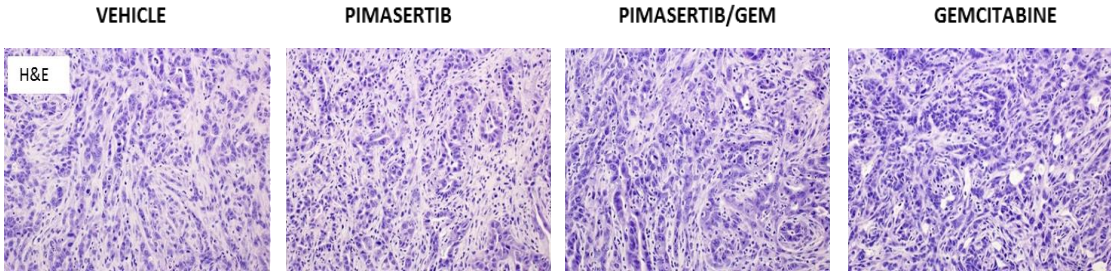

Figure 5.7: TB32048 mice develop pancreatic tumor morphology.
Representative H&E staining from mouse pancreas were performed to determine tissue morphology.

A

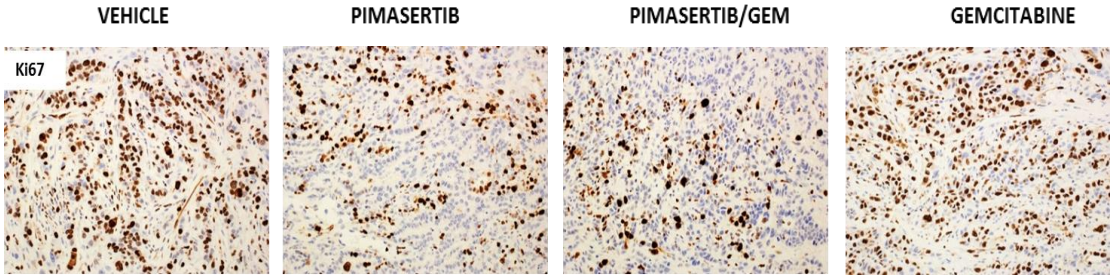

B

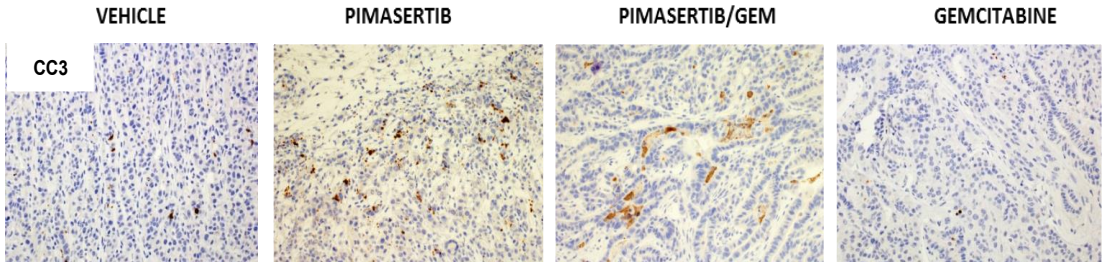

C

	Percentage of stained CC3 cells			Percentage of stained Ki67 cells	
	< 1%	**1-5%**		**< 40%**	**> 40%**
Vehicle	6	0	Vehicle	2	4
Gem 80mg/kg	1	5	Gem 80mg/kg	4	2
Pim 5mg/kg	2	4	Pim 5mg/kg	5	1
Pim/Gem	0	6	Pim/Gem	4	2

Figure 5.8: Effects of pimasertib and gemcitabine on proliferation and apoptosis of TB32048 mice.
A. Representative Images of Ki67 staining of paraformaldehyde-fixed sections derived from tumors treated with the indicated drugs or vehicle. **B.** Representative Images of CC3 staining of paraformaldehyde-fixed sections derived from tumors treated with the indicated drugs or vehicle.
C. Ki67 and CC3 staining were quantified as previously described and scored.

5.3.4 Pimasertib inhibits P-ERK activation *in vivo*

The molecular mechanism of action of pimasertib and gemcitabine was investigated in the TB32048 orthotopic mouse model of pancreatic cancer. First, to test the specificity of the MEK inhibitor, P-ERK staining was performed. Immunohistochemical analysis revealed that ERK phosphorylation was significantly reduced in TB32048 tumors harvested from the pimasertib and gemcitabine/pimasertib cohorts. On the other hand, gemcitabine activated phosphorylation of ERK (Fig. 5.9A). Gemcitabine induced activation of MAPK signaling in PDAC tumors have already been observed in other preclinical studies (Miyabayashi et al. 2013). Quantification of P-ERK staining was performed as described in the methods section and showed in Figure 5.9B

A

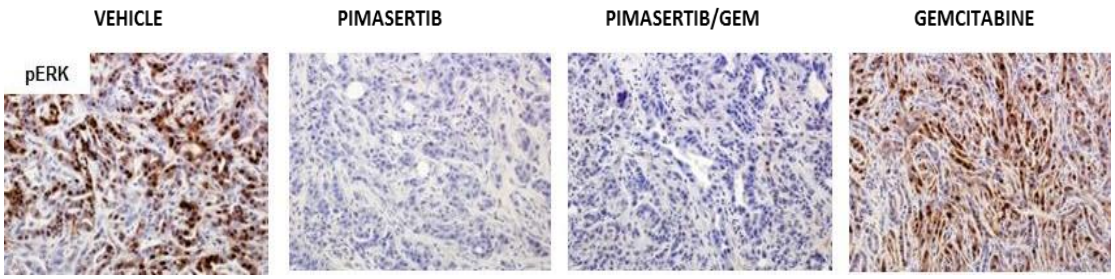

B

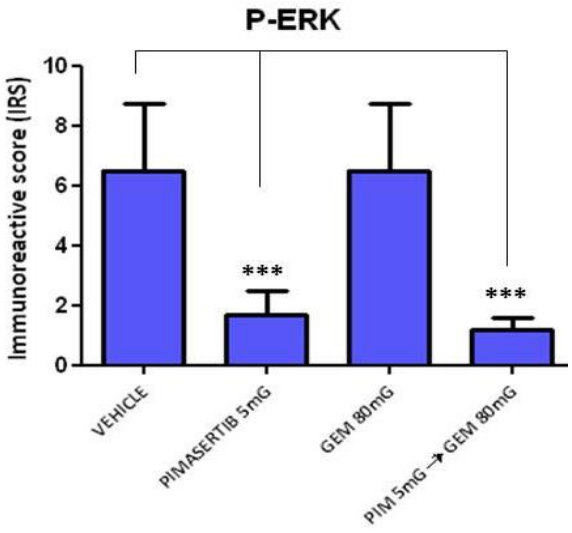

Figure 5.9: Pimasertib inhibits P-ERK protein expression in TB32048 mice.
A. Representative images of P-ERK staining of paraformaldehyde-fixed sections derived from tumors treated with the indicated drugs or vehicle (brown staining indicates detection of P-ERK in paraffin tissue sections). **B.** P-ERK staining was quantified and scored. Results are represented in the column graph. (n= 6/ group). One-way Anova was performed for statistical analysis (***P<0.001).

5.3.5 Pimasertib reduces RRM1 protein levels *in vivo*

We have previously demonstrated that pharmacological or biological inhibition of MEK protein reduces RRM1 protein levels in human pancreatic cancer cell lines (Fig.3.23, 3.25) and mouse KPC cell line (TB32048) (Fig. 5.3). Immunohistochemical analysis showed a significant reduction in the expression of RRM1 in mouse tumors from pimasertib- and pimasertib/gemcitabine cohorts (Fig. 5.10A), a result comparable to what was observed *in vitro*. Quantification of RRM1 staining was performed and showed in Figure 5.10B.

A

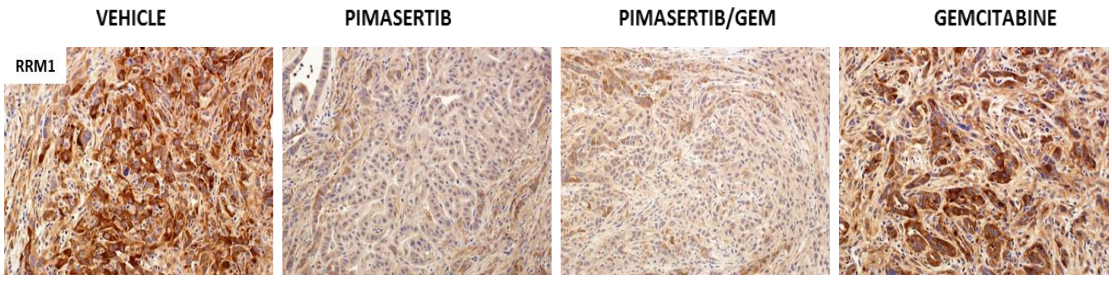

B

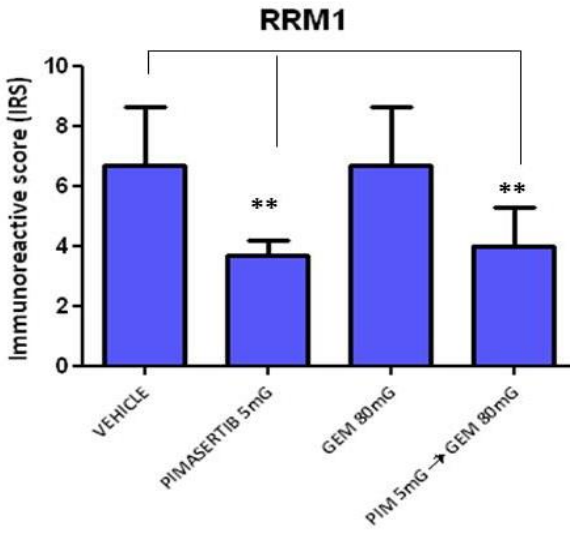

Figure.5.10: Pimasertib destabilizes RRM1 protein inTB32048 mice.
A. Representative Images of RRM1 staining of paraformaldehyde-fixed sections derived from tumors treated with the indicated drugs or vehicle. B. RRM1 staining was quantified and scored. Results are represented in the column graph. (n= 6/ group). One-way Anova was performed for statistical analysis (**P<0.01).

5.3.6 Pimasertib increases P-AKT expression *in vivo*

Previous reports have shown that MEK inhibitors activate the PI3K/AKT signalling pathway through mechanisms of feedback regulation. (Duncan et al. 2012). Our *in vitro* results showed an increase of AKT phosphorylation upon treatment with pimasertib (Fig. 4.12-4.13 and 5.3). To determine whether pimasertib activates P-AKT *in vivo*, we analysed its expression by immunohistochemistry. A significant increase in AKT phosphorylation was observed after pimasertib treatment in TB32048 xenograft tumors (Fig. 5.11A). Quantification of P-AKT staining was performed and showed in Figure 5.11B.

A

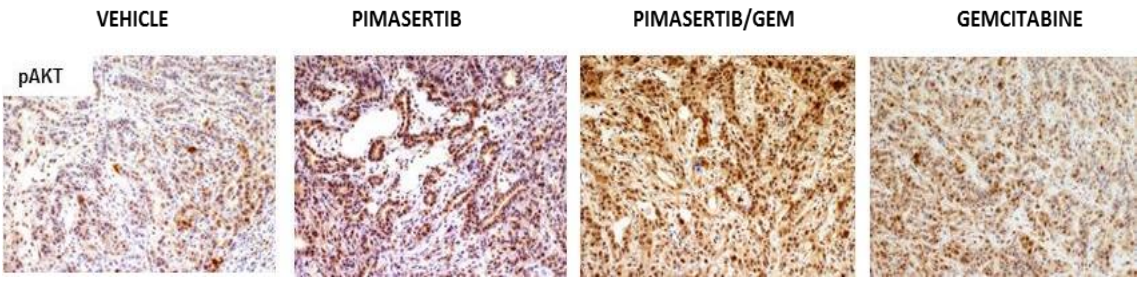

B

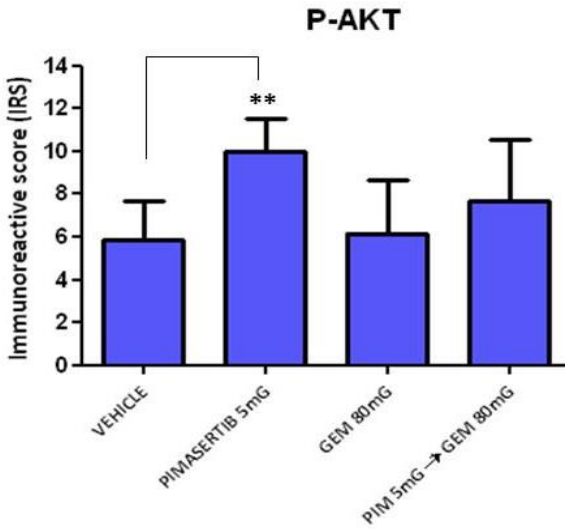

Figure 5.11: Pimasertib increases P-AKT expression in xenograft mice.
A. Representative Images of P-AKT staining of paraformaldehyde-fixed sections derived from tumors treated with the indicated drugs or vehicle. **B.** P-AKT staining was quantified and scored. Results are represented in the column graph (n= 6/ group). One-way Anova was performed for statistical analysis (**P<0.01).

5.3.7 High dose of pimasertib induces tumor growth delay in TB32048 mice when combined with gemcitabine

A second *in vivo* experiment was carried out using the same schedule described in 5.3.2 but with a different dosing regimen of pimasertib (15mg/kg). The pimasertib/gemcitabine regimen produced significantly smaller tumors compared to vehicle (*P< 0.05) gemcitabine alone (**P< 0.01) and pimasertib alone (*P<0.05) (Fig. 5.12A). Representative gross images of tumor from each group are shown (Fig. 5.12B). The higher dose of pimasertib was still well tolerated with no apparent signs of acute toxicity.

A

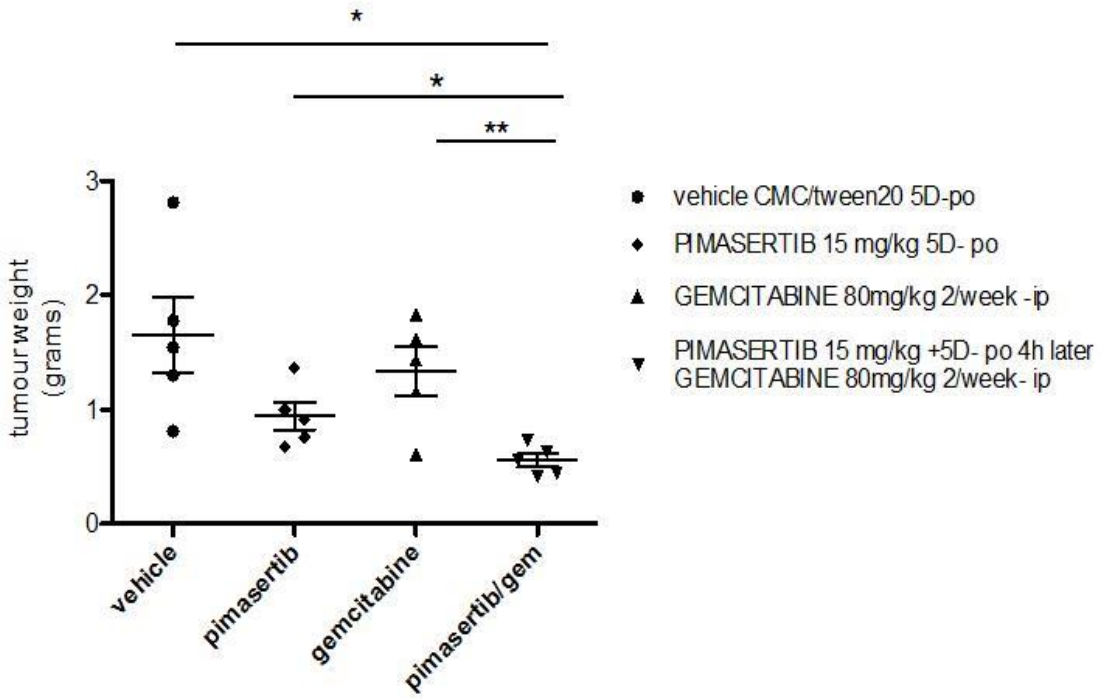

Figure 5.12: Pimasertib (15mg/kg) in combination with gemcitabine delays tumor growth in vivo.
A. TB32048 tumor-bearing mice were treated with vehicle, 15mg/kg pimasertib (daily) by oral gavage, gemcitabine 80mg/kg (twice/week) intraperitoneally or a sequential combination of pimasertib 15mg/kg followed by gemcitabine 80mg/kg. After 12 days mice were sacrificed and tumor weight was measured. Student's t test was used to determine the statistical significance of differences in tumor weight (**P<0.01 and *P<0.05).

B

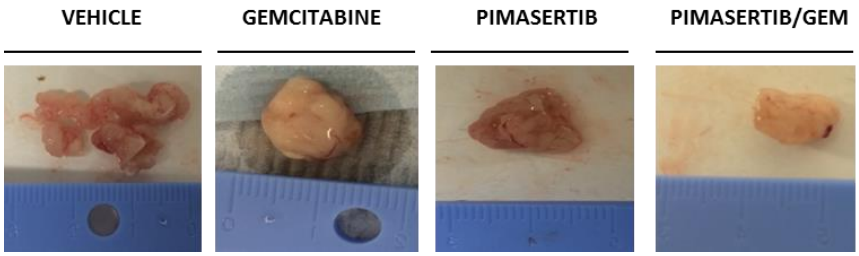

Figure 5.12 continued: Pimasertib (15mg/kg) in combination with gemcitabine delays tumor growth *in vivo*.
B. Gross images from representative excised tumors of TB32048 mice treated with the indicated drugs.

Immunohistochemical analysis on TB32048 mouse tumors showed a significant reduction in the expression of P-ERK and RRM1 in tumors from pimasertib (15mg/kg)- and pimasertib (15mg/kg) plus gemcitabine (80mg/kg) cohorts (Figure 5.13).

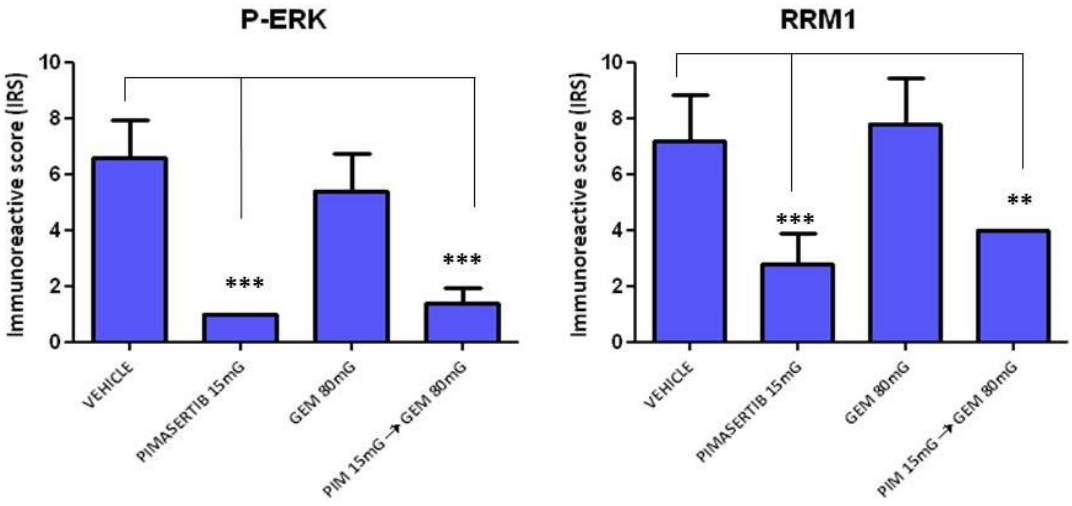

Fig. 5.13: 15mg/kg pimasertib reduces P-ERK and RRM1 expression in TB32048 mice.
P-ERK and RRM1 staining was quantified and scored. Results are represented in the column graph. (n= 5/ group). One-way Anova was performed for statistical analysis (***P<0.001 **P<0.01).

5.3.8 Metastatic spread is reduced in the combination cohort

At the end of drugs treatment, mice were sacrificed and visible metastases were counted. No significant difference in the incidence of metastasis was observed between the groups when mice were treated with 5mg/kg pimasertib and 80mg/kg gemcitabine (Fig. 5.15). The combination cohort had significantly reduced metastases incidence compared with vehicle cohorts when pimasertib was administered at 15mg/kg (Fig. 5.16A). In particular, visible liver and spleen metastasis were observed in mice treated with vehicle. Mice treated with pimasertib plus gemcitabine showed metastasis only in the spleen. Representative images are illustrated in figure 5.16B.

One limitation of this result was due to the fact that visible metastases were counted by naked eye and no methods were used for this analysis.

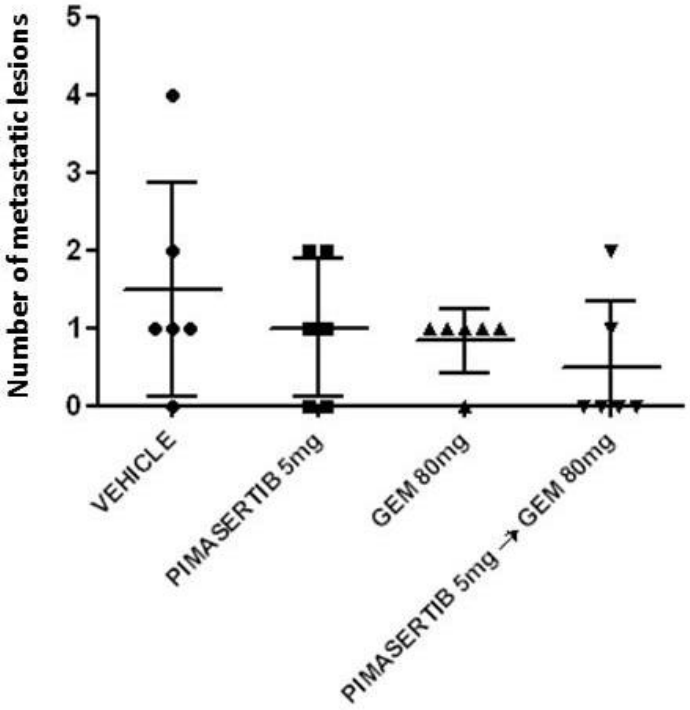

Figure 5.15 Pimasertib 5mg/kg plus gemcitabine-treated mice do not reduce the incidence of metastases compared to other cohorts.

Visible metastases in mice treated with pimasertib, gemcitabine or their combinations were counted and the number of metastases in each individual mouse was quantified and showed in the graphs. The graph shows the number of metastases in each individual mouse.

A

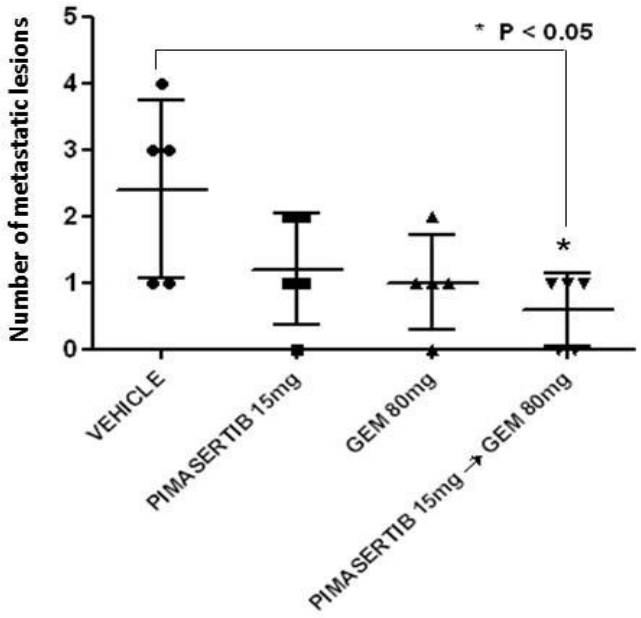

B

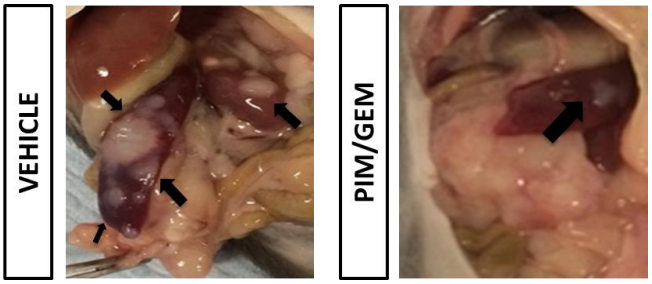

Figure 5.16: pimasertib 15mg/kg plus gemcitabine-treated mice develop less metastases compared to vehicle-treated mice.

A. Visible metastases in mice treated with 15mg/kg pimasertib, 80mg/kg gemcitabine or their combinations were counted and the number of metastases in each individual mouse was quantified and showed in the graphs (*P<0.05). **B.** Gross Images of TB32048 mouse tumors from vehicle or gemcitabine/pimasertib cohorts. Arrows indicate liver and spleen metastases.

5.4 DISCUSSION

5.4.1 *In vivo* model systems to study cancer therapeutics

An important challenge in cancer research is to generate predictive experimental models to study the function of genes in a particular tumor with the aim of improving patient's personalized treatment (Dow and Lowe 2012). Several *in vivo* models of pancreatic tumors have been established and have helped to better understand the biology of this aggressive disease (Herreros-Villanueva et al. 2012). For example, patient-derived xenograft (PDX) models, developed from patients' tumor tissues, are now an important system to study PDAC. To generate these models, tumors, obtained fresh after surgical resection or from tumor biopsies, are implanted into immunodeficient mice (Siolas and Hannon 2013). PDX models of pancreatic cancer have shown to recapitulate the genetic features found in the human disease but one limitation is the absence of an intact immunity. A recent study adopted PDX models as an investigational platform for drug response with the aim of personalizing treatment course for PDAC patients (Hidalgo et al. 2014). In particular, the patient's treatment choice was based on the drug response against the xenograft models developed from the patient's tumor. The results demonstrated that drugs activity in PDX models was in many cases correlated with the patient's outcome, suggesting that the use of PDX models as a tool to predict patients' drug response should be further investigated (Hidalgo et al. 2014).

Organoids represent a recently established model system to grow pancreatic tissue in a three-dimensional culture system (Boj et al. 2015). Organoids can be generated from human patient tissues, by performing small patient biopsies, or from mice tissues (Fig. 5.17). Because they can be genetically manipulated, they represent a powerful tool for the discovery of novel mediators of PDAC progression (Boj et al. 2015). Recently, organoids have been generated from adult $KRAS^{G12D}$ GEM mouse ductal cells. Once isolated from murine tissues, ductal cells were embedded in matrigel and started folding and to develop into budding structures within 2-3 days (Huch et al. 2013). These organoids could then be orthotopically transplanted in mice, where they fully developed all the common features of human PDAC (Boj et al. 2015).

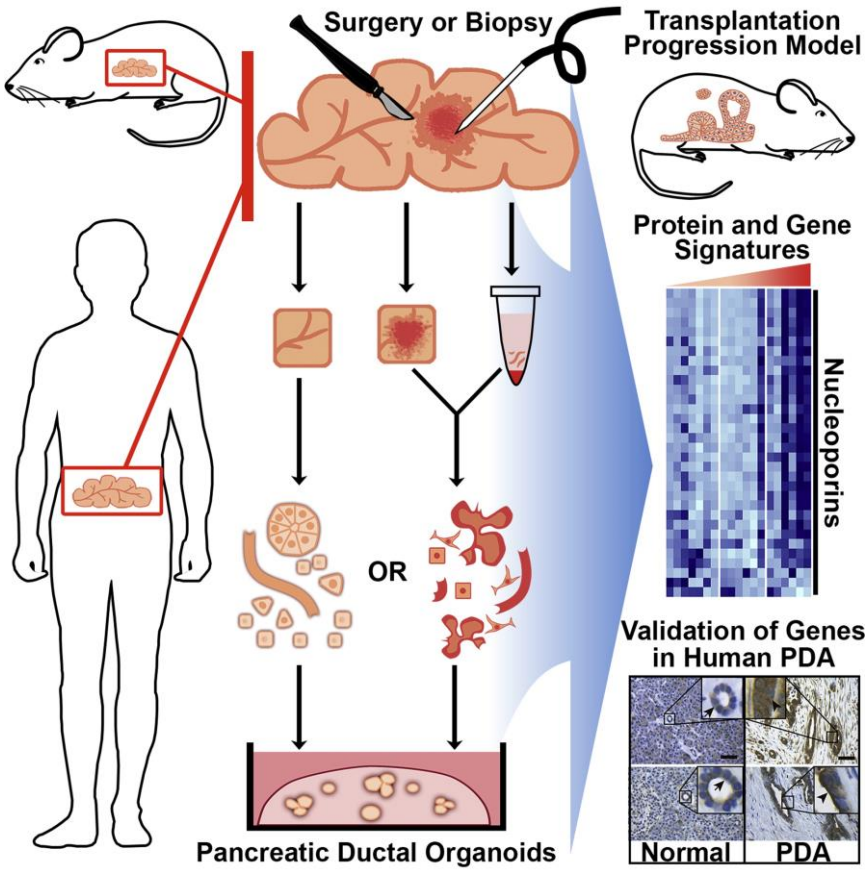

Figure 5.17: Establishment of pancreatic ductal organoids.
Ductal cells from adult mice or patients biopsies are isolated and embedded in matrigel. Duct cells formed cystic structures after 24 hours and passaged in cultures. After 2-3 days cells started to fold and acquired cuboidal structures (Boj et al. 2015).

The development of genetically engineered mouse models (GEMMs), such as the KPC mouse model, where mutant K-RAS and mutant TP53 is expressed specifically in the mouse pancreatic tissue, has been crucial to explore the role of these genetic alterations in pancreatic tumor initiation, development and progression (Ardito et al. 2012) (Collins et al. 2012). However, these models require long times to develop and are extremely expensive, thus xenograft (orthotopic or heterotopic) mouse models are widely used instead as a model system to explore the effects of novel anticancer therapies. In the orthotopic model cells are implanted directly into the mouse organ of the corresponding tumor of origin. These models are less time consuming than GEM models and they rapidly develop palpable tumors. Orthotopic syngeneic mouse models established in immunocompetent mice have been demonstrated to be more effective than orthotopic isogenic models (generated from human tumor cell lines) at

predicting patient response to therapy. In fact, transplanted cells and mouse hosts share the same genetic background and this allow maintenance of an intact immune system development of a tumor microenvironment similar to what is observed in human tumors (Tseng et al. 2010). One disadvantage of these models is represented by the fact that transplanted mouse tissue might not fully recapitulate the complexity of human cancers in the clinical setting (Loukopoulos et al. 2004).

5.4.2 MEK inhibition plus gemcitabine combination induces antitumor activity in an orthotopic mouse model of pancreatic cancer

New therapies are urgently needed for PDAC patients since the current available treatments provide small survival benefit (Garrido-Laguna and Hidalgo 2015). MEK inhibitors in combination with gemcitabine, one of the standard chemotherapeutic agents used in PDAC, induced tumor stasis but not regression in a mutant K-RAS GEM model of pancreatic cancer (Junttila et al. 2015). However, the improvement in survival was not dramatic compared to the effects obtained by the combination of gemcitabine with the EGFR inhibitor erlotinib in the same model (Singh et al. 2010). This modest survival benefit was associated with the dose of the MEK inhibitor used, which produced only partial and not sustained MAPK pathway suppression (Junttila et al. 2015).

For this project, we developed an orthotopic mouse model of pancreatic cancer by implanting tumor cells derived from the established KPC mouse model into the pancreas of immunocompetent mice. The biological matrix matrigel was used to inject the cells into the pancreas. This biological matrix remains in a liquid state at low temperatures but forms a gel once is injected into the mice where the local tissue temperature is increased. The use of this three-dimensional matrix prevents any injection site leakage (Jiang et al. 2014). These mice developed tumors within two weeks, after which they were treated with gemcitabine and pimasertib. Our study provided *in vivo* evidence that gemcitabine alone did not result in relevant slowing of tumor growth. The weak antitumor activity of gemcitabine *in vivo* has already been shown and it is often attributed to its short half-life (Frese et al. 2012). The addition of the MEK inhibitor pimasertib to gemcitabine induced significant tumor growth

attenuation (Fig. 5.5-5.12). No tumor regression was observed, as expected, since the treatment period in these experiments was brief (12 days). The purpose of the study was to examine dynamic effects on gene expression as in *in vitro* studies. Pimasertib induced strong pathway inhibition as shown by the reduction of phospho-ERK expression (Fig. 5.9, 5.15) and upregulation of phospho-AKT in pancreatic xenograft models (Fig. 5.11), further highlighting the existence of a feedback loop between MEK and PI3K signalling.

The results of our experiments indicate that low doses of pimasertib are sufficient at inducing specific target inhibition and are effective at sensitizing mouse models of pancreatic cancer to gemcitabine treatment, supporting evaluation of such dosing schedules for future clinical trials to reduce the common side effects experienced with MEK inhibitors.

5.4.3 Pimasertib modulates RRM1 expression *in vivo*

Gemcitabine diphosphate covalently binds and inhibits Ribonucleotide Reductase (RR) large subunit-1 (RRM1) as one of its mechanisms of cytotoxicity (Gesto et al. 2012).

Our *in vitro* results obtained from human pancreatic cancer cell lines identified RR large subunit-1 (RRM1) to be modulated by pimasertib treatment. This is an important finding since RRM1 overexpression has been frequently associated with increased resistance to gemcitabine (Zhang et al. 2014) (Bepler et al. 2006). Consistent with our *in vitro* observation, pimasertib induced downregulation of RRM1 protein in the KPC mouse cell line (Fig. 5.3). In addition, a significant decrease of RRM1 protein levels was observed in our pancreatic xenograft models treated with pimasertib alone and in combination with gemcitabine (Fig. 5.10, 5.13).

5.5 CONCLUSIONS

The use of a syngeneic orthotopic mouse model of pancreatic cancer was valuable in the preclinical evaluation of the antitumor activity between pimasertib and gemcitabine. The orthotopic mouse model generated for this study was not significantly impacted by MEK inhibition or gemcitabine administration. However, sequential combination treatment of the two agents resulted in significantly delayed tumor growth. Moreover, pimasertib efficiently suppressed MAPK pathway activation and decreased RRM1 protein levels in mouse tumors, a mechanism that might explain why these models benefit from pimasertib plus gemcitabine combination.

Our *in vivo* results further provide a biological rationale for further investigation of gemcitabine in combination with MEK inhibitors in the clinical setting for improving PDAC patient's outcome.

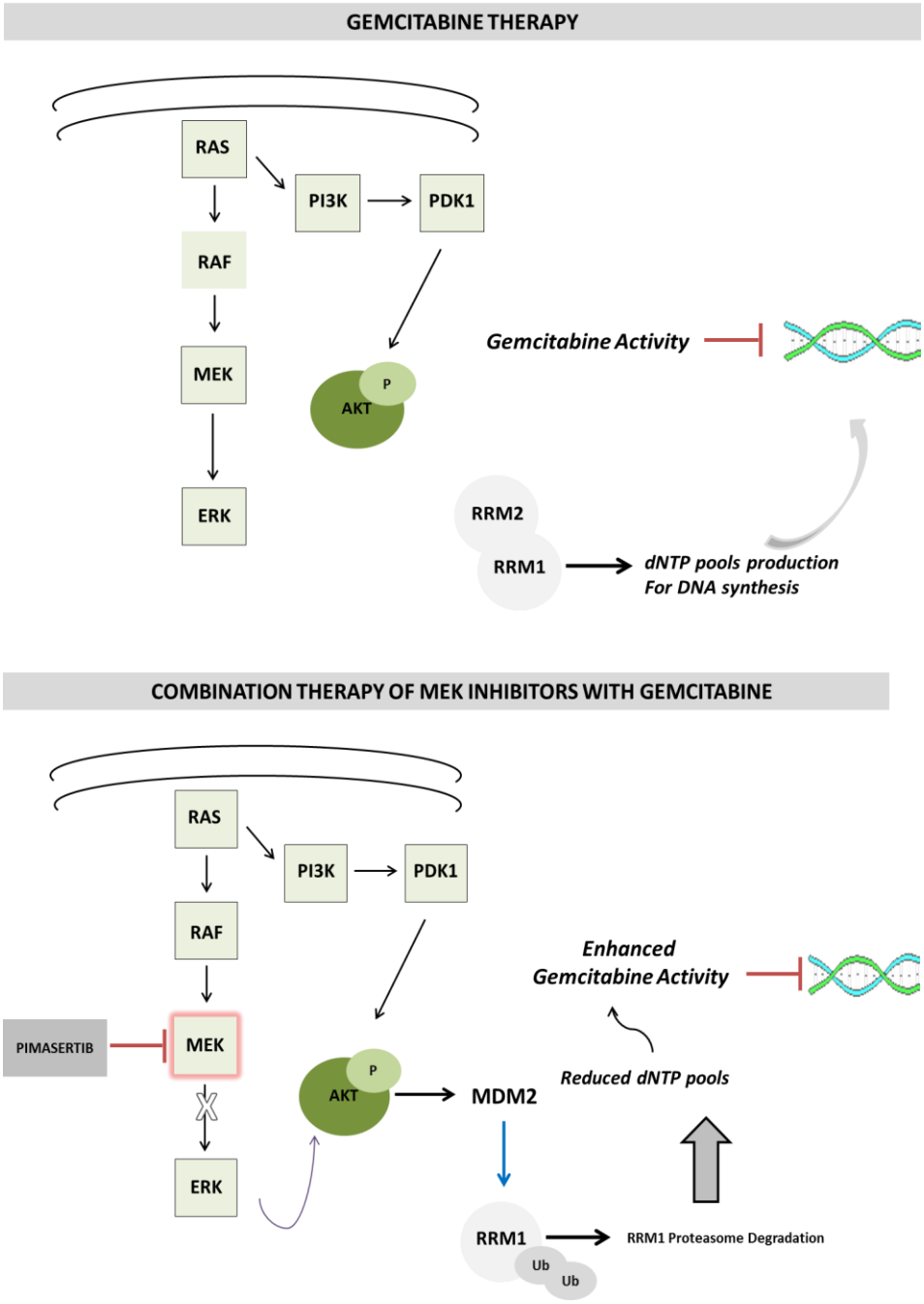

Figure 5.18: Graphical abstract of the mechanism of action of pimasertib with gemcitabine.
In normal conditions GTP-bound RAS activates RAF, which in turn phosphorylates and activates MEK, which ultimately phosphorylates ERK and induces its translocation into the nucleus where it induces expression of genes associated with cell proliferation, differentiation and survival. The active form of gemcitabine gets incorporated into the DNA double strand and leads to termination of DNA duplication. The MEK inhibitor pimasertib blocks MEK into a catalytically inactive conformation that blocks MEK from binding ERK. When MEK signalling is inhibited, there is an increase in AKT activation, which triggers MDM2 to ubiquitinate and degrade RRM1. As a result gemcitabine activity is potentiated.

CHAPTER 6

CONCLUSIONS AND FUTURE WORK

Pancreatic ductal adenocarcinoma (PDAC) is a lethal malignancy characterised by a 1-year survival rate of 18% (Hidalgo 2015). Less than 20% of PDAC patients are candidates for surgery at time of diagnosis, which is the only curative option available. However, almost 90% of these patients still die of local recurrence or metastatic disease (Hidalgo et al. 2015). In the adjuvant setting, gemcitabine, a deoxycytidine analogue, whose active form interferes with DNA synthesis leading to its termination, was approved in 1997 as a standard care for PDAC on the basis of improved quality of life indicators (Burris et al. 1997). Unfortunately, the survival benefit of gemcitabine is rather modest (median survival less than 6 months) and its limited efficacy is mainly caused by intrinsic and acquired resistance (Werner et al. 2013). Therapeutic strategies against PDAC have been the focus of intense studies for the last decade and have led to the approval of two novel chemotherapeutic regimens that produced a small but significant effect on survival: FOLFIRINOX and nab-paclitaxel plus gemcitabine combination (Conroy et al. 2011) (Von Hoff et al. 2013).

The majority of PDAC patients harbour a mutation within the K-RAS gene, which is required for tumor initiation and development (di Magliano and Logsdon 2013). There has been extensive interest in the development of inhibitors of downstream effectors of K-RAS effectors as a strategy for PDAC therapy; in particular, MEK protein, a dual-specific kinase, represents a potential target of therapeutic intervention since it is downstream RAS and activates ERK to stimulate proliferation, differentiation, migration and survival (Neuzillet et al. 2014) (Neuzillet et al. 2013).

Ribonucleotide Reductase enzyme catalyses the conversion of ribonucleosides to deoxyribonucleosides triphosphates needed for new DNA synthesis and repair. Gemcitabine diphosphate is a direct inhibitor of Ribonucleotide Reductase subunit-1 (RRM1) (Heinemann et al. 1990), whose expression has been frequently associated with gemcitabine resistance (Wang et al. 2013) (Wonganan et al. 2012) (Zhang et al. 2014). Therefore, molecular agents that alter RRM1 stability could be a promising strategy for the management of gemcitabine resistance.

In this study we sought to investigate the effects of combining gemcitabine with pimasertib, an allosteric MEK1/2 inhibitor and to explore their mechanisms of interaction in pancreatic cancer models.

Chapter three determined the biological effects of pimasertib and analysed the effects of pimasertib in combination with gemcitabine on proliferation, apoptosis and cell signalling pathway genes in human pancreatic cancer cell lines. Strong inhibition of ERK phosphorylation was observed upon pimasertib treatment. Simultaneous administration of pimasertib with gemcitabine was not effective at inhibiting proliferation or at enhancing apoptosis. On the other hand, synergistic antiproliferative effects and enhanced apoptosis were observed upon sequential treatment with pimasertib followed by gemcitabine. Our results showed that pimasertib arrested the cells at G1-phase and gemcitabine induced an S-phase arrest. Therefore we suggest that concomitant treatment would suppress the effects of gemcitabine to act as an S-phase specific agent.

We then investigated whether the expression of genes associated with gemcitabine response could be modulated by MEK inhibition. To our surprise we found RRM1 to be significantly downregulated by pimasertib treatment. This effect was specifically dependent on MEK protein inhibition and was not induced by blocking upstream activators of the MEK pathway such as EGFR.

Finally, the data provided confirmed the role of RRM1 in affecting gemcitabine response, since its depletion increased gemcitabine-induced apoptosis in human pancreatic cancer cell lines.

Chapter four explored the molecular mechanisms by which pimasertib reduces RRM1 protein expression. Subsequent mechanistic studies focusing on modulation of RRM1 stability indicated that pimasertib reduced RRM1 protein by enhancing its ubiquitin-dependent proteasomal degradation. Additionally, the results found MDM2 to be involved in mediating RRM1 polyubiquitination, since biological or pharmacologic inhibition of MDM2 impaired RRM1 downregulation occurring after pimasertib treatment.

The involvement of PI3K/AKT signalling in the degradation of RRM1 induced by pimasertib was also studied. We observed increased phosphorylation of AKT after pimasertib treatment. Furthermore, co-treatment with pimasertib and a PI3K inhibitor impaired RRM1 downregulation triggered by the MEK inhibitor, thus we believe that

AKT activation induced by MEK inhibition is in part associated with MDM2-mediated degradation of RRM1 protein.

Chapter five aimed to confirm the synergistic antitumour activity of pimasertib with gemcitabine combination observed *in vitro*, in an orthotopic pancreatic tumour model. Sequential combination of pimasertib followed by gemcitabine inhibited tumour growth. Additionally, the MEK inhibitor abrogated P-ERK signalling and markedly decreased RRM1 protein levels *in vivo,* an effect we believe is associated with the synergistic antitumour activity observed between pimasertib and gemcitabine.

6.1 FUTURE DIRECTIONS:

6.1.1 What are the effects of simultaneous administrations of gemcitabine with pimasertib *in vivo*?

The results presented in this thesis indicate that sequential but not concomitant combination of MEK inhibitors with gemcitabine produces synergistic anti-proliferative and pro-apoptotic effects *in vitro*. The schedule that induced the best synergism was used for assessing the antitumour activity of pimasertib plus gemcitabine combination in an orthotopic model of pancreatic cancer. It would be of great interest to investigate the effects of simultaneous administration of pimasertib with gemcitabine in the same model to confirm the antagonism observed *in vitro*.

6.1.2 Does knockdown of MDM2 sensitize pancreatic tumour mouse models to gemcitabine treatment?

Our study shows that pimasertib treatment reduces RRM1 protein levels and this occurs through its polyubiquitination and proteasomal degradation mediated by the E3 ligase MDM2. Transient inhibition of MDM2 would cause accumulation of intracellular RRM1, thus antagonising gemcitabine activity. This hypothesis could be explored further by examining gemcitabine cytotoxicity in MDM2 siRNA transfected mice. Potentially, shRNA against MDM2 in mouse models of pancreatic cancer treated

with gemcitabine could reveal some insights into the mechanism of gemcitabine efficacy.

6.1.3 Can pre-treatment with pimasertib sensitize pancreatic cancer models to PI3K inhibitors plus gemcitabine combination?

Several preclinical studies have focused on the evaluation of concurrent blockade of K-RAS downstream pathways (MEK and PI3K) to overcome the effects of compensatory feedback loop mechanisms between the two pathways (Wee et al. 2009). Results obtained from human pancreatic cancer cell lines and GEM models of PDAC have shown modest but significant survival improvement upon combination of PI3K/AKT inhibitors with MEK inhibitors (Junttila et al. 2015) (Chang et al. 2010). Evaluation of novel therapeutic strategies that combine PI3K inhibitor, MEK inhibitors and gemcitabine should be explored. However, since we believe that pimasertib sensitizing effects on gemcitabine response is due to RRM1 degradation and we think AKT activation is involved in this mechanism, it would be rational to explore the effects of pre-treating pancreatic cancer mouse models with pimasertib for a window of time necessary to downregulate RRM1 protein, followed by gemcitabine treatment and finally administer a PI3K inhibitor to allow sustained inhibition of the MAPK pathway.

6.1.4 Effect of RRM1 inhibition in a mouse model of pancreatic cancer

Small interfering RNA (siRNA) represents a powerful method to achieve efficient knock down of a target gene (Burnett et al. 2011). This study showed that inhibition of RRM1 expression by siRNA enhanced gemcitabine cytotoxicity in human pancreatic cancer cells. It would be interesting to explore whether systemic administration of RRM1 specific siRNA in the orthotopic mouse model would be efficiently delivered into the tumour, downregulate RRM1 and would potentiate the antitumour activity of gemcitabine. In addition to this, RRM1 knock out pancreatic cancer cell lines, by using the CRISPR-Cas9 system could be developed and used as a platform to study the cytotoxic effects of gemcitabine.

6.1.5 Analysis of RRM1 expression on human samples of pancreatic cancer

Our studies thus far have focused on *in vitro* models and animal models. It is also critical to evaluate clinical samples. Circulating tumour cells, detected in the blood stream of patients with solid cancers, represent an important tool for diagnosis and for monitoring response to chemotherapy (Rhim et al. 2012). The isolation of circulating tumour cells would allow analysis of RRM1 expression on pancreatic tumour specimens from patients treated with pimasertib and gemcitabine. This method would be important to confirm whether downregulation of RRM1 occurs in these patients. This could be done in a neoadjuvant 'window study'.

6.2 CONCLUSIONS

The lack of efficacious therapies available for patients diagnosed with advanced PDAC increases the need to explore novel therapeutic strategies to target this disease. Combination treatments that include targeted agents represent a potential approach to potentiate the antitumour activity of chemotherapy. In particular, MEK proteins, downstream components of the RAS signalling pathway, are ideal therapeutic targets since this pathway is frequently deregulated in human cancers. The most recently developed MEK inhibitors do not affect other serine/threonine or tyrosine protein kinases targeting the ATP-binding site; therefore they overcome any adverse effects associated with this (Ohren et al. 2004). In the clinic, MEK inhibitors have proved to be well tolerated and have provided significant survival benefit in melanoma, a result that led to the FDA approval of these agents (Flaherty et al. 2012).

The results obtained in this study support the clinical use of MEK inhibitors to enhance gemcitabine efficacy for pancreatic cancer treatment. The importance of drug scheduling as a factor by which MEK inhibition increases gemcitabine efficacy will inform future clinical investigations for combinations and schedules of gemcitabine with MEK inhibitors. Our hypothesis based on the results obtained suggests that the administration of pimasertib increases gemcitabine cytotoxicity in pancreatic cancer models in part by interfering with an important mechanism that contributes to

gemcitabine resistance. This study has provided mechanism insights to the synergistic interaction observed between gemcitabine and pimasertib that should be further investigated. The frequent use of gemcitabine in pancreatic cancer therapy and the awareness of RRM1 being an important factor in determining gemcitabine sensitivity urge a deeper understanding of the detailed mechanism of modulation of RRM1 expression by MEK inhibition, to allow a better design of future clinical trials involving gemcitabine with MEK inhibitors and possibly other targeted therapies downstream RAS and to predict PDAC patient's outcome.

REFERENCES

Adams, J. M. and S. Cory (2007). "The Bcl-2 apoptotic switch in cancer development and therapy." Oncogene **26**(9): 1324-1337.

Aguirre, A. J., N. Bardeesy, M. Sinha, L. Lopez, D. A. Tuveson, J. Horner, M. S. Redston and R. A. DePinho (2003). "Activated Kras and Ink4a/Arf deficiency cooperate to produce metastatic pancreatic ductal adenocarcinoma." Genes Dev **17**(24): 3112-3126.

Airiau, K., V. Prouzet-Mauleon, B. Rousseau, A. Pigneux, M. Jeanneteau, M. Giraudon, K. Allou, P. Dubus, F. Belloc and F. X. Mahon (2015). "Synergistic cooperation between ABT-263 and MEK1/2 inhibitor: effect on apoptosis and proliferation of acute myeloid leukemia cells." Oncotarget.

Akinleye, A., M. Furqan, N. Mukhi, P. Ravella and D. Liu (2013). "MEK and the inhibitors: from bench to bedside." J Hematol Oncol **6**: 27.

Akita, H., Z. Zheng, Y. Takeda, C. Kim, N. Kittaka, S. Kobayashi, S. Marubashi, I. Takemasa, H. Nagano, K. Dono, S. Nakamori, M. Monden, M. Mori, Y. Doki and G. Bepler (2009). "Significance of RRM1 and ERCC1 expression in resectable pancreatic adenocarcinoma." Oncogene **28**(32): 2903-2909.

Alagesan, B., G. Contino, A. R. Guimaraes, R. B. Corcoran, V. Deshpande, G. R. Wojtkiewicz, A. F. Hezel, K. K. Wong, M. Loda, R. Weissleder, C. Benes, J. A. Engelman and N. Bardeesy (2015). "Combined MEK and PI3K inhibition in a mouse model of pancreatic cancer." Clin Cancer Res **21**(2): 396-404.

Almond, J. B. and G. M. Cohen (2002). "The proteasome: a novel target for cancer chemotherapy." Leukemia **16**(4): 433-443.

Altomare, D. A., S. Tanno, A. De Rienzo, A. J. Klein-Szanto, S. Tanno, K. L. Skele, J. P. Hoffman and J. R. Testa (2002). "Frequent activation of AKT2 kinase in human pancreatic carcinomas." J Cell Biochem **87**(4): 470-476.

Ambrosini, G., E. B. Sambol, D. Carvajal, L. T. Vassilev, S. Singer and G. K. Schwartz (2007). "Mouse double minute antagonist Nutlin-3a enhances chemotherapy-induced apoptosis in cancer cells with mutant p53 by activating E2F1." Oncogene **26**(24): 3473-3481.

Anastas, J. N. and R. T. Moon (2013). "WNT signalling pathways as therapeutic targets in cancer." Nat Rev Cancer **13**(1): 11-26.

Anderson, N. G., J. L. Maller, N. K. Tonks and T. W. Sturgill (1990). "Requirement for integration of signals from two distinct phosphorylation pathways for activation of MAP kinase." Nature **343**(6259): 651-653.

Ardito, C. M., B. M. Gruner, K. K. Takeuchi, C. Lubeseder-Martellato, N. Teichmann, P. K. Mazur, K. E. Delgiorno, E. S. Carpenter, C. J. Halbrook, J. C. Hall, D. Pal, T. Briel, A. Herner, M. Trajkovic-Arsic, B. Sipos, G. Y. Liou, P. Storz, N. R. Murray, D. W. Threadgill, M. Sibilia, M. K. Washington, C. L. Wilson, R. M. Schmid, E. W. Raines, H. C. Crawford and J. T. Siveke (2012). "EGF receptor is required for KRAS-induced pancreatic tumorigenesis." Cancer cell **22**(3): 304-317.

Artandi, S. E., S. Chang, S. L. Lee, S. Alson, G. J. Gottlieb, L. Chin and R. A. DePinho (2000). "Telomere dysfunction promotes non-reciprocal translocations and epithelial cancers in mice." Nature **406**(6796): 641-645.

Asano, T., Y. Yao, J. Zhu, D. Li, J. L. Abbruzzese and S. A. Reddy (2004). "The PI 3-kinase/Akt signaling pathway is activated due to aberrant Pten expression and targets transcription factors NF-kappaB and c-Myc in pancreatic cancer cells." Oncogene **23**(53): 8571-8580.

Aye, Y., M. Li, M. J. Long and R. S. Weiss (2015). "Ribonucleotide reductase and cancer: biological mechanisms and targeted therapies." Oncogene **34**(16): 2011-2021.

Balmanno, K. and S. J. Cook (2009). "Tumour cell survival signalling by the ERK1/2 pathway." Cell Death Differ **16**(3): 368-377.

Bardeesy, N., K. H. Cheng, J. H. Berger, G. C. Chu, J. Pahler, P. Olson, A. F. Hezel, J. Horner, G. Y. Lauwers, D. Hanahan and R. A. DePinho (2006). "Smad4 is dispensable for normal pancreas development yet critical in progression and tumor biology of pancreas cancer." Genes Dev **20**(22): 3130-3146.

Bardeesy, N. and R. A. DePinho (2002). "Pancreatic cancer biology and genetics." Nature reviews. Cancer **2**(12): 897-909.

Barrett, S. D., A. J. Bridges, D. T. Dudley, A. R. Saltiel, J. H. Fergus, C. M. Flamme, A. M. Delaney, M. Kaufman, S. LePage, W. R. Leopold, S. A. Przybranowski, J. Sebolt-Leopold, K. Van Becelaere, A. M. Doherty, R. M. Kennedy, D. Marston, W. A. Howard, Jr., Y. Smith, J. S. Warmus and H. Tecle (2008). "The discovery of the benzhydroxamate MEK inhibitors CI-1040 and PD 0325901." Bioorg Med Chem Lett **18**(24): 6501-6504.

Bartsch, D. K., M. Sina-Frey, S. Lang, A. Wild, B. Gerdes, P. Barth, R. Kress, R. Grutzmann, M. Colombo-Benkmann, A. Ziegler, S. A. Hahn, M. Rothmund and H. Rieder (2002). "CDKN2A germline mutations in familial pancreatic cancer." Ann Surg **236**(6): 730-737.

Bepler, G., I. Kusmartseva, S. Sharma, A. Gautam, A. Cantor, A. Sharma and G. Simon (2006). "RRM1 modulated in vitro and in vivo efficacy of gemcitabine and platinum in non-small-cell lung cancer." Journal of clinical oncology : official journal of the American Society of Clinical Oncology **24**(29): 4731-4737.

Bepler, G., S. Sharma, A. Cantor, A. Gautam, E. Haura, G. Simon, A. Sharma, E. Sommers and L. Robinson (2004). "RRM1 and PTEN as prognostic parameters for overall and disease-free survival in patients with non-small-cell lung cancer." J Clin Oncol **22**(10): 1878-1885.

Berndt, N., A. D. Hamilton and S. M. Sebti (2011). "Targeting protein prenylation for cancer therapy." Nat Rev Cancer **11**(11): 775-791.

Bieging, K. T., S. S. Mello and L. D. Attardi (2014). "Unravelling mechanisms of p53-mediated tumour suppression." Nat Rev Cancer **14**(5): 359-370.

Bijnsdorp, I. V., E. Giovannetti and G. J. Peters (2011). "Analysis of drug interactions." Methods Mol Biol **731**: 421-434.

Blackstock, A. W., S. A. Bernard, F. Richards, K. S. Eagle, L. D. Case, M. E. Poole, P. D. Savage and J. E. Tepper (1999). "Phase I trial of twice-weekly gemcitabine and concurrent radiation in patients with advanced pancreatic cancer." J Clin Oncol **17**(7): 2208-2212.

Blackstock, A. W., F. Mornex, C. Partensky, L. Descos, L. D. Case, S. A. Melin, E. A. Levine, G. Mishra, S. A. Limentani, L. A. Kachnic and J. E. Tepper (2006). "Adjuvant gemcitabine and concurrent radiation for patients with resected pancreatic cancer: a phase II study." Br J Cancer **95**(3): 260-265.

Blackstock, A. W., J. E. Tepper, D. Niedwiecki, D. R. Hollis, R. J. Mayer and M. A. Tempero (2003). "Cancer and leukemia group B (CALGB) 89805: phase II chemoradiation trial using gemcitabine in patients with locoregional adenocarcinoma of the pancreas." Int J Gastrointest Cancer **34**(2-3): 107-116.

Bodoky, G., C. Timcheva, D. R. Spigel, P. J. La Stella, T. E. Ciuleanu, G. Pover and N. C. Tebbutt (2012). "A phase II open-label randomized study to assess the efficacy and safety of selumetinib (AZD6244 [ARRY-142886]) versus capecitabine in patients with advanced or metastatic pancreatic cancer who have failed first-line gemcitabine therapy." Invest New Drugs **30**(3): 1216-1223.

Boj, S. F., C. I. Hwang, L. A. Baker, Chio, II, D. D. Engle, V. Corbo, M. Jager, M. Ponz-Sarvise, H. Tiriac, M. S. Spector, A. Gracanin, T. Oni, K. H. Yu, R. van Boxtel, M. Huch, K. D. Rivera, J. P. Wilson, M. E. Feigin, D. Ohlund, A. Handly-Santana, C. M. Ardito-Abraham, M. Ludwig, E. Elyada, B. Alagesan, G. Biffi, G. N. Yordanov, B. Delcuze, B. Creighton, K. Wright, Y. Park, F. H. Morsink, I. Q. Molenaar, I. H. Borel Rinkes, E. Cuppen, Y. Hao, Y. Jin, I. J. Nijman, C. Iacobuzio-Donahue, S. D. Leach, D. J. Pappin, M.

Hammell, D. S. Klimstra, O. Basturk, R. H. Hruban, G. J. Offerhaus, R. G. Vries, H. Clevers and D. A. Tuveson (2015). "Organoid models of human and mouse ductal pancreatic cancer." Cell **160**(1-2): 324-338.

Bouffard, D. Y., J. Laliberte and R. L. Momparler (1993). "Kinetic studies on 2',2'-difluorodeoxycytidine (Gemcitabine) with purified human deoxycytidine kinase and cytidine deaminase." Biochem Pharmacol **45**(9): 1857-1861.

Bouska, A. and C. M. Eischen (2009). "Mdm2 affects genome stability independent of p53." Cancer Res **69**(5): 1697-1701.

Brummer, T., H. Naegele, M. Reth and Y. Misawa (2003). "Identification of novel ERK-mediated feedback phosphorylation sites at the C-terminus of B-Raf." Oncogene **22**(55): 8823-8834.

Burgess, A. W., H. S. Cho, C. Eigenbrot, K. M. Ferguson, T. P. Garrett, D. J. Leahy, M. A. Lemmon, M. X. Sliwkowski, C. W. Ward and S. Yokoyama (2003). "An open-and-shut case? Recent insights into the activation of EGF/ErbB receptors." Mol Cell **12**(3): 541-552.

Burnett, J. C., J. J. Rossi and K. Tiemann (2011). "Current progress of siRNA/shRNA therapeutics in clinical trials." Biotechnol J **6**(9): 1130-1146.

Burris, H. A., 3rd, M. J. Moore, J. Andersen, M. R. Green, M. L. Rothenberg, M. R. Modiano, M. C. Cripps, R. K. Portenoy, A. M. Storniolo, P. Tarassoff, R. Nelson, F. A. Dorr, C. D. Stephens and D. D. Von Hoff (1997). "Improvements in survival and clinical benefit with gemcitabine as first-line therapy for patients with advanced pancreas cancer: a randomized trial." Journal of clinical oncology : official journal of the American Society of Clinical Oncology **15**(6): 2403-2413.

Campbell, P. J., S. Yachida, L. J. Mudie, P. J. Stephens, E. D. Pleasance, L. A. Stebbings, L. A. Morsberger, C. Latimer, S. McLaren, M. L. Lin, D. J. McBride, I. Varela, S. A. Nik-Zainal, C. Leroy, M. Jia, A. Menzies, A. P. Butler, J. W. Teague, C. A. Griffin, J. Burton, H. Swerdlow, M. A. Quail, M. R. Stratton, C. Iacobuzio-Donahue and P. A. Futreal (2010). "The patterns and dynamics of genomic instability in metastatic pancreatic cancer." Nature **467**(7319): 1109-1113.

Caras, I. W. and D. W. Martin, Jr. (1988). "Molecular cloning of the cDNA for a mutant mouse ribonucleotide reductase M1 that produces a dominant mutator phenotype in mammalian cells." Mol Cell Biol **8**(7): 2698-2704.

Catalanotti, F., G. Reyes, V. Jesenberger, G. Galabova-Kovacs, R. de Matos Simoes, O. Carugo and M. Baccarini (2009). "A Mek1-Mek2 heterodimer determines the strength and duration of the Erk signal." Nat Struct Mol Biol **16**(3): 294-303.

Cavallaro, U. and G. Christofori (2004). "Cell adhesion and signalling by cadherins and Ig-CAMs in cancer." Nat Rev Cancer **4**(2): 118-132.

Chabes, A. and L. Thelander (2000). "Controlled protein degradation regulates ribonucleotide reductase activity in proliferating mammalian cells during the normal cell cycle and in response to DNA damage and replication blocks." J Biol Chem **275**(23): 17747-17753.

Chandler, N. M., J. J. Canete and M. P. Callery (2004). "Caspase-3 drives apoptosis in pancreatic cancer cells after treatment with gemcitabine." J Gastrointest Surg **8**(8): 1072-1078.

Chang, L. and M. Karin (2001). "Mammalian MAP kinase signalling cascades." Nature **410**(6824): 37-40.

Chang, L., B. Zhou, S. Hu, R. Guo, X. Liu, S. N. Jones and Y. Yen (2008). "ATM-mediated serine 72 phosphorylation stabilizes ribonucleotide reductase small subunit p53R2 protein against MDM2 to DNA damage." Proc Natl Acad Sci U S A **105**(47): 18519-18524.

Chang, Q., M. S. Chapman, J. N. Miner and D. W. Hedley (2010). "Antitumour activity of a potent MEK inhibitor RDEA119/BAY 869766 combined with rapamycin in human orthotopic primary pancreatic cancer xenografts." BMC Cancer **10**: 515.

Chapman, T. R. and T. J. Kinsella (2011). "Ribonucleotide reductase inhibitors: a new look at an old target for radiosensitization." Front Oncol **1**: 56.

Cheng, Y., G. Zhang and G. Li (2013). "Targeting MAPK pathway in melanoma therapy." Cancer Metastasis Rev **32**(3-4): 567-584.

Chou, T. C. (2006). "Theoretical basis, experimental design, and computerized simulation of synergism and antagonism in drug combination studies." Pharmacol Rev **58**(3): 621-681.

Chou, T. C. (2010). "Drug combination studies and their synergy quantification using the Chou-Talalay method." Cancer Res **70**(2): 440-446.

Ciccolini, J., L. Dahan, N. Andre, A. Evrard, M. Duluc, A. Blesius, C. Yang, S. Giacometti, C. Brunet, C. Raynal, A. Ortiz, N. Frances, A. Iliadis, F. Duffaud, J. F. Seitz and C. Mercier (2010). "Cytidine deaminase residual activity in serum is a predictive marker of early severe toxicities in adults after gemcitabine-based chemotherapies." J Clin Oncol **28**(1): 160-165.

Colburn, W. A. (2003). "Biomarkers in drug discovery and development: from target identification through drug marketing." J Clin Pharmacol **43**(4): 329-341.

Collado, M. and M. Serrano (2010). "Senescence in tumours: evidence from mice and humans." Nat Rev Cancer **10**(1): 51-57.

Collins, M. A., F. Bednar, Y. Zhang, J. C. Brisset, S. Galban, C. J. Galban, S. Rakshit, K. S. Flannagan, N. V. Adsay and M. Pasca di Magliano (2012). "Oncogenic Kras is required for both the initiation and maintenance of pancreatic cancer in mice." J Clin Invest **122**(2): 639-653.

Collisson, E. A., A. De, H. Suzuki, S. S. Gambhir and M. S. Kolodney (2003). "Treatment of metastatic melanoma with an orally available inhibitor of the Ras-Raf-MAPK cascade." Cancer Res **63**(18): 5669-5673.

Collisson, E. A., C. L. Trejo, J. M. Silva, S. Gu, J. E. Korkola, L. M. Heiser, R. P. Charles, B. A. Rabinovich, B. Hann, D. Dankort, P. T. Spellman, W. A. Phillips, J. W. Gray and M. McMahon (2012). "A central role for RAF-->MEK-->ERK signaling in the genesis of pancreatic ductal adenocarcinoma." Cancer discovery **2**(8): 685-693.

Conroy, T., F. Desseigne, M. Ychou, O. Bouche, R. Guimbaud, Y. Becouarn, A. Adenis, J. L. Raoul, S. Gourgou-Bourgade, C. de la Fouchardiere, J. Bennouna, J. B. Bachet, F. Khemissa-Akouz, D. Pere-Verge, C. Delbaldo, E. Assenat, B. Chauffert, P. Michel, C. Montoto-Grillot and M. Ducreux (2011). "FOLFIRINOX versus gemcitabine for metastatic pancreatic cancer." The New England journal of medicine **364**(19): 1817-1825.

Conroy, T., F. Desseigne, M. Ychou, O. Bouche, R. Guimbaud, Y. Becouarn, A. Adenis, J. L. Raoul, S. Gourgou-Bourgade, C. de la Fouchardiere, J. Bennouna, J. B. Bachet, F. Khemissa-Akouz, D. Pere-Verge, C. Delbaldo, E. Assenat, B. Chauffert, P. Michel, C. Montoto-Grillot, M. Ducreux, U. Groupe Tumeurs Digestives of and P. Intergroup (2011). "FOLFIRINOX versus gemcitabine for metastatic pancreatic cancer." N Engl J Med **364**(19): 1817-1825.

Costello, E., W. Greenhalf and J. P. Neoptolemos (2012). "New biomarkers and targets in pancreatic cancer and their application to treatment." Nature reviews. Gastroenterology & hepatology **9**(8): 435-444.

Courtin, A., F. M. Richards, T. E. Bapiro, J. L. Bramhall, A. Neesse, N. Cook, B. F. Krippendorff, D. A. Tuveson and D. I. Jodrell (2013). "Anti-tumour efficacy of capecitabine in a genetically engineered mouse model of pancreatic cancer." PLoS One **8**(6): e67330.

Croce, C. M. (2008). "Oncogenes and cancer." N Engl J Med **358**(5): 502-511.

Cunningham, D., I. Chau, D. D. Stocken, J. W. Valle, D. Smith, W. Steward, P. G. Harper, J. Dunn, C. Tudur-Smith, J. West, S. Falk, A. Crellin, F. Adab, J. Thompson, P. Leonard, J. Ostrowski, M. Eatock, W. Scheithauer, R. Herrmann and J. P. Neoptolemos (2009). "Phase III randomized comparison of gemcitabine versus gemcitabine plus

capecitabine in patients with advanced pancreatic cancer." J Clin Oncol **27**(33): 5513-5518.

D'Angiolella, V., V. Donato, F. M. Forrester, Y. T. Jeong, C. Pellacani, Y. Kudo, A. Saraf, L. Florens, M. P. Washburn and M. Pagano (2012). "Cyclin F-mediated degradation of ribonucleotide reductase M2 controls genome integrity and DNA repair." Cell **149**(5): 1023-1034.

Dahlmann, B. (2007). "Role of proteasomes in disease." BMC Biochem **8 Suppl 1**: S3.

Davidson, J. D., L. Ma, M. Flagella, S. Geeganage, L. M. Gelbert and C. A. Slapak (2004). "An increase in the expression of ribonucleotide reductase large subunit 1 is associated with gemcitabine resistance in non-small cell lung cancer cell lines." Cancer Res **64**(11): 3761-3766.

Davidson, J. D., L. Ma, M. Flagella, S. Geeganage, L. M. Gelbert and C. A. Slapak (2004). "An increase in the expression of ribonucleotide reductase large subunit 1 is associated with gemcitabine resistance in non-small cell lung cancer cell lines." Cancer research **64**(11): 3761-3766.

Deutsch, M., M. M. Rosenstein and R. K. Ramanathan (1999). "Pancreatic cancer in a young adult after treatment for Hodgkin's disease." Clin Oncol (R Coll Radiol) **11**(4): 280-282.

Dhanasekaran, N. and E. Premkumar Reddy (1998). "Signaling by dual specificity kinases." Oncogene **17**(11 Reviews): 1447-1455.

Di Fiore, F., F. Blanchard, F. Charbonnier, F. Le Pessot, A. Lamy, M. P. Galais, L. Bastit, A. Killian, R. Sesboue, J. J. Tuech, A. M. Queuniet, B. Paillot, J. C. Sabourin, F. Michot, P. Michel and T. Frebourg (2007). "Clinical relevance of KRAS mutation detection in metastatic colorectal cancer treated by Cetuximab plus chemotherapy." Br J Cancer **96**(8): 1166-1169.

di Magliano, M. P. and C. D. Logsdon (2013). "Roles for KRAS in pancreatic tumor development and progression." Gastroenterology **144**(6): 1220-1229.

Dow, L. E. and S. W. Lowe (2012). "Life in the fast lane: mammalian disease models in the genomics era." Cell **148**(6): 1099-1109.

Downward, J. (2003). "Targeting RAS signalling pathways in cancer therapy." Nat Rev Cancer **3**(1): 11-22.

Duncan, J. S., M. C. Whittle, K. Nakamura, A. N. Abell, A. A. Midland, J. S. Zawistowski, N. L. Johnson, D. A. Granger, N. V. Jordan, D. B. Darr, J. Usary, P. F. Kuan, D. M. Smalley, B. Major, X. He, K. A. Hoadley, B. Zhou, N. E. Sharpless, C. M. Perou, W. Y. Kim, S. M. Gomez, X. Chen, J. Jin, S. V. Frye, H. S. Earp, L. M. Graves and G. L. Johnson

(2012). "Dynamic reprogramming of the kinome in response to targeted MEK inhibition in triple-negative breast cancer." Cell **149**(2): 307-321.

Duxbury, M. S., H. Ito, M. J. Zinner, S. W. Ashley and E. E. Whang (2004). "RNA interference targeting the M2 subunit of ribonucleotide reductase enhances pancreatic adenocarcinoma chemosensitivity to gemcitabine." Oncogene **23**(8): 1539-1548.

Engelman, J. A. (2009). "Targeting PI3K signalling in cancer: opportunities, challenges and limitations." Nat Rev Cancer **9**(8): 550-562.

Everhart, J. and D. Wright (1995). "Diabetes mellitus as a risk factor for pancreatic cancer. A meta-analysis." JAMA **273**(20): 1605-1609.

Ewald, B., D. Sampath and W. Plunkett (2008). "Nucleoside analogs: molecular mechanisms signaling cell death." Oncogene **27**(50): 6522-6537.

Fairman, J. W., S. R. Wijerathna, M. F. Ahmad, H. Xu, R. Nakano, S. Jha, J. Prendergast, R. M. Welin, S. Flodin, A. Roos, P. Nordlund, Z. Li, T. Walz and C. G. Dealwis (2011). "Structural basis for allosteric regulation of human ribonucleotide reductase by nucleotide-induced oligomerization." Nat Struct Mol Biol **18**(3): 316-322.

Fan, H., A. Huang, C. Villegas and J. A. Wright (1997). "The R1 component of mammalian ribonucleotide reductase has malignancy-suppressing activity as demonstrated by gene transfer experiments." Proc Natl Acad Sci U S A **94**(24): 13181-13186.

Farrell, J. J., H. Elsaleh, M. Garcia, R. Lai, A. Ammar, W. F. Regine, R. Abrams, A. B. Benson, J. Macdonald, C. E. Cass, A. P. Dicker and J. R. Mackey (2009). "Human equilibrative nucleoside transporter 1 levels predict response to gemcitabine in patients with pancreatic cancer." Gastroenterology **136**(1): 187-195.

Fernandez-Medarde, A. and E. Santos (2011). "Ras in cancer and developmental diseases." Genes Cancer **2**(3): 344-358.

Fidler, I. J. (2003). "The pathogenesis of cancer metastasis: the 'seed and soil' hypothesis revisited." Nat Rev Cancer **3**(6): 453-458.

Fitzgerald, J. B., B. Schoeberl, U. B. Nielsen and P. K. Sorger (2006). "Systems biology and combination therapy in the quest for clinical efficacy." Nat Chem Biol **2**(9): 458-466.

Flaherty, K. T., J. R. Infante, A. Daud, R. Gonzalez, R. F. Kefford, J. Sosman, O. Hamid, L. Schuchter, J. Cebon, N. Ibrahim, R. Kudchadkar, H. A. Burris, 3rd, G. Falchook, A. Algazi, K. Lewis, G. V. Long, I. Puzanov, P. Lebowitz, A. Singh, S. Little, P. Sun, A. Allred,

D. Ouellet, K. B. Kim, K. Patel and J. Weber (2012). "Combined BRAF and MEK inhibition in melanoma with BRAF V600 mutations." N Engl J Med **367**(18): 1694-1703.

Flaherty, K. T., C. Robert, P. Hersey, P. Nathan, C. Garbe, M. Milhem, L. V. Demidov, J. C. Hassel, P. Rutkowski, P. Mohr, R. Dummer, U. Trefzer, J. M. Larkin, J. Utikal, B. Dreno, M. Nyakas, M. R. Middleton, J. C. Becker, M. Casey, L. J. Sherman, F. S. Wu, D. Ouellet, A. M. Martin, K. Patel, D. Schadendorf and M. S. Group (2012). "Improved survival with MEK inhibition in BRAF-mutated melanoma." N Engl J Med **367**(2): 107-114.

Freed-Pastor, W. A., H. Mizuno, X. Zhao, A. Langerod, S. H. Moon, R. Rodriguez-Barrueco, A. Barsotti, A. Chicas, W. Li, A. Polotskaia, M. J. Bissell, T. F. Osborne, B. Tian, S. W. Lowe, J. M. Silva, A. L. Borresen-Dale, A. J. Levine, J. Bargonetti and C. Prives (2012). "Mutant p53 disrupts mammary tissue architecture via the mevalonate pathway." Cell **148**(1-2): 244-258.

Freedman, D. A., L. Wu and A. J. Levine (1999). "Functions of the MDM2 oncoprotein." Cellular and molecular life sciences : CMLS **55**(1): 96-107.

Frese, K. K., A. Neesse, N. Cook, T. E. Bapiro, M. P. Lolkema, D. I. Jodrell and D. A. Tuveson (2012). "nab-Paclitaxel potentiates gemcitabine activity by reducing cytidine deaminase levels in a mouse model of pancreatic cancer." Cancer discovery **2**(3): 260-269.

Frese, K. K., A. Neesse, N. Cook, T. E. Bapiro, M. P. Lolkema, D. I. Jodrell and D. A. Tuveson (2012). "nab-Paclitaxel potentiates gemcitabine activity by reducing cytidine deaminase levels in a mouse model of pancreatic cancer." Cancer Discov **2**(3): 260-269.

Frese, K. K. and D. A. Tuveson (2007). "Maximizing mouse cancer models." Nat Rev Cancer **7**(9): 645-658.

Friday, B. B., C. Yu, G. K. Dy, P. D. Smith, L. Wang, S. N. Thibodeau and A. A. Adjei (2008). "BRAF V600E disrupts AZD6244-induced abrogation of negative feedback pathways between extracellular signal-regulated kinase and Raf proteins." Cancer Res **68**(15): 6145-6153.

Garrido-Laguna, I. and M. Hidalgo (2015). "Pancreatic cancer: from state-of-the-art treatments to promising novel therapies." Nat Rev Clin Oncol **12**(6): 319-334.

Gautam, A., Z. R. Li and G. Bepler (2003). "RRM1-induced metastasis suppression through PTEN-regulated pathways." Oncogene **22**(14): 2135-2142.

Gesto, D. S., N. M. Cerqueira, P. A. Fernandes and M. J. Ramos (2012). "Gemcitabine: a critical nucleoside for cancer therapy." Current medicinal chemistry **19**(7): 1076-1087.

Gillen, S., T. Schuster, C. Meyer Zum Buschenfelde, H. Friess and J. Kleeff (2010). "Preoperative/neoadjuvant therapy in pancreatic cancer: a systematic review and meta-analysis of response and resection percentages." PLoS Med **7**(4): e1000267.

Gilmartin, A. G., M. R. Bleam, A. Groy, K. G. Moss, E. A. Minthorn, S. G. Kulkarni, C. M. Rominger, S. Erskine, K. E. Fisher, J. Yang, F. Zappacosta, R. Annan, D. Sutton and S. G. Laquerre (2011). "GSK1120212 (JTP-74057) is an inhibitor of MEK activity and activation with favorable pharmacokinetic properties for sustained in vivo pathway inhibition." Clin Cancer Res **17**(5): 989-1000.

Giovannetti, E., M. Del Tacca, V. Mey, N. Funel, S. Nannizzi, S. Ricci, C. Orlandini, U. Boggi, D. Campani, M. Del Chiaro, M. Iannopollo, G. Bevilacqua, F. Mosca and R. Danesi (2006). "Transcription analysis of human equilibrative nucleoside transporter-1 predicts survival in pancreas cancer patients treated with gemcitabine." Cancer research **66**(7): 3928-3935.

Golan, T., Z. S. Kanji, R. Epelbaum, N. Devaud, E. Dagan, S. Holter, D. Aderka, S. Paluch-Shimon, B. Kaufman, R. Gershoni-Baruch, D. Hedley, M. J. Moore, E. Friedman and S. Gallinger (2014). "Overall survival and clinical characteristics of pancreatic cancer in BRCA mutation carriers." Br J Cancer **111**(6): 1132-1138.

Goldberg, A. L. (2012). "Development of proteasome inhibitors as research tools and cancer drugs." J Cell Biol **199**(4): 583-588.

Goodsell, D. S. (1999). "The molecular perspective: the ras oncogene." Stem Cells **17**(4): 235-236.

Gopinathan, A. and D. A. Tuveson (2008). "The use of GEM models for experimental cancer therapeutics." Dis Model Mech **1**(2-3): 83-86.

Greenhalf, W., P. Ghaneh, J. P. Neoptolemos, D. H. Palmer, T. F. Cox, R. F. Lamb, E. Garner, F. Campbell, J. R. Mackey, E. Costello, M. J. Moore, J. W. Valle, A. C. McDonald, R. Carter, N. C. Tebbutt, D. Goldstein, J. Shannon, C. Dervenis, B. Glimelius, M. Deakin, R. M. Charnley, F. Lacaine, A. G. Scarfe, M. R. Middleton, A. Anthoney, C. M. Halloran, J. Mayerle, A. Olah, R. Jackson, C. L. Rawcliffe, A. Scarpa, C. Bassi, M. W. Buchler and C. European Study Group for Pancreatic (2014). "Pancreatic cancer hENT1 expression and survival from gemcitabine in patients from the ESPAC-3 trial." J Natl Cancer Inst **106**(1): djt347.

Grossmann, M. E., H. Huang and D. J. Tindall (2001). "Androgen receptor signaling in androgen-refractory prostate cancer." J Natl Cancer Inst **93**(22): 1687-1697.

Grunewald, R., H. Kantarjian, M. J. Keating, J. Abbruzzese, P. Tarassoff and W. Plunkett (1990). "Pharmacologically directed design of the dose rate and schedule of 2',2'-difluorodeoxycytidine (Gemcitabine) administration in leukemia." Cancer Res **50**(21): 6823-6826.

Gschwind, A., E. Zwick, N. Prenzel, M. Leserer and A. Ullrich (2001). "Cell communication networks: epidermal growth factor receptor transactivation as the paradigm for interreceptor signal transmission." Oncogene **20**(13): 1594-1600.

Guerra, C. and M. Barbacid (2013). "Genetically engineered mouse models of pancreatic adenocarcinoma." Mol Oncol **7**(2): 232-247.

Guerra, C., A. J. Schuhmacher, M. Canamero, P. J. Grippo, L. Verdaguer, L. Perez-Gallego, P. Dubus, E. P. Sandgren and M. Barbacid (2007). "Chronic pancreatitis is essential for induction of pancreatic ductal adenocarcinoma by K-Ras oncogenes in adult mice." Cancer Cell **11**(3): 291-302.

Haeno, H., M. Gonen, M. B. Davis, J. M. Herman, C. A. Iacobuzio-Donahue and F. Michor (2012). "Computational modeling of pancreatic cancer reveals kinetics of metastasis suggesting optimum treatment strategies." Cell **148**(1-2): 362-375.

Hanahan, D. and J. Folkman (1996). "Patterns and emerging mechanisms of the angiogenic switch during tumorigenesis." Cell **86**(3): 353-364.

Hanahan, D. and R. A. Weinberg (2011). "Hallmarks of cancer: the next generation." Cell **144**(5): 646-674.

Haura, E. B., A. D. Ricart, T. G. Larson, P. J. Stella, L. Bazhenova, V. A. Miller, R. B. Cohen, P. D. Eisenberg, P. Selaru, K. D. Wilner and S. M. Gadgeel (2010). "A phase II study of PD-0325901, an oral MEK inhibitor, in previously treated patients with advanced non-small cell lung cancer." Clin Cancer Res **16**(8): 2450-2457.

Hayflick, L. (1997). "Mortality and immortality at the cellular level. A review." Biochemistry (Mosc) **62**(11): 1180-1190.

Heinemann, V., L. W. Hertel, G. B. Grindey and W. Plunkett (1988). "Comparison of the cellular pharmacokinetics and toxicity of 2',2'-difluorodeoxycytidine and 1-beta-D-arabinofuranosylcytosine." Cancer Res **48**(14): 4024-4031.

Heinemann, V., L. Schulz, R. D. Issels and W. Wilmanns (1998). "Regulation of deoxycytidine kinase by deoxycytidine and deoxycytidine 5' triphosphate in whole leukemia and tumor cells." Adv Exp Med Biol **431**: 249-253.

Heinemann, V., Y. Z. Xu, S. Chubb, A. Sen, L. W. Hertel, G. B. Grindey and W. Plunkett (1990). "Inhibition of ribonucleotide reduction in CCRF-CEM cells by 2',2'-difluorodeoxycytidine." Mol Pharmacol **38**(4): 567-572.

Heinemann, V., Y. Z. Xu, S. Chubb, A. Sen, L. W. Hertel, G. B. Grindey and W. Plunkett (1992). "Cellular elimination of 2',2'-difluorodeoxycytidine 5'-triphosphate: a mechanism of self-potentiation." Cancer Res **52**(3): 533-539.

Heldin, C. H., K. Rubin, K. Pietras and A. Ostman (2004). "High interstitial fluid pressure - an obstacle in cancer therapy." Nat Rev Cancer **4**(10): 806-813.

Herman, J. M., M. J. Swartz, C. C. Hsu, J. Winter, T. M. Pawlik, E. Sugar, R. Robinson, D. A. Laheru, E. Jaffee, R. H. Hruban, K. A. Campbell, C. L. Wolfgang, F. Asrari, R. Donehower, M. Hidalgo, L. A. Diaz, Jr., C. Yeo, J. L. Cameron, R. D. Schulick and R. Abrams (2008). "Analysis of fluorouracil-based adjuvant chemotherapy and radiation after pancreaticoduodenectomy for ductal adenocarcinoma of the pancreas: results of a large, prospectively collected database at the Johns Hopkins Hospital." J Clin Oncol **26**(21): 3503-3510.

Herreros-Villanueva, M., E. Hijona, A. Cosme and L. Bujanda (2012). "Mouse models of pancreatic cancer." World J Gastroenterol **18**(12): 1286-1294.

Hers, I., E. E. Vincent and J. M. Tavare (2011). "Akt signalling in health and disease." Cell Signal **23**(10): 1515-1527.

Hershko, A. and A. Ciechanover (1998). "The ubiquitin system." Annu Rev Biochem **67**: 425-479.

Hezel, A. F., A. C. Kimmelman, B. Z. Stanger, N. Bardeesy and R. A. Depinho (2006). "Genetics and biology of pancreatic ductal adenocarcinoma." Genes Dev **20**(10): 1218-1249.

Hidalgo, M. (2010). "Pancreatic cancer." N Engl J Med **362**(17): 1605-1617.

Hidalgo, M., F. Amant, A. V. Biankin, E. Budinska, A. T. Byrne, C. Caldas, R. B. Clarke, S. de Jong, J. Jonkers, G. M. Maelandsmo, S. Roman-Roman, J. Seoane, L. Trusolino and A. Villanueva (2014). "Patient-derived xenograft models: an emerging platform for translational cancer research." Cancer Discov **4**(9): 998-1013.

Hidalgo, M., S. Cascinu, J. Kleeff, R. Labianca, J. M. Lohr, J. Neoptolemos, F. X. Real, J. L. Van Laethem and V. Heinemann (2015). "Addressing the challenges of pancreatic cancer: future directions for improving outcomes." Pancreatology **15**(1): 8-18.

Hidalgo, M., C. Plaza, M. Musteanu, P. Illei, C. B. Brachmann, C. Heise, D. Pierce, P. P. Lopez-Casas, C. Menendez, J. Tabernero, A. Romano, X. Wei, F. Lopez-Rios and D. D. Von Hoff (2015). "SPARC Expression Did Not Predict Efficacy of nab-Paclitaxel plus Gemcitabine or Gemcitabine Alone for Metastatic Pancreatic Cancer in an Exploratory Analysis of the Phase III MPACT Trial." Clin Cancer Res.

Hingorani, S. R., E. F. Petricoin, A. Maitra, V. Rajapakse, C. King, M. A. Jacobetz, S. Ross, T. P. Conrads, T. D. Veenstra, B. A. Hitt, Y. Kawaguchi, D. Johann, L. A. Liotta, H. C. Crawford, M. E. Putt, T. Jacks, C. V. Wright, R. H. Hruban, A. M. Lowy and D. A. Tuveson (2003). "Preinvasive and invasive ductal pancreatic cancer and its early detection in the mouse." Cancer Cell **4**(6): 437-450.

Hingorani, S. R. and D. A. Tuveson (2003). "Targeting oncogene dependence and resistance." Cancer Cell **3**(5): 414-417.

Hingorani, S. R., L. Wang, A. S. Multani, C. Combs, T. B. Deramaudt, R. H. Hruban, A. K. Rustgi, S. Chang and D. A. Tuveson (2005). "Trp53R172H and KrasG12D cooperate to promote chromosomal instability and widely metastatic pancreatic ductal adenocarcinoma in mice." Cancer Cell **7**(5): 469-483.

Hochstrasser, M. (2009). "Origin and function of ubiquitin-like proteins." Nature **458**(7237): 422-429.

Hoy, S. M. (2014). "Albumin-bound paclitaxel: a review of its use for the first-line combination treatment of metastatic pancreatic cancer." Drugs **74**(15): 1757-1768.

Hruban, R. H., N. V. Adsay, J. Albores-Saavedra, C. Compton, E. S. Garrett, S. N. Goodman, S. E. Kern, D. S. Klimstra, G. Kloppel, D. S. Longnecker, J. Luttges and G. J. Offerhaus (2001). "Pancreatic intraepithelial neoplasia: a new nomenclature and classification system for pancreatic duct lesions." Am J Surg Pathol **25**(5): 579-586.

Hruban, R. H., K. Takaori, D. S. Klimstra, N. V. Adsay, J. Albores-Saavedra, A. V. Biankin, S. A. Biankin, C. Compton, N. Fukushima, T. Furukawa, M. Goggins, Y. Kato, G. Kloppel, D. S. Longnecker, J. Luttges, A. Maitra, G. J. Offerhaus, M. Shimizu and S. Yonezawa (2004). "An illustrated consensus on the classification of pancreatic intraepithelial neoplasia and intraductal papillary mucinous neoplasms." Am J Surg Pathol **28**(8): 977-987.

Huang, M., A. Shen, J. Ding and M. Geng (2014). "Molecularly targeted cancer therapy: some lessons from the past decade." Trends Pharmacol Sci **35**(1): 41-50.

Huang, P., S. Chubb, L. W. Hertel, G. B. Grindey and W. Plunkett (1991). "Action of 2',2'-difluorodeoxycytidine on DNA synthesis." Cancer Res **51**(22): 6110-6117.

Huang, P. and W. Plunkett (1995). "Induction of apoptosis by gemcitabine." Semin Oncol **22**(4 Suppl 11): 19-25.

Huch, M., P. Bonfanti, S. F. Boj, T. Sato, C. J. Loomans, M. van de Wetering, M. Sojoodi, V. S. Li, J. Schuijers, A. Gracanin, F. Ringnalda, H. Begthel, K. Hamer, J. Mulder, J. H. van Es, E. de Koning, R. G. Vries, H. Heimberg and H. Clevers (2013). "Unlimited in vitro expansion of adult bi-potent pancreas progenitors through the Lgr5/R-spondin axis." EMBO J **32**(20): 2708-2721.

Hunter, T. (1997). "Oncoprotein networks." Cell **88**(3): 333-346.

Hynes, N. E. and H. A. Lane (2005). "ERBB receptors and cancer: the complexity of targeted inhibitors." Nat Rev Cancer **5**(5): 341-354.

Infante, J. R., H. Matsubayashi, N. Sato, J. Tonascia, A. P. Klein, T. A. Riall, C. Yeo, C. Iacobuzio-Donahue and M. Goggins (2007). "Peritumoral fibroblast SPARC expression and patient outcome with resectable pancreatic adenocarcinoma." J Clin Oncol **25**(3): 319-325.

Infante, J. R., B. G. Somer, J. O. Park, C. P. Li, M. E. Scheulen, S. M. Kasubhai, D. Y. Oh, Y. Liu, S. Redhu, K. Steplewski and N. Le (2014). "A randomised, double-blind, placebo-controlled trial of trametinib, an oral MEK inhibitor, in combination with gemcitabine for patients with untreated metastatic adenocarcinoma of the pancreas." Eur J Cancer **50**(12): 2072-2081.

Iodice, S., S. Gandini, P. Maisonneuve and A. B. Lowenfels (2008). "Tobacco and the risk of pancreatic cancer: a review and meta-analysis." Langenbecks Arch Surg **393**(4): 535-545.

Ishimura, N., K. Yamasawa, M. A. Karim Rumi, Y. Kadowaki, S. Ishihara, Y. Amano, Y. Nio, T. Higami and Y. Kinoshita (2003). "BRAF and K-ras gene mutations in human pancreatic cancers." Cancer Lett **199**(2): 169-173.

Iwakuma, T. and G. Lozano (2003). "MDM2, an introduction." Mol Cancer Res **1**(14): 993-1000.

Jacobetz, M. A., D. S. Chan, A. Neesse, T. E. Bapiro, N. Cook, K. K. Frese, C. Feig, T. Nakagawa, M. E. Caldwell, H. I. Zecchini, M. P. Lolkema, P. Jiang, A. Kultti, C. B. Thompson, D. C. Maneval, D. I. Jodrell, G. I. Frost, H. M. Shepard, J. N. Skepper and D. A. Tuveson (2013). "Hyaluronan impairs vascular function and drug delivery in a mouse model of pancreatic cancer." Gut **62**(1): 112-120.

Jaffee, E. M., R. H. Hruban, M. Canto and S. E. Kern (2002). "Focus on pancreas cancer." Cancer Cell **2**(1): 25-28.

Jaster, R. (2004). "Molecular regulation of pancreatic stellate cell function." Mol Cancer **3**: 26.

Jiang, Y. J., C. L. Lee, Q. Wang, Z. W. Zhou, F. Yang, C. Jin and D. L. Fu (2014). "Establishment of an orthotopic pancreatic cancer mouse model: cells suspended and injected in Matrigel." World J Gastroenterol **20**(28): 9476-9485.

Johnson, G. L. and R. Lapadat (2002). "Mitogen-activated protein kinase pathways mediated by ERK, JNK, and p38 protein kinases." Science **298**(5600): 1911-1912.

Jones, S., X. Zhang, D. W. Parsons, J. C. Lin, R. J. Leary, P. Angenendt, P. Mankoo, H. Carter, H. Kamiyama, A. Jimeno, S. M. Hong, B. Fu, M. T. Lin, E. S. Calhoun, M. Kamiyama, K. Walter, T. Nikolskaya, Y. Nikolsky, J. Hartigan, D. R. Smith, M. Hidalgo, S. D. Leach, A. P. Klein, E. M. Jaffee, M. Goggins, A. Maitra, C. Iacobuzio-Donahue, J. R. Eshleman, S. E. Kern, R. H. Hruban, R. Karchin, N. Papadopoulos, G. Parmigiani, B.

Vogelstein, V. E. Velculescu and K. W. Kinzler (2008). "Core signaling pathways in human pancreatic cancers revealed by global genomic analyses." Science **321**(5897): 1801-1806.

Jones, S. N., A. E. Roe, L. A. Donehower and A. Bradley (1995). "Rescue of embryonic lethality in Mdm2-deficient mice by absence of p53." Nature **378**(6553): 206-208.

Junttila, M. R., V. Devasthali, J. H. Cheng, J. Castillo, C. Metcalfe, A. C. Clermont, D. D. Otter, E. Chan, H. Bou-Reslan, T. Cao, W. Forrest, M. A. Nannini, D. French, R. Carano, M. Merchant, K. P. Hoeflich and M. Singh (2015). "Modeling targeted inhibition of MEK and PI3 kinase in human pancreatic cancer." Mol Cancer Ther **14**(1): 40-47.

Jura, N., N. F. Endres, K. Engel, S. Deindl, R. Das, M. H. Lamers, D. E. Wemmer, X. Zhang and J. Kuriyan (2009). "Mechanism for activation of the EGF receptor catalytic domain by the juxtamembrane segment." Cell **137**(7): 1293-1307.

Kanda, M., H. Matthaei, J. Wu, S. M. Hong, J. Yu, M. Borges, R. H. Hruban, A. Maitra, K. Kinzler, B. Vogelstein and M. Goggins (2012). "Presence of somatic mutations in most early-stage pancreatic intraepithelial neoplasia." Gastroenterology **142**(4): 730-733 e739.

Kelland, L. R. (2004). "Of mice and men: values and liabilities of the athymic nude mouse model in anticancer drug development." Eur J Cancer **40**(6): 827-836.

Kerr, M., H. E. Scott, B. Groselj, M. R. Stratford, K. Karaszi, N. L. Sharma and A. E. Kiltie (2014). "Deoxycytidine kinase expression underpins response to gemcitabine in bladder cancer." Clin Cancer Res **20**(21): 5435-5445.

Killion, J. J., R. Radinsky and I. J. Fidler (1998). "Orthotopic models are necessary to predict therapy of transplantable tumors in mice." Cancer Metastasis Rev **17**(3): 279-284.

Kim, K., S. Y. Kong, M. Fulciniti, X. Li, W. Song, S. Nahar, P. Burger, M. J. Rumizen, K. Podar, D. Chauhan, T. Hideshima, N. C. Munshi, P. Richardson, A. Clark, J. Ogden, A. Goutopoulos, L. Rastelli, K. C. Anderson and Y. T. Tai (2010). "Blockade of the MEK/ERK signalling cascade by AS703026, a novel selective MEK1/2 inhibitor, induces pleiotropic anti-myeloma activity in vitro and in vivo." British journal of haematology **149**(4): 537-549.

Kim, K., S. Y. Kong, M. Fulciniti, X. Li, W. Song, S. Nahar, P. Burger, M. J. Rumizen, K. Podar, D. Chauhan, T. Hideshima, N. C. Munshi, P. Richardson, A. Clark, J. Ogden, A. Goutopoulos, L. Rastelli, K. C. Anderson and Y. T. Tai (2010). "Blockade of the MEK/ERK signalling cascade by AS703026, a novel selective MEK1/2 inhibitor, induces pleiotropic anti-myeloma activity in vitro and in vivo." Br J Haematol **149**(4): 537-549.

Kim, N. W., M. A. Piatyszek, K. R. Prowse, C. B. Harley, M. D. West, P. L. Ho, G. M. Coviello, W. E. Wright, S. L. Weinrich and J. W. Shay (1994). "Specific association of human telomerase activity with immortal cells and cancer." Science **266**(5193): 2011-2015.

Kim, S. O., J. Y. Jeong, M. R. Kim, H. J. Cho, J. Y. Ju, Y. S. Kwon, I. J. Oh, K. S. Kim, Y. I. Kim, S. C. Lim and Y. C. Kim (2008). "Efficacy of gemcitabine in patients with non-small cell lung cancer according to promoter polymorphisms of the ribonucleotide reductase M1 gene." Clin Cancer Res **14**(10): 3083-3088.

Kleeff, J., C. Reiser, U. Hinz, J. Bachmann, J. Debus, D. Jaeger, H. Friess and M. W. Buchler (2007). "Surgery for recurrent pancreatic ductal adenocarcinoma." Annals of surgery **245**(4): 566-572.

Kroep, J. R., W. J. Loves, C. L. van der Wilt, E. Alvarez, I. Talianidis, E. Boven, B. J. Braakhuis, C. J. van Groeningen, H. M. Pinedo and G. J. Peters (2002). "Pretreatment deoxycytidine kinase levels predict in vivo gemcitabine sensitivity." Mol Cancer Ther **1**(6): 371-376.

Kunz, B. A. and S. E. Kohalmi (1991). "Modulation of mutagenesis by deoxyribonucleotide levels." Annu Rev Genet **25**: 339-359.

Lavoie, H. and M. Therrien (2015). "Regulation of RAF protein kinases in ERK signalling." Nat Rev Mol Cell Biol **16**(5): 281-298.

Lee, J. J., C. H. Maeng, S. K. Baek, G. Y. Kim, J. H. Yoo, C. W. Choi, Y. H. Kim, Y. T. Kwak, D. H. Kim, Y. K. Lee, J. B. Kim and S. Y. Kim (2010). "The immunohistochemical overexpression of ribonucleotide reductase regulatory subunit M1 (RRM1) protein is a predictor of shorter survival to gemcitabine-based chemotherapy in advanced non-small cell lung cancer (NSCLC)." Lung Cancer **70**(2): 205-210.

Lee, J. M., S. Dedhar, R. Kalluri and E. W. Thompson (2006). "The epithelial-mesenchymal transition: new insights in signaling, development, and disease." J Cell Biol **172**(7): 973-981.

Lee, M. J., A. S. Ye, A. K. Gardino, A. M. Heijink, P. K. Sorger, G. MacBeath and M. B. Yaffe (2012). "Sequential application of anticancer drugs enhances cell death by rewiring apoptotic signaling networks." Cell **149**(4): 780-794.

Lemmon, M. A. (2009). "Ligand-induced ErbB receptor dimerization." Exp Cell Res **315**(4): 638-648.

Li, D., K. Xie, R. Wolff and J. L. Abbruzzese (2004). "Pancreatic cancer." Lancet **363**(9414): 1049-1057.

Lilienbaum, A. (2013). "Relationship between the proteasomal system and autophagy." Int J Biochem Mol Biol **4**(1): 1-26.

Lim, K. H. and C. M. Counter (2005). "Reduction in the requirement of oncogenic Ras signaling to activation of PI3K/AKT pathway during tumor maintenance." Cancer Cell **8**(5): 381-392.

Lin, H. K., L. Wang, Y. C. Hu, S. Altuwaijri and C. Chang (2002). "Phosphorylation-dependent ubiquitylation and degradation of androgen receptor by Akt require Mdm2 E3 ligase." EMBO J **21**(15): 4037-4048.

Lito, P., N. Rosen and D. B. Solit (2013). "Tumor adaptation and resistance to RAF inhibitors." Nat Med **19**(11): 1401-1409.

Liu, P., H. Cheng, T. M. Roberts and J. J. Zhao (2009). "Targeting the phosphoinositide 3-kinase pathway in cancer." Nat Rev Drug Discov **8**(8): 627-644.

Lohr, M., G. Faulmann, F. Hummel and M. V. Singer (2001). "[Gene therapy of pancreatic cancer with microencapsulated CYP2B1-expressing cells]." Onkologie **24 Suppl 5**: 60-64.

Lohr, M., B. Trautmann, M. Gottler, S. Peters, I. Zauner, B. Maillet and G. Kloppel (1994). "Human ductal adenocarcinomas of the pancreas express extracellular matrix proteins." Br J Cancer **69**(1): 144-151.

Longley, D. B., D. P. Harkin and P. G. Johnston (2003). "5-fluorouracil: mechanisms of action and clinical strategies." Nature reviews. Cancer **3**(5): 330-338.

Lord, C. J. and A. Ashworth (2012). "The DNA damage response and cancer therapy." Nature **481**(7381): 287-294.

Lorusso, P. M., A. A. Adjei, M. Varterasian, S. Gadgeel, J. Reid, D. Y. Mitchell, L. Hanson, P. DeLuca, L. Bruzek, J. Piens, P. Asbury, K. Van Becelaere, R. Herrera, J. Sebolt-Leopold and M. B. Meyer (2005). "Phase I and pharmacodynamic study of the oral MEK inhibitor CI-1040 in patients with advanced malignancies." J Clin Oncol **23**(23): 5281-5293.

Loughran, O. and N. B. La Thangue (2000). "Apoptotic and growth-promoting activity of E2F modulated by MDM2." Mol Cell Biol **20**(6): 2186-2197.

Loukopoulos, P., K. Kanetaka, M. Takamura, T. Shibata, M. Sakamoto and S. Hirohashi (2004). "Orthotopic transplantation models of pancreatic adenocarcinoma derived from cell lines and primary tumors and displaying varying metastatic activity." Pancreas **29**(3): 193-203.

Luttges, J., A. Reinecke-Luthge, B. Mollmann, M. A. Menke, A. Clemens, M. Klimpfinger, B. Sipos and G. Kloppel (1999). "Duct changes and K-ras mutations in the disease-free pancreas: analysis of type, age relation and spatial distribution." Virchows Arch **435**(5): 461-468.

Lynch, H. T., R. E. Brand, J. F. Lynch, R. M. Fusaro and S. E. Kern (2002). "Hereditary factors in pancreatic cancer." J Hepatobiliary Pancreat Surg **9**(1): 12-31.

Ma, W. W. and M. Hidalgo (2013). "The winning formulation: the development of paclitaxel in pancreatic cancer." Clin Cancer Res **19**(20): 5572-5579.

Macarulla, T., A. Cervantes, J. Tabernero, S. Rosello, E. Van Cutsem, S. Tejpar, H. Prenen, E. Martinelli, T. Troiani, B. Laffranchi, V. Jego, O. von Richter and F. Ciardiello (2015). "Phase I study of FOLFIRI plus pimasertib as second-line treatment for KRAS-mutated metastatic colorectal cancer." Br J Cancer **112**(12): 1874-1881.

Maisonneuve, P., B. C. Marshall and A. B. Lowenfels (2007). "Risk of pancreatic cancer in patients with cystic fibrosis." Gut **56**(9): 1327-1328.

Malka, D., P. Hammel, F. Maire, P. Rufat, I. Madeira, F. Pessione, P. Levy and P. Ruszniewski (2002). "Risk of pancreatic adenocarcinoma in chronic pancreatitis." Gut **51**(6): 849-852.

Malumbres, M. and M. Barbacid (2003). "RAS oncogenes: the first 30 years." Nat Rev Cancer **3**(6): 459-465.

Martinelli, E., T. Troiani, E. D'Aiuto, F. Morgillo, D. Vitagliano, A. Capasso, S. Costantino, L. P. Ciuffreda, F. Merolla, L. Vecchione, V. De Vriendt, S. Tejpar, A. Nappi, V. Sforza, G. Martini, L. Berrino, R. De Palma and F. Ciardiello (2013). "Antitumor activity of pimasertib, a selective MEK 1/2 inhibitor, in combination with PI3K/mTOR inhibitors or with multi-targeted kinase inhibitors in pimasertib-resistant human lung and colorectal cancer cells." Int J Cancer **133**(9): 2089-2101.

Massague, J., S. W. Blain and R. S. Lo (2000). "TGFbeta signaling in growth control, cancer, and heritable disorders." Cell **103**(2): 295-309.

Matsuda, Y., T. Ishiwata, N. Izumiyama-Shimomura, H. Hamayasu, M. Fujiwara, K. Tomita, N. Hiraishi, K. Nakamura, N. Ishikawa, J. Aida, K. Takubo and T. Arai (2015). "Gradual telomere shortening and increasing chromosomal instability among PanIN grades and normal ductal epithelia with and without cancer in the pancreas." PLoS One **10**(2): e0117575.

Mayo, L. D. and D. B. Donner (2001). "A phosphatidylinositol 3-kinase/Akt pathway promotes translocation of Mdm2 from the cytoplasm to the nucleus." Proc Natl Acad Sci U S A **98**(20): 11598-11603.

Mazur, P. K. and J. T. Siveke (2012). "Genetically engineered mouse models of pancreatic cancer: unravelling tumour biology and progressing translational oncology." Gut **61**(10): 1488-1500.

McCubrey, J. A., L. S. Steelman, S. L. Abrams, W. H. Chappell, S. Russo, R. Ove, M. Milella, A. Tafuri, P. Lunghi, A. Bonati, F. Stivala, F. Nicoletti, M. Libra, A. M. Martelli, G. Montalto and M. Cervello (2010). "Emerging MEK inhibitors." Expert Opin Emerg Drugs **15**(2): 203-223.

McCubrey, J. A., L. S. Steelman, S. L. Abrams, W. H. Chappell, S. Russo, R. Ove, M. Milella, A. Tafuri, P. Lunghi, A. Bonati, F. Stivala, F. Nicoletti, M. Libra, A. M. Martelli, G. Montalto and M. Cervello (2010). "Emerging MEK inhibitors." Expert opinion on emerging drugs **15**(2): 203-223.

Mehlen, P. and A. Puisieux (2006). "Metastasis: a question of life or death." Nat Rev Cancer **6**(6): 449-458.

Mendoza, M. C., E. E. Er and J. Blenis (2011). "The Ras-ERK and PI3K-mTOR pathways: cross-talk and compensation." Trends Biochem Sci **36**(6): 320-328.

Michael, D. and M. Oren (2003). "The p53-Mdm2 module and the ubiquitin system." Semin Cancer Biol **13**(1): 49-58.

Michalski, C. W., J. Weitz and M. W. Buchler (2007). "Surgery insight: surgical management of pancreatic cancer." Nat Clin Pract Oncol **4**(9): 526-535.

Mini, E., S. Nobili, B. Caciagli, I. Landini and T. Mazzei (2006). "Cellular pharmacology of gemcitabine." Annals of oncology : official journal of the European Society for Medical Oncology / ESMO **17 Suppl 5**: v7-12.

Mini, E., S. Nobili, B. Caciagli, I. Landini and T. Mazzei (2006). "Cellular pharmacology of gemcitabine." Ann Oncol **17 Suppl 5**: v7-12.

Mirzoeva, O. K., E. A. Collisson, P. M. Schaefer, B. Hann, Y. K. Hom, A. H. Ko and W. M. Korn (2013). "Subtype-specific MEK-PI3 kinase feedback as a therapeutic target in pancreatic adenocarcinoma." Mol Cancer Ther **12**(10): 2213-2225.

Miyabayashi, K., H. Ijichi, D. Mohri, M. Tada, K. Yamamoto, Y. Asaoka, T. Ikenoue, K. Tateishi, Y. Nakai, H. Isayama, Y. Morishita, M. Omata, H. L. Moses and K. Koike (2013). "Erlotinib prolongs survival in pancreatic cancer by blocking gemcitabine-induced MAPK signals." Cancer Res **73**(7): 2221-2234.

Mo, P., H. Wang, H. Lu, D. D. Boyd and C. Yan (2010). "MDM2 mediates ubiquitination and degradation of activating transcription factor 3." J Biol Chem **285**(35): 26908-26915.

Montagut, C. and J. Settleman (2009). "Targeting the RAF-MEK-ERK pathway in cancer therapy." Cancer Lett **283**(2): 125-134.

Moore, M. J., D. Goldstein, J. Hamm, A. Figer, J. R. Hecht, S. Gallinger, H. J. Au, P. Murawa, D. Walde, R. A. Wolff, D. Campos, R. Lim, K. Ding, G. Clark, T. Voskoglou-Nomikos, M. Ptasynski, W. Parulekar and G. National Cancer Institute of Canada Clinical Trials (2007). "Erlotinib plus gemcitabine compared with gemcitabine alone in patients with advanced pancreatic cancer: a phase III trial of the National Cancer Institute of Canada Clinical Trials Group." J Clin Oncol **25**(15): 1960-1966.

Moore, P. S., B. Sipos, S. Orlandini, C. Sorio, F. X. Real, N. R. Lemoine, T. Gress, C. Bassi, G. Kloppel, H. Kalthoff, H. Ungefroren, M. Lohr and A. Scarpa (2001). "Genetic profile of 22 pancreatic carcinoma cell lines. Analysis of K-ras, p53, p16 and DPC4/Smad4." Virchows Arch **439**(6): 798-802.

Morgan, M. A., L. A. Parsels, L. E. Kollar, D. P. Normolle, J. Maybaum and T. S. Lawrence (2008). "The combination of epidermal growth factor receptor inhibitors with gemcitabine and radiation in pancreatic cancer." Clinical cancer research : an official journal of the American Association for Cancer Research **14**(16): 5142-5149.

Mori, R., T. Ishikawa, Y. Ichikawa, K. Taniguchi, R. Matsuyama, M. Ueda, Y. Fujii, I. Endo, S. Togo, P. V. Danenberg and H. Shimada (2007). "Human equilibrative nucleoside transporter 1 is associated with the chemosensitivity of gemcitabine in human pancreatic adenocarcinoma and biliary tract carcinoma cells." Oncol Rep **17**(5): 1201-1205.

Morris, J. P. t., D. A. Cano, S. Sekine, S. C. Wang and M. Hebrok (2010). "Beta-catenin blocks Kras-dependent reprogramming of acini into pancreatic cancer precursor lesions in mice." J Clin Invest **120**(2): 508-520.

Morris, J. P. t., S. C. Wang and M. Hebrok (2010). "KRAS, Hedgehog, Wnt and the twisted developmental biology of pancreatic ductal adenocarcinoma." Nat Rev Cancer **10**(10): 683-695.

Morton, J. P., N. B. Jamieson, S. A. Karim, D. Athineos, R. A. Ridgway, C. Nixon, C. J. McKay, R. Carter, V. G. Brunton, M. C. Frame, A. Ashworth, K. A. Oien, T. R. Evans and O. J. Sansom (2010). "LKB1 haploinsufficiency cooperates with Kras to promote pancreatic cancer through suppression of p21-dependent growth arrest." Gastroenterology **139**(2): 586-597, 597 e581-586.

Morton, J. P., P. Timpson, S. A. Karim, R. A. Ridgway, D. Athineos, B. Doyle, N. B. Jamieson, K. A. Oien, A. M. Lowy, V. G. Brunton, M. C. Frame, T. R. Evans and O. J. Sansom (2010). "Mutant p53 drives metastasis and overcomes growth arrest/senescence in pancreatic cancer." Proc Natl Acad Sci U S A **107**(1): 246-251.

Mukherjee, S., C. N. Hurt, J. Bridgewater, S. Falk, S. Cummins, H. Wasan, T. Crosby, C. Jephcott, R. Roy, G. Radhakrishna, A. McDonald, R. Ray, G. Joseph, J. Staffurth, R. A. Abrams, G. Griffiths and T. Maughan (2013). "Gemcitabine-based or capecitabine-based chemoradiotherapy for locally advanced pancreatic cancer (SCALOP): a multicentre, randomised, phase 2 trial." Lancet Oncol **14**(4): 317-326.

Murphy, K. M., K. A. Brune, C. Griffin, J. E. Sollenberger, G. M. Petersen, R. Bansal, R. H. Hruban and S. E. Kern (2002). "Evaluation of candidate genes MAP2K4, MADH4, ACVR1B, and BRCA2 in familial pancreatic cancer: deleterious BRCA2 mutations in 17%." Cancer Res **62**(13): 3789-3793.

Nakahira, S., S. Nakamori, M. Tsujie, Y. Takahashi, J. Okami, S. Yoshioka, M. Yamasaki, S. Marubashi, I. Takemasa, A. Miyamoto, Y. Takeda, H. Nagano, K. Dono, K. Umeshita, M. Sakon and M. Monden (2007). "Involvement of ribonucleotide reductase M1 subunit overexpression in gemcitabine resistance of human pancreatic cancer." Int J Cancer **120**(6): 1355-1363.

Nakahira, S., S. Nakamori, M. Tsujie, Y. Takahashi, J. Okami, S. Yoshioka, M. Yamasaki, S. Marubashi, I. Takemasa, A. Miyamoto, Y. Takeda, H. Nagano, K. Dono, K. Umeshita, M. Sakon and M. Monden (2007). "Involvement of ribonucleotide reductase M1 subunit overexpression in gemcitabine resistance of human pancreatic cancer." International journal of cancer. Journal international du cancer **120**(6): 1355-1363.

Nakano, Y., S. Tanno, K. Koizumi, T. Nishikawa, K. Nakamura, M. Minoguchi, T. Izawa, Y. Mizukami, T. Okumura and Y. Kohgo (2007). "Gemcitabine chemoresistance and molecular markers associated with gemcitabine transport and metabolism in human pancreatic cancer cells." Br J Cancer **96**(3): 457-463.

Navas, C., I. Hernandez-Porras, A. J. Schuhmacher, M. Sibilia, C. Guerra and M. Barbacid (2012). "EGF receptor signaling is essential for k-ras oncogene-driven pancreatic ductal adenocarcinoma." Cancer Cell **22**(3): 318-330.

Neesse, A., K. K. Frese, D. S. Chan, T. E. Bapiro, W. J. Howat, F. M. Richards, V. Ellenrieder, D. I. Jodrell and D. A. Tuveson (2014). "SPARC independent drug delivery and antitumour effects of nab-paclitaxel in genetically engineered mice." Gut **63**(6): 974-983.

Neesse, A., P. Michl, K. K. Frese, C. Feig, N. Cook, M. A. Jacobetz, M. P. Lolkema, M. Buchholz, K. P. Olive, T. M. Gress and D. A. Tuveson (2011). "Stromal biology and therapy in pancreatic cancer." Gut **60**(6): 861-868.

Neoptolemos, J. P., D. D. Stocken, J. A. Dunn, J. Almond, H. G. Beger, P. Pederzoli, C. Bassi, C. Dervenis, L. Fernandez-Cruz, F. Lacaine, J. Buckels, M. Deakin, F. A. Adab, R. Sutton, C. Imrie, I. Ihse, T. Tihanyi, A. Olah, S. Pedrazzoli, D. Spooner, D. J. Kerr, H. Friess, M. W. Buchler and C. European Study Group for Pancreatic (2001). "Influence of resection margins on survival for patients with pancreatic cancer treated by

adjuvant chemoradiation and/or chemotherapy in the ESPAC-1 randomized controlled trial." Ann Surg **234**(6): 758-768.

Neoptolemos, J. P., D. D. Stocken, H. Friess, C. Bassi, J. A. Dunn, H. Hickey, H. Beger, L. Fernandez-Cruz, C. Dervenis, F. Lacaine, M. Falconi, P. Pederzoli, A. Pap, D. Spooner, D. J. Kerr, M. W. Buchler and C. European Study Group for Pancreatic (2004). "A randomized trial of chemoradiotherapy and chemotherapy after resection of pancreatic cancer." N Engl J Med **350**(12): 1200-1210.

Neuzillet, C., P. Hammel, A. Tijeras-Raballand, A. Couvelard and E. Raymond (2012). "Targeting the Ras-ERK pathway in pancreatic adenocarcinoma." Cancer metastasis reviews.

Neuzillet, C., P. Hammel, A. Tijeras-Raballand, A. Couvelard and E. Raymond (2013). "Targeting the Ras-ERK pathway in pancreatic adenocarcinoma." Cancer Metastasis Rev **32**(1-2): 147-162.

Neuzillet, C., A. Tijeras-Raballand, L. de Mestier, J. Cros, S. Faivre and E. Raymond (2014). "MEK in cancer and cancer therapy." Pharmacol Ther **141**(2): 160-171.

Nordlund, P. and P. Reichard (2006). "Ribonucleotide reductases." Annu Rev Biochem **75**: 681-706.

Nordlund, P. and P. Reichard (2006). "Ribonucleotide reductases." Annual review of biochemistry **75**: 681-706.

Normanno, N., A. De Luca, C. Bianco, L. Strizzi, M. Mancino, M. R. Maiello, A. Carotenuto, G. De Feo, F. Caponigro and D. S. Salomon (2006). "Epidermal growth factor receptor (EGFR) signaling in cancer." Gene **366**(1): 2-16.

Oettle, H. and P. Neuhaus (2007). "Adjuvant therapy in pancreatic cancer: a critical appraisal." Drugs **67**(16): 2293-2310.

Oettle, H., S. Post, P. Neuhaus, K. Gellert, J. Langrehr, K. Ridwelski, H. Schramm, J. Fahlke, C. Zuelke, C. Burkart, K. Gutberlet, E. Kettner, H. Schmalenberg, K. Weigang-Koehler, W. O. Bechstein, M. Niedergethmann, I. Schmidt-Wolf, L. Roll, B. Doerken and H. Riess (2007). "Adjuvant chemotherapy with gemcitabine vs observation in patients undergoing curative-intent resection of pancreatic cancer: a randomized controlled trial." JAMA **297**(3): 267-277.

Ogawa, M., H. Hori, T. Ohta, K. Onozato, M. Miyahara and Y. Komada (2005). "Sensitivity to gemcitabine and its metabolizing enzymes in neuroblastoma." Clin Cancer Res **11**(9): 3485-3493.

Ohhashi, S., K. Ohuchida, K. Mizumoto, H. Fujita, T. Egami, J. Yu, H. Toma, S. Sadatomi, E. Nagai and M. Tanaka (2008). "Down-regulation of deoxycytidine kinase enhances

acquired resistance to gemcitabine in pancreatic cancer." Anticancer Res **28**(4B): 2205-2212.

Ohren, J. F., H. Chen, A. Pavlovsky, C. Whitehead, E. Zhang, P. Kuffa, C. Yan, P. McConnell, C. Spessard, C. Banotai, W. T. Mueller, A. Delaney, C. Omer, J. Sebolt-Leopold, D. T. Dudley, I. K. Leung, C. Flamme, J. Warmus, M. Kaufman, S. Barrett, H. Tecle and C. A. Hasemann (2004). "Structures of human MAP kinase kinase 1 (MEK1) and MEK2 describe novel noncompetitive kinase inhibition." Nat Struct Mol Biol **11**(12): 1192-1197.

Ohren, J. F., H. Chen, A. Pavlovsky, C. Whitehead, E. Zhang, P. Kuffa, C. Yan, P. McConnell, C. Spessard, C. Banotai, W. T. Mueller, A. Delaney, C. Omer, J. Sebolt-Leopold, D. T. Dudley, I. K. Leung, C. Flamme, J. Warmus, M. Kaufman, S. Barrett, H. Tecle and C. A. Hasemann (2004). "Structures of human MAP kinase kinase 1 (MEK1) and MEK2 describe novel noncompetitive kinase inhibition." Nature structural & molecular biology **11**(12): 1192-1197.

Olive, K. P., M. A. Jacobetz, C. J. Davidson, A. Gopinathan, D. McIntyre, D. Honess, B. Madhu, M. A. Goldgraben, M. E. Caldwell, D. Allard, K. K. Frese, G. Denicola, C. Feig, C. Combs, S. P. Winter, H. Ireland-Zecchini, S. Reichelt, W. J. Howat, A. Chang, M. Dhara, L. Wang, F. Ruckert, R. Grutzmann, C. Pilarsky, K. Izeradjene, S. R. Hingorani, P. Huang, S. E. Davies, W. Plunkett, M. Egorin, R. H. Hruban, N. Whitebread, K. McGovern, J. Adams, C. Iacobuzio-Donahue, J. Griffiths and D. A. Tuveson (2009). "Inhibition of Hedgehog signaling enhances delivery of chemotherapy in a mouse model of pancreatic cancer." Science **324**(5933): 1457-1461.

Oliver, T. G., E. Meylan, G. P. Chang, W. Xue, J. R. Burke, T. J. Humpton, D. Hubbard, A. Bhutkar and T. Jacks (2011). "Caspase-2-mediated cleavage of Mdm2 creates a p53-induced positive feedback loop." Mol Cell **43**(1): 57-71.

Orlowski, M. and S. Wilk (2000). "Catalytic activities of the 20 S proteasome, a multicatalytic proteinase complex." Arch Biochem Biophys **383**(1): 1-16.

Ostruszka, L. J. and D. S. Shewach (2000). "The role of cell cycle progression in radiosensitization by 2',2'-difluoro-2'-deoxycytidine." Cancer Res **60**(21): 6080-6088.

Ottenhof, N. A., R. F. de Wilde, A. Maitra, R. H. Hruban and G. J. Offerhaus (2011). "Molecular characteristics of pancreatic ductal adenocarcinoma." Pathology research international **2011**: 620601.

Ozcelik, H., B. Schmocker, N. Di Nicola, X. H. Shi, B. Langer, M. Moore, B. R. Taylor, S. A. Narod, G. Darlington, I. L. Andrulis, S. Gallinger and M. Redston (1997). "Germline BRCA2 6174delT mutations in Ashkenazi Jewish pancreatic cancer patients." Nat Genet **16**(1): 17-18.

Park, S. J., S. W. Hong, J. H. Moon, D. H. Jin, J. S. Kim, C. K. Lee, K. P. Kim, Y. S. Hong, E. K. Choi, J. S. Lee, J. L. Lee and T. W. Kim (2013). "The MEK1/2 inhibitor AS703026 circumvents resistance to the BRAF inhibitor PLX4032 in human malignant melanoma cells." Am J Med Sci **346**(6): 494-498.

Pasca di Magliano, M., A. V. Biankin, P. W. Heiser, D. A. Cano, P. J. Gutierrez, T. Deramaudt, D. Segara, A. C. Dawson, J. G. Kench, S. M. Henshall, R. L. Sutherland, A. Dlugosz, A. K. Rustgi and M. Hebrok (2007). "Common activation of canonical Wnt signaling in pancreatic adenocarcinoma." PLoS One **2**(11): e1155.

Pazdur, R., A. P. Kudelka, J. J. Kavanagh, P. R. Cohen and M. N. Raber (1993). "The taxoids: paclitaxel (Taxol) and docetaxel (Taxotere)." Cancer Treat Rev **19**(4): 351-386.

Philip, P. A., J. Benedetti, C. L. Corless, R. Wong, E. M. O'Reilly, P. J. Flynn, K. M. Rowland, J. N. Atkins, B. C. Mirtsching, S. E. Rivkin, A. A. Khorana, B. Goldman, C. M. Fenoglio-Preiser, J. L. Abbruzzese and C. D. Blanke (2010). "Phase III study comparing gemcitabine plus cetuximab versus gemcitabine in patients with advanced pancreatic adenocarcinoma: Southwest Oncology Group-directed intergroup trial S0205." Journal of clinical oncology : official journal of the American Society of Clinical Oncology **28**(22): 3605-3610.

Piao, C., C. K. Youn, M. Jin, S. P. Yoon, I. Y. Chang, J. H. Lee and H. J. You (2012). "MEK2 regulates ribonucleotide reductase activity through functional interaction with ribonucleotide reductase small subunit p53R2." Cell Cycle **11**(17): 3237-3249.

Plunkett, W., P. Huang and V. Gandhi (1995). "Preclinical characteristics of gemcitabine." Anticancer Drugs **6 Suppl 6**: 7-13.

Polyak, K. and R. A. Weinberg (2009). "Transitions between epithelial and mesenchymal states: acquisition of malignant and stem cell traits." Nature reviews. Cancer **9**(4): 265-273.

Poplin, E., H. Wasan, L. Rolfe, M. Raponi, T. Ikdahl, I. Bondarenko, I. Davidenko, V. Bondar, A. Garin, S. Boeck, S. Ormanns, V. Heinemann, C. Bassi, T. R. Evans, R. Andersson, H. Hahn, V. Picozzi, A. Dicker, E. Mann, C. Voong, P. Kaur, J. Isaacson and A. Allen (2013). "Randomized, multicenter, phase II study of CO-101 versus gemcitabine in patients with metastatic pancreatic ductal adenocarcinoma: including a prospective evaluation of the role of hENT1 in gemcitabine or CO-101 sensitivity." J Clin Oncol **31**(35): 4453-4461.

Pourquier, P., C. Gioffre, G. Kohlhagen, Y. Urasaki, F. Goldwasser, L. W. Hertel, S. Yu, R. T. Pon, W. H. Gmeiner and Y. Pommier (2002). "Gemcitabine (2',2'-difluoro-2'-deoxycytidine), an antimetabolite that poisons topoisomerase I." Clin Cancer Res **8**(8): 2499-2504.

Provenzano, P. P., C. Cuevas, A. E. Chang, V. K. Goel, D. D. Von Hoff and S. R. Hingorani (2012). "Enzymatic targeting of the stroma ablates physical barriers to treatment of pancreatic ductal adenocarcinoma." Cancer Cell **21**(3): 418-429.

Pylayeva-Gupta, Y., E. Grabocka and D. Bar-Sagi (2011). "RAS oncogenes: weaving a tumorigenic web." Nat Rev Cancer **11**(11): 761-774.

Qiu, W., F. Sahin, C. A. Iacobuzio-Donahue, D. Garcia-Carracedo, W. M. Wang, C. Y. Kuo, D. Chen, D. E. Arking, A. M. Lowy, R. H. Hruban, H. E. Remotti and G. H. Su (2011). "Disruption of p16 and activation of Kras in pancreas increase ductal adenocarcinoma formation and metastasis in vivo." Oncotarget **2**(11): 862-873.

Qiu, W. and G. H. Su (2013). "Development of orthotopic pancreatic tumor mouse models." Methods Mol Biol **980**: 215-223.

Raimondi, S., P. Maisonneuve and A. B. Lowenfels (2009). "Epidemiology of pancreatic cancer: an overview." Nat Rev Gastroenterol Hepatol **6**(12): 699-708.

Rajalingam, K., R. Schreck, U. R. Rapp and S. Albert (2007). "Ras oncogenes and their downstream targets." Biochim Biophys Acta **1773**(8): 1177-1195.

Reichard, P. (1993). "From RNA to DNA, why so many ribonucleotide reductases?" Science **260**(5115): 1773-1777.

Reichert, M. and A. K. Rustgi (2011). "Pancreatic ductal cells in development, regeneration, and neoplasia." J Clin Invest **121**(12): 4572-4578.

Reichert, M., D. Saur, R. Hamacher, R. M. Schmid and G. Schneider (2007). "Phosphoinositide-3-kinase signaling controls S-phase kinase-associated protein 2 transcription via E2F1 in pancreatic ductal adenocarcinoma cells." Cancer Res **67**(9): 4149-4156.

Rhim, A. D., E. T. Mirek, N. M. Aiello, A. Maitra, J. M. Bailey, F. McAllister, M. Reichert, G. L. Beatty, A. K. Rustgi, R. H. Vonderheide, S. D. Leach and B. Z. Stanger (2012). "EMT and dissemination precede pancreatic tumor formation." Cell **148**(1-2): 349-361.

Rinehart, J., A. A. Adjei, P. M. Lorusso, D. Waterhouse, J. R. Hecht, R. B. Natale, O. Hamid, M. Varterasian, P. Asbury, E. P. Kaldjian, S. Gulyas, D. Y. Mitchell, R. Herrera, J. S. Sebolt-Leopold and M. B. Meyer (2004). "Multicenter phase II study of the oral MEK inhibitor, CI-1040, in patients with advanced non-small-cell lung, breast, colon, and pancreatic cancer." J Clin Oncol **22**(22): 4456-4462.

Ritzel, M. W., A. M. Ng, S. Y. Yao, K. Graham, S. K. Loewen, K. M. Smith, R. J. Hyde, E. Karpinski, C. E. Cass, S. A. Baldwin and J. D. Young (2001). "Recent molecular advances in studies of the concentrative Na+-dependent nucleoside transporter (CNT) family: identification and characterization of novel human and mouse proteins (hCNT3 and

mCNT3) broadly selective for purine and pyrimidine nucleosides (system cib)." Mol Membr Biol **18**(1): 65-72.

Robert, C., R. Dummer, R. Gutzmer, P. Lorigan, K. B. Kim, M. Nyakas, A. Arance, G. Liszkay, D. Schadendorf, M. Cantarini, S. Spencer and M. R. Middleton (2013). "Selumetinib plus dacarbazine versus placebo plus dacarbazine as first-line treatment for BRAF-mutant metastatic melanoma: a phase 2 double-blind randomised study." Lancet Oncol **14**(8): 733-740.

Roberts, P. J. and C. J. Der (2007). "Targeting the Raf-MEK-ERK mitogen-activated protein kinase cascade for the treatment of cancer." Oncogene **26**(22): 3291-3310.

Roskoski, R., Jr. (2012). "MEK1/2 dual-specificity protein kinases: structure and regulation." Biochem Biophys Res Commun **417**(1): 5-10.

Roy, R., J. Chun and S. N. Powell (2012). "BRCA1 and BRCA2: different roles in a common pathway of genome protection." Nat Rev Cancer **12**(1): 68-78.

Rozenblum, E., M. Schutte, M. Goggins, S. A. Hahn, S. Panzer, M. Zahurak, S. N. Goodman, T. A. Sohn, R. H. Hruban, C. J. Yeo and S. E. Kern (1997). "Tumor-suppressive pathways in pancreatic carcinoma." Cancer Res **57**(9): 1731-1734.

Rubio-Viqueira, B., A. Jimeno, G. Cusatis, X. Zhang, C. Iacobuzio-Donahue, C. Karikari, C. Shi, K. Danenberg, P. V. Danenberg, H. Kuramochi, K. Tanaka, S. Singh, H. Salimi-Moosavi, N. Bouraoud, M. L. Amador, S. Altiok, P. Kulesza, C. Yeo, W. Messersmith, J. Eshleman, R. H. Hruban, A. Maitra and M. Hidalgo (2006). "An in vivo platform for translational drug development in pancreatic cancer." Clin Cancer Res **12**(15): 4652-4661.

Saborowski, M., A. Saborowski, J. P. t. Morris, B. Bosbach, L. E. Dow, J. Pelletier, D. S. Klimstra and S. W. Lowe (2014). "A modular and flexible ESC-based mouse model of pancreatic cancer." Genes Dev **28**(1): 85-97.

Sale, M. J. and S. J. Cook (2014). "Intrinsic and acquired resistance to MEK1/2 inhibitors in cancer." Biochem Soc Trans **42**(4): 776-783.

Samuel, N. and T. J. Hudson (2012). "The molecular and cellular heterogeneity of pancreatic ductal adenocarcinoma." Nature reviews. Gastroenterology & hepatology **9**(2): 77-87.

Schenk, M., A. G. Schwartz, E. O'Neal, M. Kinnard, J. K. Greenson, J. P. Fryzek, G. S. Ying and D. H. Garabrant (2001). "Familial risk of pancreatic cancer." J Natl Cancer Inst **93**(8): 640-644.

Schuller, J., J. Cassidy, E. Dumont, B. Roos, S. Durston, L. Banken, M. Utoh, K. Mori, E. Weidekamm and B. Reigner (2000). "Preferential activation of capecitabine in tumor

following oral administration to colorectal cancer patients." Cancer Chemother Pharmacol **45**(4): 291-297.

Sebastiani, V., F. Ricci, B. Rubio-Viqueira, P. Kulesza, C. J. Yeo, M. Hidalgo, A. Klein, D. Laheru and C. A. Iacobuzio-Donahue (2006). "Immunohistochemical and genetic evaluation of deoxycytidine kinase in pancreatic cancer: relationship to molecular mechanisms of gemcitabine resistance and survival." Clin Cancer Res **12**(8): 2492-2497.

Sebolt-Leopold, J. S., D. T. Dudley, R. Herrera, K. Van Becelaere, A. Wiland, R. C. Gowan, H. Tecle, S. D. Barrett, A. Bridges, S. Przybranowski, W. R. Leopold and A. R. Saltiel (1999). "Blockade of the MAP kinase pathway suppresses growth of colon tumors in vivo." Nat Med **5**(7): 810-816.

Sebolt-Leopold, J. S. and R. Herrera (2004). "Targeting the mitogen-activated protein kinase cascade to treat cancer." Nat Rev Cancer **4**(12): 937-947.

Seufferlein, T., J. B. Bachet, E. Van Cutsem, P. Rougier and E. G. W. Group (2012). "Pancreatic adenocarcinoma: ESMO-ESDO Clinical Practice Guidelines for diagnosis, treatment and follow-up." Ann Oncol **23 Suppl 7**: vii33-40.

Shi, S., W. Yao, J. Xu, J. Long, C. Liu and X. Yu (2012). "Combinational therapy: new hope for pancreatic cancer?" Cancer Lett **317**(2): 127-135.

Singh, M., A. Lima, R. Molina, P. Hamilton, A. C. Clermont, V. Devasthali, J. D. Thompson, J. H. Cheng, H. Bou Reslan, C. C. Ho, T. C. Cao, C. V. Lee, M. A. Nannini, G. Fuh, R. A. Carano, H. Koeppen, R. X. Yu, W. F. Forrest, G. D. Plowman and L. Johnson (2010). "Assessing therapeutic responses in Kras mutant cancers using genetically engineered mouse models." Nat Biotechnol **28**(6): 585-593.

Siolas, D. and G. J. Hannon (2013). "Patient-derived tumor xenografts: transforming clinical samples into mouse models." Cancer Res **73**(17): 5315-5319.

Siveke, J. T., H. Einwachter, B. Sipos, C. Lubeseder-Martellato, G. Kloppel and R. M. Schmid (2007). "Concomitant pancreatic activation of Kras(G12D) and Tgfa results in cystic papillary neoplasms reminiscent of human IPMN." Cancer Cell **12**(3): 266-279.

Slack-Davis, J. K., S. T. Eblen, M. Zecevic, S. A. Boerner, A. Tarcsafalvi, H. B. Diaz, M. S. Marshall, M. J. Weber, J. T. Parsons and A. D. Catling (2003). "PAK1 phosphorylation of MEK1 regulates fibronectin-stimulated MAPK activation." J Cell Biol **162**(2): 281-291.

Smit, V. T., A. J. Boot, A. M. Smits, G. J. Fleuren, C. J. Cornelisse and J. L. Bos (1988). "KRAS codon 12 mutations occur very frequently in pancreatic adenocarcinomas." Nucleic Acids Res **16**(16): 7773-7782.

Smith, M. P., B. Sanchez-Laorden, K. O'Brien, H. Brunton, J. Ferguson, H. Young, N. Dhomen, K. T. Flaherty, D. T. Frederick, Z. A. Cooper, J. A. Wargo, R. Marais and C. Wellbrock (2014). "The immune microenvironment confers resistance to MAPK pathway inhibitors through macrophage-derived TNFalpha." Cancer Discov **4**(10): 1214-1229.

Steelman, L. S., S. L. Abrams, J. Whelan, F. E. Bertrand, D. E. Ludwig, J. Basecke, M. Libra, F. Stivala, M. Milella, A. Tafuri, P. Lunghi, A. Bonati, A. M. Martelli and J. A. McCubrey (2008). "Contributions of the Raf/MEK/ERK, PI3K/PTEN/Akt/mTOR and Jak/STAT pathways to leukemia." Leukemia **22**(4): 686-707.

Steinman, H. A., E. Burstein, C. Lengner, J. Gosselin, G. Pihan, C. S. Duckett and S. N. Jones (2004). "An alternative splice form of Mdm2 induces p53-independent cell growth and tumorigenesis." J Biol Chem **279**(6): 4877-4886.

Sui, X., S. Shin, R. Zhang, P. F. Firozi, L. Yang, J. L. Abbruzzese and S. A. Reddy (2009). "Hdm2 is regulated by K-Ras and mediates p53-independent functions in pancreatic cancer cells." Oncogene **28**(5): 709-720.

Sun, H., C. H. Charles, L. F. Lau and N. K. Tonks (1993). "MKP-1 (3CH134), an immediate early gene product, is a dual specificity phosphatase that dephosphorylates MAP kinase in vivo." Cell **75**(3): 487-493.

Svrcek, M., J. Cros, R. Marechal, J. B. Bachet, J. F. Flejou and P. Demetter (2015). "Human equilibrative nucleoside transporter 1 testing in pancreatic ductal adenocarcinoma: a comparison between murine and rabbit antibodies." Histopathology **66**(3): 457-462.

Tanaka, H., H. Arakawa, T. Yamaguchi, K. Shiraishi, S. Fukuda, K. Matsui, Y. Takei and Y. Nakamura (2000). "A ribonucleotide reductase gene involved in a p53-dependent cell-cycle checkpoint for DNA damage." Nature **404**(6773): 42-49.

Tenno, T., K. Fujiwara, H. Tochio, K. Iwai, E. H. Morita, H. Hayashi, S. Murata, H. Hiroaki, M. Sato, K. Tanaka and M. Shirakawa (2004). "Structural basis for distinct roles of Lys63- and Lys48-linked polyubiquitin chains." Genes Cells **9**(10): 865-875.

Thomas, R. K., A. C. Baker, R. M. Debiasi, W. Winckler, T. Laframboise, W. M. Lin, M. Wang, W. Feng, T. Zander, L. MacConaill, J. C. Lee, R. Nicoletti, C. Hatton, M. Goyette, L. Girard, K. Majmudar, L. Ziaugra, K. K. Wong, S. Gabriel, R. Beroukhim, M. Peyton, J. Barretina, A. Dutt, C. Emery, H. Greulich, K. Shah, H. Sasaki, A. Gazdar, J. Minna, S. A. Armstrong, I. K. Mellinghoff, F. S. Hodi, G. Dranoff, P. S. Mischel, T. F. Cloughesy, S. F. Nelson, L. M. Liau, K. Mertz, M. A. Rubin, H. Moch, M. Loda, W. Catalona, J. Fletcher, S. Signoretti, F. Kaye, K. C. Anderson, G. D. Demetri, R. Dummer, S. Wagner, M. Herlyn, W. R. Sellers, M. Meyerson and L. A. Garraway (2007). "High-throughput oncogene mutation profiling in human cancer." Nature genetics **39**(3): 347-351.

Thota, R., J. M. Pauff and J. D. Berlin (2014). "Treatment of metastatic pancreatic adenocarcinoma: a review." Oncology (Williston Park) **28**(1): 70-74.

Tobita, K., H. Kijima, S. Dowaki, H. Kashiwagi, Y. Ohtani, Y. Oida, H. Yamazaki, M. Nakamura, Y. Ueyama, M. Tanaka, S. Inokuchi and H. Makuuchi (2003). "Epidermal growth factor receptor expression in human pancreatic cancer: Significance for liver metastasis." Int J Mol Med **11**(3): 305-309.

Tseng, W. W., D. Winer, J. A. Kenkel, O. Choi, A. H. Shain, J. R. Pollack, R. French, A. M. Lowy and E. G. Engleman (2010). "Development of an orthotopic model of invasive pancreatic cancer in an immunocompetent murine host." Clin Cancer Res **16**(14): 3684-3695.

Turke, A. B., Y. Song, C. Costa, R. Cook, C. L. Arteaga, J. M. Asara and J. A. Engelman (2012). "MEK inhibition leads to PI3K/AKT activation by relieving a negative feedback on ERBB receptors." Cancer Res **72**(13): 3228-3237.

Ueno, H., K. Kiyosawa and N. Kaniwa (2007). "Pharmacogenomics of gemcitabine: can genetic studies lead to tailor-made therapy?" Br J Cancer **97**(2): 145-151.

Valastyan, S. and R. A. Weinberg (2011). "Tumor metastasis: molecular insights and evolving paradigms." Cell **147**(2): 275-292.

van der Heijden, M. S., J. R. Brody, E. Gallmeier, S. C. Cunningham, D. A. Dezentje, D. Shen, R. H. Hruban and S. E. Kern (2004). "Functional defects in the fanconi anemia pathway in pancreatic cancer cells." Am J Pathol **165**(2): 651-657.

van Moorsel, C. J., G. Veerman, A. M. Bergman, A. Guechev, J. B. Vermorken, P. E. Postmus and G. J. Peters (1997). "Combination chemotherapy studies with gemcitabine." Semin Oncol **24**(2 Suppl 7): S7-17-S17-23.

Vassilev, L. T. (2004). "Small-molecule antagonists of p53-MDM2 binding: research tools and potential therapeutics." Cell Cycle **3**(4): 419-421.

Vassilev, L. T. (2007). "MDM2 inhibitors for cancer therapy." Trends Mol Med **13**(1): 23-31.

Veltkamp, S. A., J. H. Beijnen and J. H. Schellens (2008). "Prolonged versus standard gemcitabine infusion: translation of molecular pharmacology to new treatment strategy." The oncologist **13**(3): 261-276.

Veltkamp, S. A., D. Pluim, M. A. van Eijndhoven, M. J. Bolijn, F. H. Ong, R. Govindarajan, J. D. Unadkat, J. H. Beijnen and J. H. Schellens (2008). "New insights into the pharmacology and cytotoxicity of gemcitabine and 2',2'-difluorodeoxyuridine." Mol Cancer Ther **7**(8): 2415-2425.

Venkitaraman, A. R. (2002). "Cancer susceptibility and the functions of BRCA1 and BRCA2." Cell **108**(2): 171-182.

Vivanco, I. and C. L. Sawyers (2002). "The phosphatidylinositol 3-Kinase AKT pathway in human cancer." Nat Rev Cancer **2**(7): 489-501.

Vogelstein, B. and K. W. Kinzler (2004). "Cancer genes and the pathways they control." Nat Med **10**(8): 789-799.

Vogelstein, B., D. Lane and A. J. Levine (2000). "Surfing the p53 network." Nature **408**(6810): 307-310.

Vogelstein, B., N. Papadopoulos, V. E. Velculescu, S. Zhou, L. A. Diaz, Jr. and K. W. Kinzler (2013). "Cancer genome landscapes." Science **339**(6127): 1546-1558.

Vogelzang, N. J., S. I. Benowitz, S. Adams, C. Aghajanian, S. M. Chang, Z. E. Dreyer, P. A. Janne, A. H. Ko, G. A. Masters, O. Odenike, J. D. Patel, B. J. Roth, W. E. Samlowski, A. D. Seidman, W. D. Tap, J. S. Temel, J. H. Von Roenn and M. G. Kris (2012). "Clinical cancer advances 2011: Annual Report on Progress Against Cancer from the American Society of Clinical Oncology." J Clin Oncol **30**(1): 88-109.

Von Hoff, D. D., T. Ervin, F. P. Arena, E. G. Chiorean, J. Infante, M. Moore, T. Seay, S. A. Tjulandin, W. W. Ma, M. N. Saleh, M. Harris, M. Reni, S. Dowden, D. Laheru, N. Bahary, R. K. Ramanathan, J. Tabernero, M. Hidalgo, D. Goldstein, E. Van Cutsem, X. Wei, J. Iglesias and M. F. Renschler (2013). "Increased survival in pancreatic cancer with nab-paclitaxel plus gemcitabine." N Engl J Med **369**(18): 1691-1703.

Von Hoff, D. D., R. K. Ramanathan, M. J. Borad, D. A. Laheru, L. S. Smith, T. E. Wood, R. L. Korn, N. Desai, V. Trieu, J. L. Iglesias, H. Zhang, P. Soon-Shiong, T. Shi, N. V. Rajeshkumar, A. Maitra and M. Hidalgo (2011). "Gemcitabine plus nab-paclitaxel is an active regimen in patients with advanced pancreatic cancer: a phase I/II trial." J Clin Oncol **29**(34): 4548-4554.

Wang, Q., X. Liu, J. Zhou, Y. Huang, S. Zhang, J. Shen, S. Loera, X. Yuan, W. Chen, M. Jin, S. Shibata, Y. Liu, P. Chu, L. Wang and Y. Yen (2013). "Ribonucleotide reductase large subunit m1 predicts poor survival due to modulation of proliferative and invasive ability of gastric cancer." PloS one **8**(7): e70191.

Warshaw, A. L. and C. Fernandez-del Castillo (1992). "Pancreatic carcinoma." N Engl J Med **326**(7): 455-465.

Wee, S., Z. Jagani, K. X. Xiang, A. Loo, M. Dorsch, Y. M. Yao, W. R. Sellers, C. Lengauer and F. Stegmeier (2009). "PI3K pathway activation mediates resistance to MEK inhibitors in KRAS mutant cancers." Cancer Res **69**(10): 4286-4293.

Weissmueller, S., E. Manchado, M. Saborowski, J. P. t. Morris, E. Wagenblast, C. A. Davis, S. H. Moon, N. T. Pfister, D. F. Tschaharganeh, T. Kitzing, D. Aust, E. K. Markert, J. Wu, S. M. Grimmond, C. Pilarsky, C. Prives, A. V. Biankin and S. W. Lowe (2014). "Mutant p53 drives pancreatic cancer metastasis through cell-autonomous PDGF receptor beta signaling." Cell **157**(2): 382-394.

Werner, J., S. E. Combs, C. Springfeld, W. Hartwig, T. Hackert and M. W. Buchler (2013). "Advanced-stage pancreatic cancer: therapy options." Nat Rev Clin Oncol **10**(6): 323-333.

Westphalen, C. B. and K. P. Olive (2012). "Genetically engineered mouse models of pancreatic cancer." Cancer J **18**(6): 502-510.

Wilentz, R. E., C. H. Chung, P. D. Sturm, A. Musler, T. A. Sohn, G. J. Offerhaus, C. J. Yeo, R. H. Hruban and R. J. Slebos (1998). "K-ras mutations in the duodenal fluid of patients with pancreatic carcinoma." Cancer **82**(1): 96-103.

Witt, H., W. Luck, H. C. Hennies, M. Classen, A. Kage, U. Lass, O. Landt and M. Becker (2000). "Mutations in the gene encoding the serine protease inhibitor, Kazal type 1 are associated with chronic pancreatitis." Nat Genet **25**(2): 213-216.

Wong, A., R. A. Soo, W. P. Yong and F. Innocenti (2009). "Clinical pharmacology and pharmacogenetics of gemcitabine." Drug metabolism reviews **41**(2): 77-88.

Wonganan, P., W. G. Chung, S. Zhu, K. Kiguchi, J. Digiovanni and Z. Cui (2012). "Silencing of ribonucleotide reductase subunit M1 potentiates the antitumor activity of gemcitabine in resistant cancer cells." Cancer Biol Ther **13**(10): 908-914.

Wu, X., J. H. Bayle, D. Olson and A. J. Levine (1993). "The p53-mdm-2 autoregulatory feedback loop." Genes Dev **7**(7A): 1126-1132.

Xu, J., J. J. Knox, E. Ibrahimov, E. Chen, S. Serra, M. Tsao, P. Cao, D. Vines, D. E. Green, C. Metran-Nascente, M. G. McNamara and D. W. Hedley (2013). "Sequence dependence of MEK inhibitor AZD6244 combined with gemcitabine for the treatment of biliary cancer." Clin Cancer Res **19**(1): 118-127.

Xu, J., J. J. Knox, E. Ibrahimov, E. Chen, S. Serra, M. Tsao, P. Cao, D. Vines, D. E. Green, C. Metran-Nascente, M. G. McNamara and D. W. Hedley (2013). "Sequence dependence of MEK inhibitor AZD6244 combined with gemcitabine for the treatment of biliary cancer." Clinical cancer research : an official journal of the American Association for Cancer Research **19**(1): 118-127.

Xu, P., D. M. Duong, N. T. Seyfried, D. Cheng, Y. Xie, J. Robert, J. Rush, M. Hochstrasser, D. Finley and J. Peng (2009). "Quantitative proteomics reveals the function of unconventional ubiquitin chains in proteasomal degradation." Cell **137**(1): 133-145.

Xu, Z., A. Vonlaufen, P. A. Phillips, E. Fiala-Beer, X. Zhang, L. Yang, A. V. Biankin, D. Goldstein, R. C. Pirola, J. S. Wilson and M. V. Apte (2010). "Role of pancreatic stellate cells in pancreatic cancer metastasis." Am J Pathol **177**(5): 2585-2596.

Yao, S. Y., A. M. Ng, C. E. Cass, S. A. Baldwin and J. D. Young (2011). "Nucleobase transport by human equilibrative nucleoside transporter 1 (hENT1)." J Biol Chem **286**(37): 32552-32562.

Yarden, Y. (2001). "The EGFR family and its ligands in human cancer. signalling mechanisms and therapeutic opportunities." Eur J Cancer **37 Suppl 4**: S3-8.

Yeo, T. P., R. H. Hruban, S. D. Leach, R. E. Wilentz, T. A. Sohn, S. E. Kern, C. A. Iacobuzio-Donahue, A. Maitra, M. Goggins, M. I. Canto, R. A. Abrams, D. Laheru, E. M. Jaffee, M. Hidalgo and C. J. Yeo (2002). "Pancreatic cancer." Curr Probl Cancer **26**(4): 176-275.

Ying, H., K. G. Elpek, A. Vinjamoori, S. M. Zimmerman, G. C. Chu, H. Yan, E. Fletcher-Sananikone, H. Zhang, Y. Liu, W. Wang, X. Ren, H. Zheng, A. C. Kimmelman, J. H. Paik, C. Lim, S. R. Perry, S. Jiang, B. Malinn, A. Protopopov, S. Colla, Y. Xiao, A. F. Hezel, N. Bardeesy, S. J. Turley, Y. A. Wang, L. Chin, S. P. Thayer and R. A. DePinho (2011). "PTEN is a major tumor suppressor in pancreatic ductal adenocarcinoma and regulates an NF-kappaB-cytokine network." Cancer Discov **1**(2): 158-169.

Yoon, J., K. H. Koo and K. Y. Choi (2011). "MEK1/2 inhibitors AS703026 and AZD6244 may be potential therapies for KRAS mutated colorectal cancer that is resistant to EGFR monoclonal antibody therapy." Cancer research **71**(2): 445-453.

Yoon, J., K. H. Koo and K. Y. Choi (2011). "MEK1/2 inhibitors AS703026 and AZD6244 may be potential therapies for KRAS mutated colorectal cancer that is resistant to EGFR monoclonal antibody therapy." Cancer Res **71**(2): 445-453.

Yoon, S. and R. Seger (2006). "The extracellular signal-regulated kinase: multiple substrates regulate diverse cellular functions." Growth Factors **24**(1): 21-44.

Yuan, T. L. and L. C. Cantley (2008). "PI3K pathway alterations in cancer: variations on a theme." Oncogene **27**(41): 5497-5510.

Zhang, S. Q., W. G. Tsiaras, T. Araki, G. Wen, L. Minichiello, R. Klein and B. G. Neel (2002). "Receptor-specific regulation of phosphatidylinositol 3'-kinase activation by the protein tyrosine phosphatase Shp2." Mol Cell Biol **22**(12): 4062-4072.

Zhang, Y., X. Li, Z. Chen and G. Bepler (2014). "Ubiquitination and degradation of ribonucleotide reductase M1 by the polycomb group proteins RNF2 and Bmi1 and cellular response to gemcitabine." PLoS One **9**(3): e91186.

Zhang, Y., J. P. t. Morris, W. Yan, H. K. Schofield, A. Gurney, D. M. Simeone, S. E. Millar, T. Hoey, M. Hebrok and M. Pasca di Magliano (2013). "Canonical wnt signaling is required for pancreatic carcinogenesis." Cancer Res **73**(15): 4909-4922.

Zhang, Y., G. W. Wolf, K. Bhat, A. Jin, T. Allio, W. A. Burkhart and Y. Xiong (2003). "Ribosomal protein L11 negatively regulates oncoprotein MDM2 and mediates a p53-dependent ribosomal-stress checkpoint pathway." Mol Cell Biol **23**(23): 8902-8912.

Zhao, Y. and A. A. Adjei (2014). "The clinical development of MEK inhibitors." Nat Rev Clin Oncol **11**(7): 385-400.

Zhau, H. E., L. S. Zhao, L. W. Chung, B. Q. Chen, P. Troncoso, C. Kao, M. Kojima, W. Fraser Symmans, N. Zheng, J. L. Palmer, J. W. Moul, R. Davis, M. F. Ye, L. S. Xiao and M. Craig Hall (1995). "Comparative studies of prostate cancers among United States, Chinese, and Japanese patients: characterization of histopathology, tumor angiogenesis, neuroendocrine factors, and p53 protein accumulations." Urol Oncol **1**(2): 51-63.

Zhen, D. B., K. G. Rabe, S. Gallinger, S. Syngal, A. G. Schwartz, M. G. Goggins, R. H. Hruban, M. L. Cote, R. R. McWilliams, N. J. Roberts, L. A. Cannon-Albright, D. Li, K. Moyes, R. J. Wenstrup, A. R. Hartman, D. Seminara, A. P. Klein and G. M. Petersen (2015). "BRCA1, BRCA2, PALB2, and CDKN2A mutations in familial pancreatic cancer: a PACGENE study." Genet Med **17**(7): 569-577.

Zheng, Z., T. Chen, X. Li, E. Haura, A. Sharma and G. Bepler (2007). "DNA synthesis and repair genes RRM1 and ERCC1 in lung cancer." N Engl J Med **356**(8): 800-808.

Zhou, B., X. Liu, X. Mo, L. Xue, D. Darwish, W. Qiu, J. Shih, E. B. Hwu, F. Luh and Y. Yen (2003). "The human ribonucleotide reductase subunit hRRM2 complements p53R2 in response to UV-induced DNA repair in cells with mutant p53." Cancer Res **63**(20): 6583-6594.

Zhou, B. P., Y. Liao, W. Xia, Y. Zou, B. Spohn and M. C. Hung (2001). "HER-2/neu induces p53 ubiquitination via Akt-mediated MDM2 phosphorylation." Nat Cell Biol **3**(11): 973-982.

Zhu, C. P., J. Shi, Y. X. Chen, W. F. Xie and Y. Lin (2011). "Gemcitabine in the chemoradiotherapy for locally advanced pancreatic cancer: a meta-analysis." Radiother Oncol **99**(2): 108-113.

Zmajkovicova, K., V. Jesenberger, F. Catalanotti, C. Baumgartner, G. Reyes and M. Baccarini (2013). "MEK1 is required for PTEN membrane recruitment, AKT regulation, and the maintenance of peripheral tolerance." Mol Cell **50**(1): 43-55.

PUBLICATIONS